ABSTRACT

Title of Dissertation : AN ANALYSIS OF A NEW APPROACH TO SOL-GEL SYNTHESIS: THE REACTION OF FORMIC ACID WITH TEOS

Kimberly Ann Brown, Doctor of Philosophy, 2005

Dissertation directed by: Professor Michael T. Harris
Department of Chemical Engineering

FTIR spectroscopy was investigated as a means of monitoring the reactions of formic acid and tetraethoxy silane, TEOS, at different temperatures and molar ratios of formic acid to TEOS, r. FTIR spectra of the reactions at r values of 1, 2, and 6 showed that increasing the molar ratio and temperature significantly increased the rates of hydrolysis and condensation. An activation energy of 10.5± 0.6 kcal/mole was determined for the r= 6 system.

^{29}Si NMR was used to monitor the reaction of formic acid with TEOS at molar ratios of 1, 2, and 6. The increase in reaction rate with increasing molar ratio was clearly evident in the silica NMR spectra. The low concentration of monomeric species containing hydroxy groups was deduced from NMR spectra.

Proton NMR spectroscopy was utilized in identifying the byproducts of the reaction of formic acid with TEOS. Ethanol, ethyl formate, and SiOOCH groups were easily identified by NMR. Ethyl formate was initially the major byproduct; however, ethanol became the major low molecular weight species as the reaction proceeded.

Information on the oligomeric structures was gathered using USAXS and mass spectrometry. USAXS was used to obtain radii of gyration for the r = 6 system which increased from 5.4 nm to 9.6 nm as the reaction progressed. An analysis was performed on the mass spectrum of the reaction of formic acid with TEOS at r =6, 35 minutes. Most oligomeric species contained at least one ring, and the maximum number of silicons was 11. Furthermore, the mass spectrum indicated that OR groups were the predominant groups attached to the silica oligomers.

The analyses performed on the reaction of TEOS with formic acid provided possible explanations for the increased rate of gelation. The presence of fewer cyclic oligomers in the early stages of reactions was observed in ^{29}Si NMR spectroscopy. ^{29}Si NMR spectroscopy also indicated an increase in the rates of condensation for the reaction of formic acid with TEOS.

The results of the analyses on the reaction of formic acid with TEOS were used to propose a kinetic model.

AN ANALYSIS OF A NEW APPROACH TO SOL-GEL SYNTHESIS: THE REACTION OF FORMIC ACID WITH TEOS

By

Kimberly Ann Brown

Dissertation submitted to the Faculty of the Graduate School of the
University of Maryland, College Park in partial fulfillment
of the requirements for the degree of
Doctor of Philosophy
2005

Advisory Committee:

Professor Michael T. Harris, Chair
Professor Sandra Greer
Professor Luiz Martinez-Miranda
Professor Nam Sun Wang
Professor William Weigand

DEDICATION

I dedicate this work

to

my parents

ACKNOWLEDGEMENTS

I would like to sincerely thank my advisor, Associate Professor Michael T. Harris, for his support and guidance during my studies at the University of Maryland. His interesting and cutting edge research projects have vastly increased my knowledge base. His dedication to his graduate students is commendable.

I would like to thank Dr. Yui Fai Lam in the Department of Chemistry for all of his assistance with NMR spectroscopy analyses. I would like to also extend appreciation to Dr. Bill Wallace at NIST for his assistance with mass spectrometry. I would like to thank Dr. Ken Sharp who introduced the idea of using formic acid to catalyze sol-gel reactions.

I would like to thank David Green for assistance with SAXS experiments, and the other members of my research group. I would also like to thank Dr. Horace Russell, former Dean of the College of Engineering, for all of his help and encouragement.

The Sloan foundation, NSF foundation, and the Gem foundation provided funding for my studies at the University of Maryland.

Lastly, I would like to thank my parents and grandmother for their unconditional dedication and support.

TABLE OF CONTENTS

LIST OF TABLES

LIST OF FIGURES

Chapter 1

Introduction

A colloid is a particle or dispersed phase in the size range of 1-1000nm, and interactions are dominated by forces due to surface charges and Van der Waals attractive forces. Consequently, gravitational forces are assumed to be negligible in colloidal suspensions, and the dispersed phase exhibits Brownian motion. A colloidal suspension of solid particles in water or an organic solvent is called a hydrosol or organosol, respectively. These solid particles can agglomerate or polymerize into a network, resulting in the formation of a gel.

A gel can be defined in numerous ways; however, the most simplistic definition is a substance that contains a continuous solid phase encompassing a continuous liquid phase. The two classes that gels can be divided into are particulate and polymeric. Particulate gels are formed from the adherence of particulate sols due to Van der Waals forces and can be reversed by disturbing the system. Polymeric gels are covalently linked; therefore, they are permanent. The gel point is characterized rheologically by divergences in the viscosity (or molecular weight) and in the elastic response to stress.

1.1 Sol-gel Applications and Processing

The increase in the number of sol-gel processing applications in recent years has led to a need for the study of alkoxide chemistry. Multi-component ceramic powders and glasses used for technology applications have been produced by alkoxide based sol-gel

processing. Sol-gel processes have been used to develop thin film oxide coatings for car mirrors, to form antireflection films on glass substrates for high power lasers, to produce oxidative resistant protective coatings on stainless steel, and to prepare abrasive materials (Brinker et al., 1986). Catalyst manufacture also employs sol-gel technology to produce mixed and pure oxides for catalysts and catalyst supports (Retuert et al., 1998; Davis et al., 1997). Photo catalysis can be performed using titania as a catalyst. Titania and silica mixed oxides have been used to catalyze reactions such as phenol amination, ethene hydration, and butene isomerization. Silica with trace amounts of titanium are used to manufacture fibers, films, and optical mirrors because of their low coefficients of thermal expansion over wide temperature ranges. Sol-gel processing offers the advantage of having liquid starting materials that can readily be purified by distillation and easily mixed. Another advantage of sol-gel processing is that the processing temperatures required to prepare highly homogeneous oxide glasses are significantly lower than the melting temperatures required for conventional fusing (Artaki et al., 1985). By altering the type of medium and the types and amounts of reactants, the properties of the resulting powder or glass can be modified. Therefore, sol-gel processing has the capability of producing many different types of products.

Sol-gels can be prepared by several different methods, and there are numerous descriptions in the literature for these processes (Bailey, et al., 1990; Pouxviel & Boilot, 1987; Brinker, et al., 1984; Kursave, et al., 1998; etc.). Traditionally, alkoxide based sol-gels have been prepared using a metal alkoxide, water, an alcohol, and a catalyst. The choice of the metal alkoxide, the type of catalyst, the ratio of the water to the alkoxide, the pH of the medium, the metal concentration in solution, the reaction

pressure, and the reaction temperature affect the kinetics of the sol to gel transformation.

Silicon oxides, titanium oxides, and zirconium oxides are of particular interest. Water is added to the reaction to facilitate condensation (indirectly) and hydrolysis. Because the metal alkoxide is immiscible in water, alcohol is used as a solvent. Alkoxide gelation is catalyzed by an acidic or basic catalyst. Mineral acids or carboxylic acids are normally used as the acid catalysts in these reactions, while a base such as NH_3 can been used as a catalyst. The choice of the type of catalyst (acidic or basic) affects the rates of reaction and the rheological properties of the gel. The presence of the metal alkoxide, water, alcohol, and catalyst lead to a plethora of reaction possibilities, including carboxylation, esterification, hydrolysis, and condensation reactions. Condensation reactions are especially important because they lead to the formation of metal-oxygen-metal type bonds which are the precursors to gel and particle formation.

These condensation reactions continue after gelation to further promote growth of the gel network which is termed aging (Brinker & Scherer, 1990b). Aging may involve further condensation, monomer dissolution and reprecipitation, and phase transformation. Shrinkage may also occur due to excretion of liquid from gel pores because of bond formation or attraction between particles. Most of these gels are amorphous even after drying, but crystallization can be induced by heating (Brinker & Scherer, 1990b). The choice of the catalyst, the relative ratios, and the reaction temperature determine the types and quantities of the products.

1.2. Methods for Characterization and Identification

There are numerous techniques for identifying chemical species such as Nuclear Magnetic Resonance, Raman spectroscopy, Size Exclusion Liquid Chromatography (SEC), Fourier Transform Infra-red Spectroscopy (FTIR), and Mass Spectroscopy. Small angle X-ray scattering and light scattering techniques are used to monitor the size and microstructural evolution of the condensation products. Normally, several different techniques must be employed to characterize accurately the sol-gel process components.

1.3. Sol-gel Syntheses Utilizing Formic Acid as a Multifunctional Catalyst

Most of the current sol-gel research has been performed using TEOS as a precursor to gelation. However, this reaction system is normally performed using a mineral acid catalyst, water, and an alcohol to facilitate gelation (Malier, et al., 1992; Yoldas, 1986; Brinker, et al., 1984; Artaki, et al., 1985). Recently, non-aqueous systems comprised of TEOS and an excess of a strong carboxylic acid which functions as the catalyst, water source, and solvent have been found effective for producing gels (Sharp, 1994; Emblem, et al., 1968; Karmakar, et al., 1991). Formic acid was found to lead to shorter gelation times than acetic acid or the conventional water, solvent, and catalyst system (Sharp, 1994).

There are numerous textbooks and papers that describe silicon chemistry; however, few studies have been centered on titanium and zirconium sol-gel routes. The formic acid/metal alkoxide system exhibits a more complex system of possible

reactions. The condensation, hydrolysis, and carboxylation reactions have been well studied for the aqueous/TEOS system, and are applicable to the formic acid/metal alkoxide system. However, there are different esterification reactions that are possible, and conflicting information exists in the literature about which esterification reactions occur. ^{29}Si NMR has often been used to determine the types of products in the sol-gel process (Sharp, 1994; Brinker, et al., 1986; Malier, et al., 1992; Yoldas, 1986). ^{17}O NMR has been found useful for the characterization of titania and zirconia syntheses reactions (Dire and Babonneau, 1994; Delattre and Babonneau, 1997; Peeters et al., 1998). Further work is needed in developing the reaction pathways for these complex systems. Particular focus on the early reaction times (< 5 minutes) is necessary because the initial stages of reaction determine the major characteristics of gels (Pouxviel et al., 1987).

Studying the reaction pathways for the sol-gel process is necessary to enable control and optimization of metal oxide synthesis reactions with an ultimate goal of improving the final product. Some concerns in metal oxide processing are purity, strength, and homogeneity. The addition of additives such as amines and liquid crystals has been used to modify metal oxide properties (U.S. Patent 4732750; Adeogun et al., 1998; Retuert et al., 1998). Preparing oxides from more than one different metal alkoxide has also been employed to manipulate properties and increase possible applications (Almeida, 1998; Davis & Liu, 1997; Delattre & Babonneau, 1997; etc).

1.4. Research Objectives

The objective of this research is to investigate a novel method of producing silica sol gels using TEOS and multifunctional formic acid. The use of formic acid as a substitute for catalyst, alcohol, and water provides significant processing advantages. The cost of starting materials for sol-gel synthesis and the processing time and complexity can be reduced. The most pronounced effect of replacing the conventional method for sol-gel formation with formic acid is the rapid rate of gel formation.

Numerous analytical techniques will be explored to assist in the identification of sol-gel precursors and byproducts. The effectiveness of FTIR, which is simpler and less expensive than many analytical techniques, on characterizing the metal alkoxide/formic acid reactions will be ascertained. Additionally, characteristic infrared peaks for the metal alkoxide/ formic acid system will be identified to determine the type of information that can be deduced using this analytical tool. FTIR will also be used to determine the effect of temperature on the overall rate of hydrolysis and condensation, and the activation energy will be determined for comparison to activation energies derived from gel time data. The effect of varying the molar ratio, r, of formic acid to TEOS will also be investigated using information gathered from FTIR.

The effects of temperature and molar ratio will also be explored using NMR spectroscopy. ^{29}Si NMR will be used to explore the effects of varying reaction temperature and molar ratio of formic acid to TEOS. The NMR spectra will provide information on the distribution of Q_1, Q_2, Q_3, and Q_4 species. The activation energy will be deduced from NMR spectroscopy for comparison with activation energies

obtained from FTIR spectroscopy and gel time data. For information regarding the type and quantities of byproducts, H NMR spectroscopy will be performed on the reactions.

Oligomer identification and quantification will be obtained from mass spectroscopy and USAXS. Mass spectroscopy can provide information regarding the types of oligomers generated in these sol-gel reactions and the size of the oligomers produced. Of special interest, the extent of ring formation can readily be observed from mass spectral data. USAXS is useful for obtaining information on the size of polymeric structures such as radii of gyration, R_g.

The combination of the aforementioned analytical methods will then be used to determine appropriate reaction pathways. Incorporation of formic acid into sol-gel reactions complicates the chemistry. Additional esterification reactions are possible. The ultimate goal is to develop a realistic kinetic model to simulate the reaction of TEOS with formic acid. This model will enable apriori prediction of the effects of manipulating reaction parameters.

Chapter 2

The Chemistry of Silicon Alkoxides

2.1 Silicon Alkoxides

2.1.1. Chemistry of Silica

One-fourth of the earth's crust is comprised of silicon. Silicon can be prepared by heating sand with magnesium powder. Silica, SiO_2, is the most important compound of Si, and it can be present in a crystalline form such as quartz or an amorphous form (e.g. onyx). Silicon naturally occurs in a +4 oxidation state and with a coordination number of 4. Furthermore, Silicon, which has a partial positive charge of +0.32 in TEOS, is less electropositive than most transition metals (Brinker & Scherer, 1990).

2.1.2. Introduction to Polyalkoxy Silanes

Polyalkoxysiloxanes are polymers formed with siloxane groups, Si-O-Si, that are formed by the condensation reactions of alkoxides. Polyalkoxysiloxanes have high resistance to heat and a small dependence of physical properties to temperature. Thermal degradation of siloxane bonds only occurs at temperatures above 300°C (Voronkov, et al., 1978). Ebelman in 1844 was the first person to study polyalkoxysiloxanes (Voronkov, et al., 1978). He observed the hydrolysis of TEOS which he formed by the reaction of silicon tetrachloride with ethanol. Mendeleyev in the 1850's found that the hydrolysis of $SiCl_4$ leads to $Si(OH)_4$ which continuously

undergoes condensation to form high molecular weight polysiloxanes (Brinker & Scherer, 1990).

Friedel, Ladenburg, and Crafts developed structures of the main classes of polyalkoxysilanes in the late 1800's (Voronkov, et al., 1978). Kipping more specifically determined the structures of linear and cyclic polyalkoxysiloxanes of the $(R_2SiO)_n$ and $HO(R_2SiO)_n$ type (Voronkov, et al., 1978). Kipping also showed that silicon behaved very differently than carbon. He proved that siloxane bonds were not chemically inert and could be cleaved by acids, alkalies, and $AlCl_3$, and he also showed that silicon was not able to form a stable double bond with oxygen. Kipping was also the first to report the catalytic effect of bases and acids on alkoxide reactions to produce polyalkoxides.

The Si-O-C group of alkoxides can be cleaved by thermal degradation reactions and by reactions with myriad acids, anhydrides, esters, epoxy compounds, and metallic compounds. The thermal stability of the alkoxide varies with the structure of the alkoxy group attached to the silicon atom. Thermal stability of alkoxysilanes decreases with increase in length and branching of the alkoxy group. The phenyl substituents are the most stable (Voronkov, et al., 1978). For example, thermal studies on TEOS indicated that thermal decomposition began at 200-250°C while Ridge and Todd (1949) found that $(C_5H_{11}O)_4Si$ was stable up to 302°C. In general, compounds of the type $SiR_n(OR')_{4-n}$, maintain thermal stability up to at least 200°C where R and R' are alkyl or aryl groups with 1 to 6 carbons (Voronkov, et al., 1978). The presence of a catalyst such as KOH or $NaOC_2H_5$ can lower the thermal stablitiy of alkoxysilane compounds and even cause cleavage of the Si-C bond (Voronkov, et.al, 1978). Mineral acids and

carboxylic acids can also cleave the bonds of alkoxysilanes which make them useful in catalyzing reactions leading to gelation.

2.1.3. Significance of Silicon Alkoxide Precursors

There is an ample amount of information on the preparation of alkoxide based sol-gels from a polyalkoxysilane, catalyst, water, and an alcohol. TEOS and TMOS have both been found useful as precursors to sol-gels; however, there are advantages in using TMOS as the starting material. Brinker & Scherer (1990) reported that the rate coefficients for condensation and hydrolysis for TMOS were greater than those of TEOS; therefore, the addition of one methyl group causes steric hinderance. Consequently, larger alkyl groups and branched alkyl groups are normally not used in the manufacture of sol-gels. TMOS is also preferentially used because its hydrolysis is completed before condensation reactions begin which simplifies data analyses (Artaki,et al., 1985). Another drawback to using TEOS is that it forms more ring structures than TMOS (Bailey, et al., 1990).

Coltrain et al. (1994) investigated the use of Silicon Tetraacetate, $Si(O_2CCH_3)_4$, as a precursor to silica formation. The gel times for TEOS and TMOS were orders of magnitude longer than the observed gel times for Silicon Tetraacetate. The $Si(O_2CCH_3)_4$ system gelled after approximately 7 hours. However, the TMOS system did not gel until 239 hours of reacting, and TEOS required an even longer period of 504 hours. Chang and Ring (1986) reported the effect of alkoxy chain length on sol-gel reactions using TMOS, TEOS, and TBOS (terabutoxy silane). The hydrolysis rate was

observed to decrease with an increase in the length of the alkoxy group. Oligomeric precursors such as hexamethoxydisiloxane have also been used as alkoxide precursors, and they are used when it is necessary to increase the silicate content of a sol (Brinker & Scherer, 1990).

2.1.4. Effects of using an Acid or Base Catalyst

Acid and base catalyzed gels differ in rheological properties. Equations 2.1 and 2.2 show the different mechanisms for the acid and base catalyzed reactions.

$$(RO)_3 SiOR + H_3O^+ \rightarrow (RO)_3 SiOH + H^+ + HOR \qquad (2.1)$$

$$(RO)_3 SiOR + OH^- \rightarrow (RO)_3 SiOH + OR^- \qquad (2.2)$$

Acid catalyzed gels exhibit finer pore size, higher surface area, and higher bulk density than base catalyzed gels (Sharp, 1994). Base catalyzed gels were found to appear cloudy; however, gels catalyzed by HCl appeared clear (Brinker, et al., 1990). X-ray scattering showed that base catalyzed systems were more densely crosslinked than acid catalyzed systems (Brinker, et al., 1984). Acid catalyzed systems require less time to gel than their base catalyzed systems (Chang and Ring, 1992). Furthermore, acid catalyzed gels were spinnable, which makes them capable of being drawn into fibers, and base catalyzed gels were not spinnable (Sakka & Kamiya, 1982).

Base and acid catalyzed gels are formed by different mechanisms. Acid catalyzed hydrolysis is rapid, and monomers are slowly polymerized by cluster-cluster growth mechanisms. Lightly branched polymers entwine to form cross-linked gels

(Chang and Ring, 1986). However, condensation is faster than hydrolysis for base catalyzed systems where monomer-cluster growth mechanisms form polymers. Bailey et al. (1990) and others have reported that base catalyzed sols were colloidal and acid catalyzed sols were polymeric. However, the base catalyzed hydrolysis of TEOS performed by Brinker et al. (1984) did not show any colloidal silica due to the partially unhydrolyzed monomer. Acid catalyzed systems display a decrease in concentration of species with an increase in molecular weight; however, base catalyzed systems produce low and high molecular weight species and few intermediate molecular weight species (Bailey, et al., 1990).

NMR studies showed that both acid and base catalyzed gels contained small ring structures (Kelts et al., 1989). Primarily four membered ring structures are formed from TMOS and TEOS which were found by Eitel (1964) to be very stable. Although gelation can be catalyzed by acids or bases, acids have been reported as more effective catalysts than bases (Brinker & Scherer, 1990). Mineral acids and strong carboxylic acids have been found most useful for catalyzing sol-gel reactions.

2.1.5. Hydrolysis and Condensation Reactions for Sol-Gel Synthesis

There is a plethora of information in the literature on the use of water, an alcohol, and an acidic catalyst to produce alkoxide based sol-gels, and various aspects of the behavior of these systems have been reported. These systems undergo hydrolysis and water and alcohol condensation reactions. Equations 2.3, 2.4, and 2.5 show the generic forms of hydrolysis and condensation reactions respectively. The two modes of condensation can be classified as alcoxolation (alcohol producing) and oxolation (water producing) which are depicted by equations 2.4 and 2.5 respectively.

$$Si - OR + H_2O \Leftrightarrow Si - OH + ROH \quad (2.3)$$

$$Si - OR + HO - Si \Leftrightarrow Si - O - Si + ROH \quad (2.4)$$

$$Si - OH + HO - Si \Leftrightarrow Si - O - Si + H_2O \quad (2.5)$$

Condensation reactions lead to the formation of dimers, trimers, and tetramers. The most acidic silanols (Si-OH groups), which are the most likely to be deprotonated, are contained in the most highly condensed species; therefore, condensation occurs preferentially between more highly condensed species and less condensed species (Iler, 1979). This leads to an initially low rate of formation of dimers which react mainly with monomers to form trimers; consequently, these trimers react with monomers to form tetramers. These trimers and tetramers can then react with each other leading to the formation of a continuous network or gel. Engelhardt employed ^{29}Si NMR to

determine that condensation products formed in the following order: monomer, dimer, linear trimer, cyclic trimer, cyclic tetramer, and higher order rings (Brinker & Scherer, 1990). These siloxane bonds which are formed in condensation reactions normally do not undergo depolymerization reactions in aqueous media because of the insolubility of silica in these systems.

Artaki et al. (1985) studied the polymerization kinetics of the sol-gel process at high pressure using TMOS as the silicon alkoxide reagent. TMOS was diluted in methanol, and a methanol/HCL mixture was added to this solution to catalyze the myriad reactions. Water was added to the mixture to yield a water/alkoxide ratio (r) of 10. Pressure was varied from 1 bar to 5 kbar, and the temperature was held constant at –30°C. They found that complete hydrolysis occurred, and disilicic acid, trisilicic acid, and cyclotetrasilicic acid were formed. Increasing the pressure accelerated the condensation rate while maintaining the same reaction pathway.

The effect of catalyst, temperature, time, initial reactant ratios, solution concentration, and reaction medium on the hydrolytic polycondensation of TEOS was studied by Yoldas (1986). The addition of larger quantities of HNO_3 acid catalyst led to a decrease in the time required for the sample to reach the peak temperature; however, the catalytic effect diminished for amounts larger than 1.0 g HNO_3 per mole of TEOS. In addition to increasing the reaction rate, the molecular size distribution was also altered by increasing the amount of catalyst. Longer reaction times and higher reaction temperatures shifted the molecular size distribution to higher values. The ratio of the water to TEOS significantly affected the properties of the polyorganosiloxane polymers. An increase in the amount of higher molecular weight species occurred when the value

of r was increased from 2 to 4. Increasing the molecular separation by diluting the system with ethanol resulted in the presence of fewer bridging oxygen (or siloxane bonds). Yoldas (1986) also proposed that molecular size growth first occurs by a "growth" process, and recombination processes occur in later stages between high molecular weight species. This resulted in a bi-modal size distribution.

A two staged hydrolysis process was developed by Brinker et al. (1984) for the preparation of silica gels. TEOS, an alcohol (ethanol or n-propanol), water, and HCl were mixed in the following molar ratio: 1: 3: 1: 0.0007. The second stage was comprised of the addition of water and HCl or NH_4OH after ninety minutes of mixing. They observed the following occurrences in the first hydrolysis step: rapid hydrolysis and condensation, ester exchange, and the formation of approximately 2 Si-O-Si bridges per silicon atom after 90 minutes. In the second hydrolysis stage, addition of HCl resulted in the complete hydrolysis of the OCH_2CH_3 groups and the $O(CH_2)_2CH_3$ groups after sixty minutes. When NH_4OH was used as the catalyst instead of HCl, the solution gelled before hydrolysis was completed. Phase separation with the unhydrolyzed monomer in the solvent rich phase, which did not have water or catalyst present, probably reduced the rate of hydrolysis for the basic catalyst case. Another observation was that the rate of hydrolysis of OCH_2CH_3 groups was slightly greater than the rate of hydrolysis of $O(CH_2)_2CH_3$ groups. This was expected because of steric hinderance and inductive effects. Furthermore, they established that this method led to the formation of polymeric particles instead of colloidal silica particles, regardless of the type of catalyst utilized in the second stage. This indicated that

monomeric particles began to condense before they were fully hydrolyzed, leading to dimer formation and chain-like structures.

SAXS was used to determine porod slopes more positive than –2 for the acid catalyzed system and more negative than –2 for the base catalyzed system. This implies that the acid catalyst led to slightly branched chains while using a basic catalyst resulted in either higher branched species or more dense structures than an ideal random linear polymers. The Guinier region was also examined to determine the radius of gyration, R_g.

Diluted and undiluted samples were examined to determine if the concentration of the sample was negligible. For the acid catalyzed case, the diluted and undiluted systems showed different results. The correlation range was measured for the undiluted system while the R_g was measured for the diluted system. Initially, the correlation range and the R_g were the same; however as time progressed the R_g was significantly larger than the correlation range. The correlation range increased from 10 to 30 Angstroms, while the R_g ranged from 10 to 90 Angstroms. Therefore, the undiluted system exhibited significant overlap. Contrary to the acid catalyzed system, there was no apparent difference in the diluted and undiluted base catalyzed system. R_g increased from 10 to 100 Angstroms during the reaction.

SAXS results also indicated differences in gelation morphology. For the acid catalyzed system, there was no change in R_g during the second hydrolysis step and the subsequent gelation. However, R_g doubled during the same period for the base catalyzed system. In addition to SAXS, proton NMR was explored as a means of further quantifying these reactions.

Proton NMR enabled observation of the relative concentration of methylene groups attached to ethanol and TEOS. The appearance of numerous silica species was evidenced from proton NMR by the increase in the number of peaks in the 3.7 ppm region. The increase in hydrolysis for acid catalyzed reactions over base catalyzed reactions was again easily deduced from proton NMR spectra. The acid catalyzed reaction was shown incomplete during the first stage. The second stage hydrolysis nmr analyses indicated that the acid catalyzed system exhibited an increased extent of hydrolysis although the base system gelled faster.

Lin and Basil characterized the products of the hydrolysis and condensation reactions of TEOS (ed.Brinker, et al., 1986). The initial mole ratios of SiO_2: H_2O: HNO_3: ethanol for TEOS hydrolysis were 1: 1: 0.00056: 4.5, and the reaction was carried out at 66°C. Using ^{29}Si NMR, they identified the hydrolysis and condensation products. The following species resulted from the hydrolysis of TEOS at the above conditions: $Si(OR)_3(OH)$, $Si(OR)_2(OH)_2$, and $Si(OR)(OH)_3$. The mono-substituted hydrolysis product, $Si(OR)_3(OH)$, was the major hydrolysis product over the course of the reaction. The completely hydrolyzed product, $Si(OH)_4$, was not seen in this reaction.

The disiloxane products formed from condensation reactions of the hydrolyzed species were $Si(OET)_2(OH)OSi(OET)_{3-x}(OH)_x$ where (x=1 > x=2), $Si(OET)(OH)_2OSi(OET)_{3-x}(OH)_x$ where (x=0,1,2), and $Si(OET)_2(OH)OSi(OET)_3$. The formation of $Si(OET)_3OSi(OET)_3$ was not observed. The reactivity of silanol species to condensation obeyed the following order: $Si(OR)(OH)_3 > Si(OR)_2(OH)_2 > Si(OR)_3(OH)$, and this can be explained by inductive effects. Thus the rates of product

formation are the opposite of the species' reactivity to condensation. This indicated that inductive effects outweighed steric effects for condensation, but steric effects were dominant in hydrolysis.

Aelion et al. (1950) studied the hydrolysis of TEOS using acidic and basic catalysts. HCl was used for acid catalysis, and ammonium hydroxide, sodium hydroxide, and pyridine were used for studying the effect of basic catalysts. He found that the concentration and type of catalyst strongly influenced the hydrolysis of TEOS; however, the reaction temperature and the type of solvent effected the reactions to a lesser extent. At a ratio of initial concentration of water to TEOS of 2 and with HCl as the catalyst, a reaction order of 2 was determined. They determined the following rate expression:

$$\frac{-dx}{dt} = K(M_{to} - x)(2S_{to} - x) \qquad (2.6)$$

. where M_{to} is the concentration of water

S_{to} is the concentration of TEOS

The same rate constants were obtained when dioxane and methyl alcohol were used as the solvent which indicated that re-esterification was not important. By determining the variation of the rate of reaction with increasing acid concentration, Aelion et al. (1950) found that the rate was directly proportional to the acid concentration. Furthermore, an activation energy of 6.8 kcal/mole was determined for this system.

Aelion et al. (1950) found that a large concentration of basic catalyst was necessary to catalyze hydrolysis reactions of TEOS. The base catalyzed reactions were determined to be first order in silicate concentration for low concentrations of TEOS. However, larger concentrations of TEOS led to variations of the reaction order.

The alcoholysis of silicon tetraacetate was investigated by Coltrain et al. (1994). Ethanol was found to rapidly facilitate the alcoholysis of this metal alkoxide. All mixed alkoxy/acetoxy derivatives were formed. After thirty minutes of reaction, minute quantities of free ethanol were detected using ^{1}H NMR, and almost all of the acetic acid was liberated. The absence of ethyl acetate peaks in the NMR spectra was of particular interest. This infers that the following reaction did not occur to a detectable extent:

$$SiO_2CCH_3 + C_2H_5OH \rightarrow SiOH + C_2H_5OCOCH_3 \qquad (2.7)$$

Peeters et al. (1998) used ^{17}O NMR to study the hydrolysis and gelation behavior of TEOS and TMOS using ethanol as a solvent. ^{17}O enriched water (10 at.%) was used in the reactions to enable labeling of MOH and MOM groups, and to enhance oxygen detection. HCl was added to catalyze the reaction. The ratios of TEOS, ethanol, and water ($5x10^{-3}$ M HCl) were 1: 4: 2. The intensity of the water peak decayed exponentially to 10 mole% while the intensity of the Si-O-Si peak increased up to 40 mole% after 100 minutes. The silanol groups increased rapidly to 60 mole% after 20 minutes, and slowly decreased to 50 mole% after 100 minutes. A steady state water concentration was observed indicating an equilibrium between water consumption in hydrolysis and the water formation during condensation. The effect of the mole ratio of ethanol to TEOS was also investigated. As the mole ratio of ethanol was increased

from 2 to 20, the steady state concentration of water increased from 12% to 40% of the initial amount. This can be explained by the reaction of ethanol with a silanol group to produce water that is depicted in equation 2.8.

$$C_2H_5OH + SiOH \rightarrow C_2H_5OSi + H_2O \qquad (2.8)$$

The effect of ethanol and water concentrations on the reaction of TEOS catalyzed by HCl was also investigated by Chang and Ring (1992). They reported Newtonian behavior for open systems with the ratio of moles of water to TEOS less than four. Closed systems were non-Newtonian and either shear thinning or thixotropic. The concentrations of water and ethanol had significant effects on the gelation time. As the ratio of water to ethanol decreased, the gel time increased. The equilibrium molar ratio of TEOS to water, 0.25, represented a threshold in these reactions. The gel time increased as the molar ratio of TEOS to ethanol increased when the ratio of TEOS to water was less than the equilibrium value. However, the gel time decreased with increasing TEOS to ethanol molar ratio when the equilibrium value of TEOS to water was exceeded. Therefore, the minimum gel time occurred at the equilibrium value of TEOS concentration to water concentration which was a result of La Chatlier's principle.

Similarly, Turner and Franklin (1987) studied the reaction of TEOS, ethanol, water, and HCl using ^{1}H, ^{17}O, and ^{29}Si NMR spectroscopy. To facilitate detailed analysis of the hydrolysis and condensation reactions, sub stoichiometric amounts of

water were used in their sol-gel synthesis reactions. ^{29}Si NMR indicated that $Si(OC_2H_5)_1(OH)_3$ and $Si(OH)_4$ were condensed and completely disappeared in less than an hour. However, $Si(OC_2H_5)_2(OH)_2$ and $Si(OC_2H_5)_3(OH)_1$ decreased over a six hour period. The identification of middle groups by Si NMR indicated that condensation had resulted in linear trimers. ^{1}H and ^{17}O NMR were not helpful in these studies.

The relationship between particle size and gelation was studied by Kursawe et al. (1998). TEOS, ethanol, water, and nitric acid were used to generate sols. Excess ethanol was used to slow down the rate of gel formation. SAXS data indicated that homogenous particles of radii less than 0.5 nm were formed. As the amount of ethanol was decreased, there was an exponential increase in the particle radii. After the radii reached 2.5 nm, gel formation occurred within a short period of time.

2.1.6. The Kinetics of Silica Alkoxide Reactions

Pouxviel et al. (1987) developed reaction parameters for the sol-gel reaction of TEOS, water, ethanol and HCl . The molar ratios of TEOS, water, and ethanol were 1, 4, and 3.8 respectively which resulted in a pH equal to 2.5. This was near the isoelectric point of silica; therefore, the hydrolysis and condensation reactions could be separated. ^{29}Si NMR was used to determine the hydrolysis rate constants.

The following equations display the hydrolysis reactions for TEOS:

$$Si(OC_2H_5) + H_2O \xrightarrow{K1} Si(OH)(OC_2H_5)_3 + C_2H_5OH \quad (2.9)$$

$$Si(OH)(OC_2H_5)_3 + H_2O \xrightarrow{K2} Si(OH)_2(OC_2H_5)_2 + C_2H_5OH \quad (2.10)$$

$$Si(OH)_2(OC_2H_5)_2 + H_2O \xrightarrow{K3} Si(OH)_3(OC_2H_5) + C_2H_5OH \quad (2.11)$$

$$Si(OH)_3(OC_2H_5) + H_2O \xrightarrow{K4} Si(OH)_4 + C_2H_5OH \quad (2.12)$$

By time evolution of species, the ratio of k_2/k_1 and k_4/k_1 were determined as approximately 5 assuming the concentration of water was constant. The ratio of k_3/k_1 was a significantly greater value of 12; therefore, the number of silanol groups present had a profound effect on the kinetics. After 45 minutes, the primary species present were TEOS, $Si(OH)_4$, and $Si(OH)_3(OC_2H_5)$; and condensation peaks began to appear. The TEOS peak exponentially decayed over the four hour period studied, and the absence of disilicic ester peak at –89 ppm, (H_5C_2O)-Si-O-Si-(OC_2H_5), indicated that TEOS did not undergo condensation. ^{29}Si NMR indicated that the main condensation pathways involved species with three or four silanols. Futhermore, they discovered that condensation rate constants were higher when species consisted entirely of silanol groups. Equations 2.13 , 2.14, and 2.15 display the primary condensation reactions which are all water producing.

$$Si(OH)_4 + Si(OH)_4 \rightarrow (OH)_3 Si - O - Si(OH)_3 + H_2O \quad (2.13)$$

$$Si(OH)_4 + (H_5C_2O)Si(OH)_3 \rightarrow (OH)_3 Si - O - Si(OH)_2(OC_2H_5) + H_2O \quad (2.14)$$

$$(H_5C_2O)Si(OH)_3 + (H_5C_2O)Si(OH)_3 \rightarrow (H_5C_2O)(OH)_2 Si - O - Si(OH)_2(OC_2H_5) + H_2O \quad (2.15)$$

After eight hours of reaction, the concentration of cyclic and linear oligomers was constant, and the amount of three dimensional branched groups increased significantly.

Pouxviel et al. (1987) discovered that after 15 hours of reacting, hydrolysis was still incomplete. The hydrolysis ratio, h, is defined in equation 2.16. After 15 hours of reacting, a value of 0.60 was found for h instead of 0.50 for pure silica.

$$h = \frac{([Si - OH] + [-O-]}{4[Si]} \quad (2.16)$$

For short reaction times, a hydrolysis rate constant of 0.14 l/mole-hr was determined by assuming that the concentration of water and Si-OR groups were equal. After condensation began, the ratio of the hydrolysis rate constant to the condensation rate constant, kh/kc, was determined. This quantity was dependent on the elapsed reaction time. The value of kh/kc was 2.15 after 2.5 hours, and decreased to 1.97 after 3 hours 45 minutes of reacting. This indicated that the OR groups became less reactive as condensation proceeded. At long times, kc was approximated as 15×10^{-3} l/mole-hr by

neglecting the hydrolysis reaction. Equation 2.17 defines the condensation ratio, c. The condensation ratio was equal to 0.68 after 15 hours, and the concentration of silanol groups was high . The gelation time was approximately 35 hours.

$$c = \frac{[Q1] + 2[Q2] + 3[Q3] + 4[Q4]}{4[Si]} \qquad (2.17)$$

Respectively, [Q1], [Q2], [Q3], [Q4] are the number of Si atoms with one, two, three, and four bridging oxygen atoms respectively.

Pouxviel et al. (1987) found that the initial water concentration affected the results. Increasing the water concentration led to increases in the percentage of $Si(OH)_4$ present after 30 minutes. There were also increased production rates of disilicic acid, linear trisilicic acid, and cyclic tetramer. The condensation rate constant was higher when the ratio of water to TEOS was increased.

2.1.7. Carboxylic Acids Prove Effective as Sol-Gel Catalysts.

More recently, carboxylic acids have been investigated as multi-functional facilitators of alkoxide based gels. Some of the earliest studies in the reactions of tetra-alkoxysilanes with carboxylic acids were performed by Sumrell and Ham (1956) who discovered that reacting an alkoxysilane with an excess of a carboxylic acid resulted in the formation of the ester of the carboxylic acid. They also found that reacting TEOS

with 0.5 to 2.0 molar equivalents of a carboxylic acid produced esters of the polysilicic acid, the alcohol, and the ester of the carboxylic acid.

Emblem et al. (1968) reacted palmitic acid ($CH_3(CH_2)_{14}CO_2H$) and TEOS with molar ratios of 1 to 3 for the carboxylic acid to TEOS ratio. The reactions were carried out at elevated temperatures to liberate ethanol. At a molar ratio of 1, the product was identified as $(CH_3(CH_2)_{14}COO)Si(OC_2H_5)_3$ by determining the physical properties of the resultant white wax. As the molar ratio was increased, the reaction yielded the di-substituted product for r = 2 and the tri-substituted product for the r = 3 case. The following reaction scheme was proposed:

$$SiOR + R'COOH \rightarrow SiOOCR' + ROH \qquad (2.18)$$

They reported that the reaction mechanism involved the attack of the non-carbonyl oxygen in the carboxylic acid on the Si atom with the simultaneous association of the acid proton and the alkoxyl oxygen atom (Emblem, et al., 1968). Removal of the first ethoxy group was not difficult; however, removal of the subsequent ethoxy groups required significantly elevated temperatures. Inductive effects would indicate that removal of the second and third ethoxy groups would be easier because of the increasing electrophilicity of the Si atom. Therefore, steric hinderance must have inhibited these reactions.

Pope and Mackenzie (1986) examined the effects of myriad catalysts on the reaction of TEOS with ethanol and water. They compared the catalytic effects of HF, HCl, HNO_3, H_2SO_4, HOAC, and NH_4OH. The use of HF as the catalyst resulted in the

shortest gel time, and the acetic acid (HOAC) catalyzed system had the second shortest gel time. HF may increase the rates of hydrolysis because F^- is capable of increasing the coordination number of Si above 4 resulting in the formation of a pentavalent intermediate that weakens the Si-OR bonds (Brinker & Scherer, 1990). However, the HOAC catalyzed system displayed the largest bulk density, the smallest porosity, and the greatest gel hardness. This showed that acetic acid may better catalyze sol-gel reactions than HCl which is most commonly used. Coltrain et al. (1992) further confirmed this when they discovered that acetic acid catalyzed systems gelled 3 times faster than HCl catalyzed systems.

The reactions of TEOS, glacial acetic acid, and water at room temperature were investigated by Karmakar et al. (1991). Using FTIR spectrometry, they discovered that TEOS was attacked by acetic acid in the absence of water and that the (OC_2H_5) groups were replaced by (OH) groups. They proposed the following reaction scheme:

$$Si(OC_2H_5) + CH_3COOH \rightarrow Si - OOCCH_3 + C_2H_5OH \qquad (2.19)$$

$$Si - OOCCH_3 + C_2H_5OH \rightarrow Si(OH) + CH_3COOC_2H_5 \qquad (2.20)$$

The rate of hydrolysis of the ethoxy groups was increased when water was initially added to the reaction. Karmakar et al. (1991) determined that the silicon acetate formed initially and was converted to silicic acid rapidly with the addition of water. These results contradict the results reported by Coltrain et al. (1994).

Acetic acid was added to TEOS with a molar ratio of acid to TEOS of 4, and after thirty minutes of mixing ^{29}Si and ^{1}H NMR indicated no substitution of ethanol by

acetate groups (Coltrain et al., 1994). After HCl was added to the mixture, hydrolysis was completed within six minutes. Ethyl acetate was observed after acidic water was added. This suggests that ethyl acetate formation was a secondary reaction, and occurs after hydrolysis.

Campero et al. (199) also studied the reaction of TEOS and glacial acetic acid. Molar ratios of TEOS to acetic acid of 100, 10, and 1 were investigated. This mixture was hydrolyzed by adding water with ethanol in a molar ratio of metal alkoxide to acetic acid/ ethanol/ water of 1/ 3/ 4, and HCl was added to acidify the mixture to a pH of 3. They reported that IR and NMR showed no indication of any reaction at room temperature. After heating the solution for a few hours at reflux, proton NMR indicated the presence of $Si(O_2CCH_3)$ groups. Ethyl acetate was identified by IR peaks at 1740 and 1240 cm^{-1}. The large difference in the wavenumbers suggests that this was a monodentate acetate ligand. Campero et al. proposed the following reaction scheme for the reaction of TEOS with acetic acid heated at reflux:

$$\begin{aligned} &Si(OC_2H_5)_4 + CH_3COOH \rightarrow \\ &Si(OC_2H_5)_{4-x}(OOCCH_3)_x + xC_2H_5OH + (1-x)CH_3COOH \end{aligned} \qquad (2.21)$$

$$C_2H_5OH + CH_3COOH \rightarrow CH_3COOC_2H_5 + H_2O \qquad (2.22)$$

The value of x was significantly less than one.

Sharp (1994) studied the gelation reactions of TEOS facilitated by carboxylic acids. Studies of various carboxylic acids indicated that gelation occurs in these systems twice as fast as the corresponding aqueous system with the same pH, and he determined that the stronger the acid, the faster the gelation time (Sharp, 1994). Carboxylic acids with pKa values less than 4 were found effective in promoting gelation. Consequently, trifluoroacetic acid, dichloroacetic acid, formic acid, and glycolic acid led to rapid gelation while acetic acid and acrylic acid were less catalytic to gelation.

Sharp (1994) studied the gelation kinetics of the TEOS/formic acid system. The value of r, the ratio of moles of formic acid to moles of TEOS, for this system dramatically affected these reactions. When r was greater than 4, the TEOS/formic acid system displayed a rapid exotherm; and the maximum temperature rise for an r = 8.3 system occurred after 10 minutes (Sharp, 1994). Hydrolysis, condensation, and esterification reactions must be happening simultaneously in high r systems. He determined the activation energies for r = 3 and r = 7 systems as 11.6 and 10.1 kcal/mole respectively using the gel time. Consequently, these activation energies were 3.5 and 7.5 kcal/mole less than those reported for aqueous systems with the same molar ratios (Sharp, 1994). Furthermore, the amount of water initially present was found to be inconsequential on the rate of gelation. ^{1}H and ^{29} Si NMR were used to ascertain the behavior for the TEOS/formic acid system. The distribution of species in the TEOS/HCOOH system was similar to the distributions obtained in aqueous systems with the exception of fewer silanol groups (Sharp, 1994). He proposed the following

reaction scheme that includes carboxylation, esterification, hydrolysis, and condensation reactions for the TEOS/formic acid system.

CARBOXYLATION

$$HCOOH + Si(OC_2H_5)_4 \Leftrightarrow (H_5C_2O)_3SiOOCH + C_2H_5OH \quad (2.23)$$

$$HCOOH + SiOH \Leftrightarrow SiOOCH + H_2O \quad (2.24)$$

ESTERIFICATION

$$C_2H_5OH + HCOOH \Leftrightarrow H_5C_2OOCH + H_2O \quad (2.25)$$

HYDROLYSIS

$$SiOC_2H_5 + H_2O \Leftrightarrow SiOH + C_2H_5OH \quad (2.26)$$

$$SiOOCH + H_2O \Leftrightarrow HCOOH + SiOH \quad (2.27)$$

CONDENSATION

$$SiOH + SiOH \Leftrightarrow SiOSi + H_2O \quad (2.28)$$

$$SiOH + SiOC_2H_5 \Leftrightarrow SiOSi + C_2H_5OH \quad (2.29)$$

$$SiOH + SiOOCH \Leftrightarrow SiOSi + HCOOH \quad (2.30)$$

$$SiOOCH + SiOC_2H_5 \Leftrightarrow SiOSi + H_5C_2OOCH \quad (2.31)$$

2.2 Sol-Gel Synthesis Reactions using Transition Metal Oxides

Transition metals impart different properties to gels, films, and powders than silica which make them desirable in some sol-gel applications. The sol-gel routes to synthesize titania, TiO_2, and zirconia, ZrO_2, have been investigated. Titanium alkoxides such as titanium isopropoxide, titanium tetraethoxide, and titanium butoxide are a few of the numerous alkoxides that have been investigated (Davis and Liu, 1997; Bradley et al., 1957). Normally, zirconium propoxide is used as the starting material for the sol-gel synthesis of zirconia; however, other alkoxides may also be feasible (Laaziz et al., 1992; Delattre & Babonneau, 1997). The sol-gel reactions involving titanium and zirconium also involve hydrolysis and condensation reactions similar to silica. However, the differences in size, molecular complexity, and electronegativity along with their exhibition of multiple coordinations, and coordination expansion result in different reactivity.

The molecular weights of zirconium and titanium are significantly larger than the molecular weight of silica, 28.086. Zirconium has a molecular weight of 91.22, and titanium's molecular weight is 47.90. Therefore, these transition metals exhibit longer bond lengths which may alter the reactivity and stability of the species. Furthermore, the larger size leads to steric hinderance which decreases their susceptibility to nucleophilic attack during condensation and hydrolysis reactions.

Unlike their silicon counterparts, zirconium and titanium alkoxide

precursors are often present initially as oligomers rather than monomers. Dissolving these transition metal alkoxides in non-polar solvents leads to oligomer formation via alkoxy bridging which is displayed in equation 2.32 (Brinker & Scherer, 1990b).

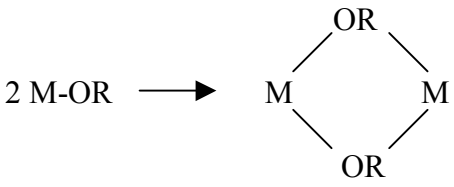

(2.32)

Silica alkoxides have the coordination number, N, and the charge, z, both equal to four. However, titanium and zirconium alkoxides are coordinately unsaturated. The quantity N-z is greater than one for these transition metals. Titanium and zirconium are group four metals; therefore, they have a charge of four. Titanium exhibits coordination numbers as high as six, and zirconium can adopt coordination numbers as large as eight (Laaziz et al., 1992). As the value of N-z increases, the activation energy decreases which leads to enhanced rates of hydrolysis and condensation (Brinker & Scherer, 1990b). These transition metals have the capability of expanding their coordination through nucleophilic association mechanisms (Brinker & Scherer, 1990b). An example of this phenomenon is the observation of bidentate bonding of transition metal acetates which is depicted in the following schematic:

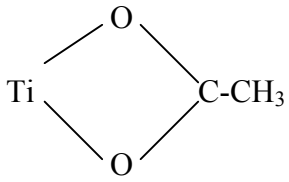

(2.33)

Bradley et al. (1955) studied the hydrolysis of titanium tetraethoxide, $Ti(OC_2H_5)_4$, in ethanol. Hydrolysis was conducted in an ebulliometer by adding water in dilute ethanol to $Ti(OC_2H_5)_4$ in boiling ethanol. Changes in the boiling were used to determine the molecular complexity which is defined as the number of titanium molecules per osmotic molecule. They discovered that the molecular complexity increased as the ratio of water to $Ti(OC_2H_5)_4$ increased. Titanium displayed a coordination number of six with respect to oxygen.

Brinker and Scherer (1990b) reported values of molecular complexity for titanium tetraethoxide and zirconium tetraethoxide as 2.9 and 3.6 respectively. These increased values of molecular complexity coincided with increases in covalent radii length. The length of the alkoxide ligand was also identified as a factor in molecular complexity. Bradley et al. (1957) studied the hydrolysis of myriad titanium alkoxides. Titanium iso-propoxide was determined to be monomeric while titanium tetraethoxide was oligomeric. Solvation in alcoholic solutions was reported to lower molecular complexity. Decreasing the

concentration of titanium alkoxide or increasing the temperature helped promote solvation.

Transition metals such as titanium and zirconium are more electropositive than silicon. This enhances their susceptibility to nucleophilic attack. The partial charge on titanium in titanium tetraethoxide is + 0.63, and + 0.65 on the zirconium in zirconium tetraethoxide (Brinker & Scherer, 1990b). These values are significantly higher than the partial charge of + 0.32 on silicon in TEOS. Therefore, hydrolysis and condensation reactions are faster for transition metal alkoxides than for silica alkoxides.

The hydrolysis and condensation reactions described previously for silica alkoxides are also valid for transition metal alkoxides. However, the enhanced coordination unsaturation for titanium and zirconium leads to an additional method of condensation called olation. Equations 2.34 and 2.35 represent the modes of olation.

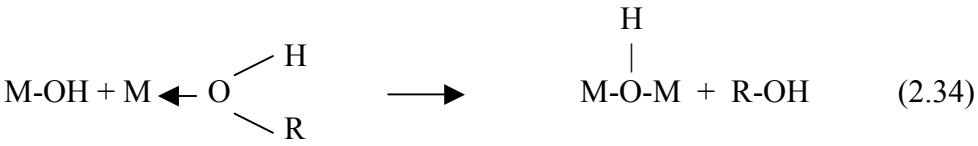

(2.34)

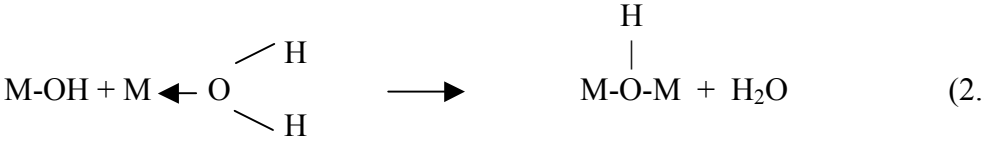

(2.35)

2.2.1. The Sol-Gel Chemistry of Titanium and Zirconium

The study of the synthesis of sol-gels from transition metal alkoxides has been reported to a much lesser extent than the silica alkoxide route of sol-gel generation. Retuert et al. (1998) attempted to increase the surface area of titania gels for implementation as a catalyst support for group eight metals in photocatalysis applications. Titanium isopropoxide was added to a solution of diethanolamine in 2-propanol. This solution was hydrolyzed by adding a mixture of water in 2-propanol. The sol was stirred for four hours, and the gel was formed upon addition of chitosan, poly-ß(1-4)-2-amino-2-deoxy-D-glucose. After a 24 hour drying period, a BET surface area of 103 m^2/g was determined for a mole ratio of chitosan to titania of 0.6. Similarly, the addition of amines to titanium tetraethoxide was reported in U.S. patent 4732750.

The hydrolysis of titanium tetraethoxide was conducted in the presence of an amine to constrain the particle size because monodisperse metal oxide powders offer processing advantages (U.S. Patent 4732750). Two mole % of triethylamine was added to a solution of $Ti(OC_2H_5)_4$ in ethanol. This was mixed with a water/ethanol mixture to facilitate hydrolysis. The average particle size was reduced from 1.3 microns (no amine was present) to 1.1 microns. When sec-butyl amine was substituted for triethyl amine, the average particle size was further reduced to 0.88 microns. Increasing the quantity of amine present resulted in a decrease in the average particle size. Average particle sizes as low as 0.21 microns were obtained. A Scanning Electron Microscope

(SEM) indicated that the particles were spherical, and that the particle size distribution was uniform for all experiments with amine additives.

As mentioned previously, the hydrolysis of various titanium alkoxides was studied by Bradley et al. (1955, 1957). They discovered that the first hydrolysis product was $Ti_6O_4(OC_2H_5)_{16}$ when titanium tetraethoxide was used as the starting metal alkoxide. The consequence of varying the ratio of water to $Ti(OC_2H_5)_4$, h, was investigated. Below a value of 0.67 for the hydrolysis ratio h, there was a mixture of $Ti_3(OC_2H_5)_{12}$ and $Ti_6O_4(OC_2H_5)_{16.}$, however, there was 100% $Ti_6O_4(OC_2H_5)_{16}$ present at a hydrolysis ratio of 0.67. Increasing the hydrolysis ratio to 0.89 led to mixtures of $Ti_6O_4(OC_2H_5)_{16}$ and $Ti_9O_8(OC_2H_5)_{20}$. At h = 0.89 no $Ti_6O_4(OC_2H_5)_{16}$ was detected. D.C. Bradley et al. (1955) predicted that a hydrolysis ratio of 1.33 should represent the limit of soluble titanium tetraethoxides. They encountered precipitation at h values larger than 1.5. Additionally, they observed different reaction behavior for various alkoxides. Titanium n-propoxide did not result in precipitation for hydrolysis ratios larger than 1.7, and residual water was present.

Zirconia synthesis was investigated by Hayashi et al. (1998). Zirconium tetrapropoxide was reacted with acetic acid and water. At a molar ratio of acetic acid to zirconium tetrapropoxide equal to one, free acetic acid was not detected by FTIR which implied that the reaction had gone to completion. For a molar ratio of acetic acid to zirconium tetrapropoxide of two, free acetic acid was detected. Increasing the amount of acetic acid above two did not eliminate all of the propoxy groups. $Zr(OCOCH_3)_2(OC_3H_7)_2$ was still detected.

Harris et al. (1997) used SAXS, FTIR, and electrical conductivity to study the hydrolysis and condensation of zirconium tetrabutoxide and titanium tetraethoxide. They studied the initial reaction kinetics using a rapid mixing technique. For $Zr(OC_4H_9)_4$, 20% of the water was consumed after 80 ms. This concentration remained the same over the monitoring period of 1000 s. The concentration of Zr-OR groups had decreased by 60% after 80 ms of reacting. Unlike the water concentration, the concentration of Zr-OR groups exponentially decayed showing more than 90% depletion after 1000 s. Titanium tetraethoxide was not as reactive as Zirconium tetrabutoxide.

The concentration of water molecules decreased by 10% after 80 ms, and continued to decrease to approximately 18% depletion at 1000 s when $Ti(OC_2H_5)_4$ was used as the starting metal alkoxide. The concentration of Ti-OR groups exponentially decayed, and 55% of the Ti-OR groups were consumed after 1000 s of reacting.

Comparisons of the water and metal alkoxide concentrations indicated that for titanium and zirconium alkoxides condensation began occurring after 1 s of reacting. The conductivity was found to correlate with the loss of M-OR ligands. As the concentration of M-OR ligands decreased, the solution conductivity simultaneously decreased.

Sanchez et al. (1988) studied the hydrolysis and condensation of titanium tetrabutoxide and zirconium propoxide. Acetic acid was used to facilitate hydrolysis and condensation. Acetic acid prevented precipitation of titania (TiO_2). Furthermore, the gel times observed were longer than the gel times obtained using the conventional HCl catalyst. Adding acetic acid to $Ti(OC_4H_9)_4$ led to an exothermic reaction, and the

resultant solution was clear. The coordination number increased from five to six when acetic acid was added to the metal alkoxide, and ^{13}C and ^{1}H NMR showed that the acetate ion behaved as a bidentate ligand.

For a molar ratio of acetic acid to titanium butoxide of one, the following reaction occurred:

$$Ti(OC_4H_9)_4 + HO_2CCH_3 \rightarrow Ti(OC_4H_9)_3(O_2CCH_3) + C_4H_9OH \qquad (2.36)$$

IR and NMR indicated that the butoxy groups were removed by hydrolysis first, and the acetate groups remained longer which could explain while gelation slowed down.

Sanchez et al. (1988) used the partial charge model to explain the order of ligand removal. The metal and the leaving group must be positively charge. Therefore, prediction of the charges on the metals and leaving groups is advantageous. The partial charge model developed by Livage and Henry is based on a linear variation of electronegativity with partial charge. The partial charge can be calculated by equations 2.37 and 2.38

$$\delta_i = \frac{(\overline{\chi} - \chi_i)}{k\sqrt{\chi_i}} \tag{2.37}$$

$$\overline{\chi} = \frac{\sum_i p_i \sqrt{\chi_i}}{(\sum_i p_i / \sqrt{\chi_i})} \tag{2.38}$$

where for molecule ($p_1X_1 \bullet p_2X_2 \bullet \ldots\ldots p_iX_i$)

χ_i is the electronegativity of the neutral atom X_i

k is 1.36 in Pauling's units

Using the partial charge model, the partial charge on acetic acid is –0.7 while the partial charge on butanol is +0.1. They further went on to study the effect of increasing the molar ratio of acetic acid to titanium tetrabutoxide. As the molar ratio was increased, the gel time also increased. This was explained by the decrease in the functionality of molecules with more acetate groups. Finally, Sanchez et al. (1988) reported that the acetic acid titanium tetrabutoxide system gelled in four days; however, the addition of acetic acid to zirconium tetrapropoxide gelled within a few minutes.

2.2.2 The Manufacture of Mixed Metal Alkoxides

More commonly, the processing of mixed alkoxides consisting of a combination of silica, titanium, and zirconium alkoxides has been investigated. A major challenge in these syntheses is producing homogenous gels or sols due to the different levels of reactivity for these different metals. Titanium and zirconium mixed oxides were formulated by Laaziz et al. (1992). Solutions of titanium and zirconium propoxides were prepared by dilution in propanol with concentrations of 0.8 mole/liter. Acetic acid was used to facilitate hydrolysis and condensation. The hydrolysis ratio h, the ratio of the number of acetic acid molecules to metal alkoxide molecules, was varied between one and eight. For h values less than five, increasing the temperature from seven degrees to forty degrees had no affect on the crystallization time or gel time. At a hydrolysis ratio of five, a gel was obtained instead of a crystal.

In general, gels derived from titanium propoxide are opaque while zirconium propoxide leads to transparent gels. Laaziz et al. (1992) discovered that for mixed systems the gels and crystals were always transparent. The presence of acetate and propoxy groups in the gels derived from their studies indicated that hydrolysis was incomplete. Furthermore, the ligands surrounding the metal atoms were identical in crystals and gels.

Delattre and Babonneau (1997) performed a comprehensive study on silica/zirconia and silica/ titania mixed gels. To compensate for the increased reactivity of the zirconium alkoxide, TEOS, water, ethanol in the ratios 1/1/0.4 was prehydrolyzed. Enriched ^{17}O water was used in their synthesis. ^{29}Si NMR was used to

detect the various oligomeric species and ^{17}O NMR was used to identify water, Si-OH groups, and Si-O-Si groups. The following assumptions were made: no condensation in the first 30 minutes, and condensation between silanol, Si-OH, groups only at low hydrolysis ratios. After 30 minutes of reaction, ^{17}O NMR indicated that 90% of the water had been consumed. The reaction mixture was comprised of 7% water, 18% Si-O-Si groups (siloxanes), and 75% Si-OH groups. Titanium terabutoxide, $Ti(OC_4H_9)_4$ was than added at a molar ratio of silicon to titanium of one. Oxygen NMR indicated that upon addition of $Ti(OC_4H_9)_4$ the silanol peaks disappeared while the amount of siloxane groups increased to 31%. Furthermore, the Ti-O-Ti groups represented 17% of the reaction media, and the Si-O-Ti groups constituted 52%. The low concentration of mixed alkoxides may have been caused by redistribution between the alkoxides. Equation 2.39 shows the possible redistribution reaction.

$$2Ti-O-Si \rightarrow Ti-O-Ti + Si-O-Si \qquad (2.39)$$

The presence of a larger amount of siloxanes after addition of titanium tetrabutoxide could also be a result of the catalytic effect of titanium tetrabutoxide on TEOS condensation. After three hours, the system reached equilibrium. The NMR intensities of Si-O-Ti groups decreased, Ti-O-Ti groups increased in intensity, and Si-O-Si groups showed no change over this period. Adding additional water to hydrolyzed Ti-OR groups further led to an increase in Ti-O-Ti groups while the quantities of Si-O-Si and Si-O-Ti groups remained constant. ^{17}O NMR indicated that formation of Si-O-Ti

groups was kinetically favored while the formation of titania and silica rich phases was thermodynamically favored. Ti-OH groups were not detected in the NMR data.

Delattre and Babonneau (1997) also synthesized zirconia/silica mixed alkoxides. $Zr(OC_3H_7)_4$ was added to prehydrolyzed TEOS. ^{29}Si NMR indicated the disappearance of all Si-OH, TEOS, and $(C_2H_5O)_3Si$-O groups. ^{17}O NMR showed Si-O-Zr bonds, Si-O-Si bonds, and water. Zirconium tetrapropoxide reacted preferentially with Si-OH to form Si-O-Zr bonds, and propanol. There were 65% Si-O-Zr groups present, and this amount did not change over 20 hours of monitoring. Adding additional water led to precipitation which suggested that unreacted $Zr(OC_3H_7)_4$ was present. This data infers that zirconium tetrapropoxide reacts with prehydrolyzed TEOS to lead to more stable sols with higher ratios of Si-O-M groups.

Silica-titania films were also investigated by Almeida (1998). TEOS and titanium tetra-isopropoxide were used as the starting alkoxides. FTIR was used to characterize the films. The Si-O-Ti peak appeared at 1056 wavenumbers. The porosity, ν_p, was determined from the following relationships:

$$A = \alpha x = \alpha_{std} x_{std} \qquad (2.40)$$

where A is the absorbance

α is the absorption coefficient of the film of interest

α_{std} is the absorption coefficient of a fully densified film

x and x_{std} are the film thickness of the film of interest and the standard film respectively

$$\nu_p = 1 - \frac{\alpha}{\alpha_{std}} \tag{2.41}$$

Yamane et al. (1982) recognized that the alkoxy group controlled the rates of hydrolysis and condensation. They used this observation to tailor the reactions to form mixed titania- silica gels. A highly branched titanium precursor, titanium ter-amyloxide, and TMOS were used as the starting metal alkoxides. Titanium ter-amyloxide (9g) was mixed with 420 ml of methanol, 20 ml of ter-amyl alcohol, 51g of TMOS, and 26 ml of ammonia water. They were able to produce monolithic clear gels that were very homogenous using these metal alkoxides.

2.3. Nuclear Magnetic Resonance Spectroscopy of Sol-Gel Reactions.

Nuclear magnetic resonance spectroscopy (NMR) is often used to characterize the structures of the silicon compounds present in the sol-gel processing of TEOS. The magnetic properties of nuclei are dependent on the spin quantum number (I) and the magnetic moment (μ). Equation 2.19 expresses the relationship between the magnetic moment of a nucleus and spin quantum number in terms of nuclear magnetons, and shows that a nucleus with a spin quantum number of zero does not have a magnetic moment.

$$\mu = \frac{geh}{2mc}(I) \qquad (2.42)$$

where e is the charge of a proton

m is the mass of a proton

g is the nuclear g factor

Only one third of the different isotopes have a spin quantum number that is not equal to zero. The following general rules apply in determining I:

a.) if the mass number of the nucleus (A) is odd, then I will be a half-integral

e.g. H^1 has an I =1/2

b.) if A and the charge (Z) are even, then I = 0

e.g. C^{12}

c.) if A is even and Z is odd, then I is an integral

e.g. H^2

When an isolated nucleus is placed in a static magnetic field it can align with the magnetic field or against the magnetic field. Because the energy difference between

these states is so small, the states exist in thermal equilibrium. The very small excess of nuclei present in the lower energy state leads to NMR signals. The applied magnetic field, H_o, causes a nucleus to spin like a top in the direction of the magnetic field, and there are 2I + 1 possible alignments for a magnetically active nucleus. The energy of the magnetic states, E, is given by equation 2.43. These different energy states are referred to as nuclear Zeeman levels.

$$E = \frac{-\mu}{I} H_o m_I \qquad (2.43)$$

where m_I is the magnetic quantum number with possible values of
I, I-1, I-2,…..,-I

A variable radio frequency is applied to the nuclei in a magnetic field to cause transitions between nuclear spin states. Only transitions where Δm_I is I or –I can occur. These transitions occur at the resonance frequency, ν, which is depicted in equation 2.44.

$$h\nu = \frac{\mu H_o}{I} \qquad (2.44)$$

The preceding analyses only considered an isolated nucleus. The diamagnetic moment produced by other atoms when many nuclei are present causes secondary magnetic fields for the individual nuclei. The electrons surrounding the nucleus provide shield from the applied magnetic field. Therefore, the actual magnetic strength, H_{eff}, is less than the applied magnetic field as shown in equation 2.45,

$$H_{eff} = H_o - \alpha H_o \qquad (2.45)$$

where α is the diamagnetic shielding constant. Therefore, NMR spectroscopy is very helpful in identifying the surrounding environments for many species. ^{29}Si NMR and ^{1}H NMR spectroscopy have often been employed in the identification of the sol-gel reactions of TEOS and TMOS.

Oldfield and Kirkpatrick (1985) performed ^{29}Si NMR spectroscopy, and reported that chemical shifts are a function of polymerization of the SiO_4 tetrahedra. In his investigation of the polycondensation of TEOS, Yoldas (1986) reported the shift of NMR peaks to higher fields as the number of bridging oxygen increased. He assigned the –90.6 ppm resonance to the Si-$(O\text{-}Si)_2$ type group, the -99.8 ppm resonance to the Si-$(O\text{-}Si)_3$ group and the –110 ppm to the silica holder.

McFarlane and Seaby (1972) studied the chemical shifts in methylsilyl carboxylates. They examined the chemical shifts of compounds of the form $(Me)_xSi(O_2CR)_{4-x}$ and found a correlation between pKa, electron density at silicon, and chemical shift. As the pK_a of the parent acid of the group attached to the Si group increased, the chemical shift also increased. Furthermore, the pKa of the parent acid affected the chemical shifts to a greater extent for compounds with x values of 3 (tri-substituted) than for compounds with mono and di-substituted groups. The number of substitutions also caused different chemical shifts. The chemical shift of $(Me)_3Si(O_2CH)$ was 25.2 ppm relative to $Si(Me)_4$, while $(Me)_2Si(O_2CH)_2$ was observed at 7.0 ppm.

Turner and Franklin (1987) used ^{29}Si NMR to identify species formed from the sol-gel synthesis reactions of TEOS, ethanol, water, and HCl. They reported that methyl and ethyl polysilicates exhibit three lines with chemical shifts in the following regions: -85 to –89 for end groups, -93 to –96 for middle groups, and –102 to –103 for trifunctional groups. The assignments are depicted in table 2.1 for the ^{29}Si NMR chemical shifts of the condensation products.

Table 2.1.: ^{29}Si NMR chemical shifts for the condensation products of TEOS reactions assigned by Turner and Franklin (1987), based on tetramethyl silane.

Peak Assignment	Chemical Shift (ppm)
End Groups	
Si-O-Si-(OH)	-86.2
Si-O-Si-(OR)	-88.9
Middle Groups	
Si-O-Si*(OH)-O-Si-	-92.65
Si-O-Si*(OH)-O-Si-O-Si-	-92.80
(OH)Si-O-Si*-O-Si-	-95.09
Si-O-Si*-O-Si-	-95.32
(HO)-Si-O-Si*-O-Si-O-Si-	-96.12
Si-O-Si*-O-Si-O-Si-	-96.29

Lin and Basil (ed. Brinker, et al., 1986) performed NMR analyses on the reaction of TEOS, HNO_3, water, and ethanol. They found that adding an OH group to TEOS resulted in downfield shifts of 2-2.5 ppm for each successive addition. They also

found that dimers and trimers appeared upfield from TEOS. Table 2.2 shows some of the chemical shifts they identified. They also showed that the chemical shifts changed when n-propanol was added as a solvent.

Table 2.2: Chemical shifts for the conventional TEOS hydrolysis reactions assigned by Lin and Basil (based on tetramethyl silane).

Compound	Chemical Shift
$Si(OET)_4$	-81.95
$(ETO)_3SiOSi(OET)_3$	-88.85
$(ETO)_3SiOSi(OET)_2OSi(OET)_3$	-88.99
$(ETO)_3SiOSi(OET)_2OSi(OET)_3$	-96.22
$Si(OR)_2(OH)OSi(OR)_3$	-86.27
$Si(OR)(OH)_2OSi(OR)_3$	-83.92
$Si(OR)_3(OH)$	-79.07
$Si(OR)_2(OH)_2$	-76.58
$Si(OR)(OH)_3$	-74.31

Coltrain et al. (1994) performed ^{29}Si NMR studies of the reaction of silicon tetraacetate with ethanol. They found that TEOS was an intermediate because of the NMR peak at –82 ppm. They also found a smaller peak at –86.5 ppm which

corresponded to $Si(OEt)_3OAc$. The reaction of TEOS with acetic acid was also studied by Coltrain et al. (1994). ^{29}Si NMR showed the appearance of broad peaks at –92 ppm, -102 ppm, and –110 ppm. These peaks were assigned to polymeric species with 2, 3, and 4 bridging oxygen atoms per silicon, respectively.

The sol-gel transition of the reaction of TEOS with ethanol and water was investigated using the magic angle spinning (MAS) technique of ^{29}Si NMR (Malier et al., 1992). During conventional static NMR, the spectra broaden with increasing degree of condensation. This occurs because of the retarded molecular motion which impairs averaging the dipolar coupling with the protons; furthermore, the multiplication of the possible neighboring configurations of silicon atoms which is caused by the rigid lattice extension broadens the isotropic chemical shift. MAS eliminates the broadening of the isotropic chemical shift due to solid state. Gadolinium nitrate was used as a relaxation agent, and relaxation times were less than one second during the liquid and gel states. This MAS method was used to determine the gel fraction of TEOS gels. A maximum degree of condensation of 0.84 was determined, and this gel fraction remained constant from $2t_g$ to $9t_g$ (where t_g is the gel time). Up until the degree of condensation increased above 80%, the gel fraction remained at zero. The gel fraction had only reached 80% after 2 t_g; therefore, the sol-gel transition is not complete after gelation. The gel fraction reaction reached 95% after a time period of 3 t_g.

These results show that NMR spectroscopy can help identify compounds. However, the similarity in the structures of the myriad compounds complicates the analyses. It is often necessary to perform additional analytical techniques such as Raman spectroscopy or FTIR spectroscopy.

2.4. Raman and FTIR Spectroscopy of Metal Alkoxide Reactions

Raman spectroscopy and FTIR spectroscopy are two commonly used methods of observing normal vibrations. These methods are based on the observation that all molecules have a certain amount of energy that causes them to bend, stretch, wag, rock, and undergo other types of molecular vibrations. The amount of energy a molecule has is quantized; therefore, the molecule can only stretch, bend, etc. at a particular frequency. When a molecule is irradiated with infrared radiation, the energy is absorbed when the energy of the infrared radiation equals the energy difference between two vibrational frequencies. Each frequency absorbed by the molecule can be related to a particular molecular motion; consequently, the type of functional group present can be determined by examining these motions. The motions of the molecule are very complex; however, they can be characterized as superpositions of simpler motions called normalmodes. A molecule with n atoms has 3n-6 normal modes of vibration (3n-5 for linear molecules).

Classical molecular vibration theory is based on the assumption that the vibrations are simple harmonic. This assumption translates into the validity of equation 2.46,

$$\nu_{qu} = \nu_{cl} \tag{2.46}$$

where ν_{qu} is the frequency of radiation absorbed or emitted due to a transition between quantized energy levels and ν_{cl} is the frequency calculated by classical theory.

To illustrate the basic principles of molecular vibrations, a simple system which consists of 3 masses joined together linearly by identical springs is shown in figure 2.1.

Figure 2.1: A linear mechanical system for illustration of molecular vibrational theory.

The displacement coordinates which are measured from the equilibrium position of each mass are x_1, x_2, and x_3. The potential energy, V, can then be expressed by equation 2.47 where f is the force constant of the springs.

$$V = \frac{1}{2} f(x_2 - x_1)^2 + \frac{1}{2} f(x_3 - x_2)^2 \qquad (2.47)$$

Equation 2.48 shows the relationship for the kinetic energy, T, as a function of the velocities, v_i.

$$T = \frac{1}{2} m_1 v_1^2 + \frac{1}{2} M_2 v_2^2 + \frac{1}{2} m_3 v_3^2 \qquad (2.48)$$

The rate of change of momentum for the ith mass is equal to the force acting upon the mass as shown in equation 2.49.

$$\frac{d}{dt}\left(\frac{\partial T}{\partial v_i}\right) + \frac{\partial V}{\partial x_i} = 0 \qquad (2.49)$$

Subsequently, the equation of motions for each mass are represented by the following equations:

$$m_1 \frac{dv_1}{dt} + f(x_1 - x_2) = 0 \qquad (2.50)$$

$$M_2 \frac{dv_2}{dt} + f(2x_2 - x_1 - x_3) = 0 \qquad (2.51)$$

$$m_3 \frac{dv_3}{dt} + f(x_3 - x_2) = 0 \qquad (2.52)$$

In every normal mode, each mass displays a simple harmonic motion with the same frequency, ν; and, all of the masses move in phase with each other but have different amplitudes, A_i. Therefore, the solutions can be represented by equation 2.53, where $\lambda=4\pi^2\nu^2$, ε is the phase angle, and (x) refers to the coordinate

.

$$x_i = A_i^{(x)} \cos(\lambda^{\frac{1}{2}} t + \varepsilon) \qquad (2.53)$$

This solution can be substituted into the equations of motions to yield the amplitude equations for each mass. The theory of linear equations states that the determinant of the coefficients must be equal to 0 for the equations to be linearly independent. This condition results in the secular equation of motion which is depicted in equation 2.54,

$$(f - m\lambda)(-2fm - fM + Mm\lambda)\lambda = 0 \qquad (2.54)$$

where the subscripts were dropped since m1=m3<M2. Therefore, this simplified mass system has the following three solutions for λ: f/m, f(M +2m)/mM, and 0. The first solution represents the case where M remains constant and m1 and m3 move in the opposite directions with equal magnitudes. The second solution represents the case where M moves in one direction and m1 and m3 move in the opposite direction. Finally, the third solution represents translation of the entire system.

The previous example illustrated the simple case of a constrained molecule. In real systems the molecules are three dimensional and are not constrained but are capable of moving in any direction. Therefore, translations, rotations, and their effect on vibrations must be accounted for in real molecules. Brame and Grasselli (1976) and

Woodward (1972) give detailed explanations and derivations of vibrational spectroscopy.

In Raman spectroscopy, a molecule is exposed to an electromagnetic wave causing the molecule to be under the influence of an electric field. Electrons are shifted by this field against the nuclei, or polarized, and the wave induces a dipole moment modulated with the frequency of the wave. The molecule then emits a wave with this frequency (Rayleigh radiation). When the molecule performs a vibration during this process, the polarizability changes and the Rayleigh radiation is modulated with the frequency of the vibration. This radiation analyzed by a spectrometer shows a central peak and 2 side bands for each vibration which are shifted to larger and smaller frequency values by the frequency of the molecular vibration. These are called Raman lines, and the intensity of these lines is proportional to the square of the change of the molecular polarizability by the vibration.

Raman and Infrared, which will be discussed in the experimental section, give complementary images with different intensities. Non-polar groups give strong bands in Raman spectroscopy, while polar groups give strong Infrared intensities.

2.5. Mass Spectroscopy of Sol-Gel Reactions

Mass spectroscopy can enable determination of the general particle distribution for sol-gel reactions. The percentage of high and low molecular weight species can qualitatively be induced from mass spectra. Mass spectrometers measure the mass-to-charge ratios, m/z, of ions formed after a sample is ionized. The molecular weight is

directly or indirectly related to the m/z ratio depending on whether sample molecules are singly ionized.

The basic parts of a mass spectrometer are the ion source, sample inlet system, separation mechanism, mass analyzer, and ion detection system. The mass resolution, mass range, and the sensitivity are the important parameters for mass spectroscopy. The resolution, R, required to separate two ions of mass m and m + Δm is represented in equation 2.55

$$R = \frac{m}{\Delta m} \tag{2.55}$$

Increasing the resolution allows for more accurate ion mass measurements. A reference compound such as perfluorokerosene, which gives mass deficient fragment ions, is often used as an internal reference in high resolution mass spectroscopy analyses. Utilizing Fourier transform mass spectrometers enables higher resolution mass spectrometry to be obtained.

Chromatographic separation or tandem mass spectrometry must be employed to analyze mixtures. The fragment ions must be identifiable from the molecular ions because the fragment ions can only be used for structure determination. Gas or liquid chromatography can be implemented to separate the molecular species before mass spectroscopy is performed. Alternatively, tandem mass spectrometry allows for selection of a particular molecular ion for activation in a collision chamber. In the collision chamber, some of the excited ions have enough energy to fragment. The

resultant fragmented ions are then mass analyzed. Tandem mass spectroscopy can not be used for mixtures that contain isobaric components; therefore, chromatography and tandem mass spectroscopy are often combined.

Mass spectroscopy requires gas phase ions which are difficult to obtain from polymer species which have large molecular weights and are often entangled. Therefore, mass spectroscopy must be tailored to convert polymers into gas phase charged species. Hanton (2001) reviewed the mass spectrometry of polymers and polymer surfaces. There are numerous mass spectroscopy techniques that have been proven useful in probing the structures of polymers. Gas chromatography-mass spectrometry (GC-MS), pyrolysis mass spectrometry, glow discharge mass spectrometry (GDMS), field desorption mass spectrometry (FD), fast atom bombardment mass spectrometry (FAB), and laser desorption mass spectrometry (LDMS) are some of the mass spectral methods shown useful in polymer analyses. However, matrix-assisted laser desorption/ionization (MALDI) is currently the method of choice for polymer mass spectroscopy.

MALDI has been applied to a variety of different polymers possessing vastly different morphology. Average molecular weights and polymer sequencing are some of the MALDI applications (Hanton, 2001). A dilute polymer solution is mixed with a matrix, and this solution is then applied either manually or via an electrospray ionization technique to a MALDI target. The target is laser irradiated which vaporizes the matrix and desorbs the polymer into the gas phase.

Wallace et al. (1999) used matrix-assisted laser desorption/ionization time-of-flight mass spectrometry (MALDI) to investigate the structure of silsesquioxane

polymers. Silsesquioxane polymers consist of silicon with three bridging oxygen and one alkyl group; therefore, they form more 3-D structures than polysiloxanes. They used 2-methacryloxypropyltrimethoxysilane to prepare the polysilsesquioxane by hydrolysis and condensation reactions. The mass spectrum obtained was consistent with a condensation polymer. Higher abundances of low molecular weight molecules were present, and the intensity exponentially decayed with increasing molecular weight. The repeat unit spacing of 188.25 u indicated that side reactions were not significant and that the oligomers were singly charged. Repeat lengths from 5 to 55 were identified in the mass spectrum. The ratio of closed loops to open loops was determined to be 0.25 for all repeat units. Therefore, Wallace et al. (1999) was able to deduce important structural information from mass spectroscopy.

Michalczyk et al. (1996) used potassium ionization (K^+IDS) of desorbed species to characterize polyfunctional alkoxysilanes for star gel precursors and tetraalkoxysilanes. K^+IDS was found useful in determining the purity of sol-gel precursors, and the extent of hydrosilylation. They were easily able to distinguish between cyclic and acyclic species using K^+IDS.

Michalczyk et al. (1996) reacted formic acid with TMOS in an equimolar ratio, and removed methanol and methyl formate by distillation during the reaction. K^+IDS analyses were performed on the polysilicate, and cyclic and acyclic distributions corresponding to n = 3 to 8 were primarily observed. The acyclic species were more abundant than the cyclic species, and there were a few bicyclic species observed. The absence of any significant silanol groups was noted, and they mentioned that silanol species were observed in the reaction of TEOS with formic acid.

2.6. Small Angle X-ray Scattering Analyses of Metal Alkoxides

X-rays are a form of electromagnetic radiation with wavelengths of interest between 0.01×10^{-9} m -7.0×10^{-9} m. These x-rays can be produced from synchrotron radiation or x-ray tubes. At synchrotron installations, x-rays are produced by decelerating energetic electrons traveling close to the speed of light. Electromagnets are used to accelerate electrons as they travel along a linear path. Deceleration is induced by inserting the electrons into a circular path of bending magnets. These electrons then lose energy by producing x-ray photons with tangential paths to the circle. Alternatively, x-ray tubes can be used to synthesize x-rays. Electrons are accelerated by high electric potentials in a x-ray tube. These electrons strike the anode of the tube and decelerate upon passing through the electron clouds of the atoms. These methods both produce a continuous x-ray spectrum of intensity as a function of wavelength.

Small angle x-ray scattering (SAXS) involves forming x-rays into a fine beam often by using slits. This beam is passed through a desired sample which causes the beam to scatter and travel in other directions upon exiting the sample. A detector is employed to record the angular dependence of the scattered intensity. Detailed information on SAXS is available in "Modern Aspects of Small Angle Scattering" edited by Brumberger.

The structure of the sample determines the scattering angle, the intensity of the scattered beam, and the mutual dependence of the scattered angle and beam intensity.

Brinker and Scherer (1990b) provided a detailed description of interpreting SAXS data. The important parameters are the Fourier spatial frequency, K; the radius of gyration, R; and the bond length, a. Equations 2.56 and 2.57 depict the relationships for K and l, the characteristic length scale.

$$K = \left(\frac{4\pi}{\lambda}\right)\sin\left(\frac{\theta}{2}\right) \qquad (2.56)$$

$$l = \frac{2\pi}{K} \qquad (2.57)$$

The scattering curve is represented as a plot of intensity, which is characterized as log K, versus log KR. This curve can be divided into the following three important regions: the Guinier region, the Porod region, and the Bragg region.

The region with KR values of approximately one, which represents low scattering angles, is classified as the Guinier region. Information regarding the polymer mass and radius may be obtained from this area of the scattering plot. Equation 2.58 depicts the exponential relationship between the scattered intensity, I, and the radius of gyration.

$$I \sim e^{-\frac{K^2 R^2}{3}} \qquad (2.58)$$

The intermediate region where $R > K^{-1} > a$ is labeled the Porod region. In this region, the scattered intensity is independent of R and a and can be represented as a decaying power law. The Porod slope, P, is related to d_f and d_s the mass fractal and surface fractal dimensions as shown in the following equation:

$$P = -2d_f + d_s \qquad (2.59)$$

Mass fractal objects characteristically display a mass that is proportional to the radius by less than a power of three ($d_f < 3$). Therefore, the density decreases with increasing radius. An object that has a surface area proportional to the radius to a power greater than two is a surface fractal ($d_s > 2$). Normally, sol-gel syntheses result in fractal objects due to the insolubility of the solid phase.

Chapter 3

Experimental Techniques

3.1. FTIR Spectroscopy

The reactions of TEOS and formic acid were investigated using FTIR. TEOS, which was obtained from J.T. Baker, and 98% formic acid, which was manufactured by EM Science, were used without additional purification. TEOS was added to formic acid to prevent formation of particles, which has been reported in the reverse addition case. After the reagents were added to a vial and sealed, the vial was briskly shaken. The vial was then placed in a temperature controlled water bath for a specific amount of time before a micro sample was taken. A fresh solution was prepared for each sampling time interval to ensure accurate results. The micro sample was then placed in 25 ml of xylene for Fourier Transform Infrared spectroscopy (FTIR) analysis. Figure 3.1 depicts the principle of operation of an FTIR spectrometer.

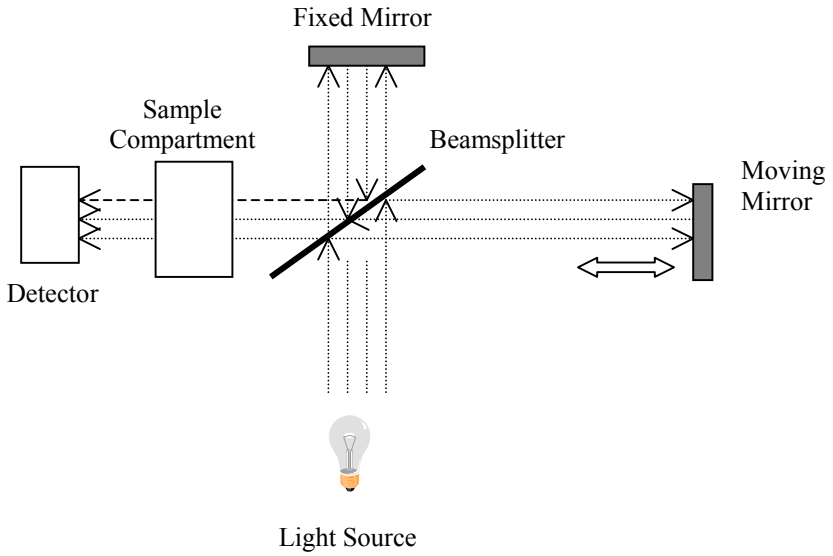

Figure 3.1. Basic principles of operation of an FTIR.

Michelson in 1891 designed an interferometer which is the basis for most FTIR spectrometers. A beam of infrared radiation is directed into the interferometer which is comprised of a fixed mirror, a moving mirror, and a beam splitter. The moving mirror glides at a constant velocity towards and away from the beamsplitter. The beamsplitter transmits approximately half of the light to one mirror and reflects the remaining light to the other mirror. The Michelson interferometer shifts the phase of one beam relative to the other by performing scans of one or both mirrors which changes the path lengths and shifts the phase of the beams. These mirrors reflect the beams back to the beamsplitter where they recombine, mutually interfere, and then leave at 90° to the original direction. The recombined beam is then focused into the sample compartment. The beam intensity is recorded as a function of optical path difference, which is called an interferogram, with an IR detector. The Fourier transform of the interferogram is computed to obtain the infrared spectra.

The interferogram and the infrared spectra are related by the Fourier transform. Equation 3.1 shows the relationship between the frequency of the signal and the wavenumber of the beam source.

$$I(\delta) = \frac{I_o}{8}(1 + \cos(2\pi\delta\sigma)) \tag{3.1}$$

Where I(δ) is the intensity measured

δ is the optical path difference

σ is the wavenumber of the light source

I_o is the incident light intensity

Equation 3.2 shows the equation of the interferogram and accounts for the presence of many frequencies.

$$I(\delta) = \frac{I_o}{16}\int_{-\infty}^{\infty} S(\sigma)e^{12\pi\delta\sigma}\,d\delta \tag{3.2}$$

The Fourier cosine transform relates the interferogram to the frequency spectrum of the infrared beam as shown in equation 3.3.

$$S(\sigma) = \int_{-\infty}^{\infty} I(\delta)e^{-12\pi\delta\sigma}\,d\delta \tag{3.3}$$

A Michelson MB-154 series FTIR spectrometer manufactured by Bomem was used for the analyses. The spectrometer is equipped with a MCT (HgCdTe) detector

which is useful in the wavenumber range from 5000-400 cm^{-1}. The beamsplitter is composed of KCl, and the window between the sample compartment and the interferometer is made of ZnSe.

Reactions of formic acid with TEOS were performed at the following molar ratios of formic acid to TEOS, r : 1, 2, and 6. These reactions were all performed in a 40°C controlled waterbath. FTIR scans were obtained at times ranging from 10 to 60 minutes. Formic acid and TEOS reactions were also carried out at various temperatures. Formic acid and TEOS were reacted at an r value of 6 and temperatures of 24, 30, and 40°C.

3.2. NMR Spectroscopy

NMR spectroscopy was used to follow the progress of a formic acid and TEOS reaction to aid in the identification of FTIR peaks. The NMR spectrometer was a Bruker Pulse Fourier Transform multi-nuclei NMR spectrometer with a 400MHz field strength. This instrument was equipped with a user tunable probe that enabled silica and proton detection. The DEPT90 (distortionless enhancement of NMR signals by polarization transfer) method was used to obtain the NMR spectra, therefore, a relaxation agent was not necessary for these experiments (Doddrell, et al., 1982). Contrary to most NMR experiments, the NMR analyses were performed on neat solutions of formic acid with TEOS. This enabled accurate kinetic analyses of the reaction with formic acid and TEOS. Also, the NMR spectra were obtained without

spinning the sample during NMR collection. Tetramethyl silane (TMS) was used as a standard for all the NMR analyses.

^{29}Si NMR and proton NMR spectra were obtained for the reaction of formic acid with TEOS. Approximately one mL of the formic acid /TEOS solution was pipetted into an NMR sample tube. In general, NMR spectroscopy analyses were performed for r values of 1, 2, and 6 at approximately 20°C. A selective set of silica NMR experiments were performed on the r = 6 formic acid /TEOS system at temperatures of 0° and -20°C.

3.3. USAXS Experiments

The reaction of formic acid with TEOS was investigated at the National Synchrotron Light Source Xray ring at Brookhaven National Laboratory. Formic acid and TEOS were reacted at molar ratios of 2 and 6 in stainless steel sample cells with 0.025 mm thick windows and 1 mm path lengths.

3.4. Mass Spectrometry

Mass Spectrometry analyses of the reactions of formic acid with TEOS were performed at NIST in Gaithersburg, Maryland. Matrix-assisted laser desorption/ionization time-of-flight (MALDI-TOF) spectrometry was used for these analyses. A Bruker REFLEX II instrument was used to perform the experiments. Ions were generated using a 337 nm wavelength nitrogen laser with a pulse duration of 3 ns

and an average energy of 5 μJ over a 200 μm x 50 μm area. All the mass spectrometry experiments were facilitated using Dimethoxy-4-hydroxy-cinnamic acid as a matrix.

Sample preparation consisted of first dissolving 50 mg of matrix into 1 ml of THF solvent. The formic acid/TEOS mixture (175 mg) was then dissolved in 1 ml of THF. The matrix solution and the formic acid/TEOS solution were then mixed together in a 1:1 ratio. The mixture of the matrix and the analyte was then electrosprayed onto a target at 5 μL/min using a steel capillary. The inner diameter of the steel capillary was 0.56 mm and 5 kV were supplied to the capillary. The distance between the target plate and the capillary tip was approximately 2 cm. The target was then placed in the mass spectrometer. The laser was continually rotated over various portions of the target for a total of 250 shots. This accounted for any possible non-uniformities in the analyte deposition onto the target. MALDI-TOF was employed in the reactions of formic acid with TEOS at r values of 1, 2, and 6. All experiments were performed at room temperature. No addition of cationizing agents was necessary for ionization. Sodium and potassium were inherently present as the cationizing agents. To alleviate the complexity of the spectra which occurred as a result of the dual cationizing agents, potassium trifluoroacetate and sodium trifluoroacetate were added to the analyte for several MALDI-TOF experiments. This did not provide any significant benefit in resolving the mass spectra.

Chapter 4

Experimental Results

4.1. FTIR Spectroscopy

Figures 4.1 and 4.2 show the infrared spectra for TEOS and formic acid. These spectra were taken to identify the characteristic peaks for each reagent and to prepare calibration curves. Both of these reagents were diluted in 100 ml of xylene to lower their respective concentrations enough to result in absorbances less than 1. The major characteristic peaks for TEOS were at 1084,1104, 1167, 966, and 804 cm^{-1}. All of these peaks were attributed to the Si-O-C linkage. The characteristic peaks for the C-H groups, which occur in the 3000 cm^{-1} region, were not clearly identifiable.

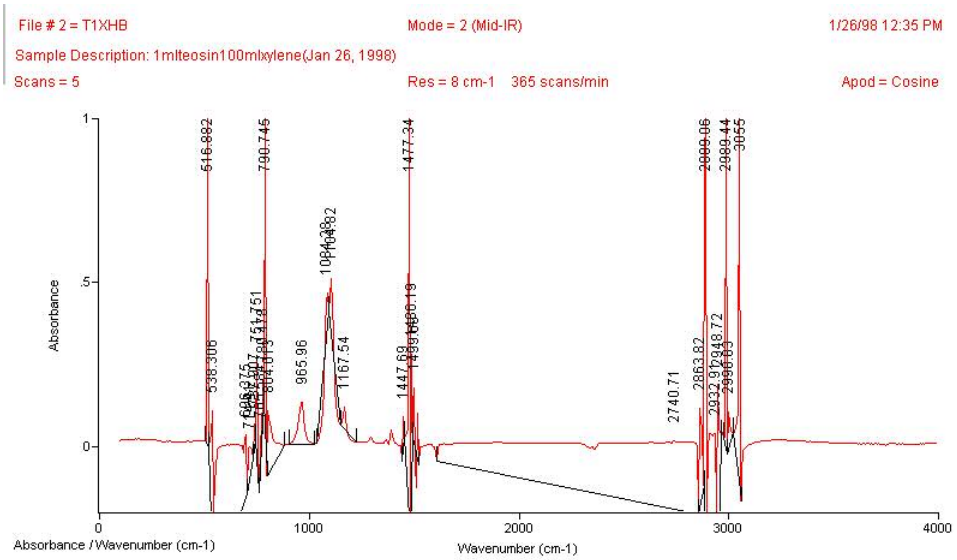

Figure 4.1: FTIR spectrum of 1 ml TEOS in 100 ml xylene.

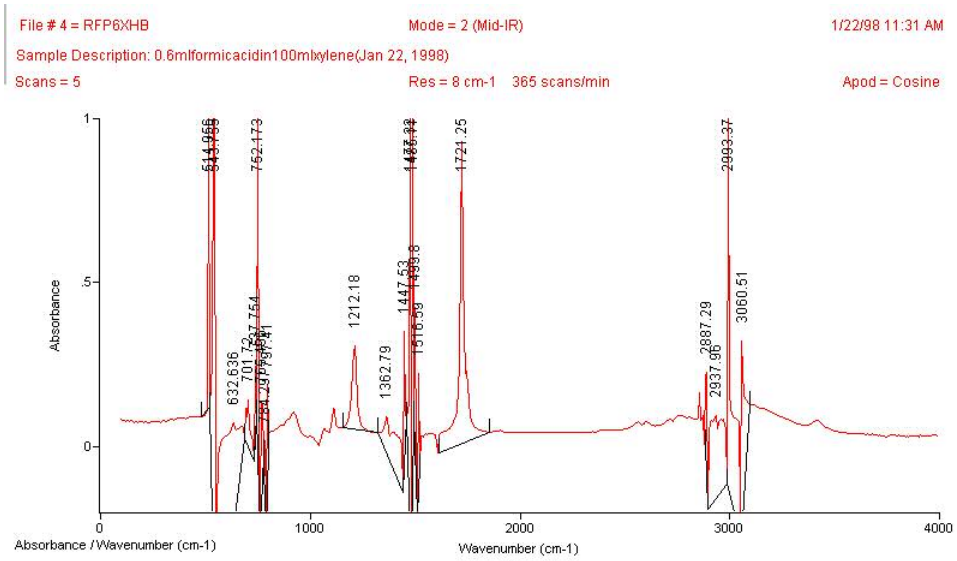

Figure 4.2: FTIR spectrum of 0.6 ml of formic acid in 100 ml of xylene.

Formic acid displayed major characteristic peaks at 1721, 1212, and 1362 cm^{-1} which coincided with previously reported FTIR spectrum. . This spectrum compared with the spectrum found in the literature for formic acid (Aldrich FTIR handbook). These peaks are the results of the vibrations of the C=O and C-O functional groups. There is a small peak at approximately 3400 cm^{-1} that is due to the OH functional group. These normal vibrations have been classified; consequently, table 4.1 shows the assignments for the major FTIR peaks (Roeges, 1994). These results showed that TEOS and formic acid have different characteristic peaks that can be easily discerned. Therefore, the concentrations of the reagents can be monitored during the course of the reaction.

Table 4.1: Assignments of the normal vibrations of formic acid.

Vibration	Observed wavenumber cm^{-1}	Reported absorption region, cm^{-1}
C=O stretching vibration	1721	1660-1790
C-O stretching vibration	1212	1170-1330
O-H stretching vibration	3400	3000-3500
O-H in-plane deformation	1362	1340-1450

FTIR spectra were obtained for different concentrations of TEOS and formic acid in order to obtain calibration curves. These calibration curves enabled monitoring of the progress of the reactions of TEOS and formic acid. The areas of the largest characteristic peaks for TEOS, 1104 cm^{-1}, and formic acid, 1721 cm^{-1}, were used to develop the calibration curves that are shown in figures 4.3, 4.4, and 4.5.

The calibration curves for TEOS and formic acid displayed highly linear behavior in the low concentration regimes. The C=O groups of formic acid vibrated at higher intensities than the Si-O-C groups of TEOS. The additional calibration curve displayed in figure 4.5 was necessary after the spacing in the sample compartment was slightly changed from cleaning the compartment.

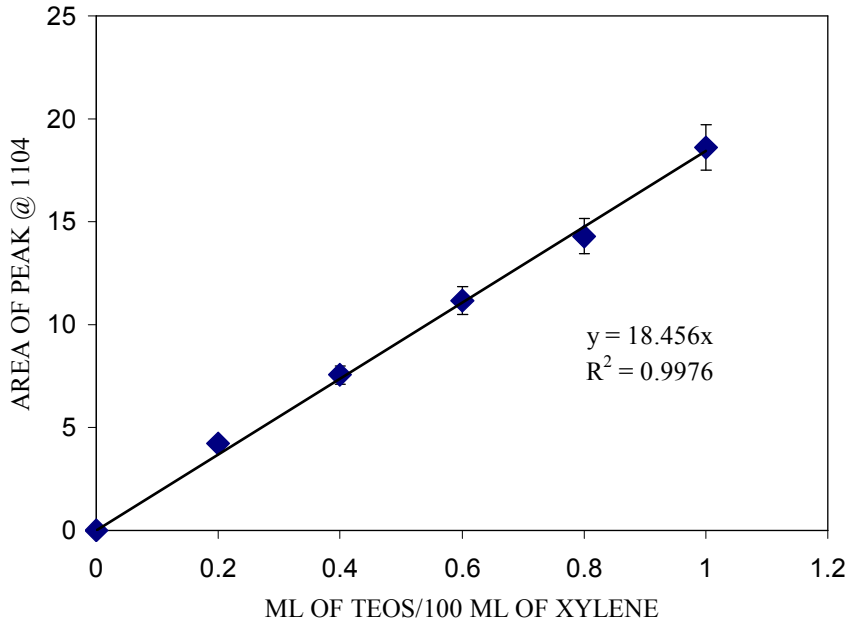

Figure 4.3: Calibration curve for TEOS.

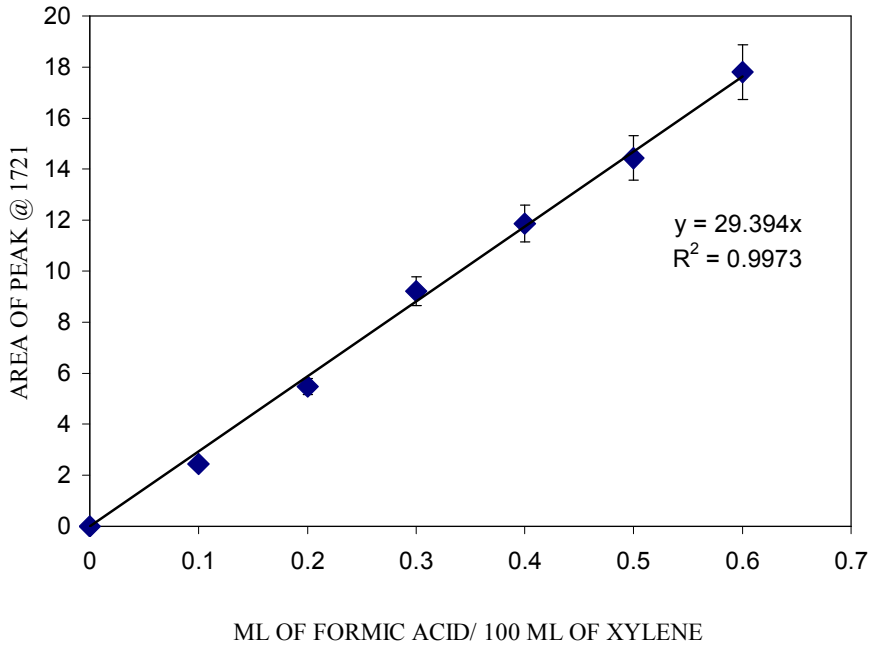

Figure 4.4: Calibration curve for formic acid @r = 6, T=40°C

Figure 4.5: Calibration curve for formic acid @ r=1, 2 & T=30°C, 24°C

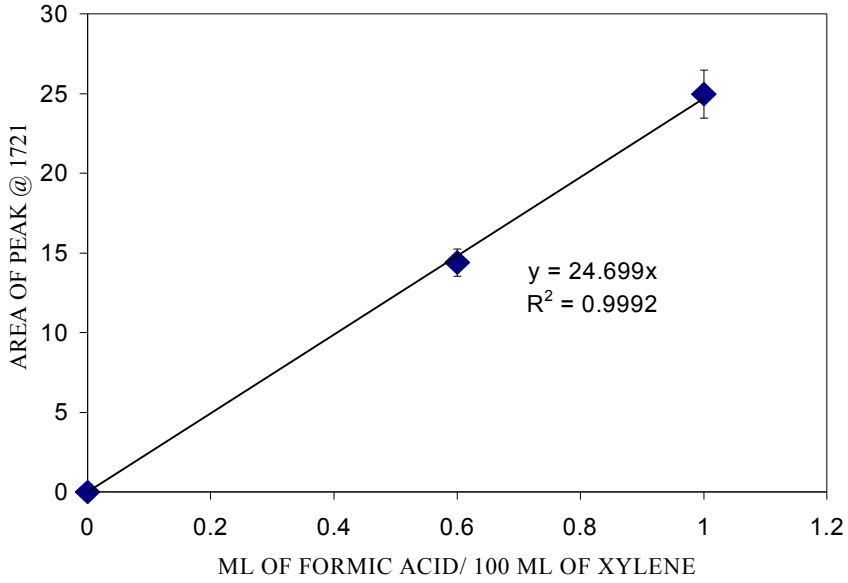

The effect of the molar ratio, r, of formic acid to TEOS was investigated at a reaction temperature of 40°C. Experiments were performed at the following r values: 1, 2, and 6. These spectra are all located in the appendix. Figures 4.6 and 4.7 show the effect of r on the concentration of carbonyl groups, which was determined from the area of the peak at 1721 cm^{-1}, and the concentration of Si-O-C groups, which was measured from the area of the peaks between 1057 cm^{-1} and 1150 cm^{-1}.

These experiments showed that the value of r significantly affected the reaction of TEOS and formic acid. At high r values, it is known that the rates of hydrolysis and condensation are increased. At r = 6 in our experiments, the concentration of the carbonyl groups decreased by 35% over the course of forty minutes. The decrease in the concentration of Si-O-C groups by 20% after 1 minute showed that the Si-O-C group concentration was affected more by the r value than the concentration of the carbonyl groups. The peaks in the region of 1104 $cm^{-1,}$ which were due to the presence of Si-O-C bonds, had disappeared after thirty minutes. The FTIR spectrum obtained at twenty minutes, which is shown in the appendix, indicated a broadening of the peaks in the 1100 cm^{-1} region.

The initial FTIR spectrum and the FTIR spectrum after forty minutes are shown in figures 4.8 and 4.9 for the r = 6 case. In addition to the loss of the characteristic TEOS peaks, the FTIR spectrum for this high r case showed the appearance of a peak at 1187 cm^{-1} after twenty minutes. The absorbance of this peak decreased from 0.134 at twenty minutes to 0.11 after reacting TEOS and formic acid for forty minutes. Consequently, this system displayed rapid gelation in less than 3 hours of reaction time.

At low r values, the initial products expected were mono and di-substitued products. The low r systems were characterized by significantly slower reactions than the r = 6 system. In our analyses, the concentration of carbonyl groups and Si-O-C groups did not vary over time but remained the same over forty minutes (sixty minutes for r = 1) at r values of 1 and 2. There was also no evidence of a peak at 1187 cm^{-1} or any other new peaks. For the r = 2 case, an FTIR spectrum was obtained after twenty-one hours of reaction time at 40°C. Figure 4.10 shows the FTIR spectrum after 1 minute of reaction for this system, and figure 4.11 shows the spectrum after twenty-one hours of reaction for r = 2. The concentration of the carbonyl groups decreased by 11%, and the characteristic TEOS peaks shifted from 1104 and 1084 cm^{-1} to lower wavenumbers of 1092 and 1059 cm^{-1} after twenty-one hours. Furthermore, a peak at

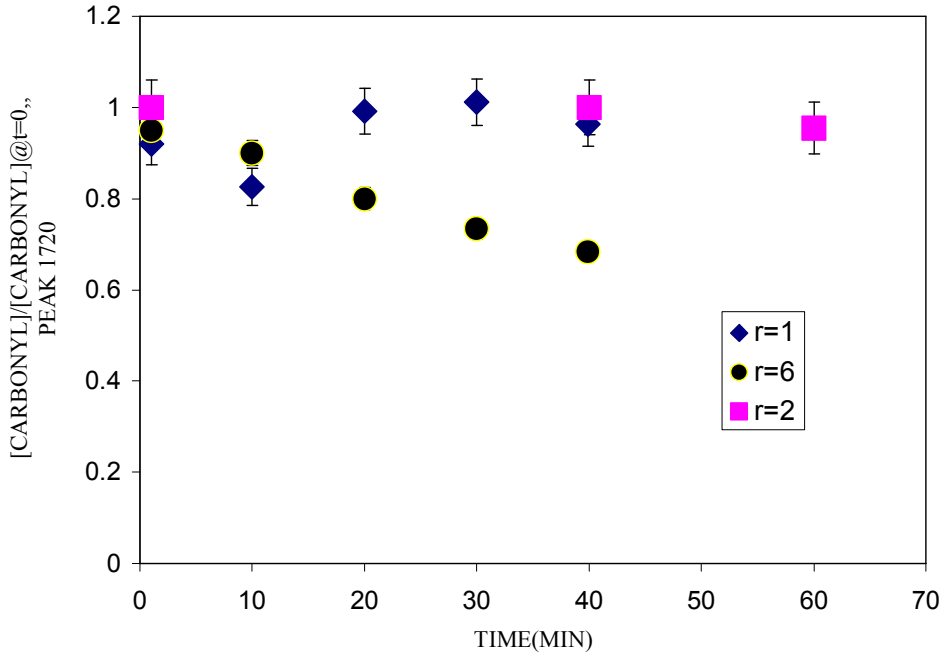

Figure 4.6: The effect of molar ratio of formic acid to TEOS on carbonyl concentration at 40°C

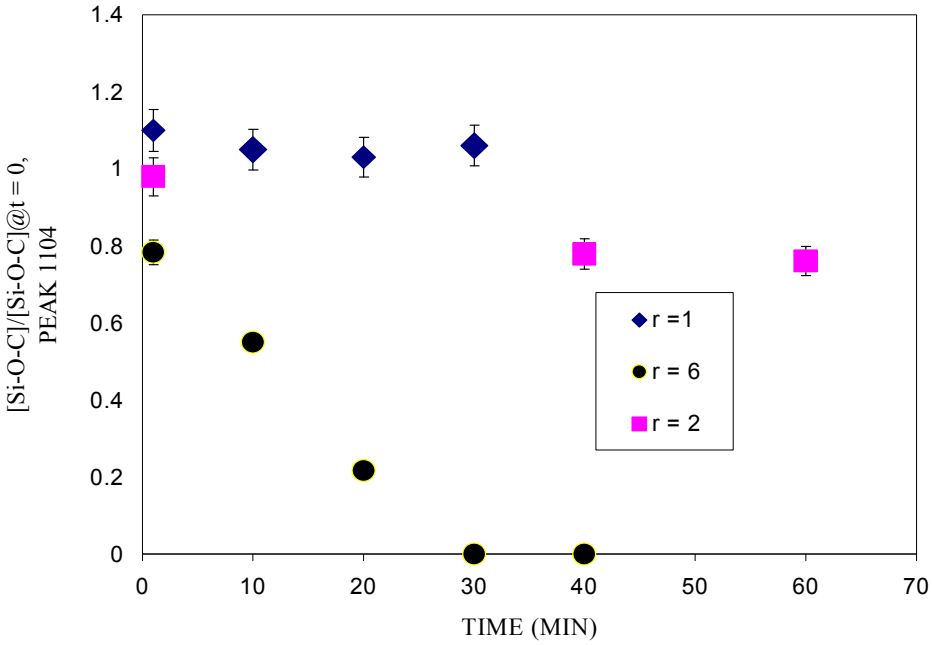

Figure 4.7: The effect of molar ratio of formic acid to TEOS on the concentration of Si-O-C groups at 40°C.

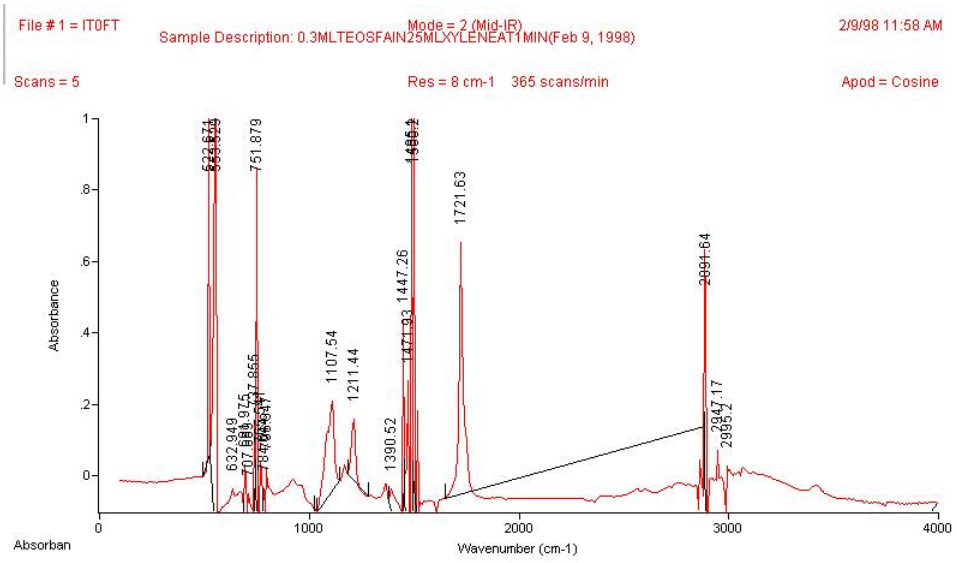

Figure 4.8: FTIR spectrum of r = 6 formic acid to TEOS at 1 minute and 40°C.

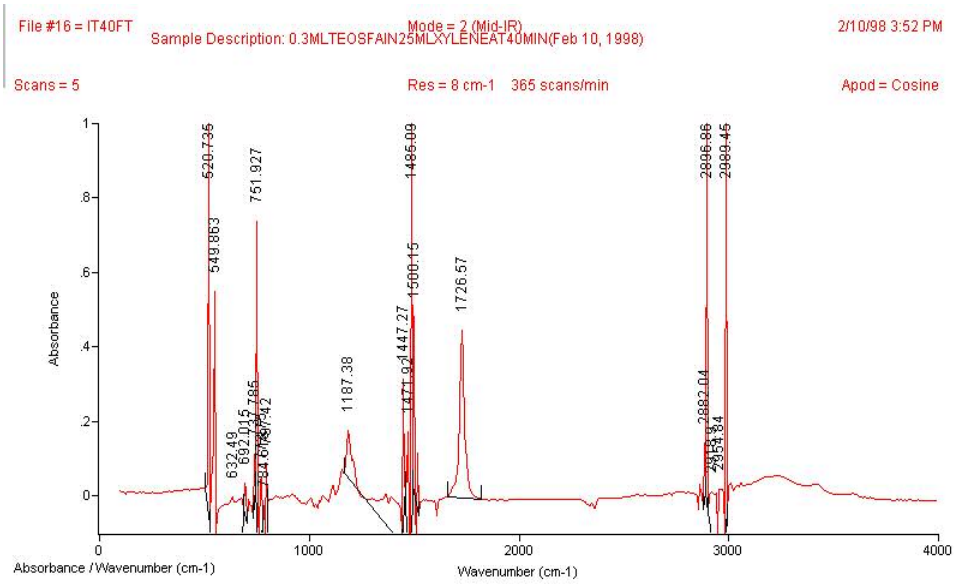

Figure 4.9: FTIR spectrum of r = 6 formic acid to TEOS at 40 minutes and 40°C.

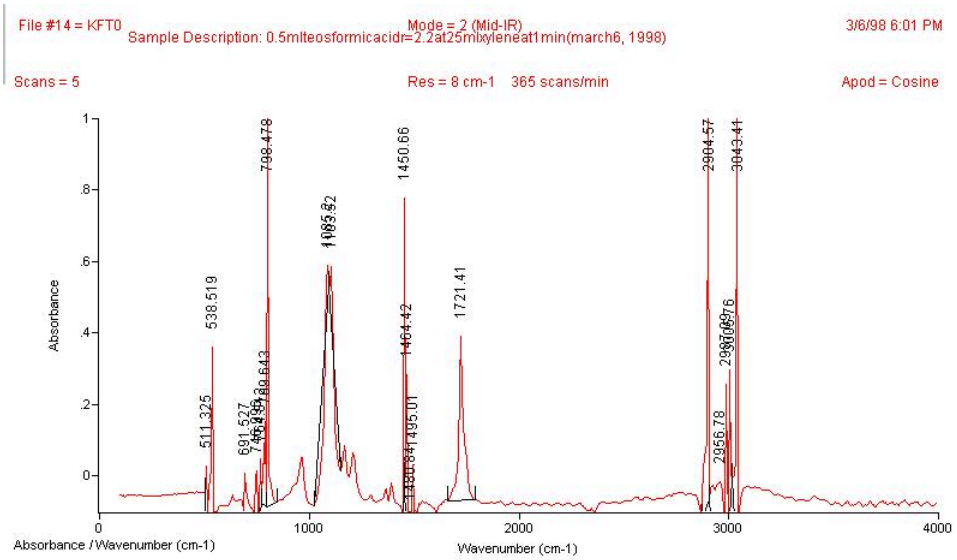

Figure 4.10: FTIR spectrum of r=2 of formic acid to TEOS at 1 minute and 40°C.

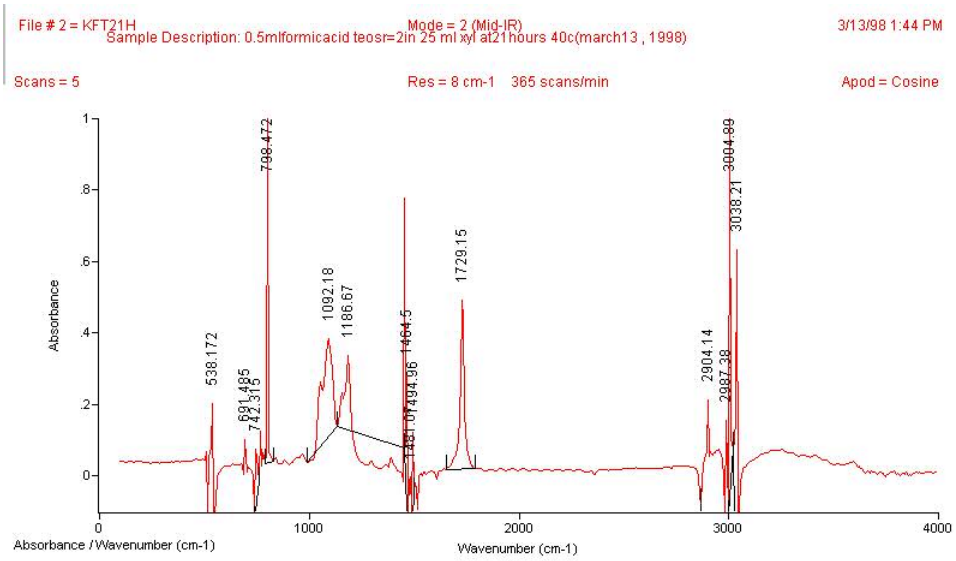

Figure 4.11: FTIR spectrum of r = 2 of formic acid to TEOS at 21 hours and 40°C.

1186 cm^{-1} with an absorbance of 0.31 had appeared. Reactions performed at r = 2 and 40°C for 6 days showed no indication of gelation.

In addition to the study of the effect of the molar ratio of formic acid to TEOS, the consequences of varying the reaction temperature were investigated at molar ratios of formic acid to TEOS of 6. The concentration of carbonyl groups and Si-O-C groups were compared at 24, 30, and 40°C. Figure 4.12 shows that temperature affected the concentration of carbonyl groups. Increasing the temperature led to a decrease in the concentration of carbonyl groups which was measured from the area of the peak at 1720 cm^{-1}. At 24°C, the concentration of carbonyl groups did not change over the course of

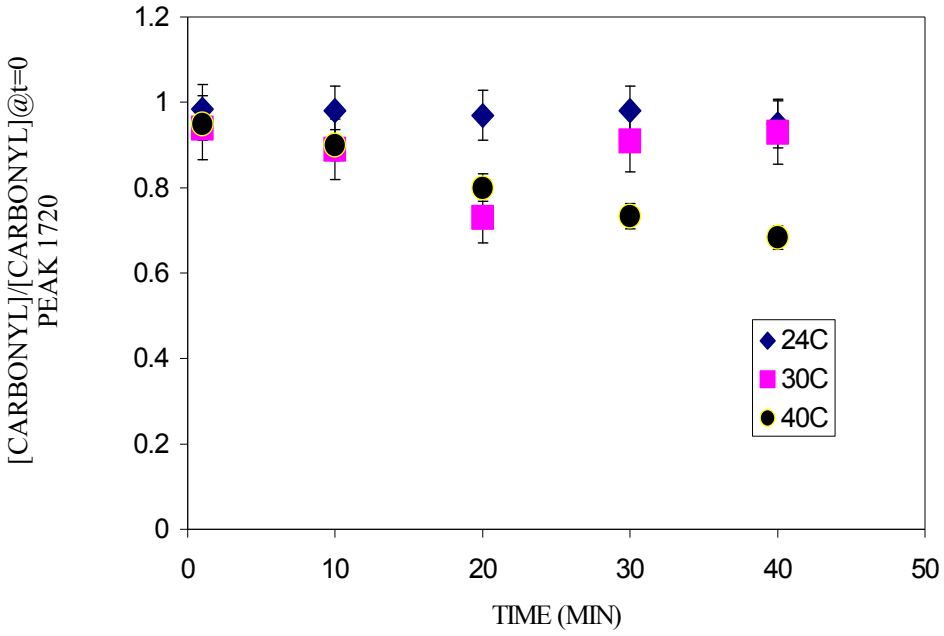

Figure 4.12: The effect of temperature on the concentration of carbonyl groups.

forty minutes. The concentration of carbonyl groups maintained a 5% decrease during forty minutes of reacting at 30°C. Contrary to the reactions performed at 24°C and

30°C, the concentration of carbonyl groups monotonically decreased when the reaction temperature was 40°C. After forty minutes of reacting TEOS and formic acid, the concentration of carbonyl groups decreased by almost 40%.

Figure 4.13 shows that increasing the reaction temperature accelerated the reaction of TEOS and formic acid. Higher reaction temperatures led to a decrease in the concentration of Si-O-C groups which was determined from measuring the area of the peaks between 1057 and 1150 cm^{-1}. Reactions performed at all 3 temperatures resulted in highly linear decreasing concentrations of Si-O-C groups. After 1 minute of reacting

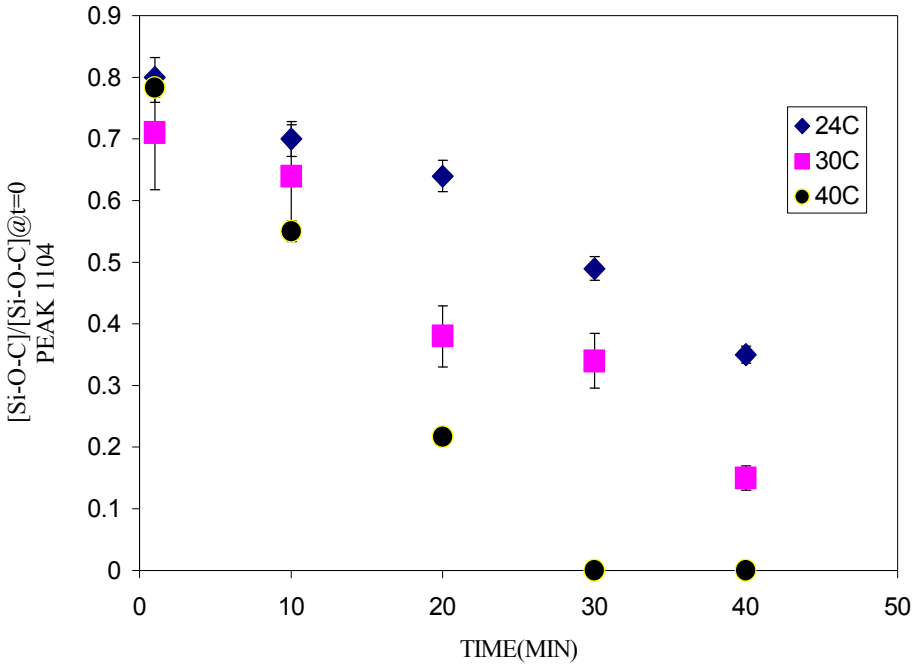

Figure 4.13: The effect of temperature on the concentration of Si-O-C groups.

TEOS and formic acid, the concentration of Si-O-C groups decreased by approximately 20% at 24, 30, and 40°C. The concentration of Si-O-C decreased by only 65% after

forty minutes at 24°C compared with a decrease by 90% for the reactions performed at 30°C. As mentioned previously, the concentration of Si-O-C groups was 0 after thirty minutes at 40°C. Furthermore, these plots indicated that the reaction was zero order in concentration of Si-O-C groups. The data on the change of the Si-O-C concentration was used to obtain the rate constants and activation energy for the r = 6 system. Table 4.2 shows the rate constants for reactions of TEOS and formic acid at 24, 30, and 40°C. Increasing the temperature from 24°c to 30°C resulted in a 30% increase in the rate constant. The reaction rate almost doubled when the temperature was raised from 30°C to 40°C.

Table 4.2: The effect of temperature on the rate constants for formic acid to TEOS molar ratio of 6.

Temperature (°C)	Rate constant (min^{-1})
24	0.0113 ± 0.0002
30	0.0145 ± 0.0005
40	0.0277 ± 0.0021

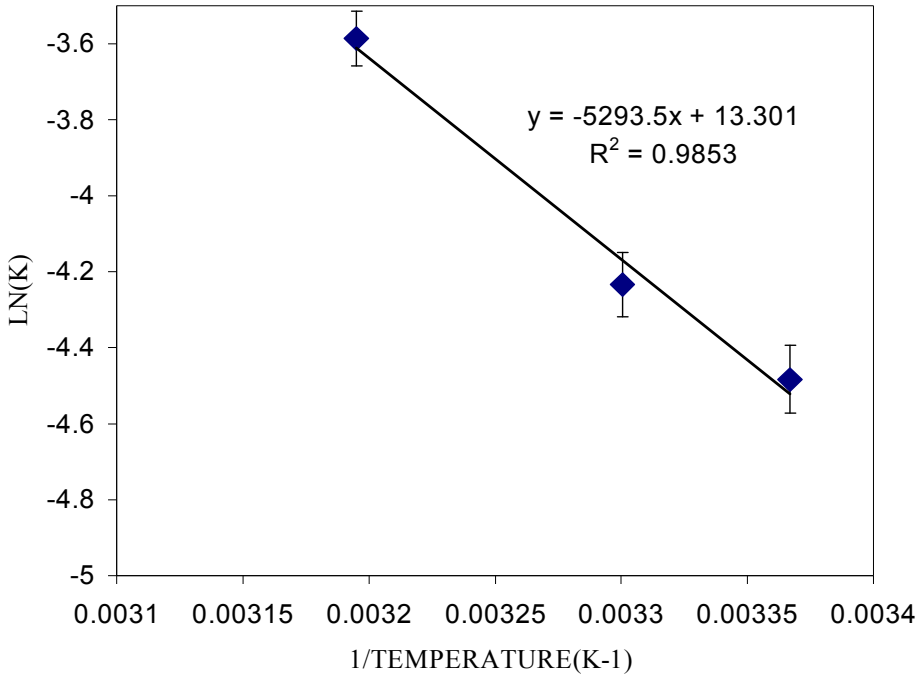

Figure 4.14: Arrhenius plot for the reactions of formic acid and TEOS with r = 6.

These rate constants were used to develop the Arrhenius plots for this system. Figure 4.14 shows that the r = 6 system displayed highly Arrhenius behavior. An activation energy of 10.5 kcal/mole was calculated from the plot of ln k vs 1/T.

FTIR spectra of pure TEOS and pure formic acid established that the peak at 1720 cm^{-1} was due to the vibration of formic acid and the peaks at 1104 and 1084 cm^{-1} represent normal modes of vibration for TEOS. However, FTIR spectroscopy indicated the presence of a new peak in the 1187 cm^{-1} region and the shift of the peaks in the 1104 cm^{-1} region to lower wavenumbers as the TEOS and formic acid reactions

progressed. Those new peaks had to be assigned from either further experiments or from results previously published in the literature.

After examining the types of intermediates and products possible in the reaction of TEOS and formic acid, reported values of the wavenumbers of the available compounds were obtained. Table 4.3 shows the ranges of wavenumbers observed for these compounds which were obtained from Roeges (1994) and Schrader in Ferraro and Krishan (1990).

Table 4.3: Typical vibrational frequencies for groups in the TEOS/formic acid system.

Vibration	Frequency range (cm^{-1})
C-O-C	1150-1060
Si-O-Si	1110-1000
Si-OH	3675
HCO_2R where R is ethyl group	~1189

These frequency ranges show that carbon and silicon vibrate similarly, and the peak that appeared at 1187 was consistent with the formation of ethyl formate, $HCO_2C_2H_5$, which is a possible intermediate in the TEOS and formic acid system. Ethyl formate can be formed by the reaction of formic acid with ethanol. Therefore, FTIR spectra were obtained for the reaction of formic acid and ethanol.

Figure 4.15 shows the spectrum for the reaction of formic acid and ethanol after twenty minutes at 40°C, and figure 4.16 shows the FTIR spectrum for pure ethanol.

These spectra showed two important things. First of all, the disappearance of the peak at 1049 cm^{-1} and the appearance of the peak at 1187 cm^{-1} indicated that formic acid and ethanol did react. Secondly, this suggested that the peak observed in the reaction of TEOS and formic acid at 1186 cm^{-1} was a result of the formation of ethyl formate. The

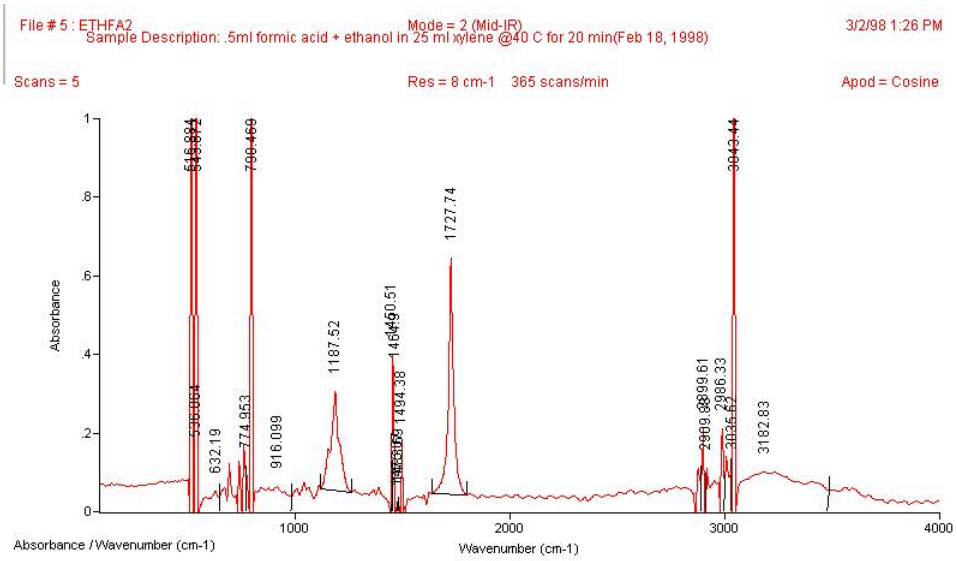

Figure 4.15: FTIR spectrum of the reaction of formic acid and ethanol at 40°C for twenty minutes.

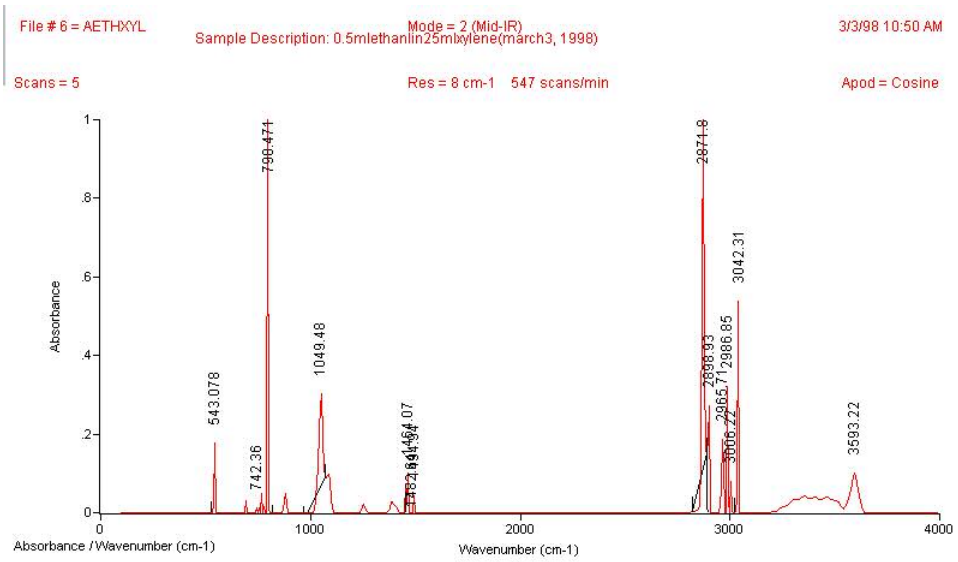

Figure 4.16: FTIR spectrum of pure ethanol.

peaks which formed from the apparent shift of the characteristic TEOS peaks to 1092 and 1059 cm^{-1} were either due to the normal vibrations of Si-O-C or Si-O-Si bonds which occur in the same region of the infrared spectrum. Based on the disappearance of these peaks seen in the r = 6 reactions at 40°C after thirty minutes, these peaks were assigned to Si-O-C vibrations of compounds other than TEOS.

FTIR spectra were obtained for various concentrations of SiO_2 particles in ethanol in order to determine if the concentration of Si-O-Si bonds was large enough to be seen in the FTIR spectra of TEOS and formic acid. The concentration of silica can be seen as the maximum possible concentration of Si-O-Si bonds. The maximum possible concentration of silica was 0.5% by weight for the reaction with r = 1, and the r = 2 and r = 6 resulted in a smaller maximum silica concentration. Figure 4.17 shows the FTIR spectrum for 0.46% by weight silica in ethanol. The silica peak is the broad peak found at 1120 cm^{-1}. This spectrum indicated that the concentration of Si-O-Si groups was too small to be seen in the FTIR spectra for the 3 cases when r was 1, 2 and 6.

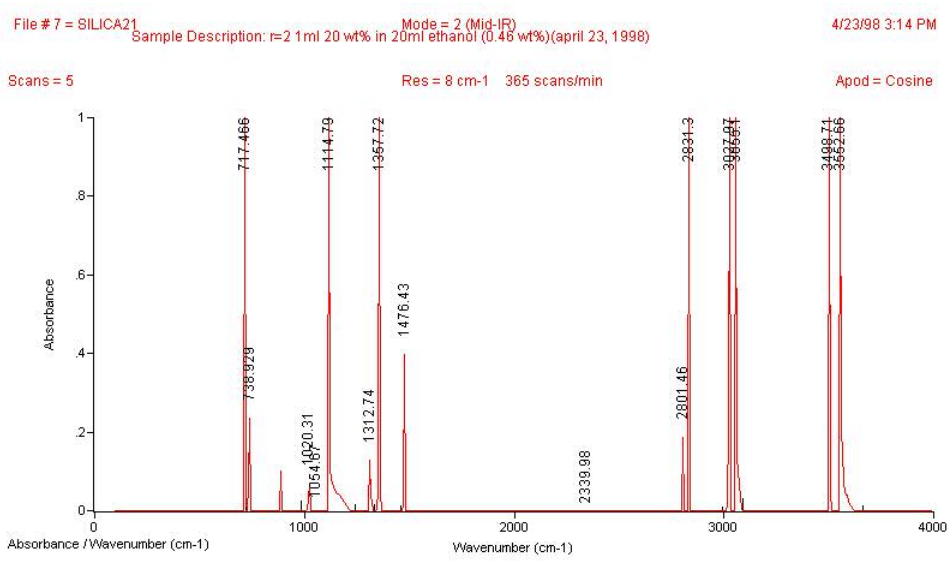

Figure 4.17: FTIR spectrum of 0.46% by weight silica in ethanol.

FTIR spectroscopy was shown to be effective and accurate in monitoring the reaction progress of the TEOS and formic acid system. The FTIR spectroscopy analyses showed differences in the spectra for different molar ratios and reaction temperatures. The systems were characterized by the decrease in the concentration of Si-O-C groups and by the appearance of a peak at 1186 cm^{-1}. The low r systems, which did not lead to gelation within 6 days, also did not show a significant decrease in the Si-O-C peaks or the appearance of a peak at 1186 cm^{-1} within sixty minutes. However, the r = 6 system gelled within 3 hours and showed no evidence of any peaks as a result of Si-O-C vibrations after thirty minutes, and did have a peak at 1186 cm^{-1}.

The peak at 1186 cm^{-1}, which is due to ethyl formate, was an indicator that the following reactions had occurred:

$$SiOR + HCOOH \Leftrightarrow SiOOCH + C_2H_5OH \quad (5.1)$$

$$SiOOCH + C_2H_5OH \Leftrightarrow C_2H_5OOCH + SiOH \quad (5.2)$$

$$HCOOH + C_2H_5OH \Leftrightarrow C_2H_5OOCH + H_2O \quad (5.3)$$

$$SiOOCH + H_2O \Leftrightarrow SiOH + HCOOH \quad (5.4)$$

For the r = 2 system, which showed an ethyl formate peak at twenty-one hours, equation 5.2 represents the most probable mode of forming ethyl formate. However, FTIR analyses do not conclusive eliminate the possibility of ethyl formate being formed

by both methods expressed in equations 5.2 and 5.3 for the r = 6 system which had a molar excess of formic acid. The presence of water in the sol-gel reactions must be determined to definitively determine the origin of ethyl formate.

The determination of an activation energy of 10.5 kcal/mole for the r = 6 system using the FTIR data for the concentration of Si-O-C groups was also very important. This compared with the results of Sharp (1994) who used gel time to calculate the activation energy. Therefore, this showed that the concentrations obtained by integrating the area of the Si-O-C region were accurate and could be used instead of gel time to obtain the activation energy.

Using the concentration of Si-O-C groups to determine activation energy is more accurate than using the gel time which has been commonly employed to characterize the kinetics of sol-gel systems. The gel time may be controlled by the kinetics of the system or the diffusion rate in the system. For very fast reactions with low activation energies, the gelation time is determined by the rate of diffusion. Usually activation energies less than 5 fall in to the previous category. The gelation time is determined by the rate of reaction for slower reacting systems with activation energies greater than 5. The reactions were controlled by the kinetics of the system for the r = 6 system, and diffusion limitations did not affect the kinetics. At larger molar ratios of formic acid to TEOS, determining the activation energy from the gel time may not give the correct results. Using the concentration of Si-O-C groups is accurate for both diffusion controlled and kinetic controlled systems. In addition to being more accurate, using the concentration of Si-O-C groups to determine activation energy is much faster.

4.2 ^{29}Si NMR Spectroscopy

After examining the effects of molar ratio and temperature on the reactions of formic acid and TEOS, ^{29}Si NMR was performed on the reaction of formic acid and TEOS. The chemical shifts were obtained relative to tetramethyl silane. Figure 4.18 shows the NMR spectrum for pure TEOS. The peak for TEOS appeared at –81.5 ppm. Formic acid and TEOS at a molar ratio of 2 were reacted for two days, and NMR spectroscopy was used to monitor the development of products. The temperature of the reaction was not controlled; however, previous studies suggest that the maximum temperature rise possible was 40°C for this exothermic reaction.

Figure 4.19 shows a stack plot of the NMR spectra for the reactions of TEOS and formic acid. The individual spectra are displayed in the appendix. The first spectrum was obtained approximately after thirty minutes of reaction, and there was a major peak at –81.6 ppm with small peaks downfield and upfield from this peak. The peak at –81.6 ppm, which represented the resonance of TEOS, showed slight increases and decreases during the reaction. This stack plot also illustrates the appearance of different compounds upfield from TEOS. The mole percent of total soluble Si as a function of time is shown in figure 4.20. As the reaction progressed, the peak at -81.65 ppm decreased while the peaks upfield increased in size and number. After sixteen hours of reaction, the peaks at –88.6 and –96.2 ppm were larger than the initial major peak, -81.6 ppm. The peak at –96.2 ppm continued to increase with time and accounted for sixty mole percent of the sol after forty-two hours. However, the peak at –88.6 ppm

reached a maximum value of 25 mole percent after eighteen hours and began to decrease.

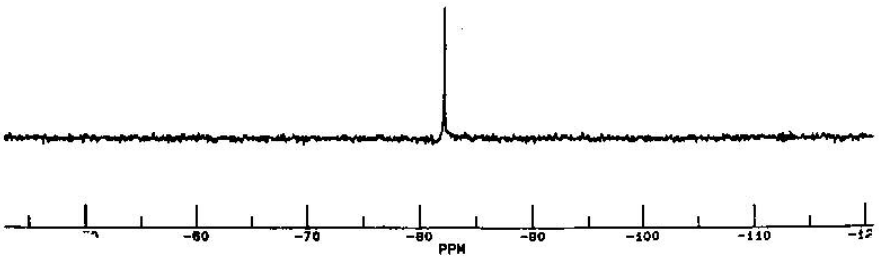

Figure 4.18: NMR spectrum of pure TEOS relative to tetramethyl silane.

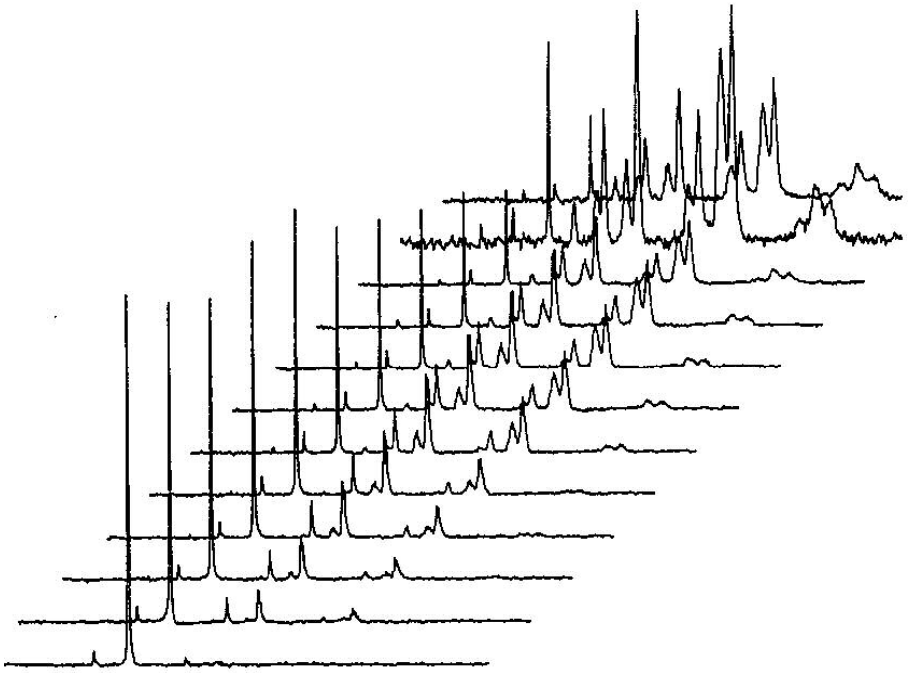

Figure 4.19: Stack plots of the NMR spectra for r = 2 formic acid to TEOS reactions over 43 hours.

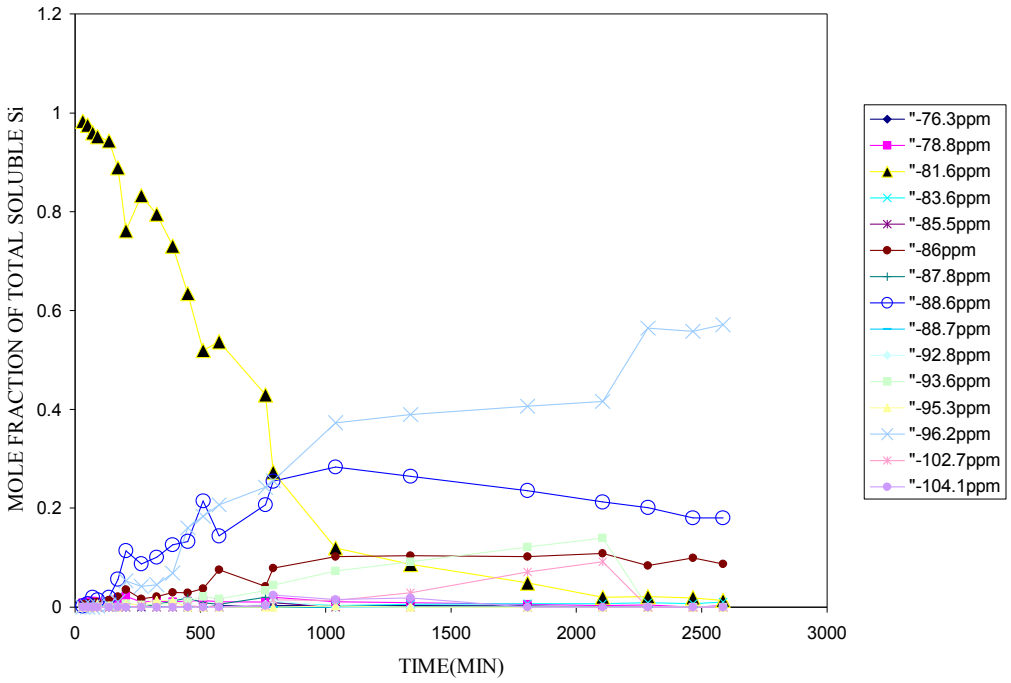

Figure 4.20: The mole fraction of total soluble Si as a function of time for an r = 2 molar ratio of formic acid to TEOS obtained from ^{29}Si NMR spectroscopy.

After examining the effects of molar ratio and temperature on the reactions of formic acid and TEOS, ^{29}Si NMR was performed on the reaction of formic acid and TEOS to provide more specific information. Assignments for the chemical shifts of the TEOS and formic acid system were made based on the reports by Lin and Basil (eds. Brinker, et al., 1984), Coltrain et al. (1994), Pouxviel et al. (1987), and McFarlane (1972), and the order of appearance of the peaks was used to identify the species.

Table 4.4 shows these assignments, and figure 8 displays the temporal evolution of these species.

Table 4.4: Chemical shifts for the NMR spectra of TEOS and formic acid reactions at r = 2.

Compound	Chemical shift (relative to tetramethylsilane)
$Si(OH)_2(OEt)_2$	-76.3
$Si(OH)(OEt)_3$	-78.8
TEOS	-81.5
$SiOSi(OH)_2(OEt)_1$	-83.6
$Si(OH)_x(OEt)_y(HC{=}OO)_z(OSi)_\alpha$	-85.3
$Si(OEt)_3(O_2CH)$	-86.06
$Si(OEt)_2(O_2CH)_2$	-87.8
Q_1: $SiOSi(OEt)_3$	-88.7
Q_2: cyclic $(SiO)_2$ $Si(OH)_1(OEt)_1$	-92.8
Q_2: linear $(SiO)_2$ $Si(OH)_1(OEt)_1$	-93.6
Q_2: cyclic $(SiO)_2$ $Si(OEt)_2$	-95.3
Q_2: linear $(SiO)_2$ $Si(OEt)_2$	-96.2
Q_3: $(SiO)_3Si(OEt)$	-102.7
Q_3: $(SiO)_3Si(OEt)$	-104.1

Figure 4.20 illustrates the exponential decrease in the TEOS peak at -81.65 ppm and the increase in the size and number of peaks upfield as the reaction progressed. The first identifiable species were the first hydrolysis product, $Si(OH)(OEt)_3$, and the carboxylation product, $Si(OEt)_3(O_2CH)$. Subsequently, the dimer, $SiOSi(OEt)_6$, was observed after 50 minutes into the reaction. Linear and then cyclic Q_2 species appeared with formate and ethoxy groups attached as the reaction progressed. The occurrence of linear Q_2 species prior to cyclic Q_2 species implied that the reactions were kinetically controlled rather than thermodynamically controlled. The second hydrolysis product, $Si(OH)_2(OEt)_2$, was detectable after eight hours. The appearance of this hydrolysis

product coincided with the appearance of the second observed dimer, $SiOSi(OH)_2(OEt)_1$. After sixteen hours of reaction, the peaks at –88.6 ($SiOSi(OEt)_3$) and –96.2 ppm (linear $(SiO)_2\ Si(OEt)_2$) were larger than the TEOS peak, -81.6 ppm . The peak at –96.2 ppm continued to increase with time and accounted for sixty mole percent of the soluble silicon species after forty-two hours. However, the peak at –88.6 ppm reached a maximum value of 25 mole percent after eighteen hours and began to decrease. Using the NMR and FTIR spectra, the following reaction scheme was proposed for the

r = 2 system:

$$SiOR + HCOOH \Leftrightarrow SiOOCH + C_2H_5OH \quad (4.1)$$

$$SiOOCH + C_2H_5OH \Leftrightarrow C_2H_5OOCH + SiOH \quad (4.2)$$

$$SiOOCH + HCOOH \Leftrightarrow Si(OOCH)_2 + C_2H_5OH \quad (4.3)$$

$$SiOOCH + Si(OR) \Leftrightarrow Q_1 \quad (4.4)$$

$$Q_1 + Si(OR) \Leftrightarrow Q_2 \Leftrightarrow Q_3 \quad (4.5)$$

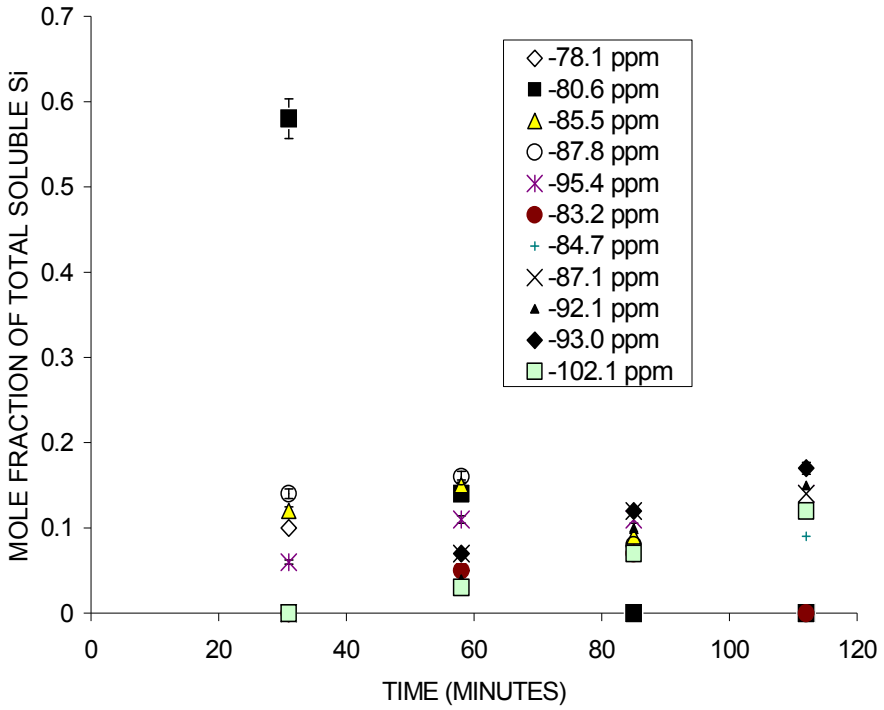

Figure 4.21 : Time evolution of species identified by ^{29}Si NMR for r = 6 formic acid to TEOS reaction.

^{29}Si NMR was also used to investigate the reactions at r=1 and r=6 molar ratios of formic acid to TEOS. NMR scans for the r=1 ratio of formic acid to TEOS showed that the reaction progression was significantly slower than r=2 system. After 12 hours, small peaks were observed at –78.2, -85.4, -87.9, and –95.3 ppm. These peaks are indicative of the presence of the following species: $Si(OH)(OEt)_3$, $Si(OEt)_3(O_2CH)$, $SiOSi(OEt)_3$, and linear $(SiO)_2$ $Si(OEt)_2$. After 36 hours of reacting, the concentration of singly hydrolyzed monomer decreased while the other peaks exhibited a slight increase.

A new peak appeared which indicated that cyclic $(SiO)_2$ $Si(OEt)_2$ was formed as the reaction progressed.

The rapidness of the r=6 reaction was illustrated in the ^{29}Si NMR spectra. After 31 minutes, peaks were already present at –78.1, -80.6, -85.5, -87.8, and –95.4 ppm. These chemical shifts correspond to Q_0, Q_1, Q_2, and Q_3 species. Q_4 species were not identified in silica NMR for any of the TEOS/formic acid reactions. Figure 4.21 displays the time evolution of species development during the r = 6 formic acid to TEOS reaction. Initially, the presence of the –80.6 ppm peak, which was the major peak after 31 minutes, was puzzling. This peak was attributed to TEOS after confirming the shift of TEOS to higher chemical shifts as the concentration of formic acid was increased. For the r=1 formic acid to TEOS reaction, the TEOS peak occurred at –81.7 ppm. The TEOS peak shifted to –81.4 ppm and –80.9 ppm for successive r=3 and r=6 formic acid to TEOS ratios. Similarly, all the peaks for the r = 6 reaction exhibited slightly higher chemical shifts than the r = 2 case.

TEOS displayed a rapid exponential decay, and had decreased to a concentration below detectable limits after 53 minutes of reacting. With one exception, the same peaks were observed for the r = 2 and r = 6 cases. For the rapid r = 6 reaction the second hydrolysis product, $Si(OH)_2(OEt)_2$, was not identifiable in the NMR spectra. One possibility for the absence of this product was that there was a different activation energy for this species at the higher molar ratio of formic acid. Alternatively, the reaction pathways may have been different as the molar ratio of formic acid to TEOS was increased. Table 4.5 shows the peak assignments for the r = 6 case which are the

same as those previously reported for the r = 2 reaction. The same reaction scheme previously reported for the r = 2 system appeared valid for the r = 6 reaction.

Table 4.5: Chemical shifts for the NMR spectra of TEOS and formic acid reactions at r = 6.

Compound	Chemical shift (relative to tetramethylsilane)
$Si(OH)(OEt)_3$	-78.1
$Si(OEt)_4$	-80.6
$SiOSi(OH)_2(OEt)_1$	-83.2
$Si(OH)_x(OEt)_y(HC{=}OO)_z(OSi)_\alpha$	-84.7
$Si(OEt)_3(O_2CH)$	-85.5
$Si(OEt)_2(O_2CH)_2$	-87.1
Q_1: $SiOSi(OEt)_3$	-87.8
Q_2: cyclic $(SiO)_2$ $Si(OH)_1(OEt)_1$	-92.1
Q_2: linear $(SiO)_2$ $Si(OH)_1(OEt)_1$	-93.0
Q_2: cyclic $(SiO)_2$ $Si(OEt)_2$	-94.7
Q_2: linear $(SiO)_2$ $Si(OEt)_2$	-95.4
Q_3: $(SiO)_3Si(OEt)$	-102.7

The extent of reaction, R, is defined by equation 4.6. Figures 4.22 and 4.23 display the extent of reaction calculated from ^{29}Si NMR for the r = 2 and r = 6 reactions of formic acid to TEOS.

$$R = \frac{Q_1 + 2Q_2 + 3Q_3 + 4Q_4}{4} \tag{4.6}$$

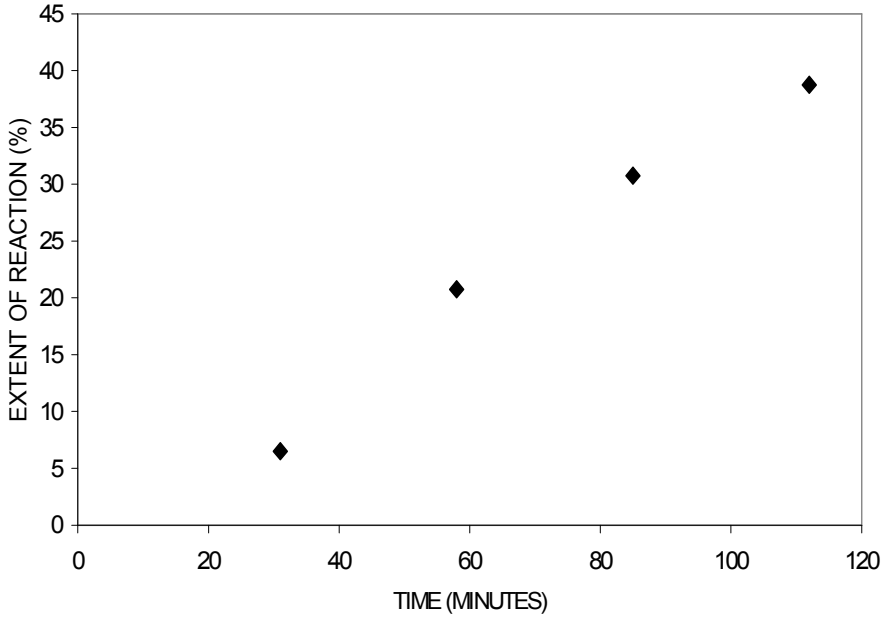

Figure 4.22 : The extent of reaction for the r = 6 formic acid to TEOS reaction measured from ^{29}Si NMR experiments.

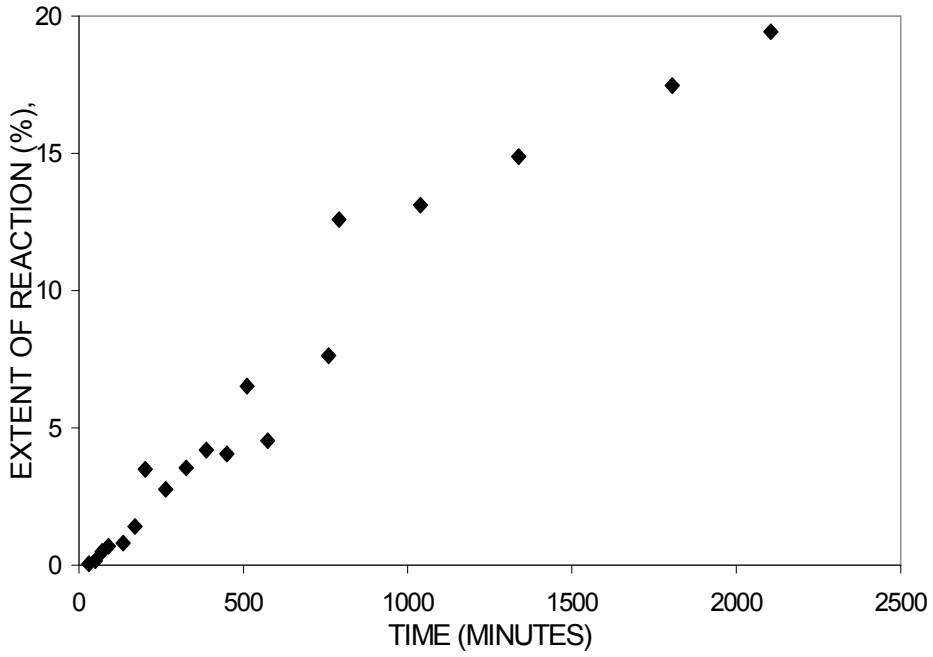

Figure 4.23 : Extent of reaction for r = 2 formic acid to TEOS reaction measured from the ^{29}Si NMR experiment.

The extent of reaction was significantly increased by raising the molar ratio of formic acid to TEOS. Figure 4.22 illustrates how rapid the r = 6 reaction progressed. After just 31 minutes of reacting, the extent of reaction had already reached 5%. The extent of reaction continued to increase in nearly a linear fashion. The NMR spectrum taken at 112 minutes indicated that the extent of reaction had increased to 35%. The r

= 2 system never reached extents of reaction as high as 35% even after 35 hours. In contrast to the r = 6 system, approximately 500 minutes were required to reach a 5% extent of reaction. The extent of reaction slowly increased with time reaching a maximum value of 20% after 35 hours. Because only the soluble silica species are measured in our NMR experiments, this extent of reaction does not account for insoluble species. The extent of reaction for the later stages of the r = 6 reactions may actually be larger.

The fraction of cyclics and linear silica compounds were determined from the Si NMR data. Figures 4.24 and 4.25 contain the percentages of cyclic dimers for the formic acid / TEOS reactions at r = 2 and r = 6.

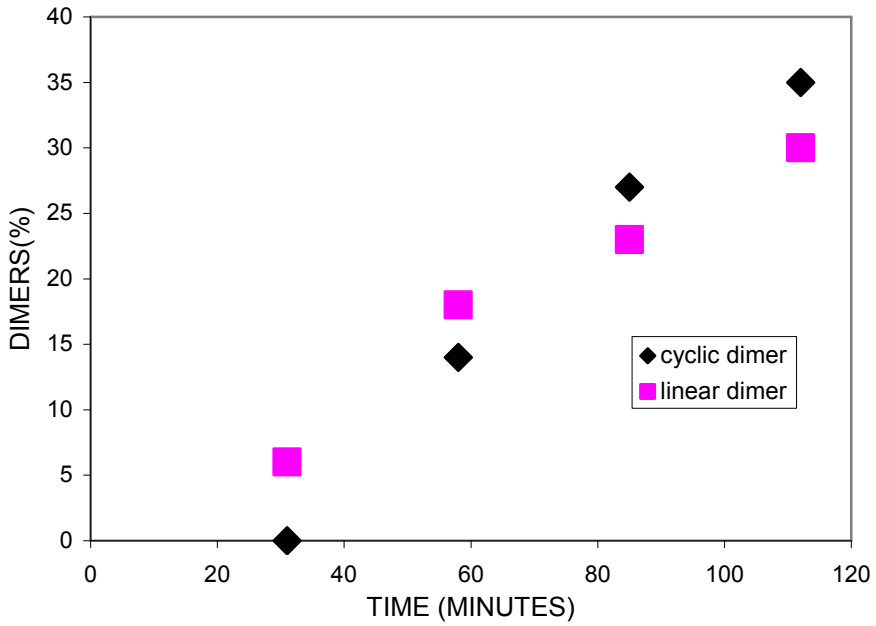

Figure 4.24: The distribution of cyclic and linear dimers in the reaction of TEOS with formic acid at r = 6.

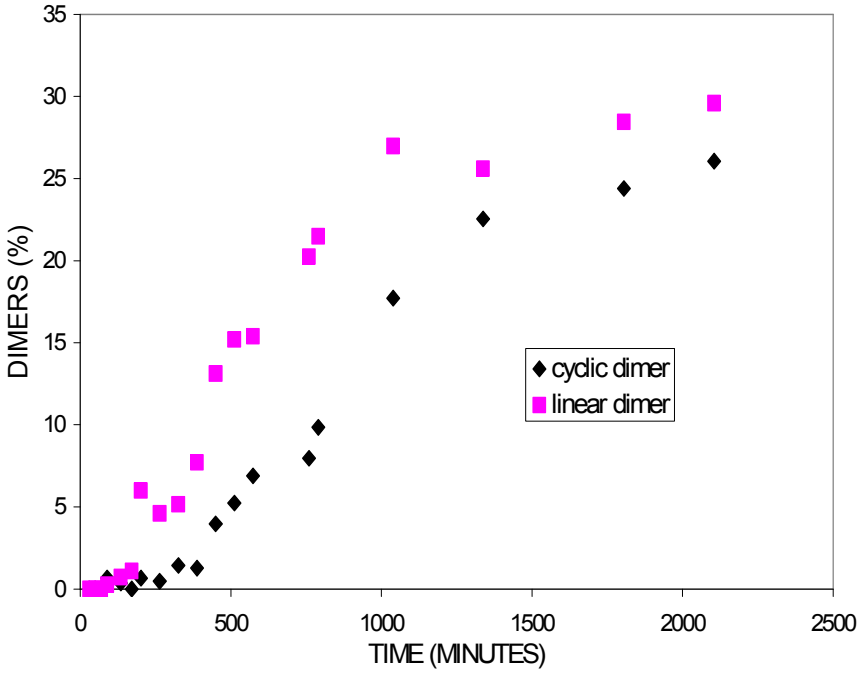

Figure 4.25: The evolution of cyclic and linear dimers in the r = 2 reaction of formic acid with TEOS.

The rapidness of the r = 6 reaction was further demonstrated by the percentages of dimers. Initially, linear dimers appeared first in the NMR spectra for the r = 2 and r = 6 reactions. However, the cyclic dimers became the primary dimers as the reaction of formic acid with TEOS at r = 6 progressed. The majority of dimers were linear throughout the entire r = 2 reaction. This may have not been the case if the reaction had been allowed to progress for a longer period of time. For the r = 6 reaction of formic acid with TEOS, the cyclic dimers and linear dimers represented 35% and 30% of the soluble silica species after 112 minutes. The significantly slower r = 2 reaction only contained 30% linear dimers and 25% cyclic dimers after 35 hours of reacting. Initially,

linear dimers appeared first in the NMR spectra for the r = 2 and r = 6 reactions. The differences in the shapes of the curves for the distribution of dimers in the r = 2 and r = 6 reactions of formic acid with TEOS is of interest. The lower activation energy r = 6 reaction shows an almost linear increase in the dimer concentrations while the dimer concentrations in the r = 2 system are nearly exponential. This same trend is illustrated with the extent of reaction in previous figures.

Silica NMR was also performed for the formic acid/TEOS system at various temperatures. The r = 6 formic acid/TEOS system was reacted at 10°C, 0°C, and -10°C with the desire of obtaining the activation energy. These reactions were also designed to decrease the rate of reaction to allow further introspection of the sol-gel kinetics. The entire collection of spectra is contained in the appendix. The following figures show the effect of reaction temperature on the major products and reactions (TEOS, $Si(OEt)_3(O_2CH)$, $SiOSi(OEt)_3$):

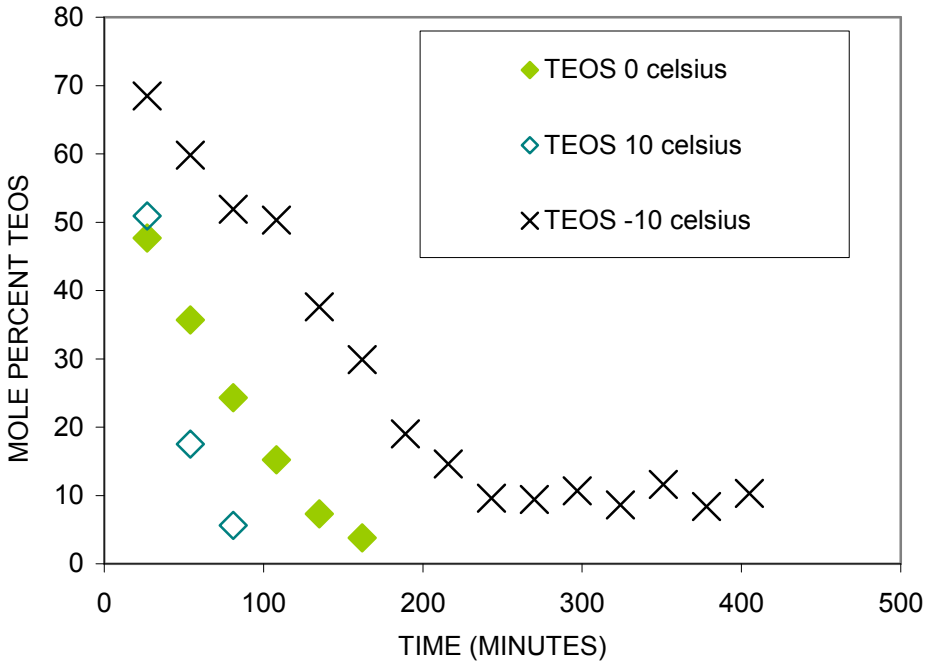

Figure 4.26: The effect of temperature on the consumption of TEOS in the reaction of formic acid with TEOS at r = 6 obtained from ^{29}Si NMR results.

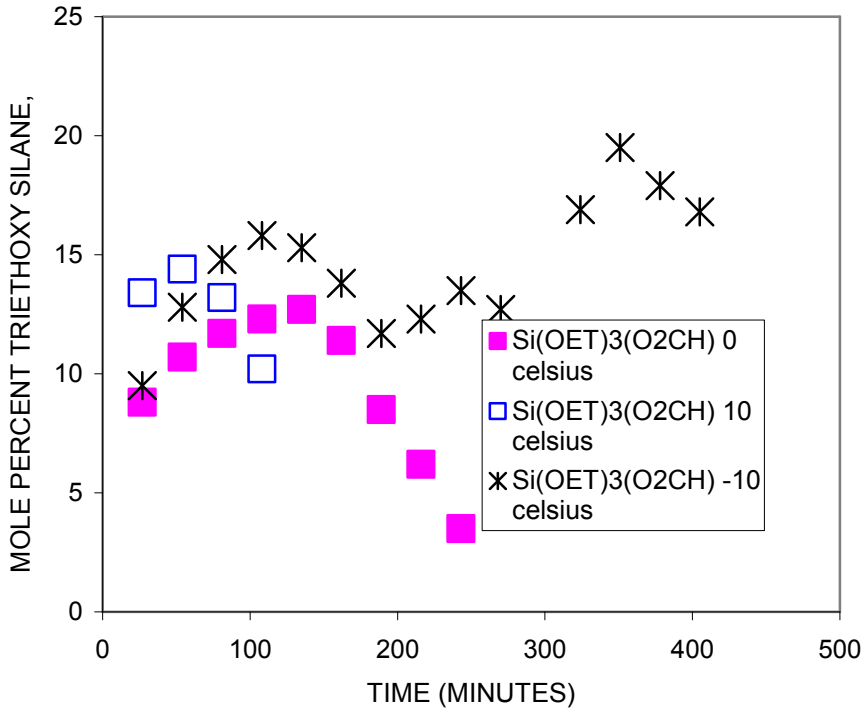

Figure 4.27: The effect of temperature on the triethoxyformyl silane product in the reaction of formic acid/TEOS at r = 6 obtained from ^{29}Si NMR results.

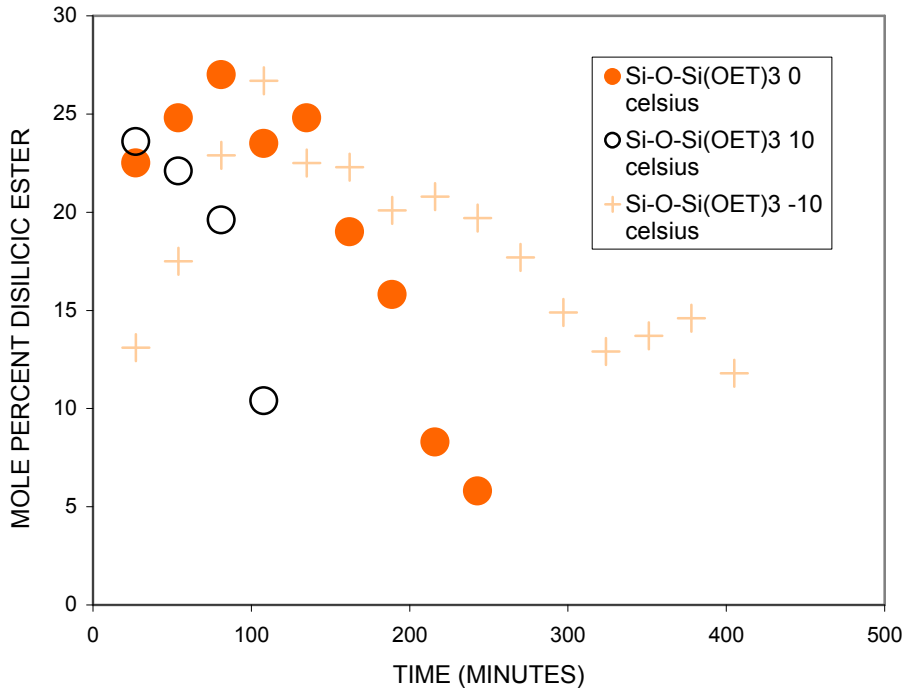

Figure 4.28: The effect of temperature on disilicic ester in the reaction of formic acid/TEOS at r = 6.

The rapid exponential decay of TEOS with increasing temperature was illustrated from ^{29}Si NMR. The effect of temperature on the extent of reaction of the TEOS/ formic acid (r = 6) system was clearly evident after 27 minutes of reaction.

TEOS represented 50% of the total soluble silica for 0° and 10°C while the significant slower -10°C reaction contained 70% TEOS after the same 27 minutes. The TEOS peak was undetectable after 162 minutes at 0°C and 81 minutes at 10°C. On the contrary, the TEOS concentration never decreased below 10% for the -10°C reaction. This appeared to be a steady state concentration because between 243 and 405 minutes the mole percent of TEOS remained constant at 10%.

The triethoxyformyl silane concentration clearly was dependent on the reaction temperature. The first data collected after 27 minutes showed that for the reactions at 10°C, 0°C, and -10°C the respective mole percent of this species were 15%, 10%, and 10%. Decreasing the reaction temperature led to an increase in the maximum triethoxyformyl silane mole percent. For reaction temperatures of 10°C and 0°C, this compound did not account for more than 15% during the reaction. The maximum mole percent of triethoxyformyl silane was obtained after 54 minutes for the 10°C reaction, and after 162 minutes at the 0°C reaction temperature. However, the mole percent for triethoxyformyl silane reached 20% after 378 minutes. This compound was undetectable after 135 minutes at a reaction temperature of 10°C, and following the NMR scan after 270 minutes at 0°C this triethoxyformyl silane was undetectable. Unlike the TEOS mole percent which remained constant at -10°C, the mole percent of triethoxyformyl silane increased over this same period.

Figure 4.28 displays the temperature effect on the primary dimmer, disilicic ester. Similar to TEOS and triethoxyformyl silane, increasing the temperature led to decreasing amounts of disilicic ester. After 27 minutes of reaction, this species represented 22% of the total silica at reaction temperatures of 10°C and 0°, this species

only accounted for 13% during the same period when the TEOS/ formic acid reaction was carried out at -10°C. The mole percent of disilic ester continuously decreased during the 10°C reaction, and was undetectable after 108 minutes. This dimer displayed a maximum mole percent of 27% after 81 minutes at 0°C, and subsequently decreased to undetectable amounts after 270 minutes. The reaction performed at a reaction temperature of -10°C resulted in a maximum of 27% after a longer duration of 108 minutes. Dissimilar to TEOS and triethoxyformyl silane, disilic ester mole percent decreased from 20% to 12% between 243 minutes of reaction and 432 minutes of reaction.

The exponential decay of TEOS which was illustrated in figure 4.26 was implemented to determine the rate constants for the reaction of TEOS and formic acid at a molar ratio of 6. Table 4.6 depicts the rate constants determined at –10, 0, and 10°C. These rate constants were used to calculate the activation energy for this system. An activation energy of 10.5 ± 0.735 kcal/mole was determined from ^{29}Si NMR as shown in figure 4.29 , and this was identical to the activation energy determined from FTIR analyses.

Table 4.6 : Rate constants for the reaction of formic acid to TEOS (r = 6) determined using ^{29}Si NMR

Temperature (°C)	Rate constant (min^{-1})
-10	0.0082 ± 0.0006
0	0.0192 ± 0.0006
10	0.0339 ± 0.002

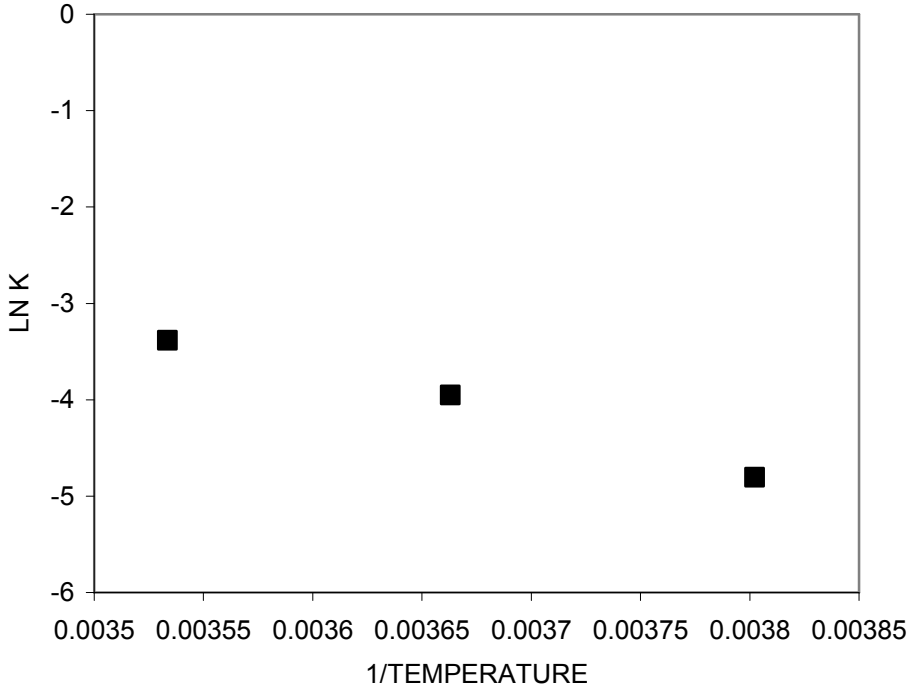

Figure 4.29: Arrhenius plot for the r = 6 reaction of formic acid to TEOS determined from ^{29}Si NMR.

Although FTIR spectra were able to determine some aspects of the formic acid/TEOS reactions, there were limitations on the ability to discern the chemical structures of the products. FTIR spectra confirmed the appearance of ethyl formate and the disappearance of Si-O-C groups. Therefore, ^{29}Si NMR was used on the r = 1, 2 and 6 systems to help determine the chemical compounds present.

^{29}Si NMR spectra for the TEOS/formic acid system provided more specific information than the FTIR spectra. Whereas the FTIR spectrum at twenty-one hours for the r =2 system only showed a slight decrease in the concentration of the carbonyl peak and shifts in the TEOS peaks, the NMR spectra showed the presence of hydrolysis products, monomers, dimers, trimers, and tetramers.

Using the NMR and FTIR spectra, the following reaction scheme was proposed for the r = 2 system:

$$SiOR + HCOOH \Leftrightarrow SiOOCH + C_2H_5OH \quad (5.5)$$

$$SiOOCH + C_2H_5OH \Leftrightarrow C_2H_5OOCH + SiOH \quad (5.6)$$

$$SiOOCH + HCOOH \Leftrightarrow Si(OOCH)_2 + C_2H_5OH \quad (5.7)$$

$$SiOOCH + Si(OR) \Leftrightarrow DIMER \quad (5.8)$$

$$DIMER + Si(OR) \Leftrightarrow TRIMER \Leftrightarrow TETRAMER \quad (5.9)$$

The r =1 system reaction scheme was probably the same except for the absence of the di-substituted acyl compound of equation 5.7. For the higher r system, the reactions were much more complex. The large excess of formic acid facilitated simultaneous hydrolysis and condensation reactions, which rapidly occurred. In addition to the di-substituted product of equation 5.7, there was most likely a tri-substituted product.

4.3. Proton NMR Spectroscopy

In order to identify and quantify the disappearance of formic acid and the appearance of low molecular weight byproducts (water, ethanol, and ethyl formate), proton NMR spectroscopy was performed for the formic acid and TEOS system. The following table displays proton NMR chemical shifts obtained for the reactants and several byproducts:

Table 4.7: Proton NMR Chemical Shifts for Pertinent Pure Compounds Relevant to the TEOS/Formic Acid System (Relative to TMS)

SPECIES NAME	CHEMICAL SHIFT A	CHEMICAL SHIFT B	CHEMICAL SHIFT C
FORMIC ACID	10.6	7.6	
TEOS	3.1	0.4	
ETHYL FORMATE	7.5	3.4	0.8

The r=2 Formic acid to TEOS reaction was investigated using proton NMR over a 60 hour period. Scans were performed every 3 hours during the reaction period. Similarly to the results from silica NMR, proton NMR depicted the depletion of TEOS during the reaction; however, additional insight was uniquely provided by the proton NMR. Before this reaction was performed, TMS was used to determine the appropriate system calibration. This resulted in a shift of chemical shifts by one ppm. The spectra are located in the appendix. The consumption of formic acid and TEOS were evidenced from these experiments. As the reaction progressed, the peak that was due to the

hydroxy proton (10.8 ppm) in formic acid shifted to lower chemical shifts. Furthermore, the attachment of the formate group to silicon species was evidenced by the shift of the peak centered at 1.6 ppm to lower chemical shifts. The quadruplet peak centered at 4.2 ppm due to TEOS showed significant decay during the period of study. In addition to the observed decrease in the quadruplet intensity, this peak broadened and increased in complexity as additional silicate species were formed.

Furthermore, additional peaks appeared in the 7 ppm region, 8 ppm region, 4 ppm region, and 1 ppm region. The emergence of the quadruplet centered at 4.3 ppm was indicative of the ethyl formate byproduct, and the appearance of a quadruplet centered at 4.1 ppm denoted ethanol formation. Figure 4.30 shows the evolution of ethyl formate and ethanol along with the depletion of Si (OC_2H_5) groups.

This graph depicts the mole percent of the following underlined protons in the three species: $O\underline{CH_2}\underline{CH_3}$. The Si ($OC_2H_5$) mole percent decreased from 35% to 15% after 30 hours, and remained nearly constant at this value for the remaining 30 hours of reaction. The mole percents of ethanol and ethyl formate were nearly the same during the entire reaction. The mole percent never reached 15% within the 60 hours of reaction.

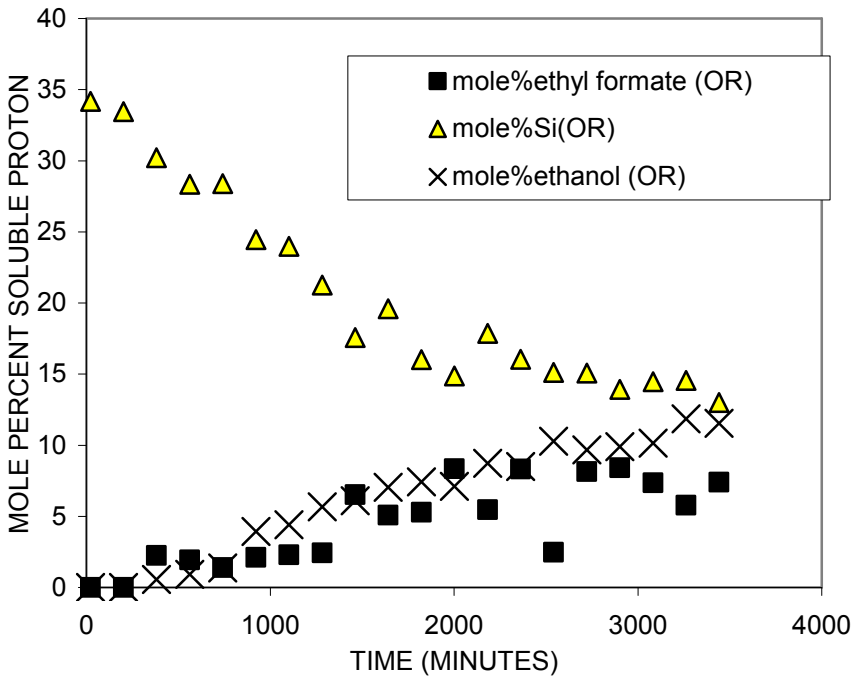

Figure 4.30 : The evolution of condensation products and depletion of $Si(OC_2H_5)$ during the r = 2 reaction of Formic acid and TEOS.

Similarly to the aforementioned experiments, the reaction of formic acid with TEOS at r = 6 was characterized using proton NMR. The reaction was monitored over 3 hours with scans every 10 minutes. The same trends observed for r = 2 were observed in the r = 6 experiments. The appendix houses the complete spectra of these reactions. The rapidness of the r = 6 reaction is clearly evident from these spectra. After 10 minutes of reaction, there were peaks consistent with ethanol formation and ethyl formate formation. The progression of condensation was characterized by the rapid depletion of detectable Si(OR) groups which were undetectable after 150 minutes of

reaction. Figure 4.31 depicts the prevalence of the significant detectable functional groups.

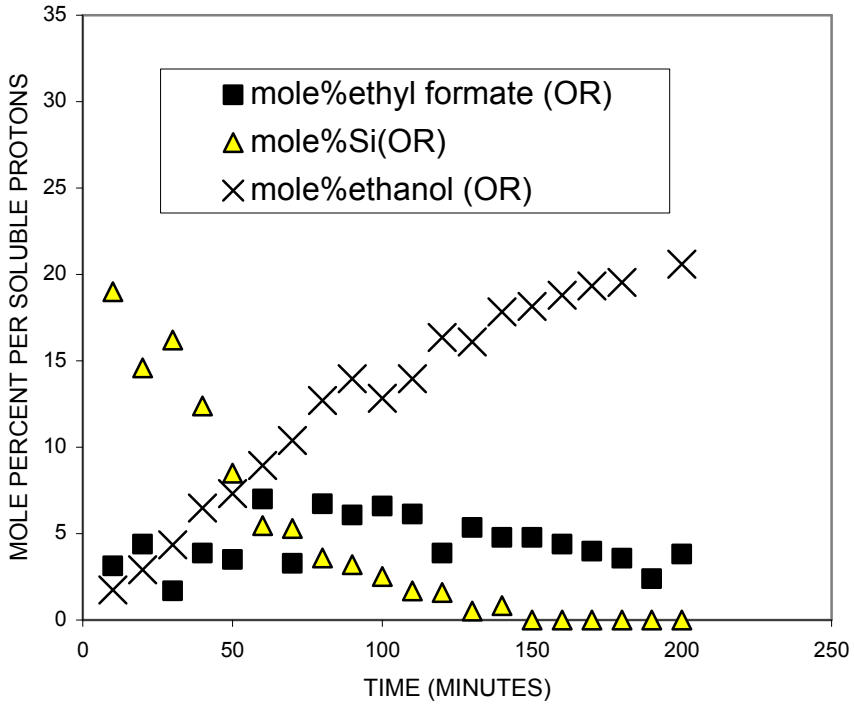

Figure 4.31: The temporal display of ethyl formate functional groups, Si(OR) groups, and ethanol functional groups during the r = 6 reaction of Formic acid with TEOS.

The relative population of species after 10 minutes into the reaction was very insightful. The mole percent of ethyl formate (3.1%) was approximately double the mole percent of ethanol (1.7%) after 10 minutes. However, the mole percent of ethanol significantly increased over the course of the reaction while the mole percent of ethyl formate remained nearly constant in the 5% range. Ethanol increased in mole percent to values exceeding 20 %. The Si(OR) group concentration decayed exponentially as condensation proceeded.

4.4. USAXS Results

The TEOS/formic acid system's microstructure was explored using USAXS. Molar ratios of formic acid to TEOS of 2 and 6 were monitored at Brookhaven National Laboratory. After 48 hours of reaction, the r = 2 case did not indicate any scattering. Silica NMR data did indicate the presence of silica species with three O-Si groups attached (Q_3); therefore, condensation reactions had progressed by 48 hours. The r = 6 case resulted in scattering after 109 minutes of reacting. Figure 4.32 shows a scattering curve for the reaction of TEOS with formic acid at r = 6 and 109 minutes . The smeared and desmeared data are graphically depicted. The corresponding radius of gyration was determined using the information shown in figure 4.33. From 109 minutes to 140 minutes, there was a rapid increase in the size of the microstructures with the Rg increasing from 5.4 nm to 8.0 nm. An Rg value of 9.4 nm was obtained after the system

had gelled, and there was no further increase in the Rg after 30 additional minutes past gelation.

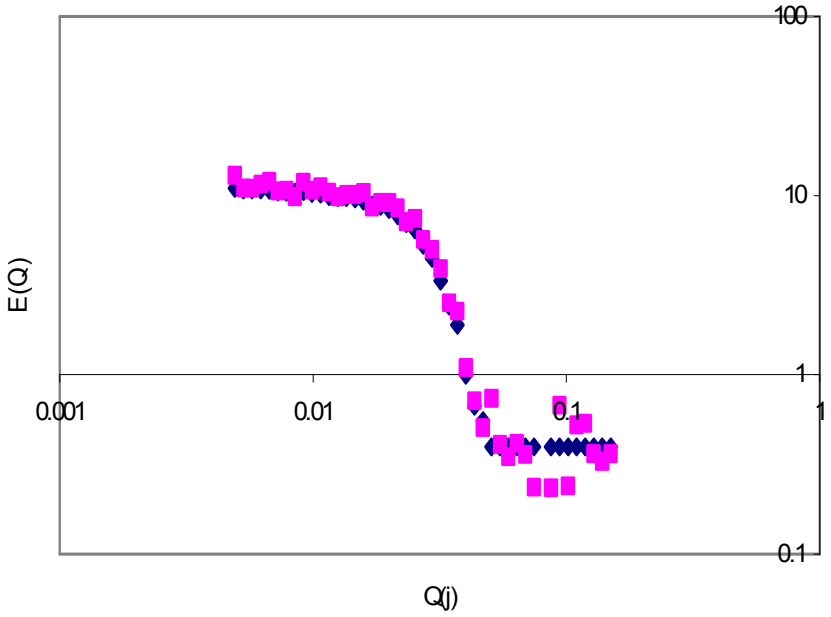

Figure 4.32: The scattering curves for the reaction of formic acid and TEOS at r = 6 after 109 minutes.

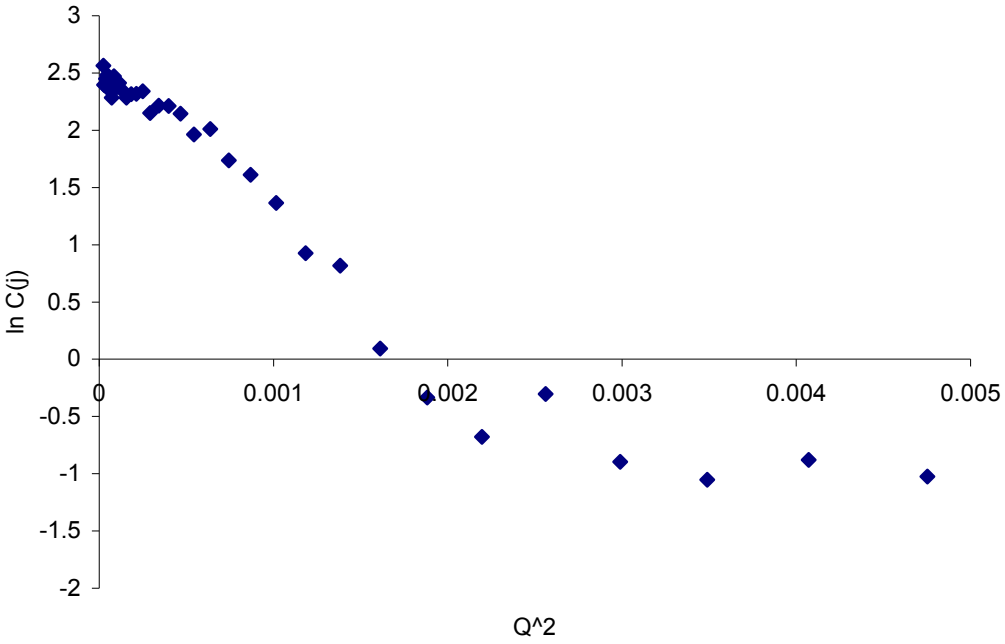

Figure 4.33: Radius of gyration plot for the reaction of TEOS with formic acid at r = 6 after 109 minutes.

4.5. Mass Spectrometry

The aforementioned experiments provided insight into the dynamics of the reaction of formic acid with TEOS with the exception of identifying and characterizing specific oligomers. Mass spectrometry was used to qualitatively determine the percentages of high and low molecular weight species and to investigate the types of oligomers that result from the reaction of TEOS with formic acid.

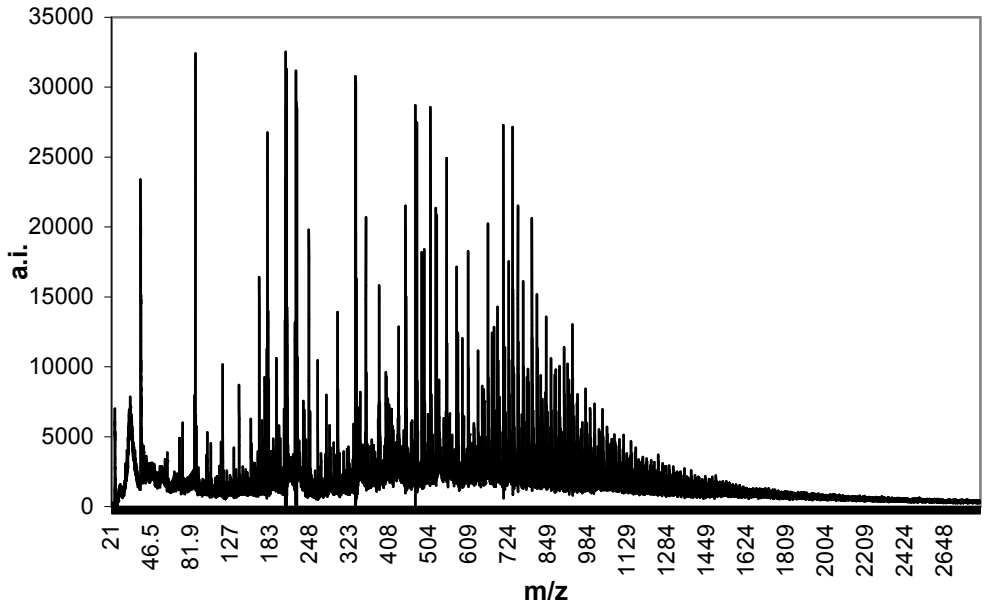

Figure 4.34 : Mass Spectrum of the reaction of TEOS with Formic acid at r = 6 after 35 minutes.

Figure 4.34 shows an apparent exponential decay in the intensity with increasing molecular weight which suggested that the reaction of TEOS with formic acid mimicked typical condensation polymerization processes. For the reaction of TEOS

with formic acid at r = 6 and 35 minutes, significant intensities were observed for molecular weights between 700 to 1230 amu's. Because of the presence of the matrix, the spectral range below 700 amu's was not considered in any analyses. The highest intensities were observed in the 800 m/z region. Identifying the oligomers that corresponded to the observed mass spectrum involved first developing a method of predicting the structures of silicate species. The high propensity to form three and four membered rings complicated the assignment of the polymeric silicate species. The following expressions are valid for straight chain silicon oligomers:

Number of Silicons : n
Number of Bridging Oxygens : n - 1
Number of Functional Groups : 2n + 2

Two of the functional groups present in the reaction of TEOS with formic acid (Ethoxy groups and Formate groups) are indistinguishable in mass spectroscopy because the molecular weights are identical. Therefore, functional groups can be classified as hydroxy groups (OH) or OR groups (OET or O=COH). The presence of ring structures leads to deviations in the numbers of bridging oxygen and functional groups denoted for straight chain silicon oligomers. With the addition of each three or four membered ring, the number of bridging oxygen is decreased by one and the number of functional groups is decreased by 2. Therefore, a silicate species with one ring and n silicon will contain n bridging oxygen and 2n functional groups. Several Microsoft Excel Macros were written to aid in the manipulation of the mass spectral data. The Macros used for

analysis of the mass spectroscopy results are contained in the appendix. The first Macro was used to select the significant molecular weights determined by the intensity. Molecular weights were considered significant at intensities greater than 3000. Approximately 1,000 of the 30,000 data points were significant in the r = 6 reaction of formic acid with TEOS. These molecular weights were then inserted into a second macro to determine a probable silicon oligomer. Figure 4.35 shows a sample of results obtained from the Microsoft Excel Macro for the r = 6 TEOS with formic acid reaction.

potassium cationized					
MW	#of Si groups	# of bridging O	# of OH	# of OR	calculated MW
`	8	9	8	6	774.8696
	10	12	15	1	773.087
	10	15	7	3	775.087
	12	21	6	0	775.3044
potassium cationized					
MW	#of Si groups	# of bridging O	# of OH	# of OR	calculated MW
774.3748	8	9	8	6	774.8696
	10	12	15	1	773.087
	10	15	7	3	775.087
	12	21	6	0	775.3044
potassium cationized					
MW	#of Si groups	# of bridging O	# of OH	# of OR	calculated MW
775.0298	9	8	18	2	776.9783
	6	6	1	11	776.6522
	8	9	8	6	774.8696
	10	12	15	1	773.087
	8	12	0	8	776.8696
	10	15	7	3	775.087
	12	21	6	0	775.3044

Figure 4.35: Results generated from the Microsoft Excel Macro for probable oligomeric species synthesized from the reaction of TEOS with formic acid.

Close introspection of the spectrum indicated potassium and sodium cationized species. These adventitious cations may have originated from the matrix, glassware, or starting materials. Therefore, each molecular weight was examined assuming the

presence of potassium or sodium cations. By process of elimination, the most probable number of Silicon, bridging Oxygen, hydroxy groups, and OR groups was selected.

Figures 4.36 and 4.37 depict the low molecular weight and high molecular weight portions of the mass spectrum for the reaction of TEOS with formic acid at r = 6, and 35 minutes.

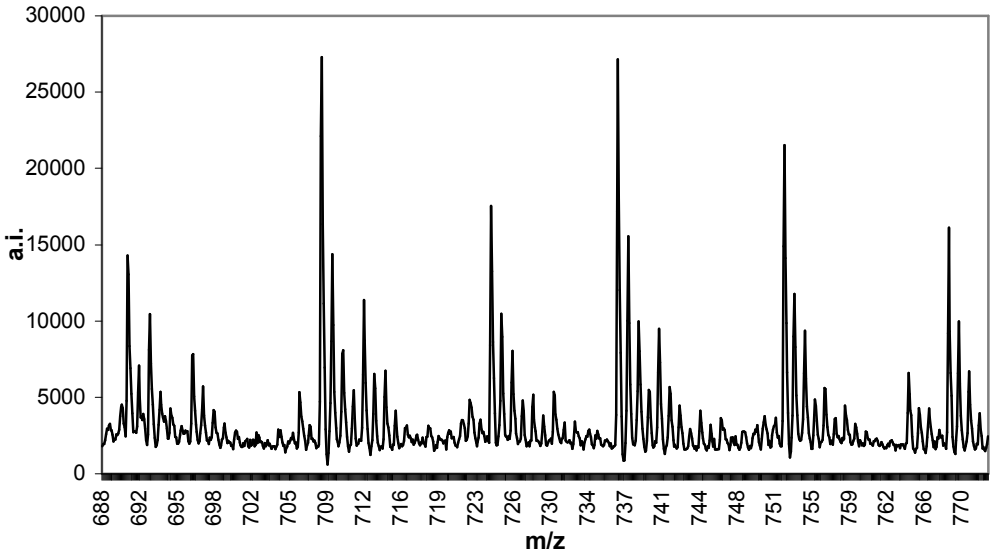

Figure 4.36: Mass Spectrum of the reaction of TEOS with formic acid at r = 6 after 35 minutes (688 – 772 m/z).

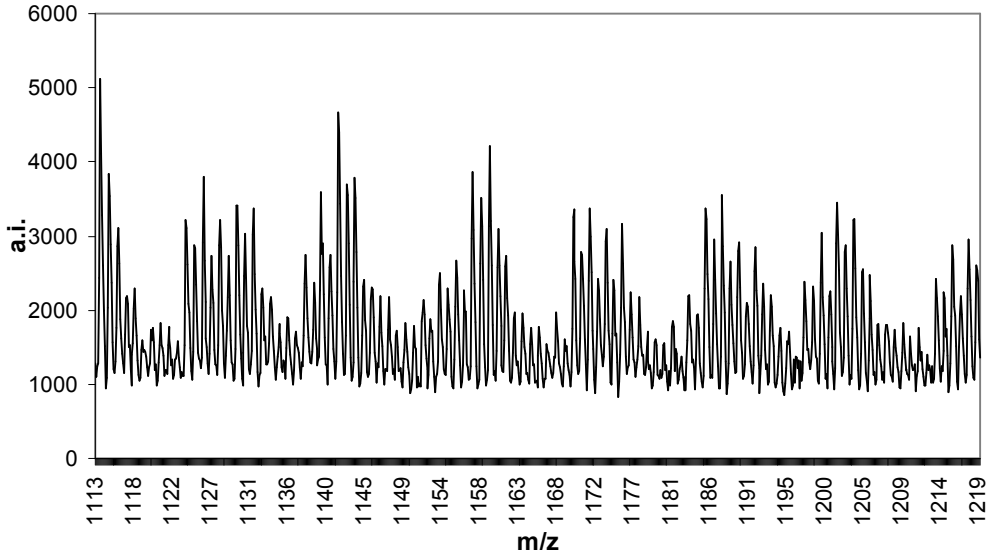

Figure 4.37: Mass Spectrum of the reaction of TEOS with formic acid at r = 6 after 35 minutes (1113 – 1219 m/z).

Analysis of the mass spectral data provided a plethora of information into the reaction of TEOS with formic acid. Species in the molecular weight range between 700 and 1265 mass units contained between five and eleven silicon atoms. Most of the lower molecular weight species contained sodium cations, while the higher molecular weight species were cationized with potassium. The OR groups accounted for the majority of all functional groups. By examination of the regions of the mass spectrum showed in the figures above, hydroxy groups accounted for 26% of all functional groups while OR groups accounted for 74% of all functional groups 35 minutes into the reaction of TEOS with formic acid at r = 6. Figure 4.38 graphically depicts the relationship between oligomer size and type of functional group. The percentage of

functional groups that were hydroxy contained in any particular species ranged on average between 10 to 45%. In general, the smaller oligomers contained fewer hydroxy groups than the larger oligomers. Approximately 20% of the silicon oligomers were comprised of only OR functional groups, while none of the oligomeric species identified contained all OH groups.

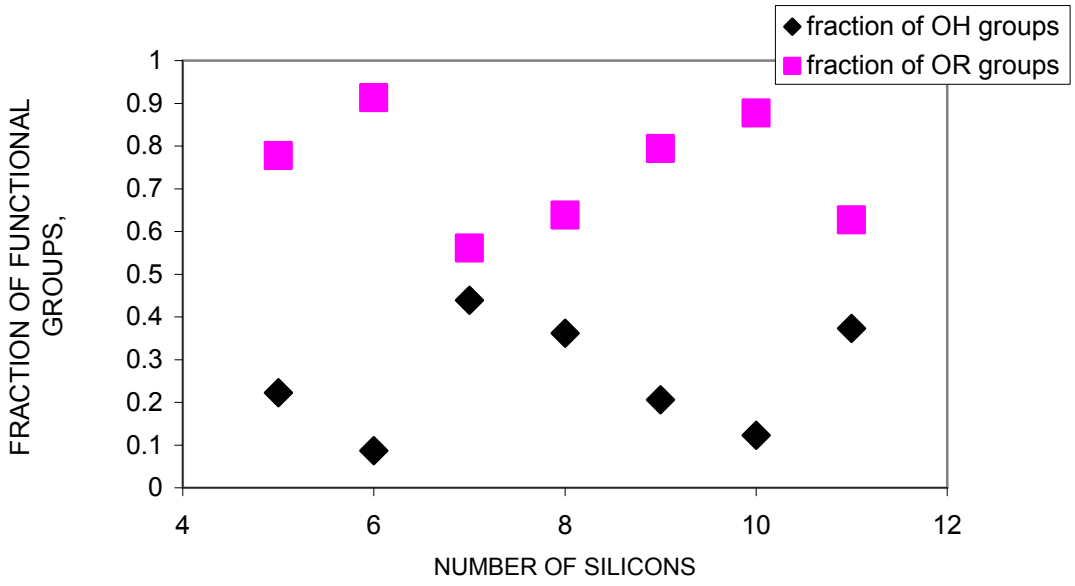

Figure 4.38 : Relationship between oligomer size and type of functional group for the reaction of TEOS with formic acid at r = 6, 35 minutes.

Mass spectroscopy provided information on ring formation in the reaction of TEOS with formic acid at r = 6. Oligomers containing as many as five rings were identified in the mass spectrum after 35 minutes. Twenty-two percent of the oligomers were straight chained containing no silica rings, and most of the rings were four

membered in the silica oligomers. The average oligomer formed in the reaction of TEOS with formic acid contained 2 rings. Figures 4.39 and 4.40 depict the ramifications of functional group type on ring formation, and the structural distribution of oligomers. All oligomeric species contained mainly OR groups regardless of the number of rings formed. Straight chained species and silica oligomers with 4 and 5 silica rings contained slightly higher abundances of OR groups than oligomers with one, two, and three rings. Straight chain oligomers were comprised of 88% OR functional groups, oligomers with 4 rings exhibited structures containing an average of 81% OR groups, and the one oligomer with 5 rings contained all OR groups.

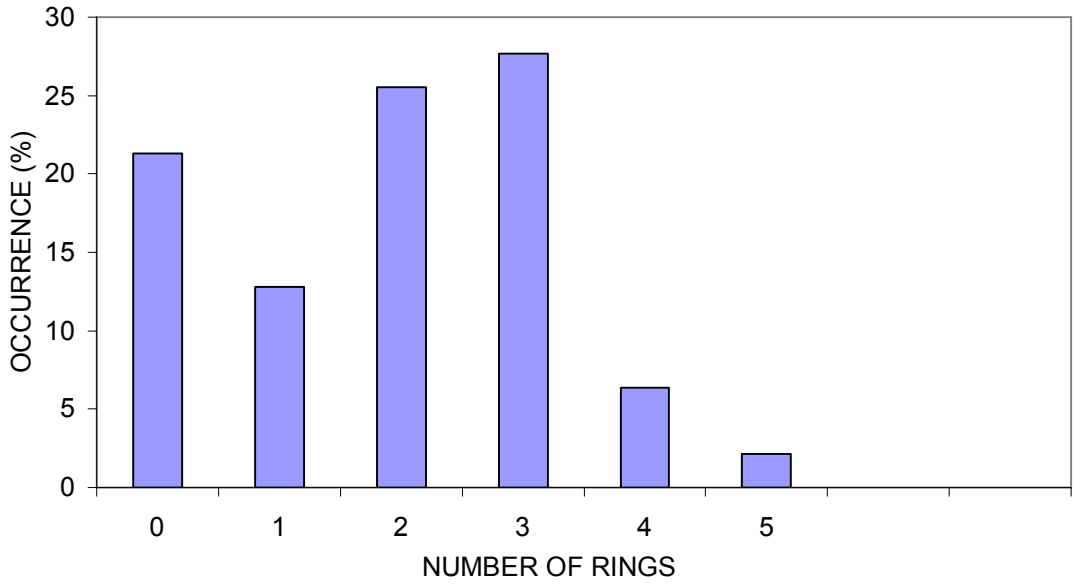

Figure 4.39 : The abundance of rings present in silica oligomers formed in the reaction of TEOS with formic acid r = 6, 35 minutes.

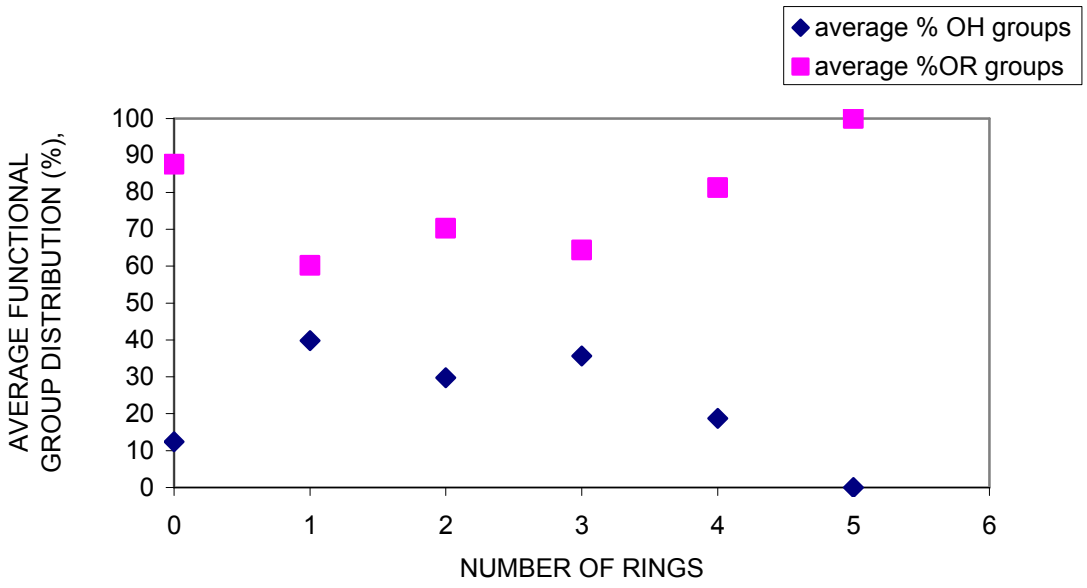

Figure 4.40 : The distribution of functional groups as a function of the number of rings present in the oligomer.

Table 4.8 shows some of the species that were identified in the mass spectrum of the reaction of TEOS with formic acid which are depicted in figures 4.36 and 4.37.

Table 4.8: Silica oligomers deduced from the mass spectrum of the reaction of TEOS with formic acid at r = 6 , 35 minutes.

OLIGOMER STRUCTURE	MOLECULAR WEIGHT
H H H H O O O O RO-Si-O-Si-O-Si- O- Si-(OH) O O O O RO-Si-O-Si-O-Si O O O R R R	650.7

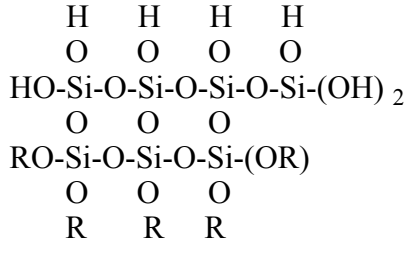	668.7
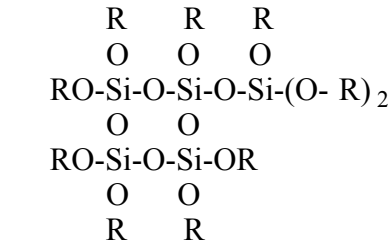	670.4
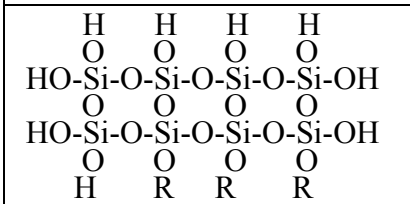	672.8
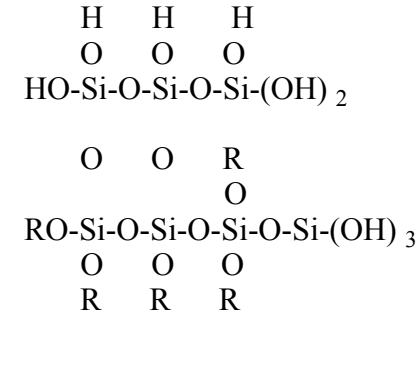	686.7
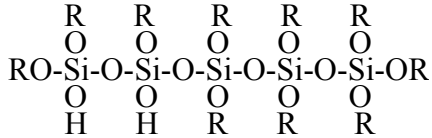	688.5

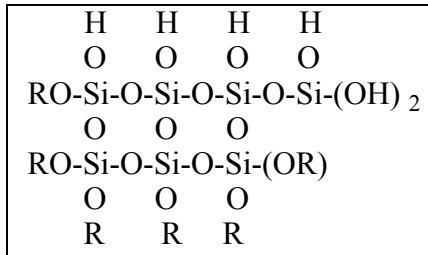	696.7
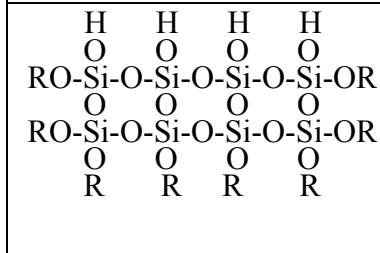	700.8
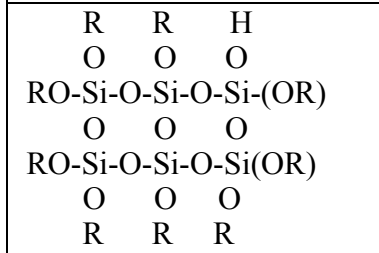	702.6
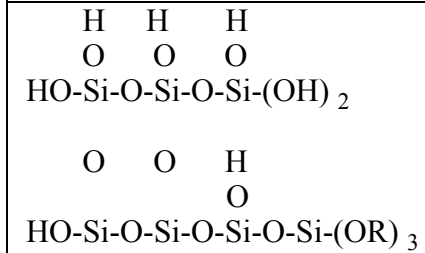	714.7
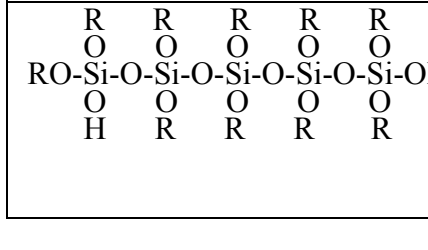	716.5

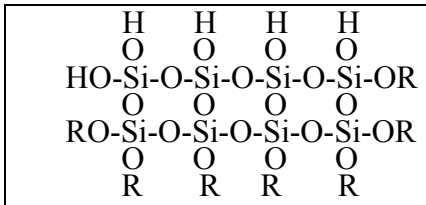	728.9
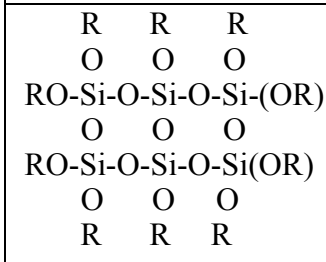	730.6
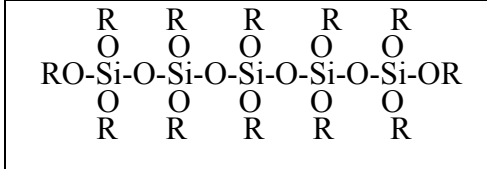	744.5
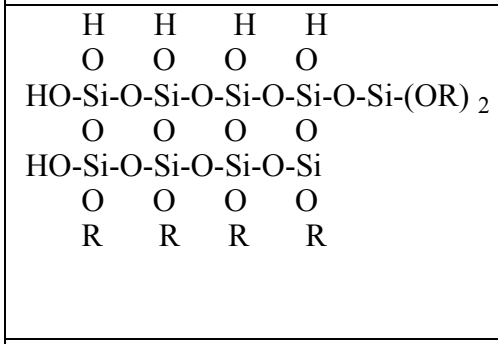	816.9
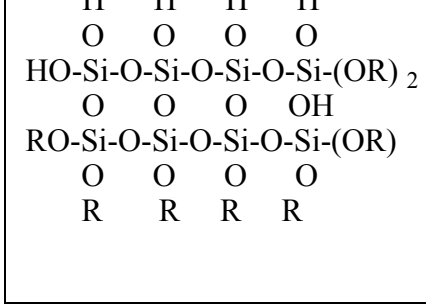	830.8

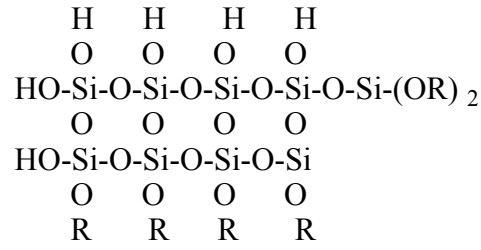	834.9
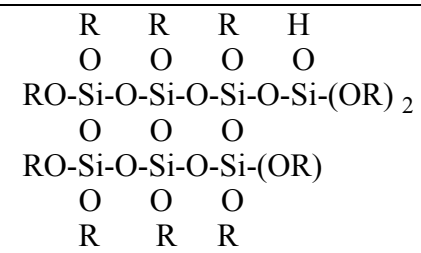	836.7
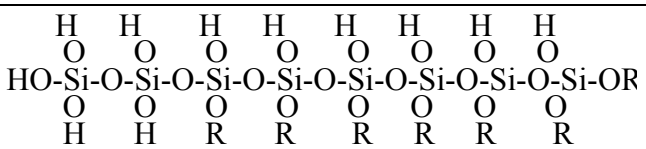	838.6
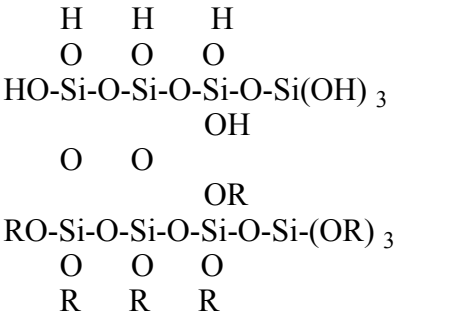	848.8
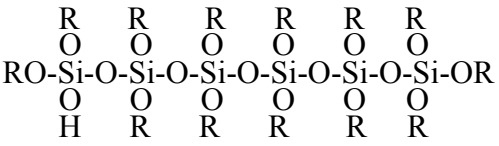	850.6

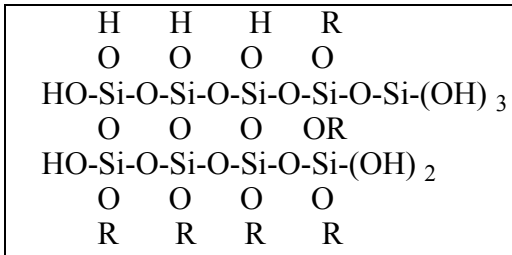	852.9
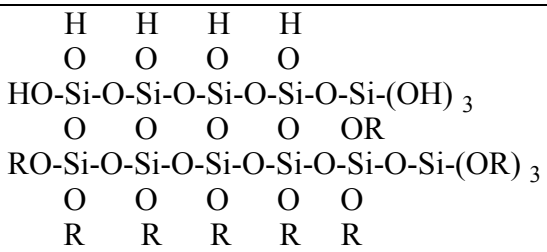	1103.1
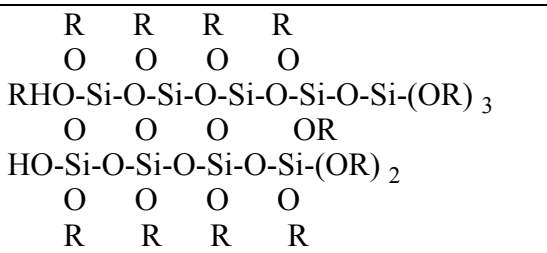	1104.9
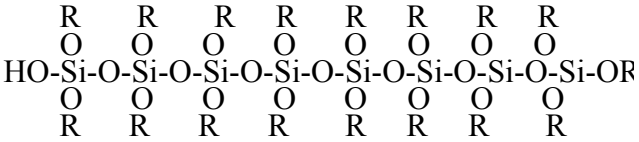	1118.0
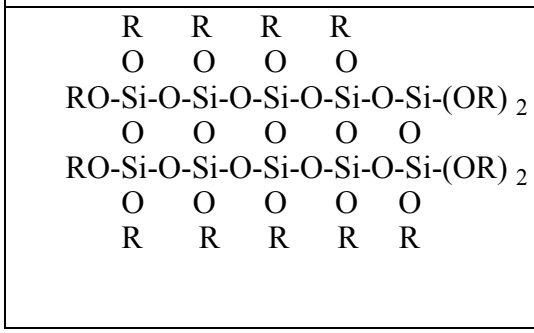	1119.0

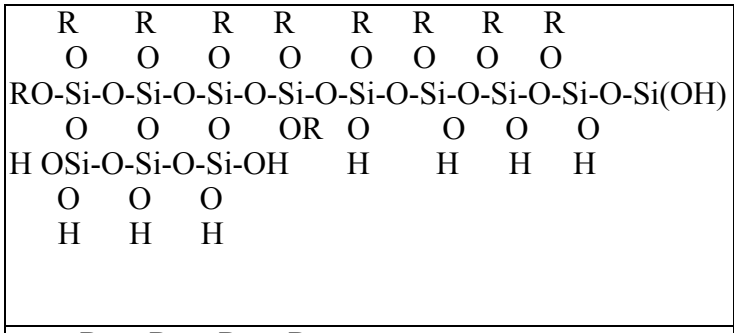	1121.1
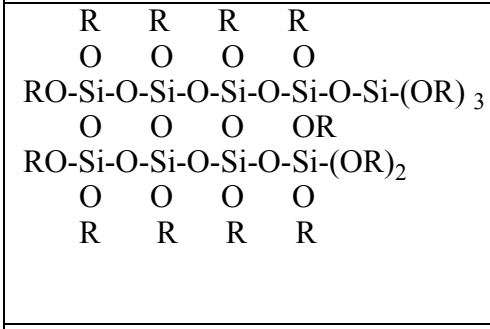	1132.9
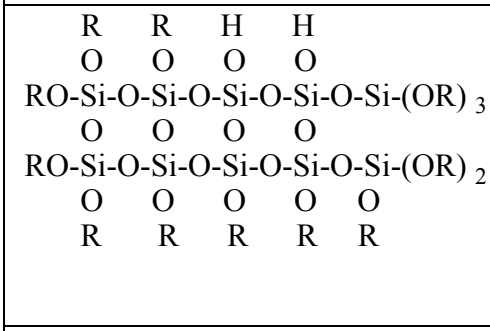	1137.0
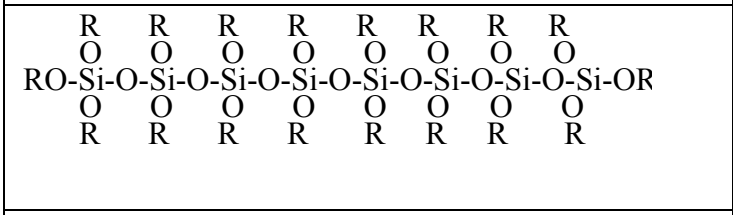	1146.8
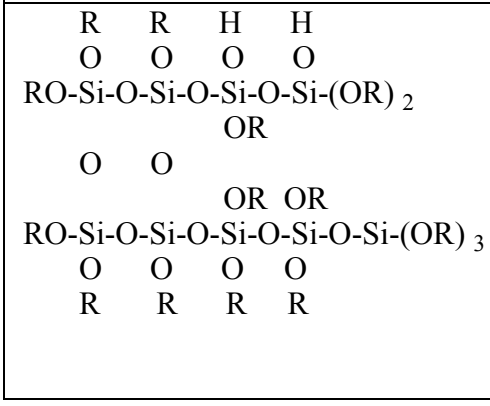	1150.9

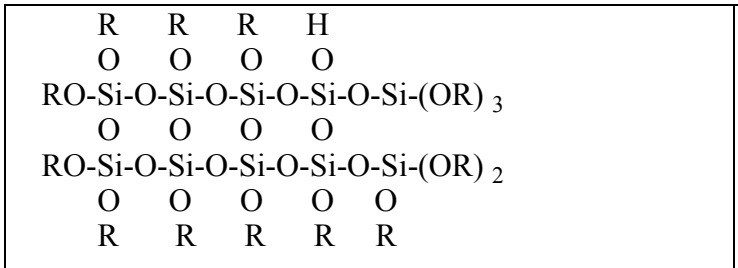	1165.0
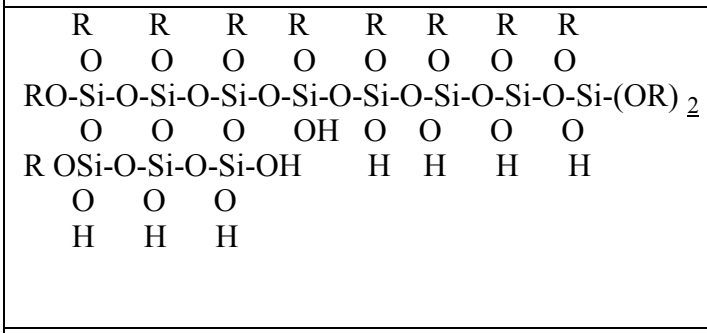	1177.1
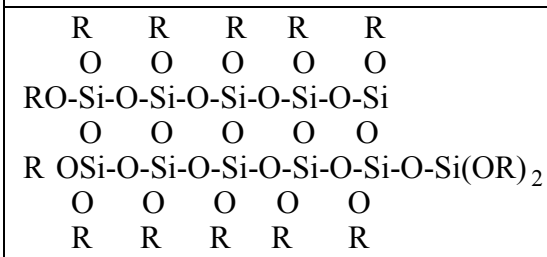	1179.1
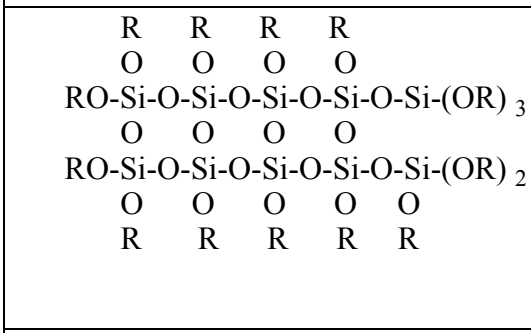	1193.0
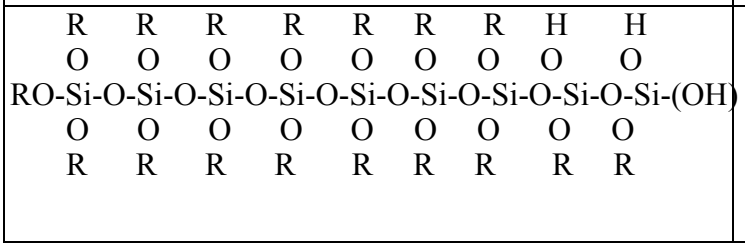	1196.9

R R R R R R R H H O O O O O O O O O RO-Si-O-Si-O-Si-O-Si-O-Si-O-Si-O-Si-O-Si-O-Si-(OR O O O O O O O O O R R R R R R R R R	1224.9
R R R H O O O O RO-Si-O-Si-O-Si-O-Si-O-Si-(OR) $_2$ O O O O O RO-Si-O-Si-O-Si-O-Si-O-Si-O-Si-(OR) $_3$ O O O O O R R R R R	1225.2
R H H H O O O O RO-Si-O-Si-O-Si-O-Si-O-Si-(OR) $_3$ O O O O OR RO-Si-O-Si-O-Si-O-Si-O-Si-O-Si-(OR) $_3$ O O O O O R R R R R	1243.1

In order to simplify the mass spectroscopy data, samples were doped with potassium trifluoroacetate and sodium trifluoroacetate. These additions were intended to separate the silica oligomers that contained potassium cations from the oligomers that contained sodium cations. Figures 4.41 and 4.42 show low molecular weight regions of the mass spectra of the reaction of TEOS with formic acid at r = 6, 30 minutes with sodium trifluoroacetate and potassium trifluoroacetate added respectively. The addition of sodium and potassium cations did not simplify the mass spectra.

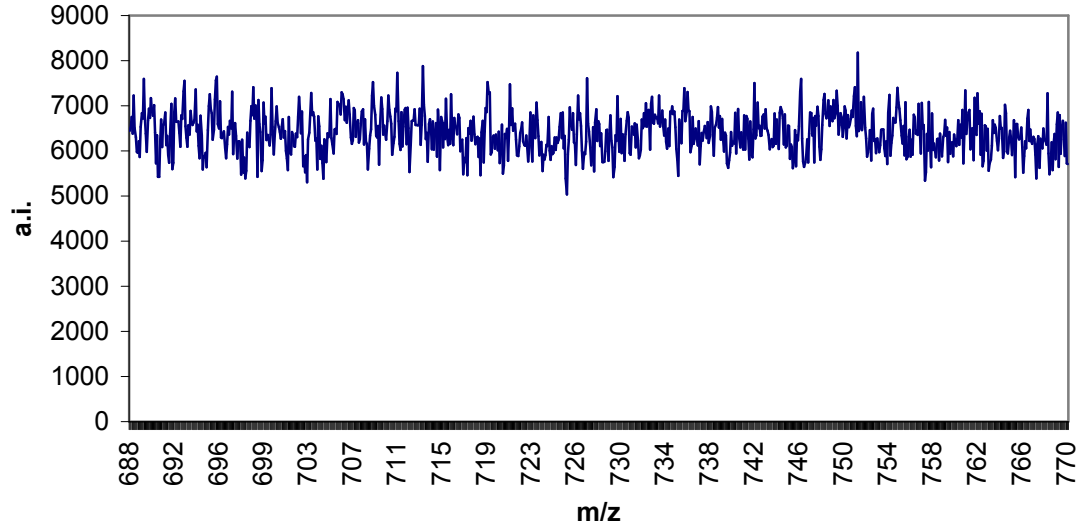

Figure 4.41 : Mass spectrum for the reaction of TEOS with formic acid at r = 6 after 30 minutes, doped with sodium trifluoroacetate.

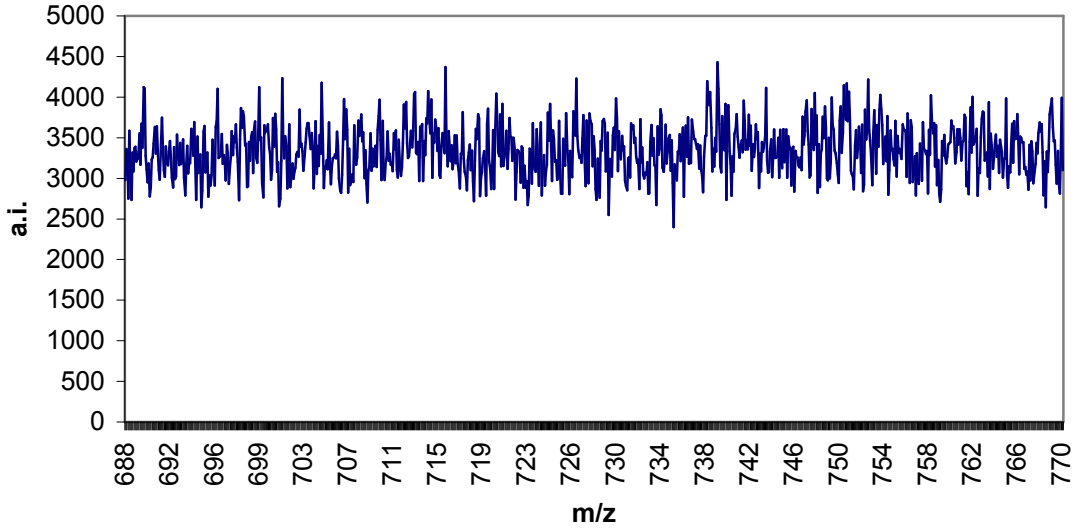

Figure 4.42: Mass spectrum for the reaction of TEOS with formic acid at r = 6 after 30 minutes, doped with potassium trifluoroacetate.

4.6. A Discussion of Results: A Comparison of all Analytical Methods

The reaction of TEOS with formic acid was studied using FTIR, ^{29}Si NMR, ^{1}H NMR, USAXS, and Mass Spectrometry. A variety of information was deduced from the analysis of the respective results. Information regarding the types and concentrations of functional groups was extracted from FTIR spectroscopy data. Because results from FTIR spectroscopy were rapidly obtained, the data from the beginning stages of the reactions was accessible for review. The reaction of TEOS with formic acid generated products that were not decipherable from FTIR analyses, because

of the similarity in functional groups between products and reactants. Therefore, additional analytical methods were required to adequately characterize the reactions. ^{29}Si NMR and ^{1}H NMR spectroscopy enabled examination of specific structures rather than functional groups. USAXS and mass spectrometry provided information on the oligomers formed in the reaction of TEOS with formic acid.

The effect of molar ratio of formic acid to TEOS was investigated using all the aforementioned analytical techniques. FTIR, ^{29}Si NMR spectroscopy, and ^{1}H NMR spectroscopy all indicated an increase in the rate of reaction with increasing the molar ratio of formic acid to TEOS. FTIR spectra did not indicate any SiOH groups or H_2O groups which are possible byproducts of the reaction of formic acid with TEOS. ^{29}Si NMR analyses provided an explanation for this observation. All of the ^{29}Si NMR experiments showed only trace amounts of SiOH groups present in the soluble phase. Similarly, proton NMR spectra did not contain the peaks consistent with the presence of water. The absence of repeat units spaced 18 amu apart in mass spectra further supported the FTIR findings that water was not a major byproduct of the reaction of formic acid with TEOS.

FTIR spectroscopy indicated that substantial amounts of ethyl formate were formed during the early stages of the reactions. Proton NMR results confirmed the presence of ethyl formate, and also indicated that ethanol was present. Initially, ethyl formate was the primary byproduct; however, ethanol became the major byproduct as the reaction progressed.

The effect of temperature on the silica sol-gel reactions was investigated using FTIR and ^{29}Si NMR spectroscopy. Results from FTIR spectroscopy and ^{29}Si NMR

spectroscopy showed that lower the reaction temperature retarded the sol-gel reactions. The same activation energy of 10.5 kcal/mole was obtained using both analytical methods. This activation energy compared with the activation energy previously determined in the literature by gel time (Sharp, 1994).

Mass spectrometry and ^{29}Si NMR spectroscopy provided conclusive information regarding oligomeric structure. Both analyses showed the presence of linear and cyclic species. Linear and cyclic dimers were observed in the NMR spectra; however, mass spectroscopy was not useful in analyzing these low molecular weight structures. At 35 minutes, NMR spectra indicated that only linear dimers were present. Mass spectrometry showed that after that same reaction time only 20% of the higher molecular weight species were linear. The insignificance of hydrolysis reactions was demonstrated in both mass spectra and NMR spectra. The majority of groups attached to oligomers were OR groups (ethoxy or formate) rather than OH groups. At 35 minutes of reaction and r = 6, OH groups accounted for 24% of all functional groups attached to oligomers and OR groups represented 76% of all functional groups. The same results were observed in silica NMR spectra with OR groups occurring in 81% of the functional group positions, and OH groups present in 19% of the functional group positions after 58 minutes .

Chapter 5

Formic Acid vs. Protic Acid, Water, Alcohol

Results from the analyses of sol-gels generated using formic acid were compared with published results of sol-gels formed using the conventional system (protic acid, water, and an alcohol). The primary aim of these comparisons is to determine the origin of rapid gelation.

5.1. Hydrolysis and Condensation Reactions

Using a protic acid, water, and an alcohol to facilitate sol-gel reactions has been well characterized. The kinetics of the hydrolysis and condensation reactions, which occur during conventional sol-gel processing, has extensively been investigated (Prabakar et al., 1994; Ng et al. 1996; Kay et al., 1988; Pouxviel et al., 1987; Peeters et al., 1998; Kelts et al., 1986; Doughty et al., 1990; Assink et al., 1988; Brinker et al., (1984); Yoldas, 1986; van Beek et al., 1991). Both hydrolysis and condensation reactions were found to concurrently lead to sol-gel formation. Brinker et al. (1987) and others reported that hydrolysis occurs and is nearly complete during the first few minutes of reaction. Kay et al. (1988) reported the following values for the hydrolysis rate constant, alcohol producing condensation rate constant, and water producing condensation rate constant : 0.20, 0.006, 0.001 (l/mol min) which further attest to the rapid rate of hydrolysis in conventional sol-gel reactions. This results in primarily a

distribution of silanol species, which then react with unreacted monomer and other hydrolyzed monomers to form condensation products. Pouxviel et al. (1987) reported that after 45 minutes of reacting the following species were primarily present: $Si(OC_2H_5)_4$, $Si(OH)_4$, $Si(OH)_3(OC_2H_5)$.

The following table shows the monomeric species that were observed from ^{29}Si NMR experiments when an acid, water, and alcohol were used to formulate sol-gels.

Table 5.1 Monomer species observed in conventional sol-gel processing.

Q_0 Species	δ_{Si}
$Si(OH)_4$	-72.4
$Si(OH)_3(OR)_1$	-73.3
$Si(OH)_2(OR)_2$	-74.3
$Si(OH)_1(OR)_3$	-76.0
$Si(OR)_4$	-78.3

The condensation reactions in the conventional system were determined to be directly correlated with the initial water concentration. Assink et al. (1988) clearly demonstrated that increasing the water concentration had an impact on the type of condensation reaction observed. At high ratios of water to Si, water producing condensation resulted. His analyses also suggested that alcohol producing and water producing condensation reactions must both be included to describe reaction kinetics.

There are discrepancies in the literature regarding the importance of alcohol producing condensation reactions. Pouxviel et al. (1987) concluded that alcohol producing condensation reactions were negligent based on the absence of dimers with fewer than 2 silanol groups. Furthermore, the type and rate of condensation reactions was determined to be a function of the initial water concentration. Different results were observed for the reaction of TEOS with formic acid. The results obtained from ^{29}Si NMR spectroscopy of the reaction of formic acid with TEOS did not indicate the presence of $Si(OH)_3(OR)_1$ or $Si(OH)_4$, and only trace amounts of $Si(OH)_2(OR)_2$ were ever observed. ^{29}Si NMR spectroscopy analyses determined that OH groups accounted for approximately 20% of all functional groups. Primarily, OH groups were observed in oligomeric species rather than monomeric species. Retarding the reaction kinetics by lowering the temperature and reducing the molar ratio of formic acid to TEOS did not result in a pronounced increase in OH concentration, nor did this result in the observation of more highly hydrolyzed species. The absence of significant amounts of SiOH groups was further confirmed in mass spectrometry analyses and FTIR spectroscopy.

The enhanced hydrolysis rates for the conventional system may be attributed to the use of water as an initial reactant. However, equations 5.1, 5.2, 5.3, and 5.4 show possible methods for producing water and silanol groups in-situ during the reaction of formic acid with TEOS.

$$Si(OOCH) + C_2H_5OH \rightarrow Si(OH) + C_2H_5OOCH \quad (5.1)$$

$$HCOOH + C_2H_5OH \rightarrow C_2H_5OOCH + H_2O \quad (5.2)$$

$$Si(OC_2H_5) + H_2O \rightarrow Si(OH) + C_2H_5OH \quad (5.3)$$

$$\mathrm{Si(OOCH)} + H_2O \rightarrow Si(OH) + HCOOH \quad (5.4)$$

$$Si(OH) + Si(OH) \rightarrow Si0Si + H_2O \quad (5.5)$$

The peaks consistent with the presence of water were not observed in FTIR which was used to explore the early stages of the reactions. The limited solubility of water in xylene may have prevented observation of small amounts of water. However, the absence of characteristic water peaks in ^{1}H NMR spectra further supported the hypothesis that insignificant amounts of water and silanol groups were produced in the reaction of formic acid with TEOS. Mass spectra also did not show a distinct pattern of peaks separated by 18 amu which would be indicative of the loss of water.

The inability to detect water during the formic acid assisted sol-gel reactions and the minor amounts of silanol groups present suggests that equations 5.2, 5.3, and 5.4 are not major determinants in reaction progression. The analyses of the kinetics and the models formulated for the sol-gel reactions using water, an alcohol, and a protic acid all conclude that under normal processing conditions (high water concentrations, low alcohol concentrations, and miniscule amounts of protic acid) these reactions are the major reactions leading to high molecular weight species. Therefore, the substitution of multi-functional formic acid in sol-gel syntheses alters the entire system kinetics.

In addition to the effects of water on the sol-gel reactions, the effect of the absence of ethanol initially must be considered. For the conventional system, the concentration of ethanol is not as important on hydrolysis and condensation reactions as the water concentration (Pouxviel et al. 1987). Equations 5.6 and 5.7 show methods of ethanol production in the absence of water. The presence of ethanol was not observed in the FTIR spectra obtained for the early stages of the formic acid/TEOS reactions. However, ^{1}H NMR spectra for formic acid/TEOS reactions did contain the characteristic ethanol peaks. Initially, small amounts of ethanol were generated; however, ethanol became the major byproduct in the reaction of formic acid with TEOS as the reaction proceeded.

$$Si(OC_2H_5) + HCOOH \rightarrow Si(OOCH) + C_2H_5OH \quad (5.6)$$

$$Si(OC_2H_5) + Si(OH) \rightarrow SiOSi + C_2H_5OH \quad (5.7)$$

Mass spectra were consistent with the presence of ethanol. There was an approximate 45 amu difference in repeat units which is indicative of the loss of ethanol or ethyl formate.

In the conventional system, ethanol is used as a solvent only. Ethanol does not participate in hydrolysis or condensation; however, it is a byproduct of both hydrolysis and condensation reactions. Equations 5.8, 5.9, and 5.10 illustrate this concept.

$$Si(OC_2H_5) + H_2O \rightarrow Si(OH) + HOC_2H_5 \quad (5.8)$$

$$Si(OH) + Si(OH) \rightarrow SiOSi + H_2O \quad (5.9)$$

$$Si(OH) + Si(OR) \rightarrow SiOSi + HOC_2H_5 \quad (5.10)$$

Ethanol appears to be significant in the reactions of formic acid with TEOS. Due to the absence of water, ethanol is the most likely source of the silanol groups that were observed (see equation 5.1).

The two byproducts of the conventional reaction to form sol-gels are water and alcohol. However, the substitution of formic acid results in esterification reactions. There are now three possible byproducts: ethanol, water, and ethyl formate. Ethyl formate is produced as a byproduct, and is not consumed in the sol-gel reactions. The presence of formic acid significantly increases the complexity of the sol-gel kinetics. In addition to the three possible byproducts, there is an additional silyl formate group (Si(OOCH)) that must be considered. This results in the consideration of eight rate expressions rather than the three that are adequate to describe the kinetics for the conventional system.

In general, the product spectra observed for the formic acid/TEOS sol-gel reactions were different from the types of products observed in the conventional TEOS sol-gel reactions. Pouxviel et al. (1987) reported ^{29}Si NMR results of the reaction of TEOS with ethanol, water, and HCl. They observed species with one, two, and three bridging oxygen after 20 hours of reaction. ^{29}Si NMR performed with the formic acid

and TEOS system showed species with one and two bridging oxygen for the r =6 system, and species with three bridging oxygen were observed for the r = 2 system. These results indicate that the higher condensed species react more rapidly to form insoluble structures in the multi-functional formic acid catalyzed sol-gel reactions than in the conventional system. This conclusion is further supported by the inability to see highly condensed structures in the ^{29}Si NMR spectra of TMOS sol-gel reactions performed using water, an alcohol, and protic acid catalyst, which are known to progress significantly faster than TEOS (Kelts et al., 1988; van Beek et al., 1991; Dougherty et al., 1990; Assink et al. 1988; Prabakar et al., 1994).

In addition to the absence of peaks associated with highly condensed species, fewer Q_1 species were observed in the reaction of formic acid with TEOS. Both methods of forming sol-gels appeared to begin in the same manner. The first three species observed in ^{29}Si NMR spectra,(TEOS, $Si(OH)(OEt)_3$, and $SiOSi(OEt)_6$), were the same for the conventional and formic acid catalyzed sol-gel reactions. However, different species were formed as the condensation reactions progressed. Primarily one dimer (Q_1), disilicic ester, was observed in the reaction of formic acid with TEOS; however, significant concentrations of dimers with one, two, and three hydroxy groups were detected by Pouxviel et al. (1987). Similar trends were observed in Q_2 species. In general, the lower concentration of OH groups inhibited the formation of many condensation species. Table 5.2 shows a comparison of the species observed in the conventional sol-gel method and in the reaction of formic acid with TEOS.

Table 5.2: A Comparison of the products of the reaction of formic acid with TEOS and the conventional method.

Formed in the reaction of TEOS with formic acid	Formed in the conventional water, alcohol, protic acid method
$Si(OH)_2(OEt)_2$	$Si(OH)_4$
$Si(OH)(OEt)_3$	$Si(OH)_3(OEt)$
TEOS	$Si(OH)_2(OEt)_2$
$SiOSi(OH)_2(OEt)_1$	$Si(OH)(OEt)_3$
$Si(OH)_x(OEt)_y(HC{=}OO)_z(OSi)_\alpha$	TEOS
$Si(OEt)_3(O_2CH)$	Q_1: $SiOSi(OH)_3$
$Si(OEt)_2(O_2CH)_2$	Q_1: $SiOSi(OH)_2(OEt)_1$
Q_1: $SiOSi(OEt)_3$	Q_1: $SiOSi(OH)_1(OEt)_2$
Q_2: cyclic $(SiO)_2$ $Si(OH)_1(OEt)_1$	Q_1: $SiOSi(OEt)_3$
Q_2: linear $(SiO)_2$ $Si(OH)_1(OEt)_1$	Q_2: cyclic $(SiO)_2$ $Si(OH)_2$
Q_2: cyclic $(SiO)_2$ $Si(OEt)_2$	Q_2: linear $(SiO)_2$ $Si(OH)_2$
Q_2: linear $(SiO)_2$ $Si(OEt)_2$	Q_2: cyclic $(SiO)_2$ $Si(OH)_1(OEt)_1$
Q_3: $(SiO)_3Si(OEt)$	Q_2: linear $(SiO)_2$ $Si(OH)_1(OEt)_1$
water	Q_2: cyclic $(SiO)_2$ $Si(OEt)_2$
ethanol	Q_2: linear $(SiO)_2$ $Si(OEt)_2$
ethyl formate	Q_3: $(SiO)_3Si(OEt)$
	Q_3: $(SiO)_3Si(OH)$

.

In addition to differences in the types of species observed, there were also differences in the extent of reactions which were measured from ^{29}Si NMR spectra. Prabakar et al. (1994) calculated the following extents of reaction for the TEOS, ethanol, water, and HCl reaction: 0.63 (1 day), 0.66 (4 days), and 0.67 (7 days). The extents of reaction determined for the reaction of formic acid with TEOS ranged from 0.05 to 0.4 during 2 hours of reacting formic acid with TEOS at r =6, and 0 to 0.2 over a two day period when formic acid was reacted with TEOS at r =2. Therefore, larger extents of reaction were determined from ^{29}Si NMR data for the conventional TEOS, ethanol, water, and HCl system. These extent of reactions would be considered small

for linear polymers; however, high molecular weights can be obtained for non-linear polymers. Thus, the determination of lower extents of reaction for systems which gel faster can be explained.

5.2. Cyclization

The formation of cyclic species has been reported in the sol-gel reactions facilitated by an alcohol, water, and protic acid using silica NMR spectroscopy results. There is conflicting information present in the literature regarding cyclization. Pouxviel et al. (1987) reported that increasing the water concentration led to a higher concentration of cyclic tetramers. Cyclic tetramers represented 20% of the total Si concentration after long periods of reaction at high water concentrations. However, high water ratios (>8 Water/Si) were reported to suppress cyclic formation by Ng et al. (1996). Kelts et al. (1988) noted that 75% of the oligomers formed in the TEOS, water, alcohol, and protic acid reaction were cyclic prior to gelation. They also discovered that replacing TEOS precursors with TMOS precursors caused a significant reduction in the concentration of cyclics. For sol-gels derived from TMOS, less than 50% of oligomers were cyclic at gelation. Linear species were present in larger quantities initially for both TMOS and TEOS; however, cyclic species became dominant as the reaction progressed (Kelts et al., 1988).

Similarly to the conventional system, linear species were observed prior to cyclic species in the sol-gel reaction of formic acid with TEOS. Results from ^{29}Si NMR analyses of the reaction of TEOS with formic acid indicated the occurrence of less

cyclic species. At 112 minutes and r = 6, cyclics accounted for 35% of the soluble Si while linear dimers accounted for 30% of the soluble Si. Lowering the ratio of formic acid to TEOS (r = 2), resulted in cyclic dimers comprising 25% of the soluble Si mole percent while linear dimers accounted for 28% of the soluble Si mole percent after 40 hours.

^{29}Si NMR only provides information for low molecular weight species. The extent of cyclic formation for oligomers must be determined by alternate methods. Currently, oligomeric structure in the sol-gel reactions of TEOS with water, an alcohol, and protic acid has not been published. Mass spectrometry analysis enabled a more comprehensive investigation into cyclic formation. Oligomers generated from the reaction of TEOS with formic acid containing 5 to 13 silica groups were extensively cyclic. Most of the rings formed were 4-membered with is consistent with the thermodynamics of silica. Analyses of 50 silica oligomers showed that 78% of these species were cyclic, and 22 % were straight chain oligomers. Therefore, cyclic formation occurred more readily in higher molecular weight species. The lower concentration of cyclics in the low molecular species may help explain the increased rates of condensation. The sol-gel reactions have been known to proceed by the reaction of low molecular species with the higher molecular weight species. The straight chain species are less sterically hindered; therefore, they react with higher molecular species more readily.

5.3. Radius of Gyration

The radius of gyration , R_g, is a measure of the effective size of polymeric structures. The R_g determined for the formic acid catalyzed TEOS system was significantly larger than the Rg reported by Brinker et al. (1984) for the conventional system. Brinker et al. (1984) deduced R_g values ranging from 2nm to 4nm during the sol-gel process from SAXS data for the conventional TEOS system. Upon gelation, the R_g values did not increase beyond 4nm in their studies. The USAXS data for the formic acid/TEOS system indicated higher R_g values. Analysis of the Gunier region indicated that the R_g increased from 5 nm to 9 nm during these sol-gel reactions at r =6. These results indicate that formic acid promotes larger structure formation. In contrast to the previously mentioned difference in R_g for the two different sol-gel techniques, both methods indicated that the size and shape of the silicate molecules did not significantly vary after gelation which was illustrated by the invariance of the R_g after gelation.

Gelation occurred for the conventional system at an R_g of 4 nm; however, formic acid catalyzed systems did not gel until the R_g reached 9 nm. This implies that the size of the structures is not the only contributing factor in determining gel time.

5.4. Gel Time

The substitution of protic acid, water, and ethanol with formic acid significantly reduced the gel time. In general, the sol-gel reactions using formic acid and TEOS led to gel times orders of magnitude lower than sol-gel reactions facilitated by water, an alcohol, and protic acid. The respective gel times for reactions of formic acid and TEOS at r =6 and r = 2 were 3 hours and approximately 40 days. For the conventional system, gel times for the reaction of TEOS with ethanol, water, and HCl gelled in 321 hours (Kelts et al., 1988). Kelts et al. (1988) reported significantly lower gel times when methanol was used as a solvent (168 hours), and using TMOS as the silica precursor led to further reductions in gel time (129 hours). This lower gel time for TMOS may be a result of reduced steric hinderance.

Examination of the results obtained for the reaction of formic acid with TEOS provides some clues regarding the rapid gelation that was observed. Gelation is directly proportional to the rate of condensation. The presence of fewer cyclics in the initial condensation products may lead to a reduction in gel time. The linear species are able to react easier with higher molecular weight condensation species, and silicate networks are formed quickly. The reduction in hydrolysis rates for the reaction of formic acid with TEOS may also contribute to the lower gel time.

For the conventional sol-gel methods, increasing the concentration of water leads to shorter gel times. This is attributed to the increased number of hydroxy groups which tend to facilitate condensation reactions. In the conventional system, these hydrolysis reactions are nearly complete before condensation reactions occur. In this

alternate method for producing sol-gels, hydrolysis reactions were determined to be negligible.

Substitution of formic acid for the water, alcohol, and protic acid significantly alters the chemistry. Instead of SiOH groups forming, SiOOCH groups are formed rapidly. The lower pka of the parent acid of the formate group , which makes this group a better leaving group, results in the promotion of nucleophilic substitution. The presence of significant amounts of ethyl formate in the early stages of the reactions of formic acid with TEOS further illustrated the importance of the silyl formate group.

5.5 Summary

Comparison of sol-gel reactions using formic acid with the conventional sol-gel reactions provided insight into this novel method . The rapid gelation observed in the formic acid/TEOS system may be attributed to several factors. The higher rates of condensation coupled with the presence of fewer cyclic species may help explain this behavior. These sol-gel reactions are governed by different chemical reactions The presence of silyl formate groups (SiOOCH) and the lower concentration of water significantly alter the sol-gel kinetics.

Chapter 6

A Kinetic Model of the Formic Acid/TEOS Reaction

The kinetics of the sol-gel reactions of TEOS with an alcohol, water, and protic acid has been investigated by several authors. Assink et al. (1988) modeled the conventional sol-gel reaction using TMOS as the silica precursor. They described the kinetics with a hydrolysis expression and two condensation expressions. Equations 6.1, 6.2, and 6.3 were used to characterize the reaction.

$$SiOR + H_2O \rightarrow SiOH + ROH \quad (6.1)$$

$$2SiOH \rightarrow 2(SiO)Si + H_2O \quad (6.2)$$

$$SiOH + SiOR \rightarrow 2(SiO)Si + ROH \quad (6.3)$$

Using proton and silica NMR spectroscopy results, the concentrations of methoxy groups, methanol, and SiOSi groups were determined. Using the limiting case at early reaction times, the rate constants were obtained. The rate constant for the water producing condensation reaction was 0.006 l/mol min, and the rate constant for the alcohol producing reaction was 0.001 l/mol min. Although the rate constant for the alcohol producing condensation reaction was largest, both condensation reactions were significant. The hydrolysis rate constant was significantly larger than either condensation rate constants. A value of 0.2 l/mol min was calculated using early reaction time approximations.

The replacement of the conventional method of making sol-gels with the reaction of formic acid with TEOS increases the complexity of the kinetics. The following equations depict all of the possible kinetic expressions that describe the sol-gel reaction.

$$SiOC_2H_5 + HCOOH \xrightarrow{k_1} SiOOCH + C_2H_5OH \quad (6.4)$$

$$SiOOCH + C_2H_5OH \xrightarrow{k_2} SiOH + C_2H_5OOCH \quad (6.5)$$

$$HCOOH + C_2H_5OH \xrightarrow{k_e} C_2H_5OOCH + H_2O \quad (6.6)$$

$$SiOOCH + H_2O \xrightarrow{kh_1} SiOH + HCOOH \quad (6.7)$$

$$SiOOCH + HCOOH \xrightarrow{k_4} SiOOCH + C_2H_5OH \quad (6.8)$$

$$SiOC_2H_5 + \mathrm{H}_2O \xrightarrow{kh_2} SiOH + C_2H_5OH \quad (6.9)$$

$$SiOOCH + SiOC_2H_5 \xrightarrow{kc_1/2} SiOSi + C_2H_5OOCH \quad (6.10)$$

$$SiOH + SiOH \xrightarrow{kc_4/2} SiOSi + \mathrm{H}_2O \quad (6.11)$$

$$SiOH + SiOOCH \xrightarrow{kc_3/2} SiOSi + HCOOH \quad (6.12)$$

$$\mathrm{SiOH} + SiOC_2H_5 \xrightarrow{kc_2/2} SiOSi + C_2H_5OH \quad (6.13)$$

Analytical results obtained by FTIR, ^{29}Si NMR spectroscopy, and ^{1}H NMR spectroscopy were employed to determine the most probable reactions in the formic acid/TEOS system. Equations 6.6, 6.7, and 6.9 were assumed negligible based on the inability to detect water by FTIR spectroscopy and ^{1}H NMR spectroscopy. Equation 6.8 was deemed insignificant based on ^{29}Si NMR spectroscopy results. Determination of appropriate rate constants was based on two assumptions.

The first assumption was irreversible reactions. Condensation reactions are known to be irreversible under the processing conditions used in this research; therefore, only the validity of this assumption on equations 6.4 and 6.5 is arguable. The results of FTIR spectroscopy indicate the disappearance of Si-O-C groups, and NMR spectroscopy indicates the increase in ethanol and ethyl formate during the reaction of TEOS with formic acid. These results support the assumption of neglecting the reverse

reactions in equations 6.4 and 6.5. Finally, Flory's equal reactivity hypothesis was assumed valid. This hypothesis states that functional groups react at the same rates independant of the species structure. This led to a system of 8 equations and 6 rate constants to describe the reaction of formic acid with TEOS which are depicted in the following equations.

$$\frac{d[SiOC_2H_5]}{dt} = -k_1[SiOC_2H_5][HCOOH] - k_{C1}[SiOC_2H_5][SiOOCH] - k_{C2}[SiOH][SiOC_2H_5] \quad (6.14)$$

$$\frac{d[HCOOH]}{dt} = -k_1[SiOC_2H_5][HCOOH] + k_{C3}[SiOH][SiOOCH] \quad (6.15)$$

$$\frac{\mathrm{d[SiOOCH]}}{\mathrm{dt}} = k_1[SiOC_2H_5][HCOOH] - k_{C1}[SiOC_2H_5][SiOOCH] - k_{C3}[SiOH][SiOOCH] \quad (6.16)$$

$$\frac{d[C_2H_5OH]}{dt} = k_1[SiOC_2H_5][HCOOH] + k_{C2}[SiOH][SiOC_2H_5] \quad (6.17)$$

$$\frac{d[SiOH]}{dt} = k_2[SiOOCH][C_2H_5OH] - k_{C2}[SiOH][SiOC_2H_5] - k_{C3}[SiOH][SiOOCH] - 2k_{C4}[SiOH]^2 \quad (6.18)$$

$$\frac{d[C_2H_5OOCH]}{dt} = k_2[SiOOCH][C_2H_5OH] + k_{C1}[SiOC_2H_5][SiOOCH] \quad (6.19)$$

$$\frac{d[SiOSi]}{dt} = k_{C1}[SiOC_2H_5][SiOOCH] + k_{C2}[SiOH][SiOC_2H_5] + k_{C3}[SiOH][SiOOCH] + 2k_{C4}[SiOH]^2 \quad (6.20)$$

$$\frac{d[H_2O]}{dt} = 2k_{C4}[SiOH]^2 \quad (6.21)$$

Table 6.1 shows concentrations for the r = 6 formic acid to TEOS system after 40 minutes of reaction. Initially, the concentration of SiOR groups was 9 mol/L and the concentration of HCOOH was 13.25 mol/L.

Table 6.1: Concentration data for the species in the reaction of TEOS with formic acid at r = 6.

Species	Concentration (40 minutes) mol/L
$SiOC_2H_5$	3.1
HCOOH	11.9
SiOH	0.6
C_2H_5OOCH	1.0
C_2H_5OH	1.7
SiOSi	4.4
SiOOCH	2.9
H_2O	0

Developing a kinetic model involved determining the four condensation rate constants and the two rate constants which described silyl formate group and silanol formation. The fortran code used to determine the rate constants is shown in the appendix. The Linpack method for solving the least squares problem Ax=b where A is the coefficient matrix and b is the data vector. The normal equations method was used to find a solution as shown in equation 6.22. The QR decomposition of A was

computed, and this enabled the normal equations to be expressed by equations 6.23, 6.24, and 6.25. If ATA is nonsingular, the equations can be solved. The IMSL routines LQRSL and LQRRR were employed in the analyses.

$$ATAx = ATb \tag{6.22}$$

$$AP = QR \tag{6.23}$$

$$(PRT)(QTQ)R(PTx) = (PRT)QTb \tag{6.24}$$

$$R(PTx) = QTb \tag{6.25}$$

where
P is the permutation matrix (P - 1 = PT)

Q is the orthogonal matrix (Q - 1 = QT)

R is the upper trapezoidal matrix

The concentration values shown in table 6.1 and the initial concentrations of SiOR groups and HCOOH were inserted into equations 6.14, 6.15, 6.17 - 6.20. The presence of six unknowns and eight equations allowed elimination of two equations. Equation 6.15 was not used in determining the rate constants after determining that the concentration of SiOOCH groups was the most uncertain. This uncertainty was based on the inability to conclusively identify these groups in ^{29}Si NMR spectroscopy. Equation 6.20 which characterized the formation of water was also omitted.

Table 6.2 shows the rate constants that were determined for the reaction of TEOS with formic acid.

The values of the rate constants varied significantly. The highest rate constants observed were k_2 and k_{c3} which represented the formation of silanol groups and the condensation of silanol groups. The reaction of $SiOC_2H_5$ with HCOOH had the smallest rate constant; therefore, equation 6.4 displays the rate determining step. The condensation rate constants increased in the following fashion: $k_{c3} > k_{c1} > k_{c2} > k_{c4}$. Therefore, the presence of silanol groups facilitated condensation reactions. The largest condensation rate constant was for the reaction between SiOH groups and SiOOCH. The rate constants for the reaction of two SiOH groups, and the reaction of SiOH groups and SiOR groups to form siloxane bonds were significantly less.

These rate constants were then utilized in modeling the TEOS/formic acid reactions using equations 6.14-6.21. The Adams-Moulton's method was used to implicitly solve the differential equations. The IVPAG IMSL routine was incorporated within a Fortran 90 computer code. See the appendix for the source code. Figure 6.1 displays the functional group concentrations determined using the kinetic rate expressions, and figure 6.2 shows a comparison of the model with the experimental results.

Table 6.2. The rate constants for the reaction of TEOS with formic acid

RATE CONSTANT	VALUE (mol/L-min)
k_1	$3x\ 10^{-5} \pm 0.00001$
k_2	$5x\ 10^{-2} \pm 0.0015$
k_{c1}	$4x\ 10^{-4} \pm 0.000012$
k_{c2}	$1x\ 10^{-3} \pm 0.00003$
k_{c3}	$9x\ 10^{-1} \pm 0.027$
k_{c4}	$2x\ 10^{-2} \pm 0.0006$

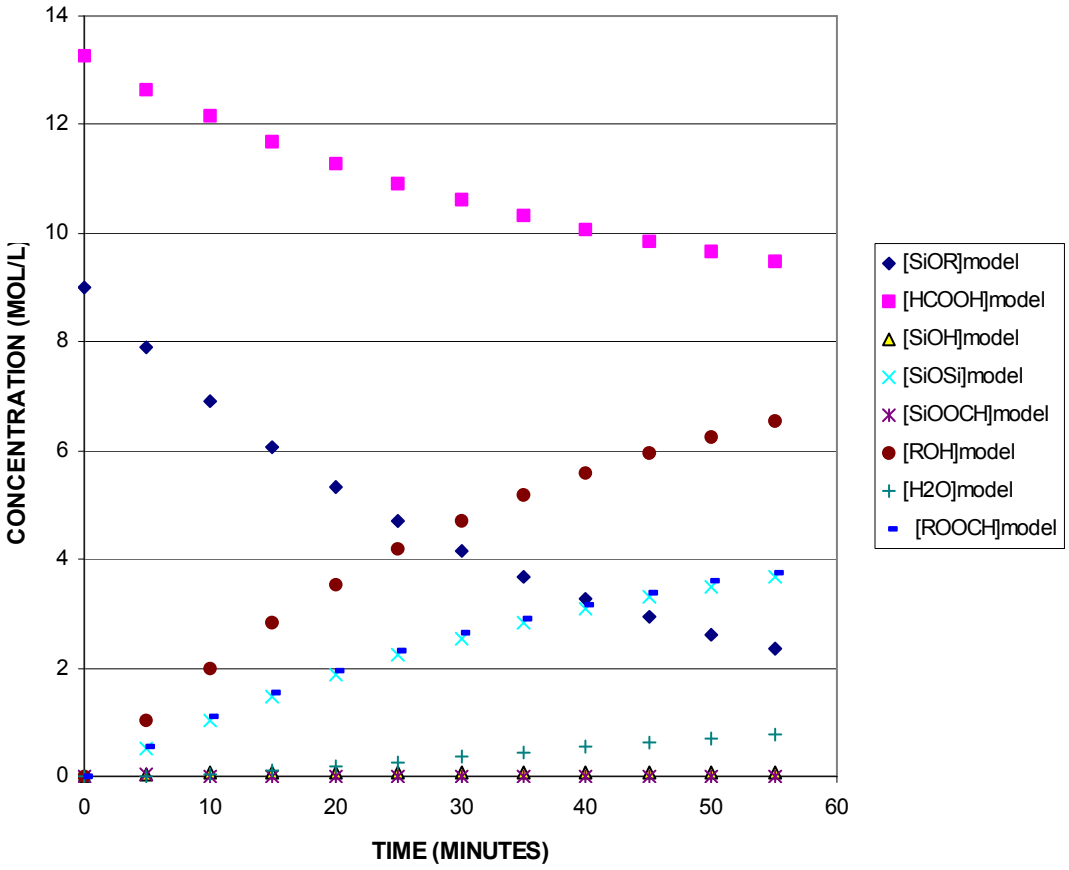

Figure 6.1: The evolution of functional group concentration determined from the kinetic model.

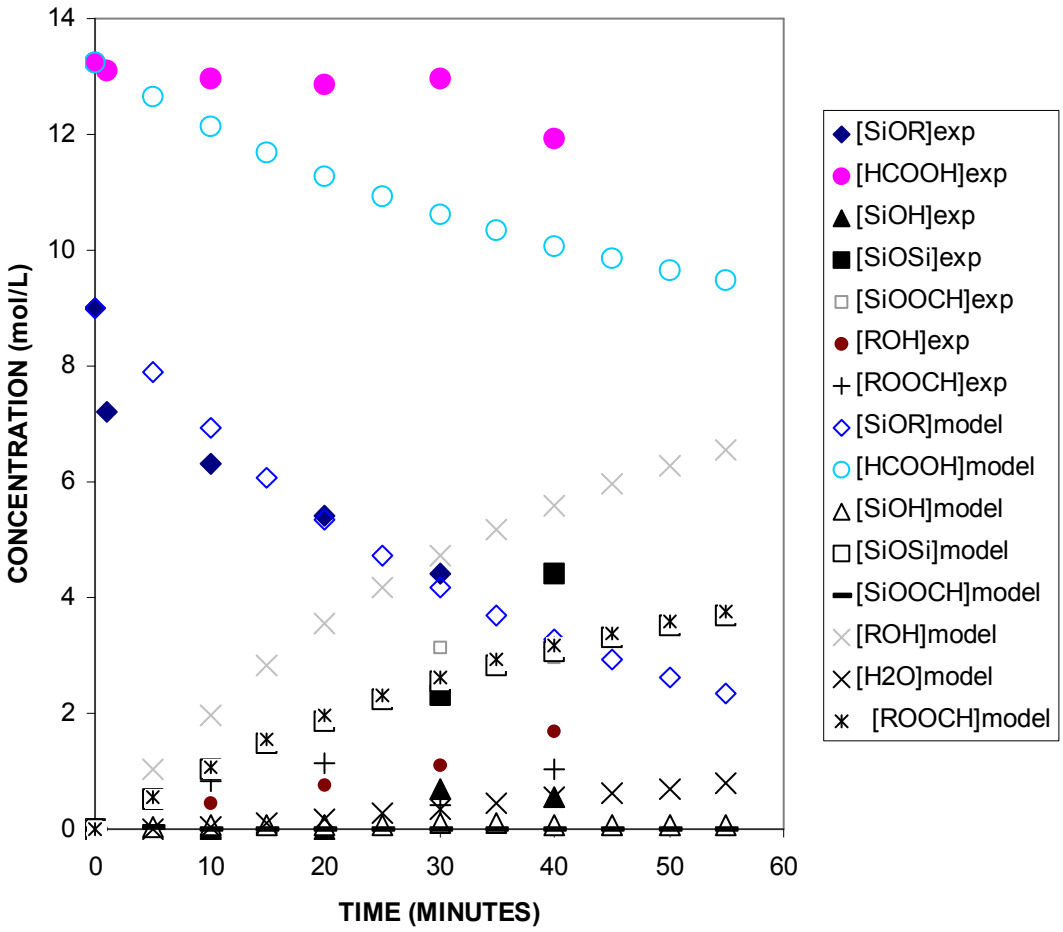

Figure 6.2.: A comparison of experimental functional group concentration obtained from proton NMR, silicon NMR, and FTIR results with the kinetic model.

The previous figures indicate that the model accurately characterized the trends observed in the reaction of formic acid with TEOS. The model shows a linear decrease in SiOR concentration that was also observed in the FTIR data. The experimental results for the SiOR concentration were in close agreement with the results generated from the kinetic model. Figure 6.2 indicates that the kinetic model predicted the same concentrations determined from FTIR spectroscopy at 20, 30, and 40 minutes.

The concentration of formic acid decayed more rapidly in the kinetic model with the concentration decreasing from 13.25 mol/L to 10 mol/L during 40 minutes. The concentration of HCOOH obtained from FTIR data was slightly higher at 40 minutes. The concentration obtained using the kinetic rate expressions may be more realistic for formic acid than the information gather using FTIR spectra. The peak at 1720 cm^{-1}, which characterizes the carbonyl group, was used to determine the conversion of formic acid. The carbonyl group is also present in ethyl formate; therefore, the decrease in the concentration of HCOOH may have actually been greater than FTIR results indicated.

The kinetic model developed for the TEOS/formic acid reaction indicated a progression in the concentration of Si-O-Si groups to a value of 3.7 mol/L after 55 minutes. The Si-O-Si concentration was only measurable in ^{29}Si NMR experiments; therefore, the Si-O-Si concentration was not determinable for short periods of time. At 30 minutes, the kinetic model predicted a concentration for Si-O-Si groups of 2.5 mol/L. Results obtained from ^{29}Si NMR indicated that an Si-O-Si concentration of 2.1 mol/L was achieved after 30 minutes. The [SiOSi] obtained from the kinetic model deviated at longer reaction times from the experimental data. At 58 minutes, the

concentration of SiOSi groups determined from NMR spectroscopy was 6.1 mol/L. However, the kinetic model only indicated a concentration of 3.7 mol/L.

The kinetic model under predicted the concentration of SiOH groups. The concentration of SiOH groups was extracted from ^{29}Si NMR spectra. At a reaction time of 30 minutes, the value of [SiOH] was 0.1 mol/L which was lower than the 0.7 mol/L determined experimentally. Similar differences between the kinetic model and experimental data were observed at 40 minutes.

The concentration of byproducts determined using the kinetic model was higher than the values obtained from proton NMR spectroscopy. The concentration of ethanol and ethyl formate, which are byproducts of the reaction of TEOS with formic acid, were respectively found to be 1.7 and 1.0 mol/L at 40 minutes using proton NMR spectroscopy. However, the values for ethanol and ethyl formate calculated using the kinetic model after 40 minutes were 5.6 and 3.1mol/L. Furthermore, small amounts of water (less than 1 mol/L) were predicted by the kinetic model. This water was formed during the condensation reactions of two silanol groups as shown in equation 6.11.

Analyzing the data generated using the kinetic model resulted in an enhanced insight into the reaction of TEOS with formic acid. The importance of the ratio of formic acid to TEOS was clearly evident after determining that the reaction of SiOR groups with formic acid was the rate determining step. The inadequacies in the model provided insight into the reaction pathways of these sol-gel reactions. Although water was not identified in any of the analytical tests, the results of this model suggest that water is present in the system. Therefore, silanol groups may be formed by hydrolysis reactions.

The incorporation of hydrolysis reactions may increase the accuracy of the kinetic model. Currently, the kinetic model contains only one method for producing silanol groups, and that is via the reaction of SiOOCH groups with ethanol as shown in equation 6.5. Incorporating alternative methods for producing silanol groups may enable conservation of silyl formate groups which were under predicted in the kinetic model.

The model under predicted the concentration of siloxane groups, and this may also be attributed to insufficient silanol group concentration. The low concentration of silanol groups retarded condensation reactions in the kinetic model. Figure 6.3 graphically summarizes the deviations between the experimental data and the kinetic model for the TEOS/formic acid system.

The kinetics of the formic acid/TEOS sol-gel reactions was vastly different than the conventional water, alcohol, protic acid sol-gel reactions. In the conventional system, the hydrolysis reactions had significantly larger rate constants than the condensation reactions. For the formic acid system, the highest rate constant was observed for a condensation reaction. The condensation rate constants on average for the formic acid catalyzed system were larger than those determined for the conventional sol-gel method. Condensation rate constants ranged between 0.9-0.0004 mol/L for the reaction of formic acid/TEOS system, while the condensation rate constants for the conventional method were 0.001 and 0.006 mol/L.

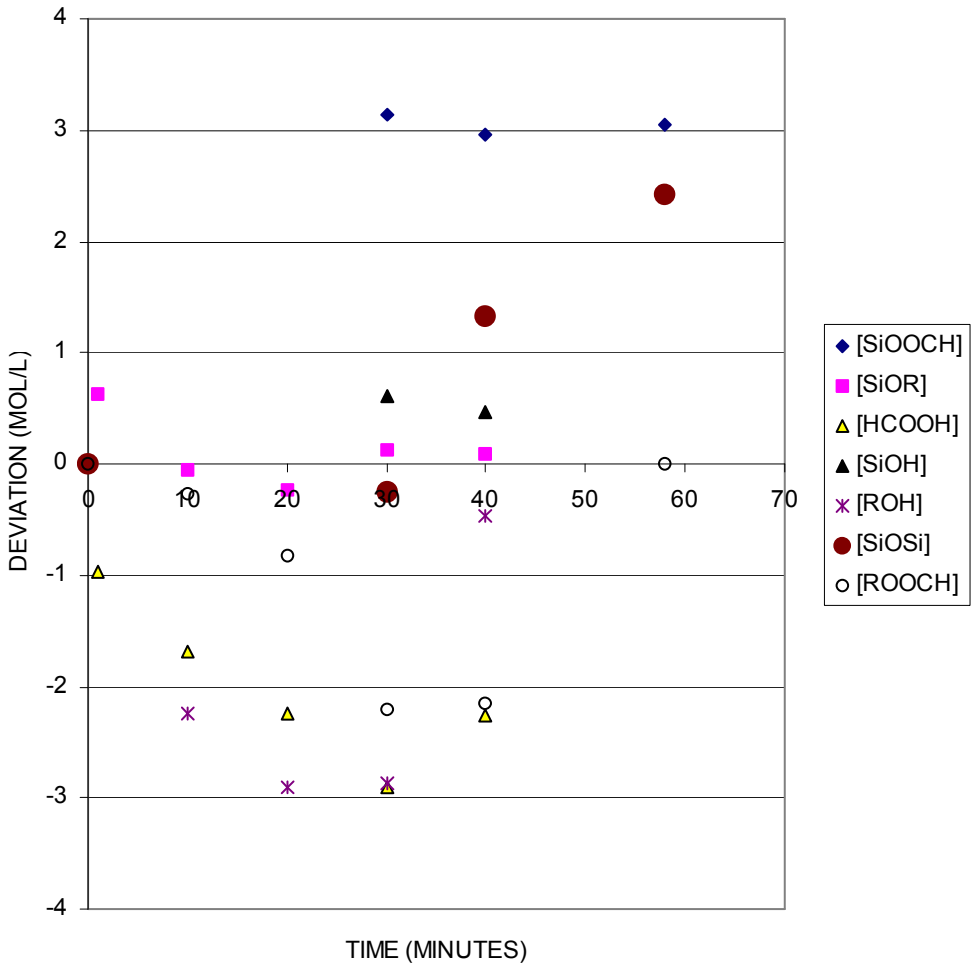

Figure 6.3. The deviation about zero for the kinetic model of the TEOS/formic acid system.

Chapter 7

Conclusions and Recommendations

Normally, silica gels are prepared using a silica precursor (e.g. TMOS), water, an alcohol, and a protic acid. However, the reaction of a silica precursor with only a carboxylic acid has been shown to lead to the formation of gels rapidly. Numerous studies have been performed using acetic acid as a multi-functional catalyst. But, limited studies have been performed using formic acid that has a lower pka than acetic acid. Analytical techniques such as FTIR spectroscopy, ^{29}Si NMR spectroscopy, ^{1}H NMR spectroscopy, mass spectrometry, and USAXS were employed to gather important information on TEOS/ formic acid reactions.

FTIR spectroscopy was used to characterize the reactions of TEOS and formic acid. FTIR spectra of the reactions of TEOS and formic acid at different molar ratios showed that increasing the molar ratio led to faster rates of condensation and esterification reactions. The decrease in SiOR concentration and the increase in ethyl formate concentration upon increasing r supported the previous conclusion. The effects of temperature on the reactions of TEOS and formic acid were readily observed in the FTIR spectra. Increasing the reaction temperature enhanced the rates of reaction. These experiments at various temperatures were used to compute the activation energy for the conversion of SiOC groups.

The activation energy was determined and compared with previous results for the TEOS and formic acid system that were determined from gel time. The same

activation energies were obtained for both methods. Therefore, FTIR proved to be an alternate method of accurately, quickly, and inexpensively determining the rates of reaction. In addition to information regarding the effect of molar ratio and temperature on the reactions, FTIR spectra indicated the appearance of ethyl formate. FTIR spectra taken at various temperatures for the r = 6 reactions was used to obtain an activation energy of 10.5 kcal/mole for the r = 6 system.

FTIR spectroscopy provided information on the types and concentration of functional groups. However, the similarity of species produced and reacted in the reaction of TEOS with formic acid limited the quantity of information obtainable from FTIR analyses alone. NMR spectroscopy was instrumental in determining the structures formed in the early sol-gel reactions of TEOS with formic acid. The ^{29}Si NMR spectra showed the evolution of different species produced during the early stages of condensation reactions including the mono and di substituted acyl compounds, hydrolyzed monomers, Q_1, Q_2, and Q_3 species.

A low rate of hydrolysis was inferred from the results of the silica NMR spectroscopy experiments. Few hydrolyzed monomers were detected from ^{29}Si NMR analyses. The first and second hydrolyzed monomers, $Si(OH)(OC_2H_5)_3$ and $Si(OH)_2(OC_2H_5)_2$, were the only observed monomers. The condensation products also were predominantly comprised of OR functional groups. Therefore, ^{29}Si NMR spectroscopy was useful for identifying the soluble low molecular weight species produced in the reaction of formic acid with TEOS.

^{1}H NMR spectroscopy was used to detect the byproducts of the sol-gel reaction of TEOS with formic acid. Ethanol and ethyl formate were identified as the major

byproducts. During the early stages of reaction, ethyl formate was the major byproduct. As the reaction progressed, ethanol concentration significantly increased and became the major byproduct. Water was not identified in the proton NMR spectroscopy. This indicated that hydrolysis and esterification reactions were negligible in the reaction of formic acid with TEOS to form sol-gels.

Information regarding the size of the oligomeric structures was obtained from USAXS and mass spectrometry. USAXS results were used to obtain radii of gyration. For the r = 2 system, no scattering was detected after 2 days of reaction. R_g values were only obtained for the r = 6 formic acid to TEOS reaction. As the reactions progressed, the R_g ranged from 5 nm to 9 nm for the r = 6 system. The radius of gyration did not increase beyond 9 nm even after gelation occurred. Porod slopes were not obtainable from the USAXS experiments.

Mass spectrometry was useful for determining the structures of the high molecular weight species. Molecular weights greater than 700 amu were analyzed in the reactions of formic acid with TEOS. Results for the r = 6 formic acid to TEOS reaction indicated that most species contained 4 membered Si rings. Also, the predominance of OR functional groups in these oligomeric silica compounds was apparent.

The results of FTIR spectroscopy, NMR Spectroscopy, USAXS, and mass spectrometry yielded insight into the reaction of formic acid with TEOS. All the analytical methods provided analogous results. The published results of conventional water, alkoxide, alcohol, protic acid system was compared to this novel method of producing sol-gels.

Higher rates of condensation were observed in the formic acid/TEOS reactions. Furthermore, fewer cyclic species were formed in the early stages of reaction in the formic acid catalyzed sol-gel reactions. As the reactions progressed, larger R_g values were obtained which indicated that sol-gels produced from formic acid resulted in larger structures. These differences ultimately contributed to rapid gelation for the reaction of formic acid with TEOS.

A kinetic model was proposed for the reaction of formic acid with TEOS. Rate constants were determined from the results of FTIR and NMR spectroscopy. The reaction of formic acid with SiOR groups was rate determining. Condensation reactions proceeded more readily when SiOH groups were present. The kinetic model predicted small quantities of water.

Future Work

The investigations of the reaction of formic acid with TEOS performed thus far have given some insight into the these sol-gel reactions. However, additional studies need to be performed. Future work needs to be done to confirm the ^{29}Si NMR assignments. The NMR theory of silicon alkoxides needs to be studied to enable apriori predictions of the chemical shifts for the condensation products. Particularly, the effect of formyl groups on the chemical shifts must be assessed because numerous authors have reported theoretical calculations for the species in the conventional TEOS, ethanol, water, and protic acid. Proton NMR spectroscopy and ^{17}O NMR spectroscopy

studies need to be performed to explore the role of water in the reaction of formic acid with TEOS.

Additional FTIR studies would also provide valuable information. FTIR spectra taken during the course of the reaction by flowing the individual reactants into the cell compartment would provide information on the early stages of the reaction . FTIR spectra can be obtained in time intervals of 200 ms. This will be particularly useful for analyzing very high molar ratios of formic acid to TEOS and for transition metal alkoxides which react extremely fast.

SAXS experiments will enable determination of the types of structures formed in the formic acid. The porod slope can be obtained for the reaction of formic acid with TEOS. This information will give an indication of the structural morphology of the oligomers. The types of structures formed can also be assessed from mass spectrometry. Preliminary mass spectrometry experiments have been performed; however, a more comprehensive investigation needs to be performed.

Additional work needs to be done to model the formic acid/TEOS system. Hydrolysis reactions must be accounted for in the kinetic model. Recursive mathematics should be investigated as a means of developing a kinetic model that will account for structure type.

The aforementioned studies need to be extended to transition metal alkoxides. The increased reactivity of these compounds complicates the investigation of these species. NMR spectroscopy and mass spectrometry experiments require extensive preparation; therefore, alternative analytical methods must be employed. Mixed and

pure titanium derived and zirconium derived sol-gel reactions need to be investigated using flow through FTIR analyses.

APPENDIX A: FTIR SPECTRA

KEY:

Spectrums labeled H: 24°C, r = 5.93

J: 30°C, r = 5.93

I: 40°C, r = 5.93

L: 40°C, r = 1.00

K: 40°C, r = 2.20

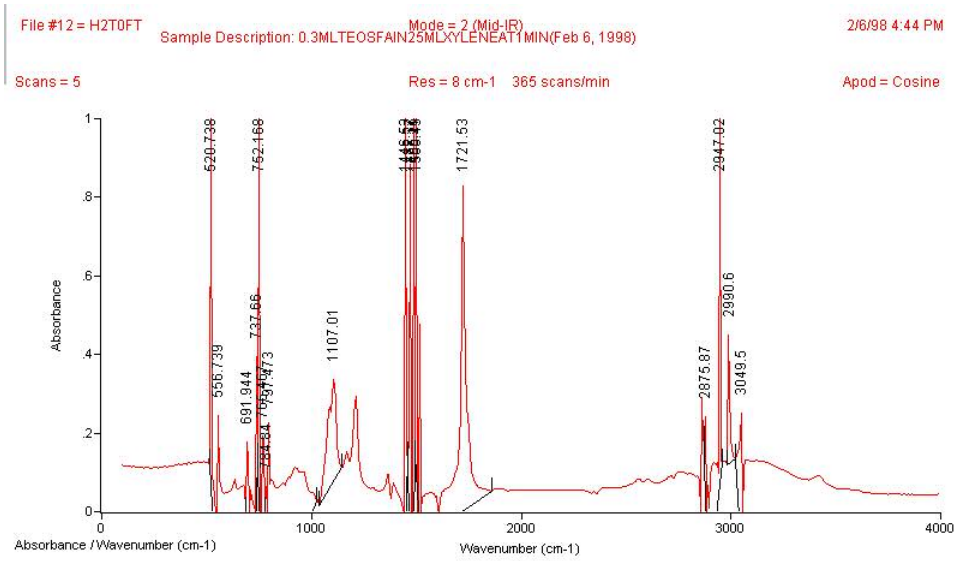
File #12 = H2T0FT
Mode = 2 (Mid-IR)
Sample Description: 0.3MLTEOSFAIN25MLXYLENEAT1MIN(Feb 6, 1998)
2/6/98 4:44 PM
Scans = 5
Res = 8 cm-1 365 scans/min
Apod = Cosine
Absorbance
Absorbance / Wavenumber (cm-1)
Wavenumber (cm-1)
620.738
752.168
1721.53
2947.02
2990.6
1107.01
737.66
556.739
691.944
2875.87
3049.5

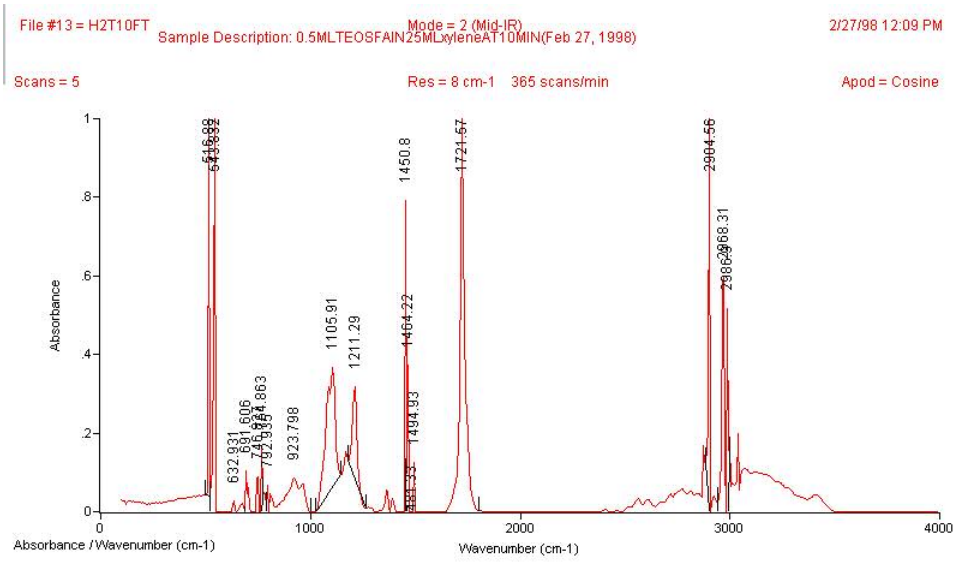
File #13 = H2T10FT
Mode = 2 (Mid-IR)
Sample Description: 0.5MLTEOSFAIN25MLxyleneAT10MIN(Feb 27, 1998)
2/27/98 12:09 PM
Scans = 5
Res = 8 cm-1 365 scans/min
Apod = Cosine
Absorbance
Absorbance / Wavenumber (cm-1)
Wavenumber (cm-1)
1450.8
1721.57
2904.56
2968.31
1105.91
1211.29
1464.22
923.798
632.931
691.606

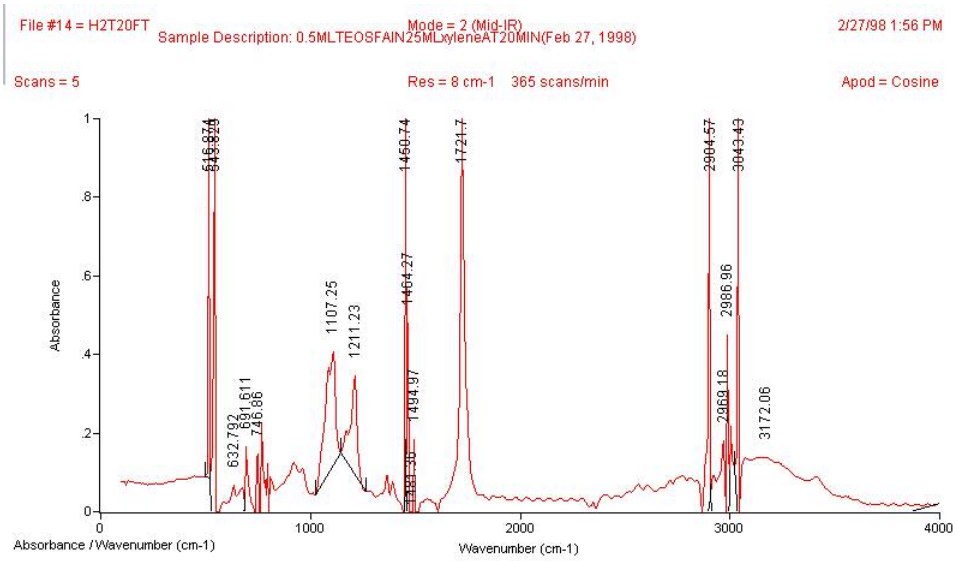
File #14 = H2T20FT
Mode = 2 (Mid-IR)
Sample Description: 0.5MLTEOSFAIN25MLxyleneAT20MIN(Feb 27, 1998)
2/27/98 1:56 PM
Scans = 5
Res = 8 cm-1 365 scans/min
Apod = Cosine
Absorbance
Absorbance / Wavenumber (cm-1)
Wavenumber (cm-1)
516.874
632.792
746.86
1107.25
1211.23
1450.74
1464.27
1494.97
1721.7
2904.57
2986.96
2969.18
3043.43
3172.06

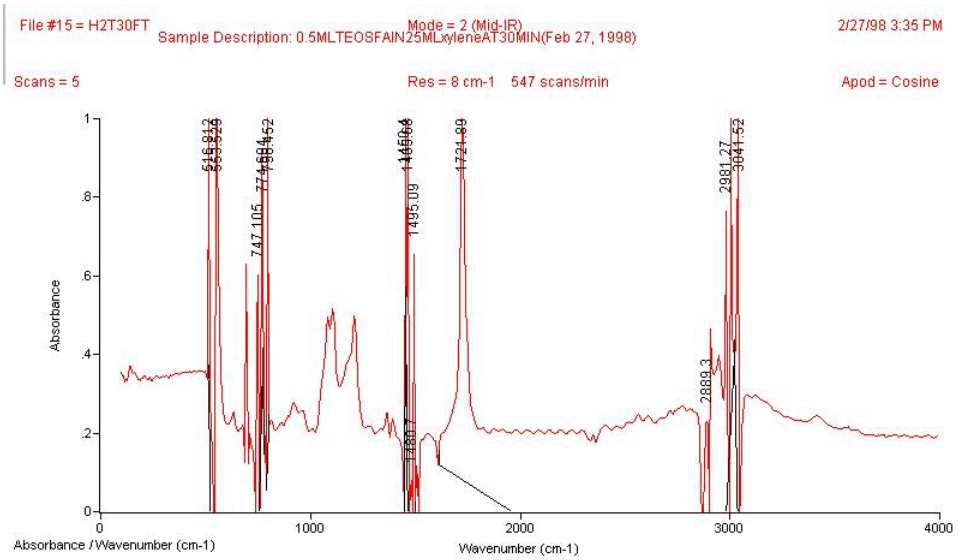
File #15 = H2T30FT
Mode = 2 (Mid-IR)
Sample Description: 0.5MLTEOSFAIN25MLxyleneAT30MIN(Feb 27, 1998)
2/27/98 3:35 PM
Scans = 5
Res = 8 cm-1 547 scans/min
Apod = Cosine
Absorbance
Absorbance / Wavenumber (cm-1)
Wavenumber (cm-1)
747.105
1495.09
1721.89
2889.3
2981.27
3041.52

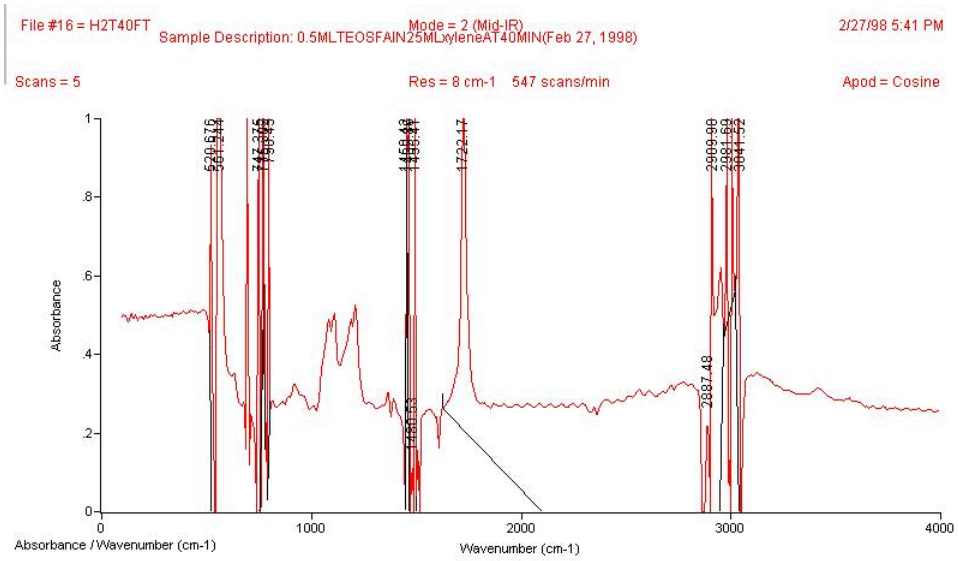
File #16 = H2T40FT
Mode = 2 (Mid-IR)
2/27/98 5:41 PM
Sample Description: 0.5MLTEOSFAIN25MLxyleneAT40MIN(Feb 27, 1998)
Scans = 5
Res = 8 cm-1 547 scans/min
Apod = Cosine
Absorbance
Wavenumber (cm-1)
Absorbance / Wavenumber (cm-1)
2887.48

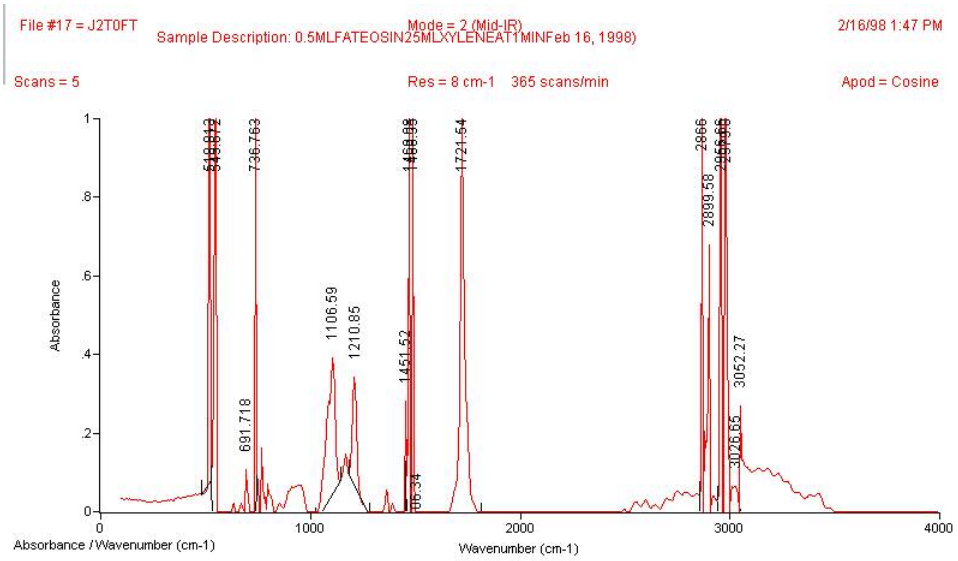
File #17 = J2T0FT
Mode = 2 (Mid-IR)
2/16/98 1:47 PM
Sample Description: 0.5MLFATEOSIN25MLXYLENEAT1MINFeb 16, 1998)
Scans = 5
Res = 8 cm-1 365 scans/min
Apod = Cosine
Absorbance
Absorbance / Wavenumber (cm-1)
Wavenumber (cm-1)
736.763
1721.64
2899.58
1106.59
1210.85
1451.52
691.718
3052.27
3026.65

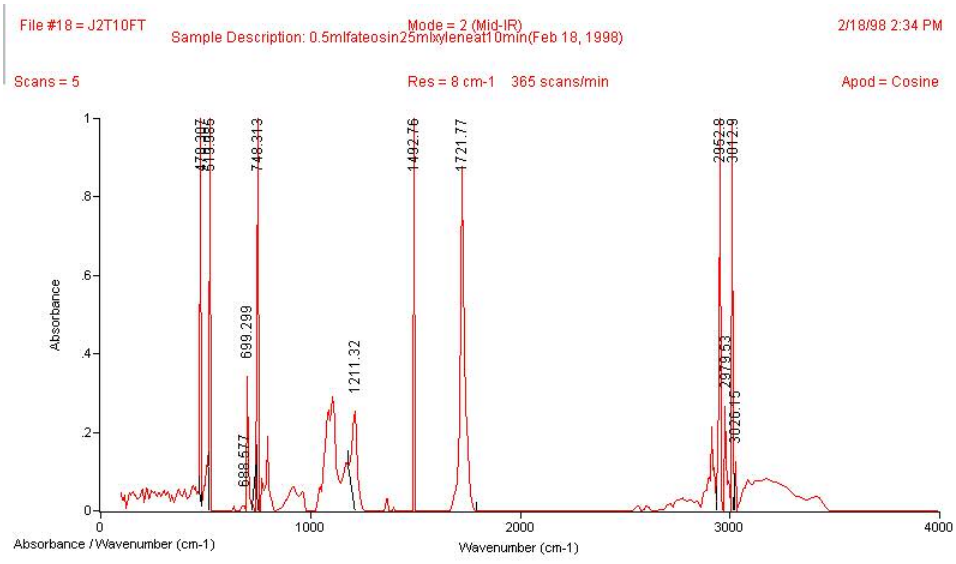
File #18 = J2T10FT
Mode = 2 (Mid-IR)
2/18/98 2:34 PM
Sample Description: 0.5mlfateosin25mlxyleneat10min(Feb 18, 1998)
Scans = 5
Res = 8 cm-1 365 scans/min
Apod = Cosine
Absorbance
Absorbance / Wavenumber (cm-1)
Wavenumber (cm-1)
748.313
1492.76
1721.77
699.299
1211.32
688.577
2978.53
3026.15

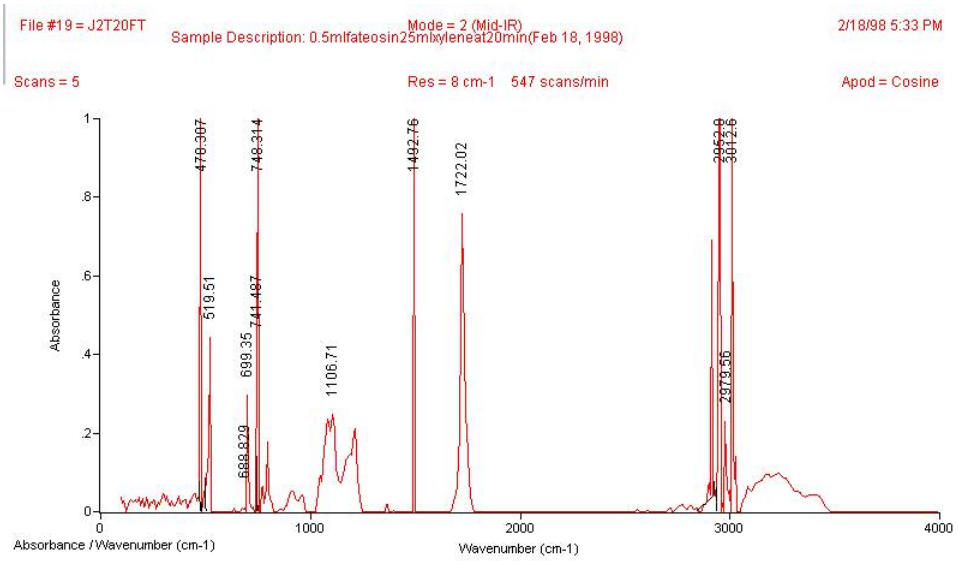
File #19 = J2T20FT
Mode = 2 (Mid-IR)
2/18/98 5:33 PM
Sample Description: 0.5mlfateosin25mlxyleneat20min(Feb 18, 1998)
Scans = 5
Res = 8 cm-1 547 scans/min
Apod = Cosine
Absorbance
Absorbance / Wavenumber (cm-1)
Wavenumber (cm-1)
470.307
519.51
688.829
699.35
741.497
748.314
1106.71
1492.76
1722.02
2953.9
3012.6
2979.56

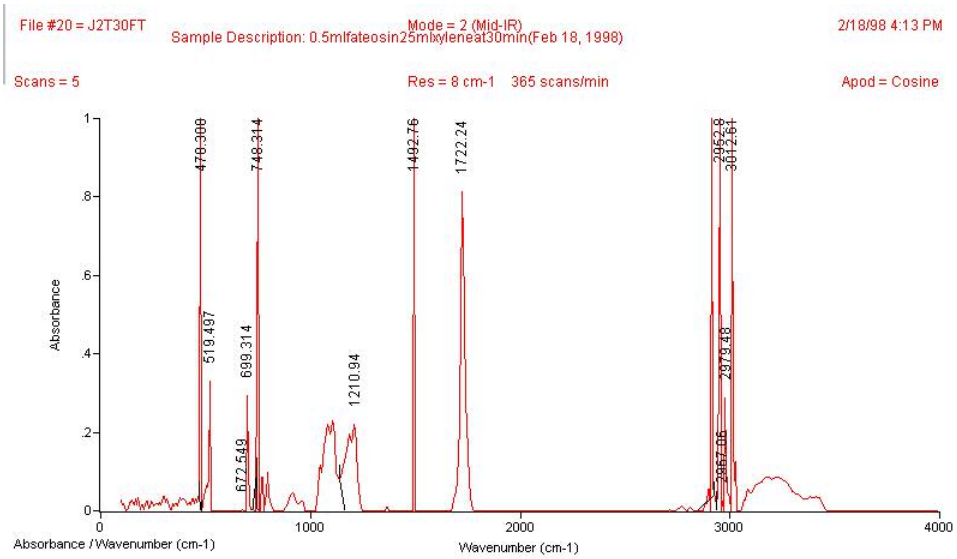
File #20 = J2T30FT
Mode = 2 (Mid-IR)
2/18/98 4:13 PM
Sample Description: 0.5mlfateosin25mlxyleneat30min(Feb 18, 1998)
Scans = 5
Res = 8 cm-1 365 scans/min
Apod = Cosine
Absorbance
Absorbance / Wavenumber (cm-1)
Wavenumber (cm-1)
470.300
519.497
672.549
699.314
748.314
1210.94
1492.76
1722.24
2952.8
3012.61
2979.48
3067.06

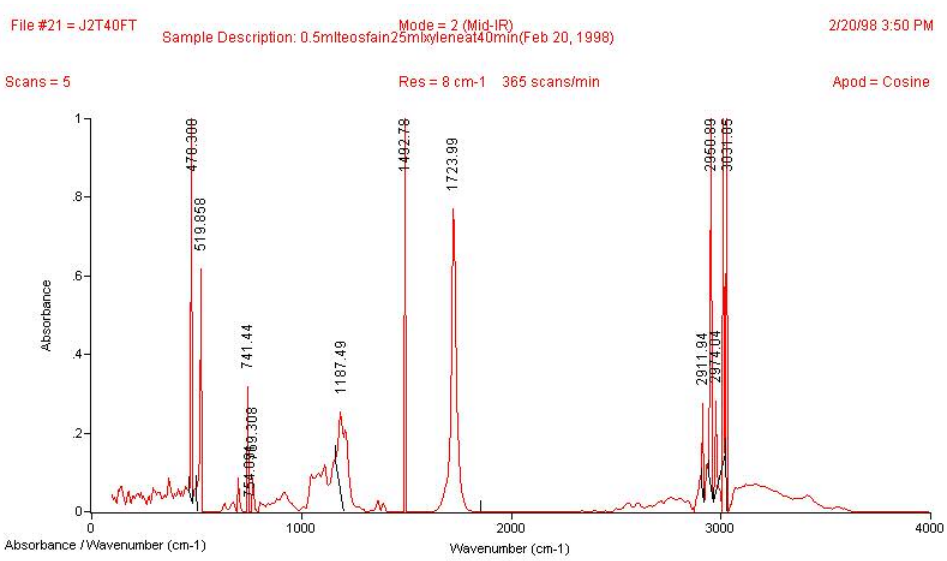
File #21 = J2T40FT
Mode = 2 (Mid-IR)
2/20/98 3:50 PM
Sample Description: 0.5mlteosfain25mlxyleneat40min(Feb 20, 1998)
Scans = 5
Res = 8 cm-1 365 scans/min
Apod = Cosine
Absorbance
Absorbance / Wavenumber (cm-1)
Wavenumber (cm-1)
470.300
519.858
741.44
1187.49
1492.78
1723.99
2911.94
2974.04
3031.85
0
.2
.4
.6
.8
1
0
1000
2000
3000
4000

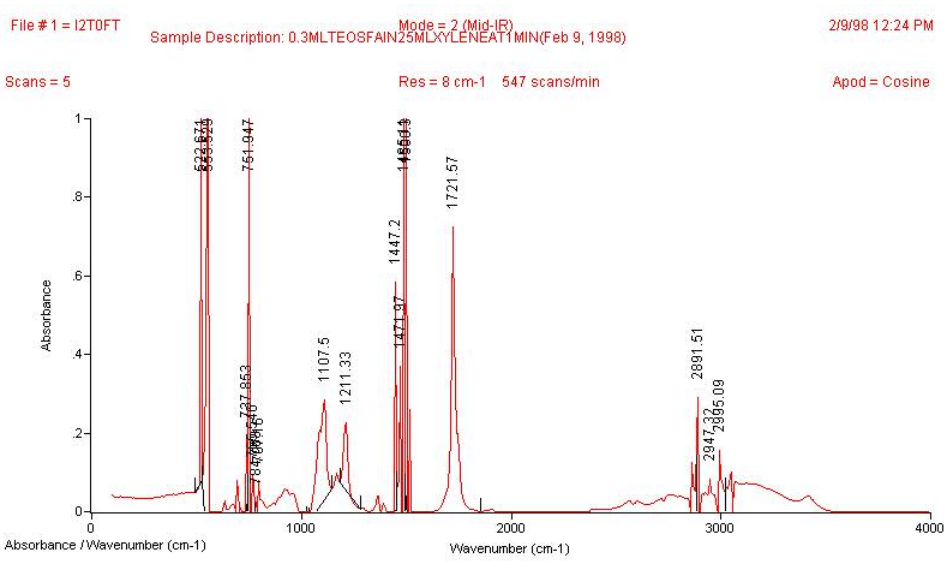
File # 1 = I2T0FT
Mode = 2 (Mid-IR)
2/9/98 12:24 PM
Sample Description: 0.3MLTEOSFAIN25MLXYLENEAT1MIN(Feb 9, 1998)
Scans = 5
Res = 8 cm-1 547 scans/min
Apod = Cosine
Absorbance
751.947
1721.57
1447.2
1471.97
1107.5
1211.33
2891.51
2947.32
2885.09
Absorbance / Wavenumber (cm-1)
Wavenumber (cm-1)

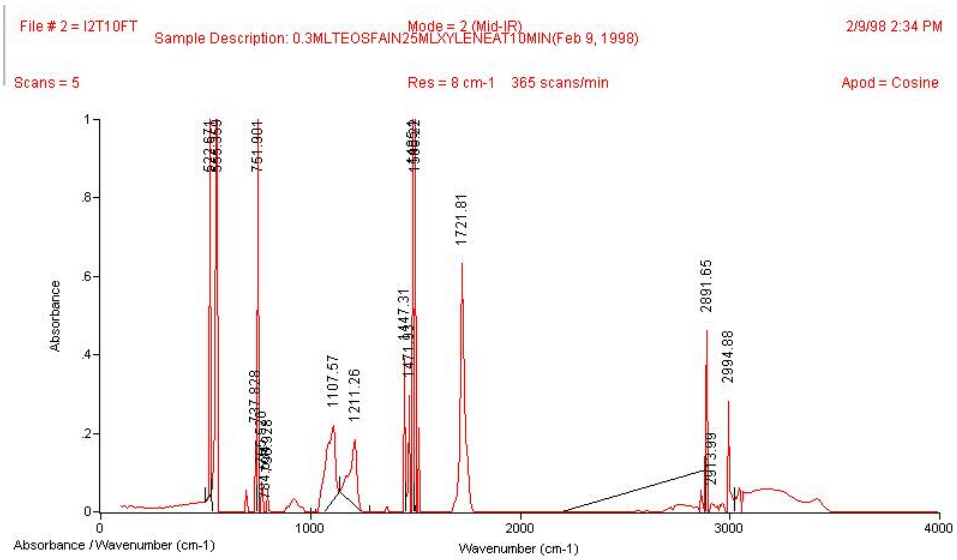
File # 2 = I2T10FT
Mode = 2 (Mid-IR)
2/9/98 2:34 PM
Sample Description: 0.3MLTEOSFAIN25MLXYLENEAT10MIN(Feb 9, 1998)
Scans = 5
Res = 8 cm-1 365 scans/min
Apod = Cosine
Absorbance
751.001
1721.81
1447.31
1107.57
1211.26
2891.65
2994.88
2913.99
Absorbance / Wavenumber (cm-1)
Wavenumber (cm-1)

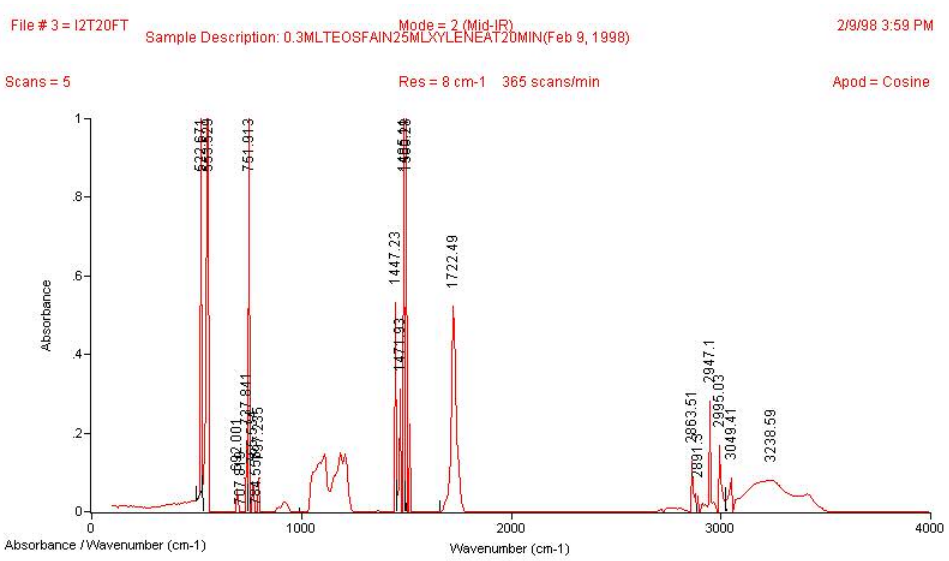
File # 3 = I2T20FT
Mode = 2 (Mid-IR)
2/9/98 3:59 PM
Sample Description: 0.3MLTEOSFAIN25MLXYLENEAT20MIN(Feb 9, 1998)
Scans = 5
Res = 8 cm-1 365 scans/min
Apod = Cosine
Absorbance
751.913
1447.23
1722.49
2863.51
2947.1
2995.03
3049.41
3238.59
Absorbance / Wavenumber (cm-1)
Wavenumber (cm-1)

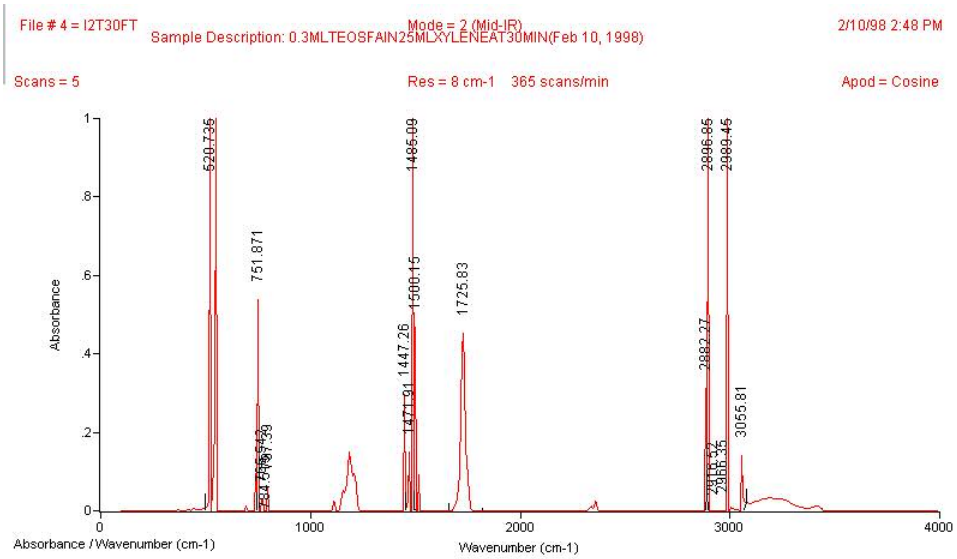
File # 4 = I2T30FT
Mode = 2 (Mid-IR)
2/10/98 2:48 PM
Sample Description: 0.3MLTEOSFAIN25MLXYLENEAT30MIN(Feb 10, 1998)
Scans = 5
Res = 8 cm-1 365 scans/min
Apod = Cosine
Absorbance
520.735
751.871
1485.09
1500.15
1725.83
2896.85
2989.45
Absorbance / Wavenumber (cm-1)
Wavenumber (cm-1)

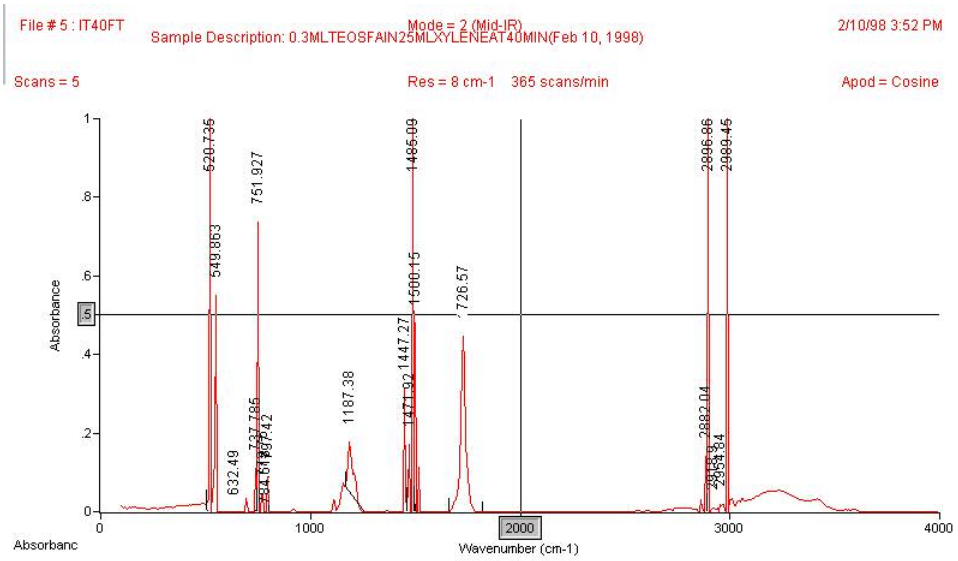
File # 5 : IT40FT
Mode = 2 (Mid-IR)
2/10/98 3:52 PM
Sample Description: 0.3MLTEOSFAIN25MLXYLENEAT40MIN(Feb 10, 1998)
Scans = 5
Res = 8 cm-1 365 scans/min
Apod = Cosine
Absorbance
Absorbanc
Wavenumber (cm-1)
620.735
751.927
549.863
1486.09
1500.15
726.57
1187.38
1447.27
2896.86
2980.45
2882.04
632.49
737.786
2954.84

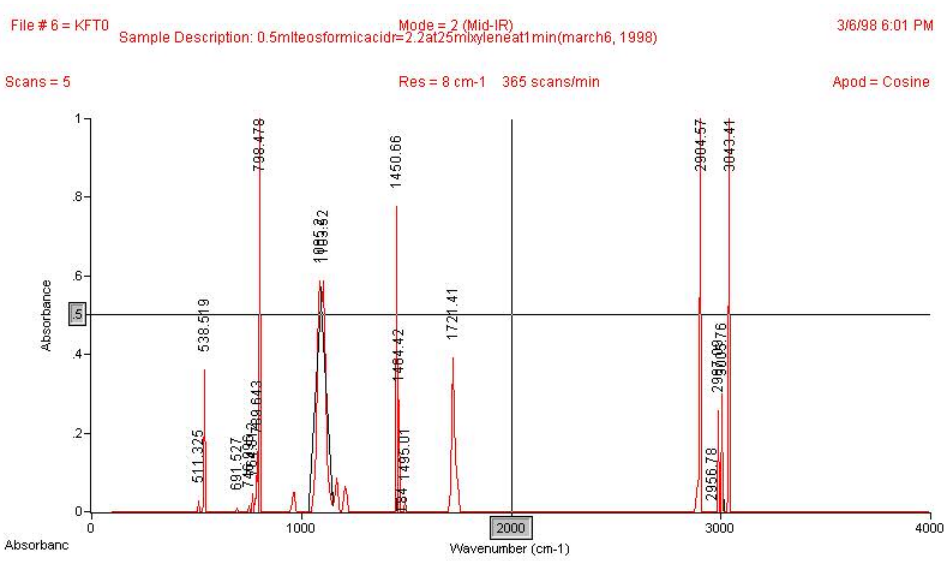
File # 6 = KFT0
Mode = 2 (Mid-IR)
3/6/98 6:01 PM
Sample Description: 0.5mlteosformicacidr=2.2at25mlxyleneat1min(march6, 1998)
Scans = 5
Res = 8 cm-1 365 scans/min
Apod = Cosine
Absorbance
Absorbanc
Wavenumber (cm-1)
538.519
798.478
1450.66
1721.41
2964.57
3043.41
511.325
691.527
1464.42
1495.01
2956.78
2000

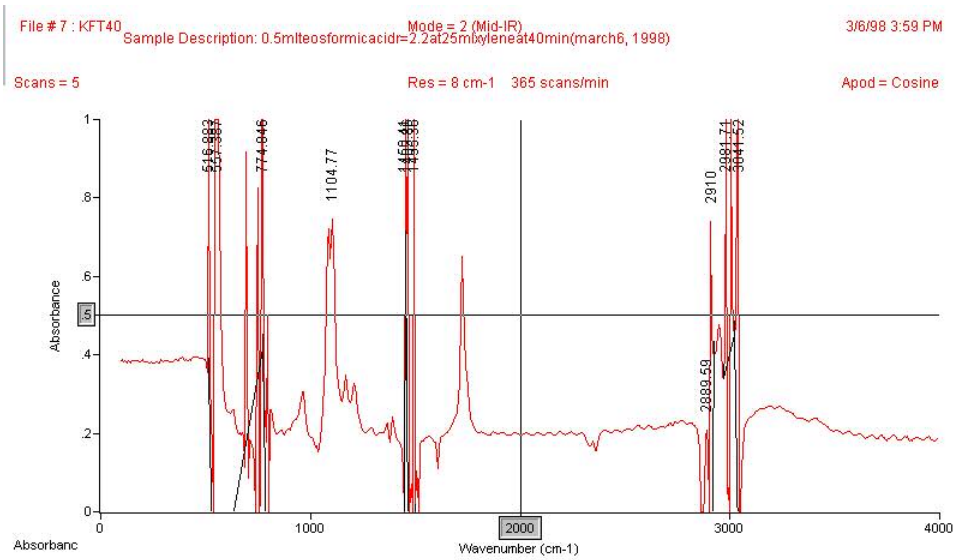
File # 7 : KFT40
Mode = 2 (Mid-IR)
3/6/98 3:59 PM
Sample Description: 0.5mlteosformicacidr=2.2at25mlxyleneat40min(march6, 1998)
Scans = 5
Res = 8 cm-1 365 scans/min
Apod = Cosine
Absorbance
Absorbanc
Wavenumber (cm-1)
774.046
1104.77
2910
2889.59
3041.52
2000

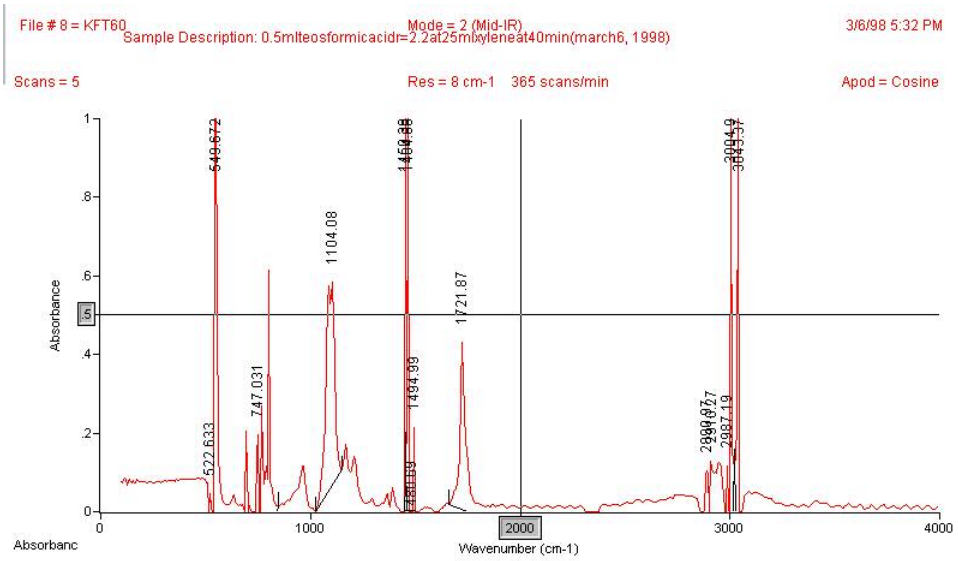
File # 8 = KFT60
Mode = 2 (Mid-IR)
3/6/98 5:32 PM
Sample Description: 0.5mlteosformicacidr=2.2at25mlxyleneat40min(march6, 1998)
Scans = 5
Res = 8 cm-1 365 scans/min
Apod = Cosine
Absorbance
549.672
1104.08
1460.88
1721.87
747.031
1494.99
522.633
2987.19
Absorbanc
Wavenumber (cm-1)

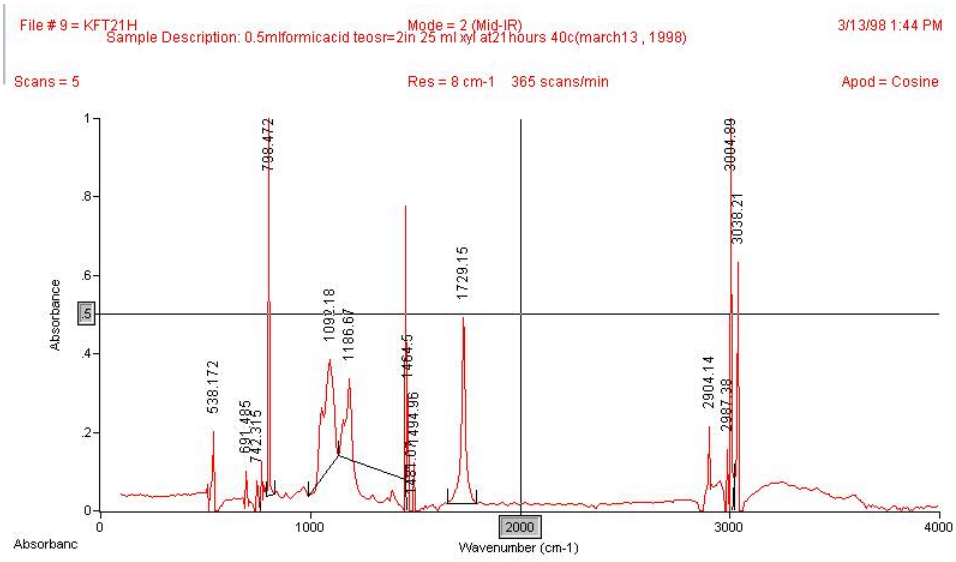
File # 9 = KFT21H
Mode = 2 (Mid-IR)
3/13/98 1:44 PM
Sample Description: 0.5mlformicacid teosr=2in 25 ml xyl at21hours 40c(march13 , 1998)
Scans = 5
Res = 8 cm-1 365 scans/min
Apod = Cosine
Absorbance
798.472
3084.89
3038.21
1729.15
1092.18
1186.67
1464.5
538.172
691.485
742.315
1494.96
2904.14
2987.38
Absorbanc
Wavenumber (cm-1)

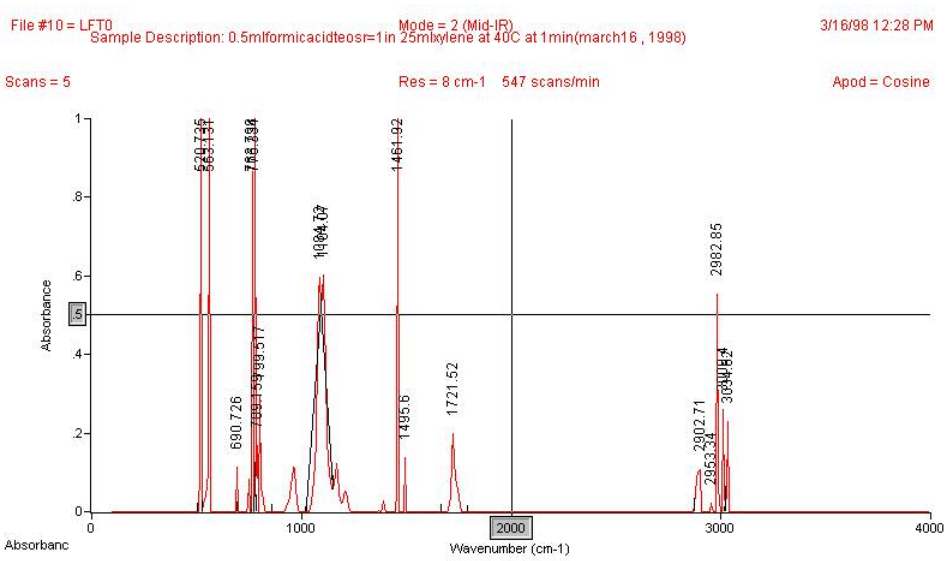
File #10 = LFT0
Mode = 2 (Mid-IR)
3/16/98 12:28 PM
Sample Description: 0.5mlformicacidteosr=1in 25mlxylene at 40C at 1min(march16 , 1998)
Scans = 5
Res = 8 cm-1 547 scans/min
Apod = Cosine
Absorbance
Wavenumber (cm-1)
1461.92
2982.85
1721.52
1495.6
690.726
2902.71
2953.34

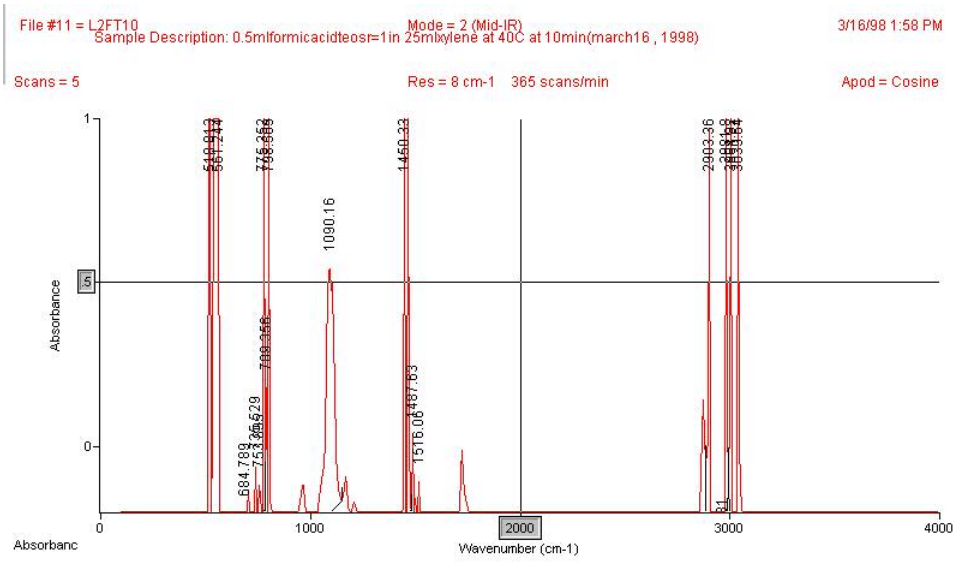
File #11 = L2FT10
Mode = 2 (Mid-IR)
3/16/98 1:58 PM
Sample Description: 0.5mlformicacidteosr=1in 25mlxylene at 40C at 10min(march16 , 1998)
Scans = 5
Res = 8 cm-1 365 scans/min
Apod = Cosine
Absorbance
Wavenumber (cm-1)
1450.33
1090.16
2903.36
1516.06
1487.63
684.789

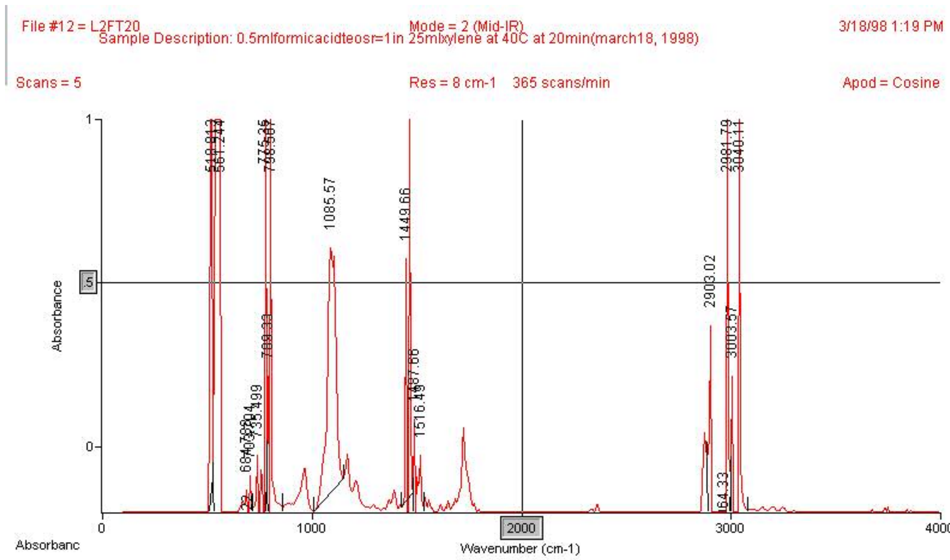
File #12 = L2FT20
Mode = 2 (Mid-IR)
3/18/98 1:19 PM
Sample Description: 0.5mlformicacidteosr=1in 25mlxylene at 40C at 20min(march18, 1998)
Scans = 5
Res = 8 cm-1 365 scans/min
Apod = Cosine
Absorbance
1085.57
1449.66
2903.02
Absorbanc
Wavenumber (cm-1)

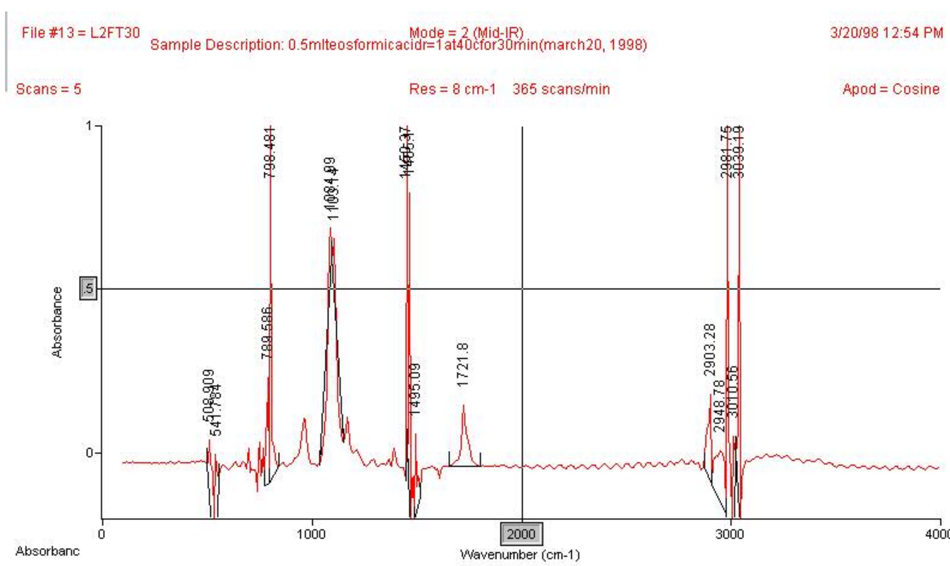
File #13 = L2FT30
Mode = 2 (Mid-IR)
3/20/98 12:54 PM
Sample Description: 0.5mlteosformicacidr=1at40cfor30min(march20, 1998)
Scans = 5
Res = 8 cm-1 365 scans/min
Apod = Cosine
Absorbance
799.481
789.586
1495.09
1721.8
2903.28
Absorbanc
Wavenumber (cm-1)

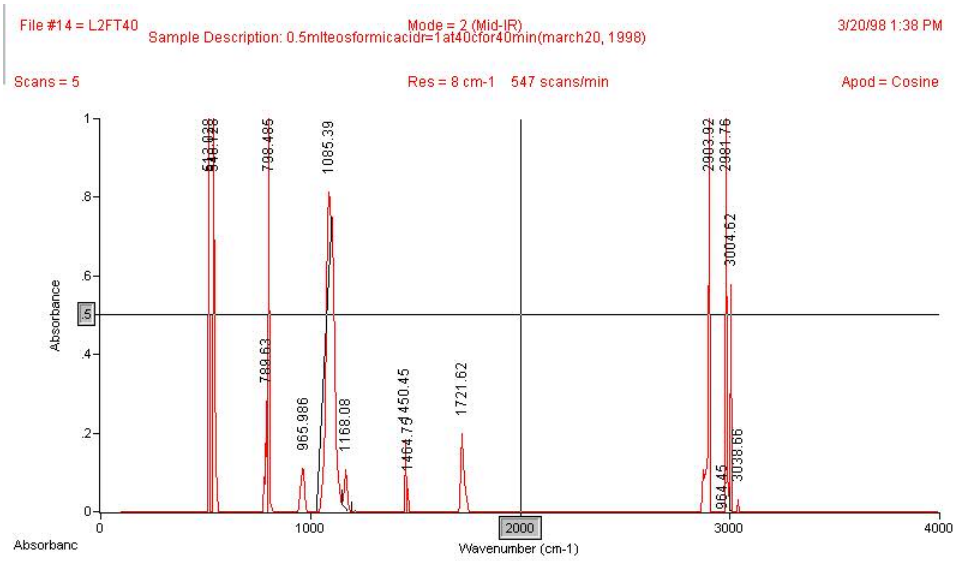
File #14 = L2FT40
Mode = 2 (Mid-IR)
3/20/98 1:38 PM
Sample Description: 0.5mlteosformicacidr=1at40cfor40min(march20, 1998)
Scans = 5
Res = 8 cm-1 547 scans/min
Apod = Cosine
Absorbance
Absorbanc
Wavenumber (cm-1)
798.495
1085.39
2903.92
2981.76
3004.62
789.63
965.986
1168.08
1450.45
1721.62
3038.66
964.45
0
1000
2000
3000
4000

Appendix B: Macro for Structure Determination of Si Compound

```
MACRO FOR DETERMINING THE STRUCTURE
OF SI COMPOUND
=INPUT("POTASSIUM OR SODIUM CATIONS",3)
=COUNTA(M:M)
=FOR("P",1,B172)
=SELECT(M1)
=IF(ISBLANK(ACTIVE.CELL()))
=SELECT(OFFSET(ACTIVE.CELL(),1,0))
=GOTO(B175)


=ELSE()
=SET.NAME("MW",ACTIVE.CELL())
=END.IF()
=SET.NAME("CATION",B171)
=IF(CATION="POTASSIUM")
=SET.NAME("MW",MW-39)
=END.IF()
=IF(CATION="SODIUM")
=SET.NAME("MW",MW-23)
=END.IF()
=FORMULA(CATION,A5)
=CLEAR()




=SELECT(A7:K140)
=CLEAR(3)

=MW
=FORMULA(MW,A7)
=0.9223*(28)+(0.0467*29)+(0.031*30)
16
17
45

=FOR("n",1,30)
=n*B202
=(n-1)*B203
=FOR("x",0,(2*n+2))
=x*B205
=((2*n+2)-x)*B204
=B212+B211+si+B209
=SET.NAME("OR",x)
=SET.NAME("OH",(2*n+2-x))
=SET.NAME("MWCALC",B213)
```

```
=SET.NAME("o",(n-1))

=IF(ABS(B200-B213)<2)
=SELECT(B7)
=IF(ISBLANK(ACTIVE.CELL()))
=FORMULA(n)
=SELECT(OFFSET(ACTIVE.CELL(),0,1))
=FORMULA(o)
=SELECT(OFFSET(ACTIVE.CELL(),0,1))
=FORMULA(OH)
=SELECT(OFFSET(ACTIVE.CELL(),0,1))
=FORMULA(OR)
=SELECT(OFFSET(ACTIVE.CELL(),0,1))
=FORMULA(MWCALC)
=ELSE()
=SELECT(,"R[1]C")
=GOTO($B$221)
=END.IF()
=END.IF()
=NEXT()
=NEXT()
=FOR("n",1,30)
=n*B202
=(n)*B203
=FOR("x",0,(2*n))
=x*B205
=((2*n)-x)*B204
=B243+B242+B239+B240
=SET.NAME("OR",x)
=SET.NAME("OH",(2*n-x))
=SET.NAME("MWCALC",B244)
=SET.NAME("o",(n))

=IF(ABS(B200-B244)<2)
=SELECT(B7)
=IF(ISBLANK(ACTIVE.CELL()))
=FORMULA(n)
=SELECT(OFFSET(ACTIVE.CELL(),0,1))
=FORMULA(o)
=SELECT(OFFSET(ACTIVE.CELL(),0,1))
=FORMULA(OH)
=SELECT(OFFSET(ACTIVE.CELL(),0,1))
=FORMULA(OR)
=SELECT(OFFSET(ACTIVE.CELL(),0,1))
=FORMULA(MWCALC)
=ELSE()
=SELECT(,"R[1]C")
=GOTO($B$252)
=END.IF()
=END.IF()
```

```
=NEXT()
=NEXT()
=FOR("n",1,30)
=n*B202
=(n+1)*B203
=FOR("x",0,(2*n-2))
=x*B205
=((2*n-2)-x)*B204
=B274+B273+B270+B271
=SET.NAME("OR",x)
=SET.NAME("OH",(2*n-2-x))
=SET.NAME("MWCALC",B275)
=SET.NAME("o",(n+1))

=IF(ABS(B200-B275)<2)
=SELECT(B7)
=IF(ISBLANK(ACTIVE.CELL()))
=FORMULA(n)
=SELECT(OFFSET(ACTIVE.CELL(),0,1))
=FORMULA(o)
=SELECT(OFFSET(ACTIVE.CELL(),0,1))
=FORMULA(OH)
=SELECT(OFFSET(ACTIVE.CELL(),0,1))
=FORMULA(OR)
=SELECT(OFFSET(ACTIVE.CELL(),0,1))
=FORMULA(MWCALC)
=ELSE()
=SELECT(,"R[1]C")
=GOTO($B$283)
=END.IF()
=END.IF()
=NEXT()
=NEXT()
=FOR("n",1,30)
=n*B202
=(n+2)*B203
=FOR("x",0,(2*n-4))
=x*B205
=((2*n-4)-x)*B204
=B305+B304+B301+B302
=SET.NAME("OR",x)
=SET.NAME("OH",(2*n-4-x))
=SET.NAME("MWCALC",B306)
=SET.NAME("o",(n+2))

=IF(ABS(B200-B306)<2)
=SELECT(B7)
=IF(ISBLANK(ACTIVE.CELL()))
=FORMULA(n)
=SELECT(OFFSET(ACTIVE.CELL(),0,1))
```

```
=FORMULA(o)
=SELECT(OFFSET(ACTIVE.CELL(),0,1))
=FORMULA(OH)
=SELECT(OFFSET(ACTIVE.CELL(),0,1))
=FORMULA(OR)
=SELECT(OFFSET(ACTIVE.CELL(),0,1))
=FORMULA(MWCALC)
```

=ELSE()
=SELECT(,"R[1]C")
=GOTO(B314)

```
=END.IF()
=END.IF()
=NEXT()
=NEXT()
=FOR("n",1,30)
=n*B202
=(n+3)*B203
=FOR("x",0,(2*n-6))
=x*B205
=((2*n-6)-x)*B204
=B336+B335+B332+B333
=SET.NAME("OR",x)
=SET.NAME("OH",(2*n-6-x))
=SET.NAME("MWCALC",B337)
=SET.NAME("o",(n+3))

=IF(ABS(B200-B337)<2)
=SELECT(B7)
```

=IF(ISBLANK(ACTIVE.CELL()))

```
=FORMULA(n)
=SELECT(OFFSET(ACTIVE.CELL(),0,1))
=FORMULA(o)
=SELECT(OFFSET(ACTIVE.CELL(),0,1))
=FORMULA(OH)
=SELECT(OFFSET(ACTIVE.CELL(),0,1))
=FORMULA(OR)
=SELECT(OFFSET(ACTIVE.CELL(),0,1))
=FORMULA(MWCALC)
```

=ELSE()
=SELECT(,"R[1]C")
=GOTO(B345)

```
=END.IF()
=END.IF()
=NEXT()
=NEXT()
=FOR("n",1,30)
=n*B202
=(n+4)*B203
=FOR("x",0,(2*n-8))
=x*B205
```

```
=((2*n-8)-x)*B204
=B367+B366+B363+B364
=SET.NAME("OR",x)
=SET.NAME("OH",(2*n-8-x))
=SET.NAME("MWCALC",B368)
=SET.NAME("o",(n+4))

=IF(ABS(B200-B368)<2)
=SELECT(B7)
=IF(ISBLANK(ACTIVE.CELL()))
=FORMULA(n)
=SELECT(OFFSET(ACTIVE.CELL(),0,1))
=FORMULA(o)
=SELECT(OFFSET(ACTIVE.CELL(),0,1))
=FORMULA(OH)
=SELECT(OFFSET(ACTIVE.CELL(),0,1))
=FORMULA(OR)
=SELECT(OFFSET(ACTIVE.CELL(),0,1))
=FORMULA(MWCALC)
=ELSE()
=SELECT(,"R[1]C")
=GOTO($B$376)
=END.IF()
=END.IF()
=NEXT()
=NEXT()
=FOR("n",1,30)
=n*B202
=(n+5)*B203
=FOR("x",0,(2*n-10))
=x*B205
=((2*n-10)-x)*B204
=B398+B397+B394+B395
=SET.NAME("OR",x)
=SET.NAME("OH",(2*n-10-x))
=SET.NAME("MWCALC",B399)
=SET.NAME("o",(n+5))

=IF(ABS(B200-B399)<2)
=SELECT(B7)
=IF(ISBLANK(ACTIVE.CELL()))
=FORMULA(n)
=SELECT(OFFSET(ACTIVE.CELL(),0,1))
=FORMULA(o)
=SELECT(OFFSET(ACTIVE.CELL(),0,1))
=FORMULA(OH)
=SELECT(OFFSET(ACTIVE.CELL(),0,1))
=FORMULA(OR)
=SELECT(OFFSET(ACTIVE.CELL(),0,1))
=FORMULA(MWCALC)
```

```
=ELSE()
=SELECT(,"R[1]C")
=GOTO($B$407)
=END.IF()
=END.IF()
=NEXT()
=NEXT()
=FOR("n",1,30)
=n*B202
=(n+6)*B203
=FOR("x",0,(2*n-12))
=x*B205
=((2*n-12)-x)*B204
=B429+B428+B425+B426
=SET.NAME("OR",x)
=SET.NAME("OH",(2*n-12-x))
=SET.NAME("MWCALC",B430)
=SET.NAME("o",(n+6))

=IF(ABS(B200-B430)<2)
=SELECT(B7)
=IF(ISBLANK(ACTIVE.CELL()))
=FORMULA(n)
=SELECT(OFFSET(ACTIVE.CELL(),0,1))
=FORMULA(o)
=SELECT(OFFSET(ACTIVE.CELL(),0,1))
=FORMULA(OH)
=SELECT(OFFSET(ACTIVE.CELL(),0,1))
=FORMULA(OR)
=SELECT(OFFSET(ACTIVE.CELL(),0,1))
=FORMULA(MWCALC)
=ELSE()
=SELECT(,"R[1]C")
=GOTO($B$438)
=END.IF()
=END.IF()
=NEXT()
=NEXT()
=FOR("n",1,30)
=n*B202
=(n+7)*B203
=FOR("x",0,(2*n-14))
=x*B205
=((2*n-14)-x)*B204
=B460+B459+B456+B457
=SET.NAME("OR",x)
=SET.NAME("OH",(2*n-14-x))
=SET.NAME("MWCALC",B461)
=SET.NAME("o",(n+7))
```

```
=IF(ABS(B200-B461)<2)
=SELECT(B7)
=IF(ISBLANK(ACTIVE.CELL()))
=FORMULA(n)
=SELECT(OFFSET(ACTIVE.CELL(),0,1))
=FORMULA(o)
=SELECT(OFFSET(ACTIVE.CELL(),0,1))
=FORMULA(OH)
=SELECT(OFFSET(ACTIVE.CELL(),0,1))
=FORMULA(OR)
=SELECT(OFFSET(ACTIVE.CELL(),0,1))
=FORMULA(MWCALC)
=ELSE()
=SELECT(,"R[1]C")
=GOTO($B$469)
=END.IF()
=END.IF()
=NEXT()
=NEXT()
=FOR("n",1,30)
=n*B202
=(n+8)*B203
=FOR("x",0,(2*n-16))
=x*B205
=((2*n-16)-x)*B204
=B491+B490+B487+B488
=SET.NAME("OR",x)
=SET.NAME("OH",(2*n-16-x))
=SET.NAME("MWCALC",B492)
=SET.NAME("o",(n+8))

=IF(ABS(B200-B492)<2)
=SELECT(B7)
=IF(ISBLANK(ACTIVE.CELL()))
=FORMULA(n)
=SELECT(OFFSET(ACTIVE.CELL(),0,1))
=FORMULA(o)
=SELECT(OFFSET(ACTIVE.CELL(),0,1))
=FORMULA(OH)
=SELECT(OFFSET(ACTIVE.CELL(),0,1))
=FORMULA(OR)
=SELECT(OFFSET(ACTIVE.CELL(),0,1))
=FORMULA(MWCALC)
=ELSE()
=SELECT(,"R[1]C")
=GOTO($B$500)
=END.IF()
=END.IF()
=NEXT()
=NEXT()
```

```
=FOR("n",1,30)
=n*B202
=(n+9)*B203
=FOR("x",0,(2*n-18))
=x*B205
=((2*n-18)-x)*B204
=B522+B521+B518+B519
=SET.NAME("OR",x)
=SET.NAME("OH",(2*n-18-x))
=SET.NAME("MWCALC",B523)
=SET.NAME("o",(n+9))

=IF(ABS(B200-B523)<2)
=SELECT(B7)
=IF(ISBLANK(ACTIVE.CELL()))
=FORMULA(n)
=SELECT(OFFSET(ACTIVE.CELL(),0,1))
=FORMULA(o)
=SELECT(OFFSET(ACTIVE.CELL(),0,1))
=FORMULA(OH)
=SELECT(OFFSET(ACTIVE.CELL(),0,1))
=FORMULA(OR)
=SELECT(OFFSET(ACTIVE.CELL(),0,1))
=FORMULA(MWCALC)
=ELSE()
=SELECT(,"R[1]C")
=GOTO($B$531)
=END.IF()
=END.IF()
=NEXT()
=NEXT()
=FOR("n",1,30)
=n*B202
=(n+10)*B203
=FOR("x",0,(2*n-20))
=x*B205
=((2*n-20)-x)*B204
=B553+B552+B549+B550
=SET.NAME("OR",x)
=SET.NAME("OH",(2*n-20-x))
=SET.NAME("MWCALC",B554)
=SET.NAME("o",(n+10))

=IF(ABS(B200-B554)<2)
=SELECT(B7)
=IF(ISBLANK(ACTIVE.CELL()))
=FORMULA(n)
=SELECT(OFFSET(ACTIVE.CELL(),0,1))
=FORMULA(o)
=SELECT(OFFSET(ACTIVE.CELL(),0,1))
```

=FORMULA(OH)
=SELECT(OFFSET(ACTIVE.CELL(),0,1))
=FORMULA(OR)
=SELECT(OFFSET(ACTIVE.CELL(),0,1))
=FORMULA(MWCALC)
=ELSE()
=SELECT(,"R[1]C")
=GOTO(B562)
=END.IF()
=END.IF()
=NEXT()
=NEXT()
=FOR("n",1,30)
=n*B202
=(n+11)*B203
=FOR("x",0,(2*n-22))
=x*B205
=((2*n-22)-x)*B204
=B584+B583+B580+B581
=SET.NAME("OR",x)
=SET.NAME("OH",(2*n-22-x))
=SET.NAME("MWCALC",B585)
=SET.NAME("o",(n+11))

=IF(ABS(B200-B585)<2)
=SELECT(B7)
=IF(ISBLANK(ACTIVE.CELL()))
=FORMULA(n)
=SELECT(OFFSET(ACTIVE.CELL(),0,1))
=FORMULA(o)
=SELECT(OFFSET(ACTIVE.CELL(),0,1))
=FORMULA(OH)
=SELECT(OFFSET(ACTIVE.CELL(),0,1))
=FORMULA(OR)
=SELECT(OFFSET(ACTIVE.CELL(),0,1))
=FORMULA(MWCALC)
=ELSE()
=SELECT(,"R[1]C")
=GOTO(B593)
=END.IF()
=END.IF()
=NEXT()
=NEXT()
=FOR("n",1,30)
=n*B202
=(n+12)*B203
=FOR("x",0,(2*n-24))
=x*B205
=((2*n-24)-x)*B204
=B615+B614+B611+B612

```
=SET.NAME("OR",x)
=SET.NAME("OH",(2*n-24-x))
=SET.NAME("MWCALC",B616)
=SET.NAME("o",(n+12))

=IF(ABS(B200-B616)<2)
=SELECT(B7)
=IF(ISBLANK(ACTIVE.CELL()))
=FORMULA(n)
=SELECT(OFFSET(ACTIVE.CELL(),0,1))
=FORMULA(o)
=SELECT(OFFSET(ACTIVE.CELL(),0,1))
=FORMULA(OH)
=SELECT(OFFSET(ACTIVE.CELL(),0,1))
=FORMULA(OR)
=SELECT(OFFSET(ACTIVE.CELL(),0,1))
=FORMULA(MWCALC)
=ELSE()
=SELECT(,"R[1]C")
=GOTO($B$593)
=END.IF()
=END.IF()
=NEXT()
=NEXT()
=FOR("n",1,30)
=n*B202
=(n+13)*B203
=FOR("x",0,(2*n-26))
=x*B205
=((2*n-26)-x)*B204
=B646+B645+B642+B643
=SET.NAME("OR",x)
=SET.NAME("OH",(2*n-26-x))
=SET.NAME("MWCALC",B647)
=SET.NAME("o",(n+13))

=IF(ABS(B200-B647)<2)
=SELECT(B7)
=IF(ISBLANK(ACTIVE.CELL()))
=FORMULA(n)
=SELECT(OFFSET(ACTIVE.CELL(),0,1))
=FORMULA(o)
=SELECT(OFFSET(ACTIVE.CELL(),0,1))
=FORMULA(OH)
=SELECT(OFFSET(ACTIVE.CELL(),0,1))
=FORMULA(OR)
=SELECT(OFFSET(ACTIVE.CELL(),0,1))
=FORMULA(MWCALC)
=ELSE()
=SELECT(,"R[1]C")
```

```
=GOTO($B$593)
=END.IF()
=END.IF()
=NEXT()
=NEXT()
=FOR("n",1,30)
=n*B202
=(n+14)*B203
=FOR("x",0,(2*n-28))
=x*B205
=((2*n-28)-x)*B205
=B677+B676+B673+B674
=SET.NAME("OR",x)
=SET.NAME("OH",(2*n-28-x))
=SET.NAME("MWCALC",B678)
=SET.NAME("o",(n+14))

=IF(ABS(B200-B678)<2)
=SELECT(B7)
=IF(ISBLANK(ACTIVE.CELL()))
=FORMULA(n)
=SELECT(OFFSET(ACTIVE.CELL(),0,1))
=FORMULA(o)
=SELECT(OFFSET(ACTIVE.CELL(),0,1))
=FORMULA(OH)
=SELECT(OFFSET(ACTIVE.CELL(),0,1))
=FORMULA(OR)
=SELECT(OFFSET(ACTIVE.CELL(),0,1))
=FORMULA(MWCALC)
=ELSE()
=SELECT(,"R[1]C")
=GOTO($B$593)
=END.IF()
=END.IF()
=NEXT()
=NEXT()
=FOR("n",1,30)
=n*B202
=(n+15)*B203
=FOR("x",0,(2*n-30))
=x*B205
=((2*n-30)-x)*B204
=B708+B707+B704+B705
=SET.NAME("OR",x)
=SET.NAME("OH",(2*n-30-x))
=SET.NAME("MWCALC",B709)
=SET.NAME("o",(n+15))

=IF(ABS(B200-B709)<2)
=SELECT(B7)
```

```
=IF(ISBLANK(ACTIVE.CELL()))
=FORMULA(n)
=SELECT(OFFSET(ACTIVE.CELL(),0,1))
=FORMULA(o)
=SELECT(OFFSET(ACTIVE.CELL(),0,1))
=FORMULA(OH)
=SELECT(OFFSET(ACTIVE.CELL(),0,1))
=FORMULA(OR)
=SELECT(OFFSET(ACTIVE.CELL(),0,1))
=FORMULA(MWCALC)
=ELSE()
=SELECT(,"R[1]C")
=GOTO($B$593)
=END.IF()
=END.IF()
=NEXT()
=NEXT()
=SELECT(A5:F109)
=COPY()
=ACTIVATE("MS")
=SELECT(!$B$2)
=IF(ISBLANK(ACTIVE.CELL()))
=SELECT(OFFSET(ACTIVE.CELL(),1,0))
=IF(ISBLANK(ACTIVE.CELL()))
=SELECT(OFFSET(ACTIVE.CELL(),-1,-1))
=PASTE()
=ELSE()
=GOTO(B738)
=END.IF()


=ELSE()
=SELECT(OFFSET(ACTIVE.CELL(),1,0))
=GOTO(B738)
=END.IF()
=ACTIVATE("MASSSPEC3.XLM")




=NEXT()
=RETURN()
```

Appendix C: Examples of Mass Spectrometry Macro Results

Mass Spec. results K potassium

MOLECULAR WEIGHT	# OF Si GROUPS	# OF BRIDGING Os	# OF OH GROUPS	# OF OR GROUPS	CALCULATED MOLECULAR WEIGHT
633.7865	5	4	4	8	632.5435
	8	9	13	1	634.8696
	7	10	3	5	632.7609
	9	16	2	2	632.9783

potassium

MOLECULAR WEIGHT	# OF Si GROUPS	# OF BRIDGING Os	# OF OH GROUPS	# OF OR GROUPS	CALCULATED MOLECULAR WEIGHT
633.9566	5	4	4	8	632.5435
	8	9	13	1	634.8696
	7	10	3	5	632.7609
	9	16	2	2	632.9783

potassium

MOLECULAR WEIGHT	# OF Si GROUPS	# OF BRIDGING Os	# OF OH GROUPS	# OF OR GROUPS	CALCULATED MOLECULAR WEIGHT
634.893	6	6	6	6	636.6522
	8	9	13	1	634.8696
	8	12	5	3	636.8696
	9	16	2	2	632.9783

potassium

MOLECULAR WEIGHT	# OF Si GROUPS	# OF BRIDGING Os	# OF OH GROUPS	# OF OR GROUPS	CALCULATED MOLECULAR WEIGHT
634.9782	6	6	6	6	636.6522
	8	9	13	1	634.8696
	8	12	5	3	636.8696
	9	16	2	2	632.9783

potassium

MOLECULAR WEIGHT	# OF Si GROUPS	# OF BRIDGING Os	# OF OH GROUPS	# OF OR GROUPS	CALCULATED MOLECULAR WEIGHT
635.404	6	6	6	6	636.6522
	8	9	13	1	634.8696
	8	12	5	3	636.8696
	10	18	4	0	637.087

potassium

MOLECULAR WEIGHT	# OF Si GROUPS	# OF BRIDGING Os	# OF OH GROUPS	# OF OR GROUPS	CALCULATED MOLECULAR WEIGHT
639.6701	7	8	8	4	640.7609
	9	14	7	1	640.9783

potassium

MOLECULAR WEIGHT	# OF Si GROUPS	# OF BRIDGING Os	# OF OH GROUPS	# OF OR GROUPS	CALCULATED MOLECULAR WEIGHT
639.7556	7	8	8	4	640.7609
	9	14	7	1	640.9783

potassium

MOLECULAR WEIGHT	# OF Si GROUPS	# OF BRIDGING Os	# OF OH GROUPS	# OF OR GROUPS	CALCULATED MOLECULAR WEIGHT
640.354	7	8	8	4	640.7609
	9	14	7	1	640.9783

potassium

MOLECULAR WEIGHT	# OF Si GROUPS	# OF BRIDGING Os	# OF OH GROUPS	# OF OR GROUPS	CALCULATED MOLECULAR WEIGHT
640.4395	7	8	8	4	640.7609
	9	14	7	1	640.9783

potassium

MOLECULAR WEIGHT	# OF Si GROUPS	# OF BRIDGING Os	# OF OH GROUPS	# OF OR GROUPS	CALCULATED MOLECULAR WEIGHT
640.525	7	8	8	4	640.7609
	9	14	7	1	640.9783

potassium

MOLECULAR WEIGHT	# OF Si GROUPS	# OF BRIDGING Os	# OF OH GROUPS	# OF OR GROUPS	CALCULATED MOLECULAR WEIGHT
640.6105	5	5	1	9	642.5435
	7	8	8	4	640.7609
	9	14	7	1	640.9783

potassium

MOLECULAR WEIGHT	# OF Si GROUPS	# OF BRIDGING Os	# OF OH GROUPS	# OF OR GROUPS	CALCULATED MOLECULAR WEIGHT
641.3803	8	7	18	0	642.8696
	5	5	1	9	642.5435
	7	8	8	4	640.7609
	7	11	0	6	642.7609
	9	14	7	1	640.9783

potassium

MOLECULAR WEIGHT	# OF Si GROUPS	# OF BRIDGING Os	# OF OH GROUPS	# OF OR GROUPS	CALCULATED MOLECULAR WEIGHT
641.5515	8	7	18	0	642.8696
	5	5	1	9	642.5435
	7	8	8	4	640.7609
	7	11	0	6	642.7609
	9	14	7	1	640.9783

potassium

MOLECULAR WEIGHT	# OF Si GROUPS	# OF BRIDGING Os	# OF OH GROUPS	# OF OR GROUPS	CALCULATED MOLECULAR WEIGHT
641.637	8	7	18	0	642.8696
	5	5	1	9	642.5435
	7	8	8	4	640.7609
	7	11	0	6	642.7609
	9	14	7	1	640.9783

potassium

MOLECULAR WEIGHT	# OF Si GROUPS	# OF BRIDGING Os	# OF OH GROUPS	# OF OR GROUPS	CALCULATED MOLECULAR WEIGHT
641.7226	8	7	18	0	642.8696
	5	5	1	9	642.5435
	7	8	8	4	640.7609
	7	11	0	6	642.7609
	9	14	7	1	640.9783

potassium

MOLECULAR WEIGHT	# OF Si GROUPS	# OF BRIDGING Os	# OF OH GROUPS	# OF OR GROUPS	CALCULATED MOLECULAR WEIGHT
641.8082	8	7	18	0	642.8696
	5	5	1	9	642.5435
	7	8	8	4	640.7609
	7	11	0	6	642.7609
	9	14	7	1	640.9783

potassium

MOLECULAR WEIGHT	# OF Si GROUPS	# OF BRIDGING Os	# OF OH GROUPS	# OF OR GROUPS	CALCULATED MOLECULAR WEIGHT
642.3219	8	7	18	0	642.8696
	5	5	1	9	642.5435
	7	8	8	4	640.7609
	7	11	0	6	642.7609
	9	14	7	1	640.9783

potassium

MOLECULAR WEIGHT	# OF Si GROUPS	# OF BRIDGING Os	# OF OH GROUPS	# OF OR GROUPS	CALCULATED MOLECULAR WEIGHT
642.4075	8	7	18	0	642.8696
	5	5	1	9	642.5435

	7	8	8	4	640.7609
	7	11	0	6	642.7609
	9	14	7	1	640.9783

potassium

MOLECULAR WEIGHT	# OF Si GROUPS	# OF BRIDGING Os	# OF OH GROUPS	# OF OR GROUPS	CALCULATED MOLECULAR WEIGHT
642.4931	8	7	18	0	642.8696
	5	5	1	9	642.5435
	7	8	8	4	640.7609
	7	11	0	6	642.7609
	9	14	7	1	640.9783

potassium

MOLECULAR WEIGHT	# OF Si GROUPS	# OF BRIDGING Os	# OF OH GROUPS	# OF OR GROUPS	CALCULATED MOLECULAR WEIGHT
642.5787	8	7	18	0	642.8696
	5	5	1	9	642.5435
	7	8	8	4	640.7609
	7	11	0	6	642.7609
	9	14	7	1	640.9783

potassium

MOLECULAR WEIGHT	# OF Si GROUPS	# OF BRIDGING Os	# OF OH GROUPS	# OF OR GROUPS	CALCULATED MOLECULAR WEIGHT
642.6644	8	7	18	0	642.8696
	5	5	1	9	642.5435
	7	8	8	4	640.7609
	7	11	0	6	642.7609
	9	14	7	1	640.9783

potassium

MOLECULAR WEIGHT	# OF Si GROUPS	# OF BRIDGING Os	# OF OH GROUPS	# OF OR GROUPS	CALCULATED MOLECULAR WEIGHT
642.75	8	7	18	0	642.8696
	5	5	1	9	642.5435
	7	8	8	4	640.7609
	7	11	0	6	642.7609
	9	14	7	1	640.9783

potassium

MOLECULAR WEIGHT	# OF Si GROUPS	# OF BRIDGING Os	# OF OH GROUPS	# OF OR GROUPS	CALCULATED MOLECULAR WEIGHT
643.4354	8	7	18	0	642.8696
	5	5	1	9	642.5435
	8	10	10	2	644.8696
	7	11	0	6	642.7609

potassium

MOLECULAR WEIGHT	# OF Si GROUPS	# OF BRIDGING Os	# OF OH GROUPS	# OF OR GROUPS	CALCULATED MOLECULAR WEIGHT
643.5211	8	7	18	0	642.8696

	5	5	1	9	642.5435
	8	10	10	2	644.8696
	7	11	0	6	642.7609

potassium

MOLECULAR WEIGHT	# OF Si GROUPS	# OF BRIDGING Os	# OF OH GROUPS	# OF OR GROUPS	CALCULATED MOLECULAR WEIGHT
643.6068	8	7	18	0	642.8696
	5	5	1	9	642.5435
	8	10	10	2	644.8696
	7	11	0	6	642.7609

potassium

MOLECULAR WEIGHT	# OF Si GROUPS	# OF BRIDGING Os	# OF OH GROUPS	# OF OR GROUPS	CALCULATED MOLECULAR WEIGHT
643.6925	8	7	18	0	642.8696
	5	5	1	9	642.5435
	8	10	10	2	644.8696
	7	11	0	6	642.7609

potassium

MOLECULAR WEIGHT	# OF Si GROUPS	# OF BRIDGING Os	# OF OH GROUPS	# OF OR GROUPS	CALCULATED MOLECULAR WEIGHT
644.4641	8	7	18	0	642.8696
	5	5	1	9	642.5435
	8	10	10	2	644.8696
	7	11	0	6	642.7609

potassium

MOLECULAR WEIGHT	# OF Si GROUPS	# OF BRIDGING Os	# OF OH GROUPS	# OF OR GROUPS	CALCULATED MOLECULAR WEIGHT
645.4078	6	7	3	7	646.6522
	8	10	10	2	644.8696
	8	13	2	4	646.8696
	10	19	1	1	647.087

potassium

MOLECULAR WEIGHT	# OF Si GROUPS	# OF BRIDGING Os	# OF OH GROUPS	# OF OR GROUPS	CALCULATED MOLECULAR WEIGHT
645.4936	6	7	3	7	646.6522
	8	10	10	2	644.8696
	8	13	2	4	646.8696
	10	19	1	1	647.087

potassium

MOLECULAR WEIGHT	# OF Si GROUPS	# OF BRIDGING Os	# OF OH GROUPS	# OF OR GROUPS	CALCULATED MOLECULAR WEIGHT
645.5794	6	7	3	7	646.6522
	8	10	10	2	644.8696
	8	13	2	4	646.8696
	10	19	1	1	647.087

potassium

MOLECULAR WEIGHT	# OF Si GROUPS	# OF BRIDGING Os	# OF OH GROUPS	# OF OR GROUPS	CALCULATED MOLECULAR WEIGHT
645.6652	6	7	3	7	646.6522
	8	10	10	2	644.8696
	8	13	2	4	646.8696
	10	19	1	1	647.087

potassium

MOLECULAR WEIGHT	# OF Si GROUPS	# OF BRIDGING Os	# OF OH GROUPS	# OF OR GROUPS	CALCULATED MOLECULAR WEIGHT
645.7511	6	7	3	7	646.6522
	8	10	10	2	644.8696
	8	13	2	4	646.8696
	10	19	1	1	647.087

potassium

MOLECULAR WEIGHT	# OF Si GROUPS	# OF BRIDGING Os	# OF OH GROUPS	# OF OR GROUPS	CALCULATED MOLECULAR WEIGHT
646.438	6	7	3	7	646.6522
	8	10	10	2	644.8696
	8	13	2	4	646.8696
	10	19	1	1	647.087

potassium

MOLECULAR WEIGHT	# OF Si GROUPS	# OF BRIDGING Os	# OF OH GROUPS	# OF OR GROUPS	CALCULATED MOLECULAR WEIGHT
646.5238	6	7	3	7	646.6522
	8	10	10	2	644.8696
	8	13	2	4	646.8696
	10	19	1	1	647.087

potassium

MOLECULAR WEIGHT	# OF Si GROUPS	# OF BRIDGING Os	# OF OH GROUPS	# OF OR GROUPS	CALCULATED MOLECULAR WEIGHT
647.4689	7	6	13	3	648.7609
	6	7	3	7	646.6522
	9	12	12	0	648.9783
	8	13	2	4	646.8696
	10	19	1	1	647.087

potassium

MOLECULAR WEIGHT	# OF Si GROUPS	# OF BRIDGING Os	# OF OH GROUPS	# OF OR GROUPS	CALCULATED MOLECULAR WEIGHT
647.5549	7	6	13	3	648.7609
	6	7	3	7	646.6522
	9	12	12	0	648.9783
	8	13	2	4	646.8696
	10	19	1	1	647.087

potassium

MOLECULAR WEIGHT	# OF Si GROUPS	# OF BRIDGING	# OF OH GROUPS	# OF OR GROUPS	CALCULATED MOLECULAR

		Os			WEIGHT
647.6408	7	6	13	3	648.7609
	6	7	3	7	646.6522
	9	12	12	0	648.9783
	8	13	2	4	646.8696
	10	19	1	1	647.087

potassium

MOLECULAR WEIGHT	# OF Si GROUPS	# OF BRIDGING Os	# OF OH GROUPS	# OF OR GROUPS	CALCULATED MOLECULAR WEIGHT
647.7268	7	6	13	3	648.7609
	6	7	3	7	646.6522
	9	12	12	0	648.9783
	8	13	2	4	646.8696
	10	19	1	1	647.087

potassium

MOLECULAR WEIGHT	# OF Si GROUPS	# OF BRIDGING Os	# OF OH GROUPS	# OF OR GROUPS	CALCULATED MOLECULAR WEIGHT
647.8127	7	6	13	3	648.7609
	6	7	3	7	646.6522
	9	12	12	0	648.9783
	8	13	2	4	646.8696
	10	19	1	1	647.087

potassium

MOLECULAR WEIGHT	# OF Si GROUPS	# OF BRIDGING Os	# OF OH GROUPS	# OF OR GROUPS	CALCULATED MOLECULAR WEIGHT
647.8987	7	6	13	3	648.7609
	6	7	3	7	646.6522
	9	12	12	0	648.9783
	8	13	2	4	646.8696
	10	19	1	1	647.087

potassium

MOLECULAR WEIGHT	# OF Si GROUPS	# OF BRIDGING Os	# OF OH GROUPS	# OF OR GROUPS	CALCULATED MOLECULAR WEIGHT
649.7053	7	6	13	3	648.7609
	7	9	5	5	650.7609
	9	12	12	0	648.9783
	9	15	4	2	650.9783

potassium

MOLECULAR WEIGHT	# OF Si GROUPS	# OF BRIDGING Os	# OF OH GROUPS	# OF OR GROUPS	CALCULATED MOLECULAR WEIGHT
649.7914	7	6	13	3	648.7609
	7	9	5	5	650.7609
	9	12	12	0	648.9783
	9	15	4	2	650.9783

potassium

MOLECULAR WEIGHT	# OF Si GROUPS	# OF BRIDGING	# OF OH GROUPS	# OF OR GROUPS	CALCULATED MOLECULAR

		Os			WEIGHT
650.7387	7	6	13	3	648.7609
	7	9	5	5	650.7609
	9	12	12	0	648.9783
	9	15	4	2	650.9783

potassium

MOLECULAR WEIGHT	# OF Si GROUPS	# OF BRIDGING Os	# OF OH GROUPS	# OF OR GROUPS	CALCULATED MOLECULAR WEIGHT
650.8249	7	9	5	5	650.7609
	9	12	12	0	648.9783
	9	15	4	2	650.9783

potassium

MOLECULAR WEIGHT	# OF Si GROUPS	# OF BRIDGING Os	# OF OH GROUPS	# OF OR GROUPS	CALCULATED MOLECULAR WEIGHT
650.9111	8	8	15	1	652.8696
	7	9	5	5	650.7609
	9	12	12	0	648.9783
	9	15	4	2	650.9783

potassium

MOLECULAR WEIGHT	# OF Si GROUPS	# OF BRIDGING Os	# OF OH GROUPS	# OF OR GROUPS	CALCULATED MOLECULAR WEIGHT
650.9972	8	8	15	1	652.8696
	7	9	5	5	650.7609
	9	15	4	2	650.9783

potassium

MOLECULAR WEIGHT	# OF Si GROUPS	# OF BRIDGING Os	# OF OH GROUPS	# OF OR GROUPS	CALCULATED MOLECULAR WEIGHT
651.0834	8	8	15	1	652.8696
	7	9	5	5	650.7609
	9	15	4	2	650.9783

potassium

MOLECULAR WEIGHT	# OF Si GROUPS	# OF BRIDGING Os	# OF OH GROUPS	# OF OR GROUPS	CALCULATED MOLECULAR WEIGHT
651.1696	8	8	15	1	652.8696
	7	9	5	5	650.7609
	9	15	4	2	650.9783

potassium

MOLECULAR WEIGHT	# OF Si GROUPS	# OF BRIDGING Os	# OF OH GROUPS	# OF OR GROUPS	CALCULATED MOLECULAR WEIGHT
651.3419	8	8	15	1	652.8696
	7	9	5	5	650.7609
	9	15	4	2	650.9783

potassium

MOLECULAR WEIGHT	# OF Si GROUPS	# OF BRIDGING Os	# OF OH GROUPS	# OF OR GROUPS	CALCULATED MOLECULAR WEIGHT
651.4281	8	8	15	1	652.8696
	7	9	5	5	650.7609
	9	15	4	2	650.9783

potassium

MOLECULAR WEIGHT	# OF Si GROUPS	# OF BRIDGING Os	# OF OH GROUPS	# OF OR GROUPS	CALCULATED MOLECULAR WEIGHT
651.5143	8	8	15	1	652.8696
	7	9	5	5	650.7609
	9	15	4	2	650.9783

potassium

MOLECULAR WEIGHT	# OF Si GROUPS	# OF BRIDGING Os	# OF OH GROUPS	# OF OR GROUPS	CALCULATED MOLECULAR WEIGHT
651.6005	8	8	15	1	652.8696
	7	9	5	5	650.7609
	9	15	4	2	650.9783

potassium

MOLECULAR WEIGHT	# OF Si GROUPS	# OF BRIDGING Os	# OF OH GROUPS	# OF OR GROUPS	CALCULATED MOLECULAR WEIGHT
651.6867	8	8	15	1	652.8696
	7	9	5	5	650.7609
	9	15	4	2	650.9783

potassium

MOLECULAR WEIGHT	# OF Si GROUPS	# OF BRIDGING Os	# OF OH GROUPS	# OF OR GROUPS	CALCULATED MOLECULAR WEIGHT
651.7729	8	8	15	1	652.8696
	7	9	5	5	650.7609
	9	15	4	2	650.9783

potassium

MOLECULAR WEIGHT	# OF Si GROUPS	# OF BRIDGING Os	# OF OH GROUPS	# OF OR GROUPS	CALCULATED MOLECULAR WEIGHT
651.8591	8	8	15	1	652.8696
	7	9	5	5	650.7609
	9	15	4	2	650.9783

potassium

MOLECULAR WEIGHT	# OF Si GROUPS	# OF BRIDGING Os	# OF OH GROUPS	# OF OR GROUPS	CALCULATED MOLECULAR WEIGHT
652.2903	8	8	15	1	652.8696
	7	9	5	5	650.7609
	9	15	4	2	650.9783

potassium

MOLECULAR WEIGHT	# OF Si GROUPS	# OF BRIDGING Os	# OF OH GROUPS	# OF OR GROUPS	CALCULATED MOLECULAR WEIGHT
652.3766	8	8	15	1	652.8696
	7	9	5	5	650.7609
	9	15	4	2	650.9783

potassium

MOLECULAR WEIGHT	# OF Si GROUPS	# OF BRIDGING Os	# OF OH GROUPS	# OF OR GROUPS	CALCULATED MOLECULAR WEIGHT
652.4628	8	8	15	1	652.8696
	7	9	5	5	650.7609
	9	15	4	2	650.9783

potassium

MOLECULAR WEIGHT	# OF Si GROUPS	# OF BRIDGING Os	# OF OH GROUPS	# OF OR GROUPS	CALCULATED MOLECULAR WEIGHT
652.5491	8	8	15	1	652.8696
	7	9	5	5	650.7609
	9	15	4	2	650.9783

potassium

MOLECULAR WEIGHT	# OF Si GROUPS	# OF BRIDGING Os	# OF OH GROUPS	# OF OR GROUPS	CALCULATED MOLECULAR WEIGHT
652.6353	8	8	15	1	652.8696
	7	9	5	5	650.7609
	9	15	4	2	650.9783

potassium

MOLECULAR WEIGHT	# OF Si GROUPS	# OF BRIDGING Os	# OF OH GROUPS	# OF OR GROUPS	CALCULATED MOLECULAR WEIGHT
652.7216	6	5	8	6	654.6522
	8	8	15	1	652.8696
	7	9	5	5	650.7609
	9	15	4	2	650.9783

potassium

MOLECULAR WEIGHT	# OF Si GROUPS	# OF BRIDGING Os	# OF OH GROUPS	# OF OR GROUPS	CALCULATED MOLECULAR WEIGHT
652.8079	6	5	8	6	654.6522
	8	8	15	1	652.8696
	9	15	4	2	650.9783

potassium

MOLECULAR WEIGHT	# OF Si GROUPS	# OF BRIDGING Os	# OF OH GROUPS	# OF OR GROUPS	CALCULATED MOLECULAR WEIGHT
652.8942	6	5	8	6	654.6522
	8	8	15	1	652.8696
	8	11	7	3	654.8696
	9	15	4	2	650.9783

potassium

MOLECULAR WEIGHT	# OF Si GROUPS	# OF BRIDGING	# OF OH GROUPS	# OF OR GROUPS	CALCULATED MOLECULAR

		Os			WEIGHT
652.9805	6	5	8	6	654.6522
	8	8	15	1	652.8696
	8	11	7	3	654.8696

potassium

MOLECULAR WEIGHT	# OF Si GROUPS	# OF BRIDGING Os	# OF OH GROUPS	# OF OR GROUPS	CALCULATED MOLECULAR WEIGHT
653.412	6	5	8	6	654.6522
	8	8	15	1	652.8696
	8	11	7	3	654.8696
	10	17	6	0	655.087

potassium

MOLECULAR WEIGHT	# OF Si GROUPS	# OF BRIDGING Os	# OF OH GROUPS	# OF OR GROUPS	CALCULATED MOLECULAR WEIGHT
653.4983	6	5	8	6	654.6522
	8	8	15	1	652.8696
	8	11	7	3	654.8696
	10	17	6	0	655.087

potassium

MOLECULAR WEIGHT	# OF Si GROUPS	# OF BRIDGING Os	# OF OH GROUPS	# OF OR GROUPS	CALCULATED MOLECULAR WEIGHT
653.5846	6	5	8	6	654.6522
	8	8	15	1	652.8696
	8	11	7	3	654.8696
	10	17	6	0	655.087

potassium

MOLECULAR WEIGHT	# OF Si GROUPS	# OF BRIDGING Os	# OF OH GROUPS	# OF OR GROUPS	CALCULATED MOLECULAR WEIGHT
653.671	6	5	8	6	654.6522
	8	8	15	1	652.8696
	8	11	7	3	654.8696
	10	17	6	0	655.087

potassium

MOLECULAR WEIGHT	# OF Si GROUPS	# OF BRIDGING Os	# OF OH GROUPS	# OF OR GROUPS	CALCULATED MOLECULAR WEIGHT
653.7573	6	5	8	6	654.6522
	8	8	15	1	652.8696
	8	11	7	3	654.8696
	10	17	6	0	655.087

potassium

MOLECULAR WEIGHT	# OF Si GROUPS	# OF BRIDGING Os	# OF OH GROUPS	# OF OR GROUPS	CALCULATED MOLECULAR WEIGHT
653.8436	6	5	8	6	654.6522
	8	8	15	1	652.8696
	8	11	7	3	654.8696
	10	17	6	0	655.087

potassium

MOLECULAR WEIGHT	# OF Si GROUPS	# OF BRIDGING Os	# OF OH GROUPS	# OF OR GROUPS	CALCULATED MOLECULAR WEIGHT
654.2754	6	5	8	6	654.6522
	8	8	15	1	652.8696
	8	11	7	3	654.8696
	10	17	6	0	655.087

potassium

MOLECULAR WEIGHT	# OF Si GROUPS	# OF BRIDGING Os	# OF OH GROUPS	# OF OR GROUPS	CALCULATED MOLECULAR WEIGHT
654.3618	6	5	8	6	654.6522
	8	8	15	1	652.8696
	8	11	7	3	654.8696
	10	17	6	0	655.087

potassium

MOLECULAR WEIGHT	# OF Si GROUPS	# OF BRIDGING Os	# OF OH GROUPS	# OF OR GROUPS	CALCULATED MOLECULAR WEIGHT
654.4482	6	5	8	6	654.6522
	8	8	15	1	652.8696
	8	11	7	3	654.8696
	10	17	6	0	655.087

potassium

MOLECULAR WEIGHT	# OF Si GROUPS	# OF BRIDGING Os	# OF OH GROUPS	# OF OR GROUPS	CALCULATED MOLECULAR WEIGHT
654.5346	6	5	8	6	654.6522
	8	8	15	1	652.8696
	8	11	7	3	654.8696
	10	17	6	0	655.087

potassium

MOLECULAR WEIGHT	# OF Si GROUPS	# OF BRIDGING Os	# OF OH GROUPS	# OF OR GROUPS	CALCULATED MOLECULAR WEIGHT
654.6209	6	5	8	6	654.6522
	8	8	15	1	652.8696
	8	11	7	3	654.8696
	10	17	6	0	655.087

potassium

MOLECULAR WEIGHT	# OF Si GROUPS	# OF BRIDGING Os	# OF OH GROUPS	# OF OR GROUPS	CALCULATED MOLECULAR WEIGHT
654.7073	6	5	8	6	654.6522
	8	8	15	1	652.8696
	6	8	0	8	656.6522
	8	11	7	3	654.8696
	10	17	6	0	655.087

potassium

MOLECULAR WEIGHT	# OF Si GROUPS	# OF BRIDGING	# OF OH GROUPS	# OF OR GROUPS	CALCULATED MOLECULAR

		Os			WEIGHT
654.7937	6	5	8	6	654.6522
	8	8	15	1	652.8696
	6	8	0	8	656.6522
	8	11	7	3	654.8696
	10	17	6	0	655.087

potassium

MOLECULAR WEIGHT	# OF Si GROUPS	# OF BRIDGING Os	# OF OH GROUPS	# OF OR GROUPS	CALCULATED MOLECULAR WEIGHT
654.8801	6	5	8	6	654.6522
	6	8	0	8	656.6522
	8	11	7	3	654.8696
	10	17	6	0	655.087

potassium

MOLECULAR WEIGHT	# OF Si GROUPS	# OF BRIDGING Os	# OF OH GROUPS	# OF OR GROUPS	CALCULATED MOLECULAR WEIGHT
654.9666	6	5	8	6	654.6522
	6	8	0	8	656.6522
	8	11	7	3	654.8696
	10	17	6	0	655.087

potassium

MOLECULAR WEIGHT	# OF Si GROUPS	# OF BRIDGING Os	# OF OH GROUPS	# OF OR GROUPS	CALCULATED MOLECULAR WEIGHT
655.3987	6	5	8	6	654.6522
	6	8	0	8	656.6522
	8	11	7	3	654.8696
	10	17	6	0	655.087

potassium

MOLECULAR WEIGHT	# OF Si GROUPS	# OF BRIDGING Os	# OF OH GROUPS	# OF OR GROUPS	CALCULATED MOLECULAR WEIGHT
655.4851	6	5	8	6	654.6522
	6	8	0	8	656.6522
	8	11	7	3	654.8696
	10	17	6	0	655.087

potassium

MOLECULAR WEIGHT	# OF Si GROUPS	# OF BRIDGING Os	# OF OH GROUPS	# OF OR GROUPS	CALCULATED MOLECULAR WEIGHT
655.5716	6	5	8	6	654.6522
	6	8	0	8	656.6522
	8	11	7	3	654.8696
	10	17	6	0	655.087

potassium

MOLECULAR WEIGHT	# OF Si GROUPS	# OF BRIDGING Os	# OF OH GROUPS	# OF OR GROUPS	CALCULATED MOLECULAR WEIGHT
655.658	6	5	8	6	654.6522
	6	8	0	8	656.6522

	8	11	7	3	654.8696
	10	17	6	0	655.087

potassium

MOLECULAR WEIGHT	# OF Si GROUPS	# OF BRIDGING Os	# OF OH GROUPS	# OF OR GROUPS	CALCULATED MOLECULAR WEIGHT
655.7445	6	5	8	6	654.6522
	6	8	0	8	656.6522
	8	11	7	3	654.8696
	10	17	6	0	655.087

potassium

MOLECULAR WEIGHT	# OF Si GROUPS	# OF BRIDGING Os	# OF OH GROUPS	# OF OR GROUPS	CALCULATED MOLECULAR WEIGHT
656.4364	6	5	8	6	654.6522
	6	8	0	8	656.6522
	8	11	7	3	654.8696
	10	17	6	0	655.087

potassium

MOLECULAR WEIGHT	# OF Si GROUPS	# OF BRIDGING Os	# OF OH GROUPS	# OF OR GROUPS	CALCULATED MOLECULAR WEIGHT
657.3017	7	7	10	4	658.7609
	6	8	0	8	656.6522
	9	13	9	1	658.9783

potassium

MOLECULAR WEIGHT	# OF Si GROUPS	# OF BRIDGING Os	# OF OH GROUPS	# OF OR GROUPS	CALCULATED MOLECULAR WEIGHT
657.3883	7	7	10	4	658.7609
	6	8	0	8	656.6522
	9	13	9	1	658.9783

potassium

MOLECULAR WEIGHT	# OF Si GROUPS	# OF BRIDGING Os	# OF OH GROUPS	# OF OR GROUPS	CALCULATED MOLECULAR WEIGHT
657.4748	7	7	10	4	658.7609
	6	8	0	8	656.6522
	9	13	9	1	658.9783

potassium

MOLECULAR WEIGHT	# OF Si GROUPS	# OF BRIDGING Os	# OF OH GROUPS	# OF OR GROUPS	CALCULATED MOLECULAR WEIGHT
657.5614	7	7	10	4	658.7609
	6	8	0	8	656.6522
	9	13	9	1	658.9783

potassium

MOLECULAR WEIGHT	# OF Si GROUPS	# OF BRIDGING Os	# OF OH GROUPS	# OF OR GROUPS	CALCULATED MOLECULAR WEIGHT
657.648	7	7	10	4	658.7609
	6	8	0	8	656.6522

	9	13	9	1	658.9783

potassium

MOLECULAR WEIGHT	# OF Si GROUPS	# OF BRIDGING Os	# OF OH GROUPS	# OF OR GROUPS	CALCULATED MOLECULAR WEIGHT
657.7346	7	7	10	4	658.7609
	6	8	0	8	656.6522
	9	13	9	1	658.9783

potassium

MOLECULAR WEIGHT	# OF Si GROUPS	# OF BRIDGING Os	# OF OH GROUPS	# OF OR GROUPS	CALCULATED MOLECULAR WEIGHT
658.2542	7	7	10	4	658.7609
	6	8	0	8	656.6522
	9	13	9	1	658.9783

potassium

MOLECULAR WEIGHT	# OF Si GROUPS	# OF BRIDGING Os	# OF OH GROUPS	# OF OR GROUPS	CALCULATED MOLECULAR WEIGHT
658.3408	7	7	10	4	658.7609
	6	8	0	8	656.6522
	9	13	9	1	658.9783

potassium

MOLECULAR WEIGHT	# OF Si GROUPS	# OF BRIDGING Os	# OF OH GROUPS	# OF OR GROUPS	CALCULATED MOLECULAR WEIGHT
658.4274	7	7	10	4	658.7609
	6	8	0	8	656.6522
	9	13	9	1	658.9783

potassium

MOLECULAR WEIGHT	# OF Si GROUPS	# OF BRIDGING Os	# OF OH GROUPS	# OF OR GROUPS	CALCULATED MOLECULAR WEIGHT
658.514	7	7	10	4	658.7609
	6	8	0	8	656.6522
	9	13	9	1	658.9783

potassium

MOLECULAR WEIGHT	# OF Si GROUPS	# OF BRIDGING Os	# OF OH GROUPS	# OF OR GROUPS	CALCULATED MOLECULAR WEIGHT
658.6007	5	4	3	9	660.5435
	7	7	10	4	658.7609
	6	8	0	8	656.6522
	9	13	9	1	658.9783

potassium

MOLECULAR WEIGHT	# OF Si GROUPS	# OF BRIDGING Os	# OF OH GROUPS	# OF OR GROUPS	CALCULATED MOLECULAR WEIGHT
659.294	5	4	3	9	660.5435
	7	7	10	4	658.7609
	7	10	2	6	660.7609
	9	13	9	1	658.9783

potassium

MOLECULAR WEIGHT	# OF Si GROUPS	# OF BRIDGING Os	# OF OH GROUPS	# OF OR GROUPS	CALCULATED MOLECULAR WEIGHT
659.3807	5	4	3	9	660.5435
	7	7	10	4	658.7609
	7	10	2	6	660.7609
	9	13	9	1	658.9783
	9	16	1	3	660.9783
	11	22	0	0	661.1957

potassium

MOLECULAR WEIGHT	# OF Si GROUPS	# OF BRIDGING Os	# OF OH GROUPS	# OF OR GROUPS	CALCULATED MOLECULAR WEIGHT
659.4674	5	4	3	9	660.5435
	7	7	10	4	658.7609
	7	10	2	6	660.7609
	9	13	9	1	658.9783
	9	16	1	3	660.9783
	11	22	0	0	661.1957

potassium

MOLECULAR WEIGHT	# OF Si GROUPS	# OF BRIDGING Os	# OF OH GROUPS	# OF OR GROUPS	CALCULATED MOLECULAR WEIGHT
659.5541	5	4	3	9	660.5435
	7	7	10	4	658.7609
	7	10	2	6	660.7609
	9	13	9	1	658.9783
	9	16	1	3	660.9783
	11	22	0	0	661.1957

potassium

MOLECULAR WEIGHT	# OF Si GROUPS	# OF BRIDGING Os	# OF OH GROUPS	# OF OR GROUPS	CALCULATED MOLECULAR WEIGHT
660.3346	5	4	3	9	660.5435
	7	7	10	4	658.7609
	7	10	2	6	660.7609
	9	13	9	1	658.9783
	9	16	1	3	660.9783
	11	22	0	0	661.1957

potassium

MOLECULAR WEIGHT	# OF Si GROUPS	# OF BRIDGING Os	# OF OH GROUPS	# OF OR GROUPS	CALCULATED MOLECULAR WEIGHT
660.4213	5	4	3	9	660.5435
	7	7	10	4	658.7609
	7	10	2	6	660.7609
	9	13	9	1	658.9783
	9	16	1	3	660.9783
	11	22	0	0	661.1957

potassium

MOLECULAR WEIGHT	# OF Si GROUPS	# OF BRIDGING Os	# OF OH GROUPS	# OF OR GROUPS	CALCULATED MOLECULAR WEIGHT
667.3787	7	8	7	5	668.7609
	9	11	14	0	666.9783
	9	14	6	2	668.9783

potassium

MOLECULAR WEIGHT	# OF Si GROUPS	# OF BRIDGING Os	# OF OH GROUPS	# OF OR GROUPS	CALCULATED MOLECULAR WEIGHT
667.4659	7	8	7	5	668.7609
	9	11	14	0	666.9783
	9	14	6	2	668.9783

potassium

MOLECULAR WEIGHT	# OF Si GROUPS	# OF BRIDGING Os	# OF OH GROUPS	# OF OR GROUPS	CALCULATED MOLECULAR WEIGHT
667.5531	7	8	7	5	668.7609
	9	11	14	0	666.9783
	9	14	6	2	668.9783

potassium

MOLECULAR WEIGHT	# OF Si GROUPS	# OF BRIDGING Os	# OF OH GROUPS	# OF OR GROUPS	CALCULATED MOLECULAR WEIGHT
667.6403	7	8	7	5	668.7609
	9	11	14	0	666.9783
	9	14	6	2	668.9783

potassium

MOLECULAR WEIGHT	# OF Si GROUPS	# OF BRIDGING Os	# OF OH GROUPS	# OF OR GROUPS	CALCULATED MOLECULAR WEIGHT
668.3381	7	8	7	5	668.7609
	9	11	14	0	666.9783
	9	14	6	2	668.9783

potassium

MOLECULAR WEIGHT	# OF Si GROUPS	# OF BRIDGING Os	# OF OH GROUPS	# OF OR GROUPS	CALCULATED MOLECULAR WEIGHT
668.4253	7	8	7	5	668.7609
	9	11	14	0	666.9783
	9	14	6	2	668.9783

potassium

MOLECULAR WEIGHT	# OF Si GROUPS	# OF BRIDGING Os	# OF OH GROUPS	# OF OR GROUPS	CALCULATED MOLECULAR WEIGHT
669.2981	8	7	17	1	670.8696
	5	5	0	10	670.5435
	7	8	7	5	668.7609
	9	14	6	2	668.9783

potassium

MOLECULAR WEIGHT	# OF Si GROUPS	# OF BRIDGING Os	# OF OH GROUPS	# OF OR GROUPS	CALCULATED MOLECULAR WEIGHT

669.3854	8	7	17	1	670.8696
	5	5	0	10	670.5435
	7	8	7	5	668.7609
	9	14	6	2	668.9783

potassium

MOLECULAR WEIGHT	# OF Si GROUPS	# OF BRIDGING Os	# OF OH GROUPS	# OF OR GROUPS	CALCULATED MOLECULAR WEIGHT
669.4727	8	7	17	1	670.8696
	5	5	0	10	670.5435
	7	8	7	5	668.7609
	9	14	6	2	668.9783

potassium

MOLECULAR WEIGHT	# OF Si GROUPS	# OF BRIDGING Os	# OF OH GROUPS	# OF OR GROUPS	CALCULATED MOLECULAR WEIGHT
669.56	8	7	17	1	670.8696
	5	5	0	10	670.5435
	7	8	7	5	668.7609
	9	14	6	2	668.9783

potassium

MOLECULAR WEIGHT	# OF Si GROUPS	# OF BRIDGING Os	# OF OH GROUPS	# OF OR GROUPS	CALCULATED MOLECULAR WEIGHT
669.6473	8	7	17	1	670.8696
	5	5	0	10	670.5435
	7	8	7	5	668.7609
	9	14	6	2	668.9783

potassium

MOLECULAR WEIGHT	# OF Si GROUPS	# OF BRIDGING Os	# OF OH GROUPS	# OF OR GROUPS	CALCULATED MOLECULAR WEIGHT
669.7347	8	7	17	1	670.8696
	5	5	0	10	670.5435
	7	8	7	5	668.7609
	9	14	6	2	668.9783

potassium

MOLECULAR WEIGHT	# OF Si GROUPS	# OF BRIDGING Os	# OF OH GROUPS	# OF OR GROUPS	CALCULATED MOLECULAR WEIGHT
670.2587	8	7	17	1	670.8696
	5	5	0	10	670.5435
	7	8	7	5	668.7609
	9	14	6	2	668.9783

potassium

MOLECULAR WEIGHT	# OF Si GROUPS	# OF BRIDGING Os	# OF OH GROUPS	# OF OR GROUPS	CALCULATED MOLECULAR WEIGHT
670.3461	8	7	17	1	670.8696
	5	5	0	10	670.5435
	7	8	7	5	668.7609
	9	14	6	2	668.9783

potassium

MOLECULAR WEIGHT	# OF Si GROUPS	# OF BRIDGING Os	# OF OH GROUPS	# OF OR GROUPS	CALCULATED MOLECULAR WEIGHT
670.4335	8	7	17	1	670.8696
	5	5	0	10	670.5435
	7	8	7	5	668.7609
	9	14	6	2	668.9783

potassium

MOLECULAR WEIGHT	# OF Si GROUPS	# OF BRIDGING Os	# OF OH GROUPS	# OF OR GROUPS	CALCULATED MOLECULAR WEIGHT
670.5208	8	7	17	1	670.8696
	5	5	0	10	670.5435
	7	8	7	5	668.7609
	9	14	6	2	668.9783

potassium

MOLECULAR WEIGHT	# OF Si GROUPS	# OF BRIDGING Os	# OF OH GROUPS	# OF OR GROUPS	CALCULATED MOLECULAR WEIGHT
670.6082	8	7	17	1	670.8696
	5	5	0	10	670.5435
	7	8	7	5	668.7609
	9	14	6	2	668.9783

potassium

MOLECULAR WEIGHT	# OF Si GROUPS	# OF BRIDGING Os	# OF OH GROUPS	# OF OR GROUPS	CALCULATED MOLECULAR WEIGHT
670.6956	8	7	17	1	670.8696
	5	5	0	10	670.5435
	7	8	7	5	668.7609
	9	14	6	2	668.9783

potassium

MOLECULAR WEIGHT	# OF Si GROUPS	# OF BRIDGING Os	# OF OH GROUPS	# OF OR GROUPS	CALCULATED MOLECULAR WEIGHT
671.3074	8	7	17	1	670.8696
	5	5	0	10	670.5435
	8	10	9	3	672.8696
	10	16	8	0	673.087

potassium

MOLECULAR WEIGHT	# OF Si GROUPS	# OF BRIDGING Os	# OF OH GROUPS	# OF OR GROUPS	CALCULATED MOLECULAR WEIGHT
671.3949	8	7	17	1	670.8696
	5	5	0	10	670.5435
	8	10	9	3	672.8696
	10	16	8	0	673.087

potassium

MOLECULAR WEIGHT	# OF Si GROUPS	# OF BRIDGING Os	# OF OH GROUPS	# OF OR GROUPS	CALCULATED MOLECULAR WEIGHT

671.4823	8	7	17	1	670.8696
	5	5	0	10	670.5435
	8	10	9	3	672.8696
	10	16	8	0	673.087

potassium

MOLECULAR WEIGHT	# OF Si GROUPS	# OF BRIDGING Os	# OF OH GROUPS	# OF OR GROUPS	CALCULATED MOLECULAR WEIGHT
671.5697	8	7	17	1	670.8696
	5	5	0	10	670.5435
	8	10	9	3	672.8696
	10	16	8	0	673.087

potassium

MOLECULAR WEIGHT	# OF Si GROUPS	# OF BRIDGING Os	# OF OH GROUPS	# OF OR GROUPS	CALCULATED MOLECULAR WEIGHT
671.6572	8	7	17	1	670.8696
	5	5	0	10	670.5435
	8	10	9	3	672.8696
	10	16	8	0	673.087

potassium

MOLECULAR WEIGHT	# OF Si GROUPS	# OF BRIDGING Os	# OF OH GROUPS	# OF OR GROUPS	CALCULATED MOLECULAR WEIGHT
671.7446	8	7	17	1	670.8696
	5	5	0	10	670.5435
	8	10	9	3	672.8696
	10	16	8	0	673.087

potassium

MOLECULAR WEIGHT	# OF Si GROUPS	# OF BRIDGING Os	# OF OH GROUPS	# OF OR GROUPS	CALCULATED MOLECULAR WEIGHT
672.3569	8	7	17	1	670.8696
	5	5	0	10	670.5435
	8	10	9	3	672.8696
	10	16	8	0	673.087

potassium

MOLECULAR WEIGHT	# OF Si GROUPS	# OF BRIDGING Os	# OF OH GROUPS	# OF OR GROUPS	CALCULATED MOLECULAR WEIGHT
672.4444	8	7	17	1	670.8696
	5	5	0	10	670.5435
	8	10	9	3	672.8696
	10	16	8	0	673.087

potassium

MOLECULAR WEIGHT	# OF Si GROUPS	# OF BRIDGING Os	# OF OH GROUPS	# OF OR GROUPS	CALCULATED MOLECULAR WEIGHT
672.5319	8	7	17	1	670.8696
	5	5	0	10	670.5435
	8	10	9	3	672.8696
	10	16	8	0	673.087

potassium

MOLECULAR WEIGHT	# OF Si GROUPS	# OF BRIDGING Os	# OF OH GROUPS	# OF OR GROUPS	CALCULATED MOLECULAR WEIGHT
673.3196	6	7	2	8	674.6522
	8	10	9	3	672.8696
	8	13	1	5	674.8696
	10	16	8	0	673.087
	10	19	0	2	675.087

potassium

MOLECULAR WEIGHT	# OF Si GROUPS	# OF BRIDGING Os	# OF OH GROUPS	# OF OR GROUPS	CALCULATED MOLECULAR WEIGHT
673.4072	6	7	2	8	674.6522
	8	10	9	3	672.8696
	8	13	1	5	674.8696
	10	16	8	0	673.087
	10	19	0	2	675.087

potassium

MOLECULAR WEIGHT	# OF Si GROUPS	# OF BRIDGING Os	# OF OH GROUPS	# OF OR GROUPS	CALCULATED MOLECULAR WEIGHT
673.4948	6	7	2	8	674.6522
	8	10	9	3	672.8696
	8	13	1	5	674.8696
	10	16	8	0	673.087
	10	19	0	2	675.087

potassium

MOLECULAR WEIGHT	# OF Si GROUPS	# OF BRIDGING Os	# OF OH GROUPS	# OF OR GROUPS	CALCULATED MOLECULAR WEIGHT
673.5823	6	7	2	8	674.6522
	8	10	9	3	672.8696
	8	13	1	5	674.8696
	10	16	8	0	673.087
	10	19	0	2	675.087

potassium

MOLECULAR WEIGHT	# OF Si GROUPS	# OF BRIDGING Os	# OF OH GROUPS	# OF OR GROUPS	CALCULATED MOLECULAR WEIGHT
673.6699	6	7	2	8	674.6522
	8	10	9	3	672.8696
	8	13	1	5	674.8696
	10	16	8	0	673.087
	10	19	0	2	675.087

potassium

MOLECULAR WEIGHT	# OF Si GROUPS	# OF BRIDGING Os	# OF OH GROUPS	# OF OR GROUPS	CALCULATED MOLECULAR WEIGHT
674.283	6	7	2	8	674.6522
	8	10	9	3	672.8696
	8	13	1	5	674.8696

	10	16	8	0	673.087
	10	19	0	2	675.087

potassium

MOLECULAR WEIGHT	# OF Si GROUPS	# OF BRIDGING Os	# OF OH GROUPS	# OF OR GROUPS	CALCULATED MOLECULAR WEIGHT
674.3706	6	7	2	8	674.6522
	8	10	9	3	672.8696
	8	13	1	5	674.8696
	10	16	8	0	673.087
	10	19	0	2	675.087

potassium

MOLECULAR WEIGHT	# OF Si GROUPS	# OF BRIDGING Os	# OF OH GROUPS	# OF OR GROUPS	CALCULATED MOLECULAR WEIGHT
674.4582	6	7	2	8	674.6522
	8	10	9	3	672.8696
	8	13	1	5	674.8696
	10	16	8	0	673.087
	10	19	0	2	675.087

potassium

MOLECULAR WEIGHT	# OF Si GROUPS	# OF BRIDGING Os	# OF OH GROUPS	# OF OR GROUPS	CALCULATED MOLECULAR WEIGHT
674.5459	6	7	2	8	674.6522
	8	10	9	3	672.8696
	8	13	1	5	674.8696
	10	16	8	0	673.087
	10	19	0	2	675.087

potassium

MOLECULAR WEIGHT	# OF Si GROUPS	# OF BRIDGING Os	# OF OH GROUPS	# OF OR GROUPS	CALCULATED MOLECULAR WEIGHT
675.3347	7	6	12	4	676.7609
	6	7	2	8	674.6522
	9	12	11	1	676.9783
	8	13	1	5	674.8696
	10	19	0	2	675.087

potassium

MOLECULAR WEIGHT	# OF Si GROUPS	# OF BRIDGING Os	# OF OH GROUPS	# OF OR GROUPS	CALCULATED MOLECULAR WEIGHT
675.4224	7	6	12	4	676.7609
	6	7	2	8	674.6522
	9	12	11	1	676.9783
	8	13	1	5	674.8696
	10	19	0	2	675.087

potassium

MOLECULAR WEIGHT	# OF Si GROUPS	# OF BRIDGING Os	# OF OH GROUPS	# OF OR GROUPS	CALCULATED MOLECULAR WEIGHT
675.5101	7	6	12	4	676.7609

	6	7	2	8	674.6522
	9	12	11	1	676.9783
	8	13	1	5	674.8696
	10	19	0	2	675.087

potassium

MOLECULAR WEIGHT	# OF Si GROUPS	# OF BRIDGING Os	# OF OH GROUPS	# OF OR GROUPS	CALCULATED MOLECULAR WEIGHT
675.5977	7	6	12	4	676.7609
	6	7	2	8	674.6522
	9	12	11	1	676.9783
	8	13	1	5	674.8696
	10	19	0	2	675.087

potassium

MOLECULAR WEIGHT	# OF Si GROUPS	# OF BRIDGING Os	# OF OH GROUPS	# OF OR GROUPS	CALCULATED MOLECULAR WEIGHT
675.6854	7	6	12	4	676.7609
	6	7	2	8	674.6522
	9	12	11	1	676.9783
	8	13	1	5	674.8696
	10	19	0	2	675.087

potassium

MOLECULAR WEIGHT	# OF Si GROUPS	# OF BRIDGING Os	# OF OH GROUPS	# OF OR GROUPS	CALCULATED MOLECULAR WEIGHT
676.2994	7	6	12	4	676.7609
	6	7	2	8	674.6522
	9	12	11	1	676.9783
	8	13	1	5	674.8696
	10	19	0	2	675.087

potassium

MOLECULAR WEIGHT	# OF Si GROUPS	# OF BRIDGING Os	# OF OH GROUPS	# OF OR GROUPS	CALCULATED MOLECULAR WEIGHT
676.3872	7	6	12	4	676.7609
	6	7	2	8	674.6522
	9	12	11	1	676.9783
	8	13	1	5	674.8696
	10	19	0	2	675.087

potassium

MOLECULAR WEIGHT	# OF Si GROUPS	# OF BRIDGING Os	# OF OH GROUPS	# OF OR GROUPS	CALCULATED MOLECULAR WEIGHT
677.4404	7	6	12	4	676.7609
	7	9	4	6	678.7609
	9	12	11	1	676.9783
	9	15	3	3	678.9783
	11	21	2	0	679.1957

potassium

MOLECULAR WEIGHT	# OF Si GROUPS	# OF BRIDGING	# OF OH GROUPS	# OF OR GROUPS	CALCULATED MOLECULAR

		Os			WEIGHT
679.4613	8	8	14	2	680.8696
	7	9	4	6	678.7609
	9	15	3	3	678.9783
	11	21	2	0	679.1957

potassium

MOLECULAR WEIGHT	# OF Si GROUPS	# OF BRIDGING Os	# OF OH GROUPS	# OF OR GROUPS	CALCULATED MOLECULAR WEIGHT
682.542	6	5	7	7	682.6522
	8	8	14	2	680.8696
	8	11	6	4	682.8696
	10	17	5	1	683.087

potassium

MOLECULAR WEIGHT	# OF Si GROUPS	# OF BRIDGING Os	# OF OH GROUPS	# OF OR GROUPS	CALCULATED MOLECULAR WEIGHT
682.6301	6	5	7	7	682.6522
	8	8	14	2	680.8696
	8	11	6	4	682.8696
	10	17	5	1	683.087

potassium

MOLECULAR WEIGHT	# OF Si GROUPS	# OF BRIDGING Os	# OF OH GROUPS	# OF OR GROUPS	CALCULATED MOLECULAR WEIGHT
682.7182	6	5	7	7	682.6522
	8	8	14	2	680.8696
	8	11	6	4	682.8696
	10	17	5	1	683.087

potassium

MOLECULAR WEIGHT	# OF Si GROUPS	# OF BRIDGING Os	# OF OH GROUPS	# OF OR GROUPS	CALCULATED MOLECULAR WEIGHT
682.8063	6	5	7	7	682.6522
	8	8	14	2	680.8696
	8	11	6	4	682.8696
	10	17	5	1	683.087

potassium

MOLECULAR WEIGHT	# OF Si GROUPS	# OF BRIDGING Os	# OF OH GROUPS	# OF OR GROUPS	CALCULATED MOLECULAR WEIGHT
683.247	6	5	7	7	682.6522
	9	10	16	0	684.9783
	8	11	6	4	682.8696
	10	17	5	1	683.087

potassium

MOLECULAR WEIGHT	# OF Si GROUPS	# OF BRIDGING Os	# OF OH GROUPS	# OF OR GROUPS	CALCULATED MOLECULAR WEIGHT
685.6292	7	7	9	5	686.7609
	9	10	16	0	684.9783
	9	13	8	2	686.9783

potassium

MOLECULAR WEIGHT	# OF Si GROUPS	# OF BRIDGING Os	# OF OH GROUPS	# OF OR GROUPS	CALCULATED MOLECULAR WEIGHT
685.7175	7	7	9	5	686.7609
	9	10	16	0	684.9783
	9	13	8	2	686.9783

potassium

MOLECULAR WEIGHT	# OF Si GROUPS	# OF BRIDGING Os	# OF OH GROUPS	# OF OR GROUPS	CALCULATED MOLECULAR WEIGHT
686.1592	7	7	9	5	686.7609
	9	10	16	0	684.9783
	9	13	8	2	686.9783

potassium

MOLECULAR WEIGHT	# OF Si GROUPS	# OF BRIDGING Os	# OF OH GROUPS	# OF OR GROUPS	CALCULATED MOLECULAR WEIGHT
686.2475	7	7	9	5	686.7609
	9	10	16	0	684.9783
	9	13	8	2	686.9783

potassium

MOLECULAR WEIGHT	# OF Si GROUPS	# OF BRIDGING Os	# OF OH GROUPS	# OF OR GROUPS	CALCULATED MOLECULAR WEIGHT
686.3358	7	7	9	5	686.7609
	9	10	16	0	684.9783
	9	13	8	2	686.9783

potassium

MOLECULAR WEIGHT	# OF Si GROUPS	# OF BRIDGING Os	# OF OH GROUPS	# OF OR GROUPS	CALCULATED MOLECULAR WEIGHT
686.4242	7	7	9	5	686.7609
	9	10	16	0	684.9783
	9	13	8	2	686.9783

potassium

MOLECULAR WEIGHT	# OF Si GROUPS	# OF BRIDGING Os	# OF OH GROUPS	# OF OR GROUPS	CALCULATED MOLECULAR WEIGHT
686.5125	7	7	9	5	686.7609
	9	10	16	0	684.9783
	9	13	8	2	686.9783

potassium

MOLECULAR	# OF Si	# OF	# OF OH	# OF OR	CALCULATED

WEIGHT	GROUPS	BRIDGING Os	GROUPS	GROUPS	MOLECULAR WEIGHT
686.6009	5	4	2	10	688.5435
	7	7	9	5	686.7609
	9	10	16	0	684.9783
	9	13	8	2	686.9783

potassium

MOLECULAR WEIGHT	# OF Si GROUPS	# OF BRIDGING Os	# OF OH GROUPS	# OF OR GROUPS	CALCULATED MOLECULAR WEIGHT
687.308	5	4	2	10	688.5435
	7	7	9	5	686.7609
	7	10	1	7	688.7609
	9	13	8	2	686.9783
	9	16	0	4	688.9783

potassium

MOLECULAR WEIGHT	# OF Si GROUPS	# OF BRIDGING Os	# OF OH GROUPS	# OF OR GROUPS	CALCULATED MOLECULAR WEIGHT
687.3964	5	4	2	10	688.5435
	7	7	9	5	686.7609
	7	10	1	7	688.7609
	9	13	8	2	686.9783
	9	16	0	4	688.9783

potassium

MOLECULAR WEIGHT	# OF Si GROUPS	# OF BRIDGING Os	# OF OH GROUPS	# OF OR GROUPS	CALCULATED MOLECULAR WEIGHT
687.4848	5	4	2	10	688.5435
	7	7	9	5	686.7609
	7	10	1	7	688.7609
	9	13	8	2	686.9783
	9	16	0	4	688.9783

potassium

MOLECULAR WEIGHT	# OF Si GROUPS	# OF BRIDGING Os	# OF OH GROUPS	# OF OR GROUPS	CALCULATED MOLECULAR WEIGHT
687.5732	5	4	2	10	688.5435
	7	7	9	5	686.7609
	7	10	1	7	688.7609
	9	13	8	2	686.9783
	9	16	0	4	688.9783

potassium

MOLECULAR WEIGHT	# OF Si GROUPS	# OF BRIDGING Os	# OF OH GROUPS	# OF OR GROUPS	CALCULATED MOLECULAR WEIGHT
687.6616	5	4	2	10	688.5435
	7	7	9	5	686.7609
	7	10	1	7	688.7609
	9	13	8	2	686.9783
	9	16	0	4	688.9783

potassium

MOLECULAR WEIGHT	# OF Si GROUPS	# OF BRIDGING Os	# OF OH GROUPS	# OF OR GROUPS	CALCULATED MOLECULAR WEIGHT
688.2807	5	4	2	10	688.5435
	7	7	9	5	686.7609
	7	10	1	7	688.7609
	9	13	8	2	686.9783
	9	16	0	4	688.9783

potassium

MOLECULAR WEIGHT	# OF Si GROUPS	# OF BRIDGING Os	# OF OH GROUPS	# OF OR GROUPS	CALCULATED MOLECULAR WEIGHT
688.3692	5	4	2	10	688.5435
	7	7	9	5	686.7609
	7	10	1	7	688.7609
	9	13	8	2	686.9783
	9	16	0	4	688.9783

potassium

MOLECULAR WEIGHT	# OF Si GROUPS	# OF BRIDGING Os	# OF OH GROUPS	# OF OR GROUPS	CALCULATED MOLECULAR WEIGHT
688.4577	5	4	2	10	688.5435
	7	7	9	5	686.7609
	7	10	1	7	688.7609
	9	13	8	2	686.9783
	9	16	0	4	688.9783

potassium

MOLECULAR WEIGHT	# OF Si GROUPS	# OF BRIDGING Os	# OF OH GROUPS	# OF OR GROUPS	CALCULATED MOLECULAR WEIGHT
689.2542	5	4	2	10	688.5435
	8	9	11	3	690.8696
	7	10	1	7	688.7609
	10	15	10	0	691.087
	9	16	0	4	688.9783

potassium

MOLECULAR WEIGHT	# OF Si GROUPS	# OF BRIDGING Os	# OF OH GROUPS	# OF OR GROUPS	CALCULATED MOLECULAR WEIGHT
689.3427	5	4	2	10	688.5435
	8	9	11	3	690.8696
	7	10	1	7	688.7609
	10	15	10	0	691.087
	9	16	0	4	688.9783

potassium

MOLECULAR WEIGHT	# OF Si GROUPS	# OF BRIDGING Os	# OF OH GROUPS	# OF OR GROUPS	CALCULATED MOLECULAR WEIGHT
689.4312	5	4	2	10	688.5435
	8	9	11	3	690.8696
	7	10	1	7	688.7609
	10	15	10	0	691.087

	9	16	0	4	688.9783

potassium

MOLECULAR WEIGHT	# OF Si GROUPS	# OF BRIDGING Os	# OF OH GROUPS	# OF OR GROUPS	CALCULATED MOLECULAR WEIGHT
689.5197	5	4	2	10	688.5435
	8	9	11	3	690.8696
	7	10	1	7	688.7609
	10	15	10	0	691.087
	9	16	0	4	688.9783

potassium

MOLECULAR WEIGHT	# OF Si GROUPS	# OF BRIDGING Os	# OF OH GROUPS	# OF OR GROUPS	CALCULATED MOLECULAR WEIGHT
690.3168	5	4	2	10	688.5435
	8	9	11	3	690.8696
	7	10	1	7	688.7609
	10	15	10	0	691.087
	9	16	0	4	688.9783

potassium

MOLECULAR WEIGHT	# OF Si GROUPS	# OF BRIDGING Os	# OF OH GROUPS	# OF OR GROUPS	CALCULATED MOLECULAR WEIGHT
690.4054	5	4	2	10	688.5435
	8	9	11	3	690.8696
	7	10	1	7	688.7609
	10	15	10	0	691.087
	9	16	0	4	688.9783

potassium

MOLECULAR WEIGHT	# OF Si GROUPS	# OF BRIDGING Os	# OF OH GROUPS	# OF OR GROUPS	CALCULATED MOLECULAR WEIGHT
691.2916	6	6	4	8	692.6522
	8	9	11	3	690.8696
	8	12	3	5	692.8696
	10	15	10	0	691.087
	10	18	2	2	693.087

potassium

MOLECULAR WEIGHT	# OF Si GROUPS	# OF BRIDGING Os	# OF OH GROUPS	# OF OR GROUPS	CALCULATED MOLECULAR WEIGHT
691.3803	6	6	4	8	692.6522
	8	9	11	3	690.8696
	8	12	3	5	692.8696
	10	15	10	0	691.087
	10	18	2	2	693.087

potassium

MOLECULAR WEIGHT	# OF Si GROUPS	# OF BRIDGING Os	# OF OH GROUPS	# OF OR GROUPS	CALCULATED MOLECULAR WEIGHT
691.4689	6	6	4	8	692.6522
	8	9	11	3	690.8696

	8	12	3	5	692.8696
	10	15	10	0	691.087
	10	18	2	2	693.087

potassium

MOLECULAR WEIGHT	# OF Si GROUPS	# OF BRIDGING Os	# OF OH GROUPS	# OF OR GROUPS	CALCULATED MOLECULAR WEIGHT
691.5576	6	6	4	8	692.6522
	8	9	11	3	690.8696
	8	12	3	5	692.8696
	10	15	10	0	691.087
	10	18	2	2	693.087

potassium

MOLECULAR WEIGHT	# OF Si GROUPS	# OF BRIDGING Os	# OF OH GROUPS	# OF OR GROUPS	CALCULATED MOLECULAR WEIGHT
692.3558	6	6	4	8	692.6522
	8	9	11	3	690.8696
	8	12	3	5	692.8696
	10	15	10	0	691.087
	10	18	2	2	693.087

potassium

MOLECULAR WEIGHT	# OF Si GROUPS	# OF BRIDGING Os	# OF OH GROUPS	# OF OR GROUPS	CALCULATED MOLECULAR WEIGHT
693.3319	6	6	4	8	692.6522
	9	11	13	1	694.9783
	8	12	3	5	692.8696
	10	18	2	2	693.087

potassium

MOLECULAR WEIGHT	# OF Si GROUPS	# OF BRIDGING Os	# OF OH GROUPS	# OF OR GROUPS	CALCULATED MOLECULAR WEIGHT
697.243	8	7	16	2	698.8696
	7	8	6	6	696.7609
	9	14	5	3	696.9783
	11	20	4	0	697.1957

potassium

MOLECULAR WEIGHT	# OF Si GROUPS	# OF BRIDGING Os	# OF OH GROUPS	# OF OR GROUPS	CALCULATED MOLECULAR WEIGHT
697.332	8	7	16	2	698.8696
	7	8	6	6	696.7609
	9	14	5	3	696.9783
	11	20	4	0	697.1957

potassium

MOLECULAR WEIGHT	# OF Si GROUPS	# OF BRIDGING Os	# OF OH GROUPS	# OF OR GROUPS	CALCULATED MOLECULAR WEIGHT
697.421	8	7	16	2	698.8696
	7	8	6	6	696.7609
	9	14	5	3	696.9783

	11	20	4	0	697.1957

potassium

MOLECULAR WEIGHT	# OF Si GROUPS	# OF BRIDGING Os	# OF OH GROUPS	# OF OR GROUPS	CALCULATED MOLECULAR WEIGHT
697.5101	8	7	16	2	698.8696
	7	8	6	6	696.7609
	9	14	5	3	696.9783
	11	20	4	0	697.1957

potassium

MOLECULAR WEIGHT	# OF Si GROUPS	# OF BRIDGING Os	# OF OH GROUPS	# OF OR GROUPS	CALCULATED MOLECULAR WEIGHT
697.5991	8	7	16	2	698.8696
	7	8	6	6	696.7609
	9	14	5	3	696.9783
	11	20	4	0	697.1957

potassium

MOLECULAR WEIGHT	# OF Si GROUPS	# OF BRIDGING Os	# OF OH GROUPS	# OF OR GROUPS	CALCULATED MOLECULAR WEIGHT
697.6881	8	7	16	2	698.8696
	7	8	6	6	696.7609
	9	14	5	3	696.9783
	11	20	4	0	697.1957

potassium

MOLECULAR WEIGHT	# OF Si GROUPS	# OF BRIDGING Os	# OF OH GROUPS	# OF OR GROUPS	CALCULATED MOLECULAR WEIGHT
697.7771	8	7	16	2	698.8696
	7	8	6	6	696.7609
	9	14	5	3	696.9783
	11	20	4	0	697.1957

potassium

MOLECULAR WEIGHT	# OF Si GROUPS	# OF BRIDGING Os	# OF OH GROUPS	# OF OR GROUPS	CALCULATED MOLECULAR WEIGHT
698.2224	8	7	16	2	698.8696
	7	8	6	6	696.7609
	9	14	5	3	696.9783
	11	20	4	0	697.1957

potassium

MOLECULAR WEIGHT	# OF Si GROUPS	# OF BRIDGING Os	# OF OH GROUPS	# OF OR GROUPS	CALCULATED MOLECULAR WEIGHT
698.3115	8	7	16	2	698.8696
	7	8	6	6	696.7609
	9	14	5	3	696.9783
	11	20	4	0	697.1957

potassium

MOLECULAR WEIGHT	# OF Si GROUPS	# OF BRIDGING Os	# OF OH GROUPS	# OF OR GROUPS	CALCULATED MOLECULAR WEIGHT
699.2916	8	7	16	2	698.8696
	8	10	8	4	700.8696
	10	16	7	1	701.087

potassium

MOLECULAR WEIGHT	# OF Si GROUPS	# OF BRIDGING Os	# OF OH GROUPS	# OF OR GROUPS	CALCULATED MOLECULAR WEIGHT
699.3807	8	7	16	2	698.8696
	8	10	8	4	700.8696
	10	16	7	1	701.087

potassium

MOLECULAR WEIGHT	# OF Si GROUPS	# OF BRIDGING Os	# OF OH GROUPS	# OF OR GROUPS	CALCULATED MOLECULAR WEIGHT
699.4699	8	7	16	2	698.8696
	8	10	8	4	700.8696
	10	16	7	1	701.087

potassium

MOLECULAR WEIGHT	# OF Si GROUPS	# OF BRIDGING Os	# OF OH GROUPS	# OF OR GROUPS	CALCULATED MOLECULAR WEIGHT
699.559	8	7	16	2	698.8696
	8	10	8	4	700.8696
	10	16	7	1	701.087

potassium

MOLECULAR WEIGHT	# OF Si GROUPS	# OF BRIDGING Os	# OF OH GROUPS	# OF OR GROUPS	CALCULATED MOLECULAR WEIGHT
699.6482	8	7	16	2	698.8696
	8	10	8	4	700.8696
	10	16	7	1	701.087

potassium

MOLECULAR WEIGHT	# OF Si GROUPS	# OF BRIDGING Os	# OF OH GROUPS	# OF OR GROUPS	CALCULATED MOLECULAR WEIGHT
700.2724	8	7	16	2	698.8696
	8	10	8	4	700.8696
	10	16	7	1	701.087

potassium

MOLECULAR WEIGHT	# OF Si GROUPS	# OF BRIDGING Os	# OF OH GROUPS	# OF OR GROUPS	CALCULATED MOLECULAR WEIGHT
700.3615	8	7	16	2	698.8696
	8	10	8	4	700.8696
	10	16	7	1	701.087

potassium

MOLECULAR	# OF Si	# OF	# OF OH	# OF OR	CALCULATED

WEIGHT	GROUPS	BRIDGING Os	GROUPS	GROUPS	MOLECULAR WEIGHT
700.4507	8	7	16	2	698.8696
	8	10	8	4	700.8696
	10	16	7	1	701.087

potassium

MOLECULAR WEIGHT	# OF Si GROUPS	# OF BRIDGING Os	# OF OH GROUPS	# OF OR GROUPS	CALCULATED MOLECULAR WEIGHT
700.54	8	7	16	2	698.8696
	8	10	8	4	700.8696
	10	16	7	1	701.087

potassium

MOLECULAR WEIGHT	# OF Si GROUPS	# OF BRIDGING Os	# OF OH GROUPS	# OF OR GROUPS	CALCULATED MOLECULAR WEIGHT
701.1645	9	9	18	0	702.9783
	6	7	1	9	702.6522
	8	10	8	4	700.8696
	8	13	0	6	702.8696
	10	16	7	1	701.087

potassium

MOLECULAR WEIGHT	# OF Si GROUPS	# OF BRIDGING Os	# OF OH GROUPS	# OF OR GROUPS	CALCULATED MOLECULAR WEIGHT
701.2538	9	9	18	0	702.9783
	6	7	1	9	702.6522
	8	10	8	4	700.8696
	8	13	0	6	702.8696
	10	16	7	1	701.087

potassium

MOLECULAR WEIGHT	# OF Si GROUPS	# OF BRIDGING Os	# OF OH GROUPS	# OF OR GROUPS	CALCULATED MOLECULAR WEIGHT
701.343	9	9	18	0	702.9783
	6	7	1	9	702.6522
	8	10	8	4	700.8696
	8	13	0	6	702.8696
	10	16	7	1	701.087

potassium

MOLECULAR WEIGHT	# OF Si GROUPS	# OF BRIDGING Os	# OF OH GROUPS	# OF OR GROUPS	CALCULATED MOLECULAR WEIGHT
701.4323	9	9	18	0	702.9783
	6	7	1	9	702.6522
	8	10	8	4	700.8696
	8	13	0	6	702.8696
	10	16	7	1	701.087

potassium

MOLECULAR WEIGHT	# OF Si GROUPS	# OF BRIDGING Os	# OF OH GROUPS	# OF OR GROUPS	CALCULATED MOLECULAR WEIGHT

701.5215	9	9	18	0	702.9783
	6	7	1	9	702.6522
	8	10	8	4	700.8696
	8	13	0	6	702.8696
	10	16	7	1	701.087

potassium

MOLECULAR WEIGHT	# OF Si GROUPS	# OF BRIDGING Os	# OF OH GROUPS	# OF OR GROUPS	CALCULATED MOLECULAR WEIGHT
701.6108	9	9	18	0	702.9783
	6	7	1	9	702.6522
	8	10	8	4	700.8696
	8	13	0	6	702.8696
	10	16	7	1	701.087

potassium

MOLECULAR WEIGHT	# OF Si GROUPS	# OF BRIDGING Os	# OF OH GROUPS	# OF OR GROUPS	CALCULATED MOLECULAR WEIGHT
702.2358	9	9	18	0	702.9783
	6	7	1	9	702.6522
	8	10	8	4	700.8696
	8	13	0	6	702.8696
	10	16	7	1	701.087

potassium

MOLECULAR WEIGHT	# OF Si GROUPS	# OF BRIDGING Os	# OF OH GROUPS	# OF OR GROUPS	CALCULATED MOLECULAR WEIGHT
702.3251	9	9	18	0	702.9783
	6	7	1	9	702.6522
	8	10	8	4	700.8696
	8	13	0	6	702.8696
	10	16	7	1	701.087

potassium

MOLECULAR WEIGHT	# OF Si GROUPS	# OF BRIDGING Os	# OF OH GROUPS	# OF OR GROUPS	CALCULATED MOLECULAR WEIGHT
702.4145	9	9	18	0	702.9783
	6	7	1	9	702.6522
	8	10	8	4	700.8696
	8	13	0	6	702.8696
	10	16	7	1	701.087

potassium

MOLECULAR WEIGHT	# OF Si GROUPS	# OF BRIDGING Os	# OF OH GROUPS	# OF OR GROUPS	CALCULATED MOLECULAR WEIGHT
702.5038	9	9	18	0	702.9783
	6	7	1	9	702.6522
	8	10	8	4	700.8696
	8	13	0	6	702.8696
	10	16	7	1	701.087

potassium

MOLECULAR	# OF Si	# OF	# OF OH	# OF OR	CALCULATED

WEIGHT	GROUPS	BRIDGING Os	GROUPS	GROUPS	MOLECULAR WEIGHT
702.5931	9	9	18	0	702.9783
	6	7	1	9	702.6522
	8	10	8	4	700.8696
	8	13	0	6	702.8696
	10	16	7	1	701.087

potassium

MOLECULAR WEIGHT	# OF Si GROUPS	# OF BRIDGING Os	# OF OH GROUPS	# OF OR GROUPS	CALCULATED MOLECULAR WEIGHT
703.2186	7	6	11	5	704.7609
	9	9	18	0	702.9783
	6	7	1	9	702.6522
	9	12	10	2	704.9783
	8	13	0	6	702.8696

potassium

MOLECULAR WEIGHT	# OF Si GROUPS	# OF BRIDGING Os	# OF OH GROUPS	# OF OR GROUPS	CALCULATED MOLECULAR WEIGHT
703.3079	7	6	11	5	704.7609
	9	9	18	0	702.9783
	6	7	1	9	702.6522
	9	12	10	2	704.9783
	8	13	0	6	702.8696

potassium

MOLECULAR WEIGHT	# OF Si GROUPS	# OF BRIDGING Os	# OF OH GROUPS	# OF OR GROUPS	CALCULATED MOLECULAR WEIGHT
703.3973	7	6	11	5	704.7609
	9	9	18	0	702.9783
	6	7	1	9	702.6522
	9	12	10	2	704.9783
	8	13	0	6	702.8696

potassium

MOLECULAR WEIGHT	# OF Si GROUPS	# OF BRIDGING Os	# OF OH GROUPS	# OF OR GROUPS	CALCULATED MOLECULAR WEIGHT
703.4867	7	6	11	5	704.7609
	9	9	18	0	702.9783
	6	7	1	9	702.6522
	9	12	10	2	704.9783
	8	13	0	6	702.8696

potassium

MOLECULAR WEIGHT	# OF Si GROUPS	# OF BRIDGING Os	# OF OH GROUPS	# OF OR GROUPS	CALCULATED MOLECULAR WEIGHT
705.2754	7	6	11	5	704.7609
	7	9	3	7	706.7609
	9	12	10	2	704.9783
	9	15	2	4	706.9783
	11	21	1	1	707.1957

potassium

MOLECULAR WEIGHT	# OF Si GROUPS	# OF BRIDGING Os	# OF OH GROUPS	# OF OR GROUPS	CALCULATED MOLECULAR WEIGHT
705.3649	7	6	11	5	704.7609
	7	9	3	7	706.7609
	9	12	10	2	704.9783
	9	15	2	4	706.9783
	11	21	1	1	707.1957

potassium

MOLECULAR WEIGHT	# OF Si GROUPS	# OF BRIDGING Os	# OF OH GROUPS	# OF OR GROUPS	CALCULATED MOLECULAR WEIGHT
706.2602	7	6	11	5	704.7609
	7	9	3	7	706.7609
	9	12	10	2	704.9783
	9	15	2	4	706.9783
	11	21	1	1	707.1957

potassium

MOLECULAR WEIGHT	# OF Si GROUPS	# OF BRIDGING Os	# OF OH GROUPS	# OF OR GROUPS	CALCULATED MOLECULAR WEIGHT
707.2455	8	8	13	3	708.8696
	7	9	3	7	706.7609
	10	14	12	0	709.087
	9	15	2	4	706.9783
	11	21	1	1	707.1957

potassium

MOLECULAR WEIGHT	# OF Si GROUPS	# OF BRIDGING Os	# OF OH GROUPS	# OF OR GROUPS	CALCULATED MOLECULAR WEIGHT
707.3352	8	8	13	3	708.8696
	7	9	3	7	706.7609
	10	14	12	0	709.087
	9	15	2	4	706.9783
	11	21	1	1	707.1957

potassium

MOLECULAR WEIGHT	# OF Si GROUPS	# OF BRIDGING Os	# OF OH GROUPS	# OF OR GROUPS	CALCULATED MOLECULAR WEIGHT
710.7444	6	5	6	8	710.6522
	8	8	13	3	708.8696
	8	11	5	5	710.8696
	10	14	12	0	709.087
	10	17	4	2	711.087

potassium

MOLECULAR WEIGHT	# OF Si GROUPS	# OF BRIDGING Os	# OF OH GROUPS	# OF OR GROUPS	CALCULATED MOLECULAR WEIGHT
711.3733	6	5	6	8	710.6522
	9	10	15	1	712.9783
	8	11	5	5	710.8696

	10	17	4	2	711.087

potassium

MOLECULAR WEIGHT	# OF Si GROUPS	# OF BRIDGING Os	# OF OH GROUPS	# OF OR GROUPS	CALCULATED MOLECULAR WEIGHT
711.4631	6	5	6	8	710.6522
	9	10	15	1	712.9783
	8	11	5	5	710.8696
	10	17	4	2	711.087

potassium

MOLECULAR WEIGHT	# OF Si GROUPS	# OF BRIDGING Os	# OF OH GROUPS	# OF OR GROUPS	CALCULATED MOLECULAR WEIGHT
711.553	6	5	6	8	710.6522
	9	10	15	1	712.9783
	8	11	5	5	710.8696
	10	17	4	2	711.087

potassium

MOLECULAR WEIGHT	# OF Si GROUPS	# OF BRIDGING Os	# OF OH GROUPS	# OF OR GROUPS	CALCULATED MOLECULAR WEIGHT
712.362	6	5	6	8	710.6522
	9	10	15	1	712.9783
	8	11	5	5	710.8696
	10	17	4	2	711.087

potassium

MOLECULAR WEIGHT	# OF Si GROUPS	# OF BRIDGING Os	# OF OH GROUPS	# OF OR GROUPS	CALCULATED MOLECULAR WEIGHT
712.452	6	5	6	8	710.6522
	9	10	15	1	712.9783
	8	11	5	5	710.8696
	10	17	4	2	711.087

potassium

MOLECULAR WEIGHT	# OF Si GROUPS	# OF BRIDGING Os	# OF OH GROUPS	# OF OR GROUPS	CALCULATED MOLECULAR WEIGHT
712.5419	6	5	6	8	710.6522
	9	10	15	1	712.9783
	8	11	5	5	710.8696
	10	17	4	2	711.087

potassium

MOLECULAR WEIGHT	# OF Si GROUPS	# OF BRIDGING Os	# OF OH GROUPS	# OF OR GROUPS	CALCULATED MOLECULAR WEIGHT
713.1715	7	7	8	6	714.7609
	9	10	15	1	712.9783
	9	13	7	3	714.9783

potassium

MOLECULAR WEIGHT	# OF Si GROUPS	# OF BRIDGING Os	# OF OH GROUPS	# OF OR GROUPS	CALCULATED MOLECULAR WEIGHT

713.2615	7	7	8	6	714.7609
	9	10	15	1	712.9783
	9	13	7	3	714.9783
	11	19	6	0	715.1957

potassium

MOLECULAR WEIGHT	# OF Si GROUPS	# OF BRIDGING Os	# OF OH GROUPS	# OF OR GROUPS	CALCULATED MOLECULAR WEIGHT
713.3514	7	7	8	6	714.7609
	9	10	15	1	712.9783
	9	13	7	3	714.9783
	11	19	6	0	715.1957

potassium

MOLECULAR WEIGHT	# OF Si GROUPS	# OF BRIDGING Os	# OF OH GROUPS	# OF OR GROUPS	CALCULATED MOLECULAR WEIGHT
713.4414	7	7	8	6	714.7609
	9	10	15	1	712.9783
	9	13	7	3	714.9783
	11	19	6	0	715.1957

potassium

MOLECULAR WEIGHT	# OF Si GROUPS	# OF BRIDGING Os	# OF OH GROUPS	# OF OR GROUPS	CALCULATED MOLECULAR WEIGHT
713.5314	7	7	8	6	714.7609
	9	10	15	1	712.9783
	9	13	7	3	714.9783
	11	19	6	0	715.1957

potassium

MOLECULAR WEIGHT	# OF Si GROUPS	# OF BRIDGING Os	# OF OH GROUPS	# OF OR GROUPS	CALCULATED MOLECULAR WEIGHT
713.6214	7	7	8	6	714.7609
	9	10	15	1	712.9783
	9	13	7	3	714.9783
	11	19	6	0	715.1957

potassium

MOLECULAR WEIGHT	# OF Si GROUPS	# OF BRIDGING Os	# OF OH GROUPS	# OF OR GROUPS	CALCULATED MOLECULAR WEIGHT
713.7114	7	7	8	6	714.7609
	9	10	15	1	712.9783
	9	13	7	3	714.9783
	11	19	6	0	715.1957

potassium

MOLECULAR WEIGHT	# OF Si GROUPS	# OF BRIDGING Os	# OF OH GROUPS	# OF OR GROUPS	CALCULATED MOLECULAR WEIGHT
714.1614	7	7	8	6	714.7609
	9	10	15	1	712.9783
	9	13	7	3	714.9783
	11	19	6	0	715.1957

potassium

MOLECULAR WEIGHT	# OF Si GROUPS	# OF BRIDGING Os	# OF OH GROUPS	# OF OR GROUPS	CALCULATED MOLECULAR WEIGHT
733.4586	7	6	10	6	732.7609
	7	9	2	8	734.7609
	9	12	9	3	732.9783
	9	15	1	5	734.9783
	11	18	8	0	733.1957
	11	21	0	2	735.1957

potassium

MOLECULAR WEIGHT	# OF Si GROUPS	# OF BRIDGING Os	# OF OH GROUPS	# OF OR GROUPS	CALCULATED MOLECULAR WEIGHT
734.1881	7	6	10	6	732.7609
	7	9	2	8	734.7609
	9	12	9	3	732.9783
	9	15	1	5	734.9783
	11	18	8	0	733.1957
	11	21	0	2	735.1957

potassium

MOLECULAR WEIGHT	# OF Si GROUPS	# OF BRIDGING Os	# OF OH GROUPS	# OF OR GROUPS	CALCULATED MOLECULAR WEIGHT
734.2793	7	6	10	6	732.7609
	7	9	2	8	734.7609
	9	12	9	3	732.9783
	9	15	1	5	734.9783
	11	18	8	0	733.1957
	11	21	0	2	735.1957

potassium

MOLECULAR WEIGHT	# OF Si GROUPS	# OF BRIDGING Os	# OF OH GROUPS	# OF OR GROUPS	CALCULATED MOLECULAR WEIGHT
735.1918	8	8	12	4	736.8696
	7	9	2	8	734.7609
	10	14	11	1	737.087
	9	15	1	5	734.9783
	11	18	8	0	733.1957
	11	21	0	2	735.1957

potassium

MOLECULAR WEIGHT	# OF Si GROUPS	# OF BRIDGING Os	# OF OH GROUPS	# OF OR GROUPS	CALCULATED MOLECULAR WEIGHT
735.2831	8	8	12	4	736.8696
	7	9	2	8	734.7609
	10	14	11	1	737.087
	9	15	1	5	734.9783
	11	21	0	2	735.1957

potassium

MOLECULAR WEIGHT	# OF Si GROUPS	# OF BRIDGING	# OF OH GROUPS	# OF OR GROUPS	CALCULATED MOLECULAR

		Os			WEIGHT
740.403	6	5	5	9	738.6522
	9	10	14	2	740.9783
	8	11	4	6	738.8696
	10	17	3	3	739.087
	12	23	2	0	739.3044

potassium

MOLECULAR WEIGHT	# OF Si GROUPS	# OF BRIDGING Os	# OF OH GROUPS	# OF OR GROUPS	CALCULATED MOLECULAR WEIGHT
740.4946	6	5	5	9	738.6522
	9	10	14	2	740.9783
	8	11	4	6	738.8696
	10	17	3	3	739.087
	12	23	2	0	739.3044

potassium

MOLECULAR WEIGHT	# OF Si GROUPS	# OF BRIDGING Os	# OF OH GROUPS	# OF OR GROUPS	CALCULATED MOLECULAR WEIGHT
740.5862	6	5	5	9	738.6522
	9	10	14	2	740.9783
	8	11	4	6	738.8696
	10	17	3	3	739.087
	12	23	2	0	739.3044

potassium

MOLECULAR WEIGHT	# OF Si GROUPS	# OF BRIDGING Os	# OF OH GROUPS	# OF OR GROUPS	CALCULATED MOLECULAR WEIGHT
740.6778	9	10	14	2	740.9783
	8	11	4	6	738.8696
	10	17	3	3	739.087
	12	23	2	0	739.3044

potassium

MOLECULAR WEIGHT	# OF Si GROUPS	# OF BRIDGING Os	# OF OH GROUPS	# OF OR GROUPS	CALCULATED MOLECULAR WEIGHT
741.2275	7	7	7	7	742.7609
	9	10	14	2	740.9783
	9	13	6	4	742.9783
	11	19	5	1	743.1957
	12	23	2	0	739.3044

potassium

MOLECULAR WEIGHT	# OF Si GROUPS	# OF BRIDGING Os	# OF OH GROUPS	# OF OR GROUPS	CALCULATED MOLECULAR WEIGHT
741.3191	7	7	7	7	742.7609
	9	10	14	2	740.9783
	9	13	6	4	742.9783
	11	19	5	1	743.1957

potassium

MOLECULAR WEIGHT	# OF Si GROUPS	# OF BRIDGING	# OF OH GROUPS	# OF OR GROUPS	CALCULATED MOLECULAR

		Os			WEIGHT
741.4107	7	7	7	7	742.7609
	9	10	14	2	740.9783
	9	13	6	4	742.9783
	11	19	5	1	743.1957

potassium

MOLECULAR WEIGHT	# OF Si GROUPS	# OF BRIDGING Os	# OF OH GROUPS	# OF OR GROUPS	CALCULATED MOLECULAR WEIGHT
741.5024	7	7	7	7	742.7609
	9	10	14	2	740.9783
	9	13	6	4	742.9783
	11	19	5	1	743.1957

potassium

MOLECULAR WEIGHT	# OF Si GROUPS	# OF BRIDGING Os	# OF OH GROUPS	# OF OR GROUPS	CALCULATED MOLECULAR WEIGHT
741.594	7	7	7	7	742.7609
	9	10	14	2	740.9783
	9	13	6	4	742.9783
	11	19	5	1	743.1957

potassium

MOLECULAR WEIGHT	# OF Si GROUPS	# OF BRIDGING Os	# OF OH GROUPS	# OF OR GROUPS	CALCULATED MOLECULAR WEIGHT
742.2357	7	7	7	7	742.7609
	9	10	14	2	740.9783
	9	13	6	4	742.9783
	11	19	5	1	743.1957

potassium

MOLECULAR WEIGHT	# OF Si GROUPS	# OF BRIDGING Os	# OF OH GROUPS	# OF OR GROUPS	CALCULATED MOLECULAR WEIGHT
742.3274	7	7	7	7	742.7609
	9	10	14	2	740.9783
	9	13	6	4	742.9783
	11	19	5	1	743.1957

potassium

MOLECULAR WEIGHT	# OF Si GROUPS	# OF BRIDGING Os	# OF OH GROUPS	# OF OR GROUPS	CALCULATED MOLECULAR WEIGHT
742.4191	7	7	7	7	742.7609
	9	10	14	2	740.9783
	9	13	6	4	742.9783
	11	19	5	1	743.1957

potassium

MOLECULAR WEIGHT	# OF Si GROUPS	# OF BRIDGING Os	# OF OH GROUPS	# OF OR GROUPS	CALCULATED MOLECULAR WEIGHT
742.5108	7	7	7	7	742.7609
	9	10	14	2	740.9783
	9	13	6	4	742.9783

	11	19	5	1	743.1957

potassium

MOLECULAR WEIGHT	# OF Si GROUPS	# OF BRIDGING Os	# OF OH GROUPS	# OF OR GROUPS	CALCULATED MOLECULAR WEIGHT
742.6025	5	4	0	12	744.5435
	7	7	7	7	742.7609
	9	10	14	2	740.9783
	9	13	6	4	742.9783
	11	19	5	1	743.1957

potassium

MOLECULAR WEIGHT	# OF Si GROUPS	# OF BRIDGING Os	# OF OH GROUPS	# OF OR GROUPS	CALCULATED MOLECULAR WEIGHT
743.2446	5	4	0	12	744.5435
	7	7	7	7	742.7609
	10	12	16	0	745.087
	9	13	6	4	742.9783
	11	19	5	1	743.1957

potassium

MOLECULAR WEIGHT	# OF Si GROUPS	# OF BRIDGING Os	# OF OH GROUPS	# OF OR GROUPS	CALCULATED MOLECULAR WEIGHT
743.3363	5	4	0	12	744.5435
	7	7	7	7	742.7609
	10	12	16	0	745.087
	9	13	6	4	742.9783
	11	19	5	1	743.1957

potassium

MOLECULAR WEIGHT	# OF Si GROUPS	# OF BRIDGING Os	# OF OH GROUPS	# OF OR GROUPS	CALCULATED MOLECULAR WEIGHT
743.4281	5	4	0	12	744.5435
	7	7	7	7	742.7609
	10	12	16	0	745.087
	9	13	6	4	742.9783
	11	19	5	1	743.1957

potassium

MOLECULAR WEIGHT	# OF Si GROUPS	# OF BRIDGING Os	# OF OH GROUPS	# OF OR GROUPS	CALCULATED MOLECULAR WEIGHT
743.5198	5	4	0	12	744.5435
	7	7	7	7	742.7609
	10	12	16	0	745.087
	9	13	6	4	742.9783
	11	19	5	1	743.1957

potassium

MOLECULAR WEIGHT	# OF Si GROUPS	# OF BRIDGING Os	# OF OH GROUPS	# OF OR GROUPS	CALCULATED MOLECULAR WEIGHT
748.1146	9	8	19	1	748.9783
	6	6	2	10	748.6522
	8	9	9	5	746.8696
	8	12	1	7	748.8696
	10	15	8	2	747.087
	10	18	0	4	749.087

potassium

MOLECULAR WEIGHT	# OF Si GROUPS	# OF BRIDGING Os	# OF OH GROUPS	# OF OR GROUPS	CALCULATED MOLECULAR WEIGHT
748.2067	9	8	19	1	748.9783
	6	6	2	10	748.6522
	8	9	9	5	746.8696
	8	12	1	7	748.8696
	10	15	8	2	747.087
	10	18	0	4	749.087

potassium

MOLECULAR WEIGHT	# OF Si GROUPS	# OF BRIDGING Os	# OF OH GROUPS	# OF OR GROUPS	CALCULATED MOLECULAR WEIGHT
748.2987	9	8	19	1	748.9783
	6	6	2	10	748.6522
	8	9	9	5	746.8696
	8	12	1	7	748.8696
	10	15	8	2	747.087
	10	18	0	4	749.087

potassium

MOLECULAR WEIGHT	# OF Si GROUPS	# OF BRIDGING Os	# OF OH GROUPS	# OF OR GROUPS	CALCULATED MOLECULAR WEIGHT
749.1273	9	8	19	1	748.9783
	6	6	2	10	748.6522
	9	11	11	3	750.9783
	8	12	1	7	748.8696
	10	18	0	4	749.087

potassium

MOLECULAR WEIGHT	# OF Si GROUPS	# OF BRIDGING Os	# OF OH GROUPS	# OF OR GROUPS	CALCULATED MOLECULAR WEIGHT
749.2194	9	8	19	1	748.9783
	6	6	2	10	748.6522
	9	11	11	3	750.9783
	8	12	1	7	748.8696
	11	17	10	0	751.1957
	10	18	0	4	749.087

potassium

MOLECULAR	# OF Si	# OF	# OF OH	# OF OR	CALCULATED

WEIGHT	GROUPS	BRIDGING Os	GROUPS	GROUPS	MOLECULAR WEIGHT
749.3115	9	8	19	1	748.9783
	6	6	2	10	748.6522
	9	11	11	3	750.9783
	8	12	1	7	748.8696
	11	17	10	0	751.1957
	10	18	0	4	749.087

potassium

MOLECULAR WEIGHT	# OF Si GROUPS	# OF BRIDGING Os	# OF OH GROUPS	# OF OR GROUPS	CALCULATED MOLECULAR WEIGHT
757.1595	9	9	16	2	758.9783
	8	10	6	6	756.8696
	10	16	5	3	757.087
	12	22	4	0	757.3044

potassium

MOLECULAR WEIGHT	# OF Si GROUPS	# OF BRIDGING Os	# OF OH GROUPS	# OF OR GROUPS	CALCULATED MOLECULAR WEIGHT
757.2521	9	9	16	2	758.9783
	8	10	6	6	756.8696
	10	16	5	3	757.087
	12	22	4	0	757.3044

potassium

MOLECULAR WEIGHT	# OF Si GROUPS	# OF BRIDGING Os	# OF OH GROUPS	# OF OR GROUPS	CALCULATED MOLECULAR WEIGHT
757.3446	9	9	16	2	758.9783
	8	10	6	6	756.8696
	10	16	5	3	757.087
	12	22	4	0	757.3044

potassium

MOLECULAR WEIGHT	# OF Si GROUPS	# OF BRIDGING Os	# OF OH GROUPS	# OF OR GROUPS	CALCULATED MOLECULAR WEIGHT
757.4372	9	9	16	2	758.9783
	8	10	6	6	756.8696
	10	16	5	3	757.087
	12	22	4	0	757.3044

potassium

MOLECULAR WEIGHT	# OF Si GROUPS	# OF BRIDGING Os	# OF OH GROUPS	# OF OR GROUPS	CALCULATED MOLECULAR WEIGHT
757.5298	9	9	16	2	758.9783
	8	10	6	6	756.8696
	10	16	5	3	757.087
	12	22	4	0	757.3044

potassium

MOLECULAR WEIGHT	# OF Si GROUPS	# OF BRIDGING Os	# OF OH GROUPS	# OF OR GROUPS	CALCULATED MOLECULAR WEIGHT

758.0853	9	9	16	2	758.9783
	8	10	6	6	756.8696
	10	16	5	3	757.087
	12	22	4	0	757.3044

potassium

MOLECULAR WEIGHT	# OF Si GROUPS	# OF BRIDGING Os	# OF OH GROUPS	# OF OR GROUPS	CALCULATED MOLECULAR WEIGHT
758.178	9	9	16	2	758.9783
	8	10	6	6	756.8696
	10	16	5	3	757.087
	12	22	4	0	757.3044

potassium

MOLECULAR WEIGHT	# OF Si GROUPS	# OF BRIDGING Os	# OF OH GROUPS	# OF OR GROUPS	CALCULATED MOLECULAR WEIGHT
758.2706	9	9	16	2	758.9783
	8	10	6	6	756.8696
	10	16	5	3	757.087
	12	22	4	0	757.3044

potassium

MOLECULAR WEIGHT	# OF Si GROUPS	# OF BRIDGING Os	# OF OH GROUPS	# OF OR GROUPS	CALCULATED MOLECULAR WEIGHT
758.3632	9	9	16	2	758.9783
	8	10	6	6	756.8696
	10	16	5	3	757.087
	12	22	4	0	757.3044

potassium

MOLECULAR WEIGHT	# OF Si GROUPS	# OF BRIDGING Os	# OF OH GROUPS	# OF OR GROUPS	CALCULATED MOLECULAR WEIGHT
758.4558	9	9	16	2	758.9783
	8	10	6	6	756.8696
	10	16	5	3	757.087
	12	22	4	0	757.3044

potassium

MOLECULAR WEIGHT	# OF Si GROUPS	# OF BRIDGING Os	# OF OH GROUPS	# OF OR GROUPS	CALCULATED MOLECULAR WEIGHT
758.5485	9	9	16	2	758.9783
	8	10	6	6	756.8696
	10	16	5	3	757.087
	12	22	4	0	757.3044

potassium

MOLECULAR WEIGHT	# OF Si GROUPS	# OF BRIDGING Os	# OF OH GROUPS	# OF OR GROUPS	CALCULATED MOLECULAR WEIGHT
759.1044	7	6	9	7	760.7609
	9	9	16	2	758.9783
	9	12	8	4	760.9783
	12	22	4	0	757.3044

potassium

MOLECULAR WEIGHT	# OF Si GROUPS	# OF BRIDGING Os	# OF OH GROUPS	# OF OR GROUPS	CALCULATED MOLECULAR WEIGHT
759.1971	7	6	9	7	760.7609
	9	9	16	2	758.9783
	9	12	8	4	760.9783
	11	18	7	1	761.1957
	12	22	4	0	757.3044

potassium

MOLECULAR WEIGHT	# OF Si GROUPS	# OF BRIDGING Os	# OF OH GROUPS	# OF OR GROUPS	CALCULATED MOLECULAR WEIGHT
759.2898	7	6	9	7	760.7609
	9	9	16	2	758.9783
	9	12	8	4	760.9783
	11	18	7	1	761.1957
	12	22	4	0	757.3044

potassium

MOLECULAR WEIGHT	# OF Si GROUPS	# OF BRIDGING Os	# OF OH GROUPS	# OF OR GROUPS	CALCULATED MOLECULAR WEIGHT
759.3824	7	6	9	7	760.7609
	9	9	16	2	758.9783
	9	12	8	4	760.9783
	11	18	7	1	761.1957

potassium

MOLECULAR WEIGHT	# OF Si GROUPS	# OF BRIDGING Os	# OF OH GROUPS	# OF OR GROUPS	CALCULATED MOLECULAR WEIGHT
759.4751	7	6	9	7	760.7609
	9	9	16	2	758.9783
	9	12	8	4	760.9783
	11	18	7	1	761.1957

potassium

MOLECULAR WEIGHT	# OF Si GROUPS	# OF BRIDGING Os	# OF OH GROUPS	# OF OR GROUPS	CALCULATED MOLECULAR WEIGHT
759.5678	7	6	9	7	760.7609
	9	9	16	2	758.9783
	9	12	8	4	760.9783
	11	18	7	1	761.1957

potassium

MOLECULAR WEIGHT	# OF Si GROUPS	# OF BRIDGING Os	# OF OH GROUPS	# OF OR GROUPS	CALCULATED MOLECULAR WEIGHT
760.1241	7	6	9	7	760.7609
	9	9	16	2	758.9783
	9	12	8	4	760.9783
	11	18	7	1	761.1957

potassium

MOLECULAR WEIGHT	# OF Si GROUPS	# OF BRIDGING Os	# OF OH GROUPS	# OF OR GROUPS	CALCULATED MOLECULAR WEIGHT
763.0942	8	8	11	5	764.8696
	10	11	18	0	763.087
	7	9	1	9	762.7609
	10	14	10	2	765.087
	9	15	0	6	762.9783
	11	18	7	1	761.1957

potassium

MOLECULAR WEIGHT	# OF Si GROUPS	# OF BRIDGING Os	# OF OH GROUPS	# OF OR GROUPS	CALCULATED MOLECULAR WEIGHT
763.1871	8	8	11	5	764.8696
	10	11	18	0	763.087
	7	9	1	9	762.7609
	10	14	10	2	765.087
	9	15	0	6	762.9783
	11	18	7	1	761.1957

potassium

MOLECULAR WEIGHT	# OF Si GROUPS	# OF BRIDGING Os	# OF OH GROUPS	# OF OR GROUPS	CALCULATED MOLECULAR WEIGHT
763.28	8	8	11	5	764.8696
	10	11	18	0	763.087
	7	9	1	9	762.7609
	10	14	10	2	765.087
	9	15	0	6	762.9783

potassium

MOLECULAR WEIGHT	# OF Si GROUPS	# OF BRIDGING Os	# OF OH GROUPS	# OF OR GROUPS	CALCULATED MOLECULAR WEIGHT
763.373	8	8	11	5	764.8696
	10	11	18	0	763.087
	7	9	1	9	762.7609
	10	14	10	2	765.087
	9	15	0	6	762.9783

potassium

MOLECULAR WEIGHT	# OF Si GROUPS	# OF BRIDGING Os	# OF OH GROUPS	# OF OR GROUPS	CALCULATED MOLECULAR WEIGHT
764.1165	8	8	11	5	764.8696
	10	11	18	0	763.087
	7	9	1	9	762.7609
	10	14	10	2	765.087
	9	15	0	6	762.9783

potassium

MOLECULAR WEIGHT	# OF Si GROUPS	# OF BRIDGING Os	# OF OH GROUPS	# OF OR GROUPS	CALCULATED MOLECULAR WEIGHT
764.2094	8	8	11	5	764.8696
	10	11	18	0	763.087
	7	9	1	9	762.7609
	10	14	10	2	765.087

	9	15	0	6	762.9783

potassium

MOLECULAR WEIGHT	# OF Si GROUPS	# OF BRIDGING Os	# OF OH GROUPS	# OF OR GROUPS	CALCULATED MOLECULAR WEIGHT
765.1394	6	5	4	10	766.6522
	8	8	11	5	764.8696
	8	11	3	7	766.8696
	10	14	10	2	765.087
	10	17	2	4	767.087

potassium

MOLECULAR WEIGHT	# OF Si GROUPS	# OF BRIDGING Os	# OF OH GROUPS	# OF OR GROUPS	CALCULATED MOLECULAR WEIGHT
765.4185	6	5	4	10	766.6522
	8	8	11	5	764.8696
	8	11	3	7	766.8696
	10	14	10	2	765.087
	10	17	2	4	767.087
	12	23	1	1	767.3044

potassium

MOLECULAR WEIGHT	# OF Si GROUPS	# OF BRIDGING Os	# OF OH GROUPS	# OF OR GROUPS	CALCULATED MOLECULAR WEIGHT
765.5115	6	5	4	10	766.6522
	8	8	11	5	764.8696
	8	11	3	7	766.8696
	10	14	10	2	765.087
	10	17	2	4	767.087
	12	23	1	1	767.3044

potassium

MOLECULAR WEIGHT	# OF Si GROUPS	# OF BRIDGING Os	# OF OH GROUPS	# OF OR GROUPS	CALCULATED MOLECULAR WEIGHT
768.4916	6	5	4	10	766.6522
	9	10	13	3	768.9783
	8	11	3	7	766.8696
	11	16	12	0	769.1957
	10	17	2	4	767.087
	12	23	1	1	767.3044

potassium

MOLECULAR WEIGHT	# OF Si GROUPS	# OF BRIDGING Os	# OF OH GROUPS	# OF OR GROUPS	CALCULATED MOLECULAR WEIGHT
769.2375	7	7	6	8	770.7609
	9	10	13	3	768.9783
	9	13	5	5	770.9783
	11	16	12	0	769.1957
	11	19	4	2	771.1957
	12	23	1	1	767.3044

potassium

MOLECULAR WEIGHT	# OF Si GROUPS	# OF BRIDGING Os	# OF OH GROUPS	# OF OR GROUPS	CALCULATED MOLECULAR WEIGHT
769.3308	7	7	6	8	770.7609
	9	10	13	3	768.9783

	9	13	5	5	770.9783
	11	16	12	0	769.1957
	11	19	4	2	771.1957

potassium

MOLECULAR WEIGHT	# OF Si GROUPS	# OF BRIDGING Os	# OF OH GROUPS	# OF OR GROUPS	CALCULATED MOLECULAR WEIGHT
769.424	7	7	6	8	770.7609
	9	10	13	3	768.9783
	9	13	5	5	770.9783
	11	16	12	0	769.1957
	11	19	4	2	771.1957

potassium

MOLECULAR WEIGHT	# OF Si GROUPS	# OF BRIDGING Os	# OF OH GROUPS	# OF OR GROUPS	CALCULATED MOLECULAR WEIGHT
769.5173	7	7	6	8	770.7609
	9	10	13	3	768.9783
	9	13	5	5	770.9783
	11	16	12	0	769.1957
	11	19	4	2	771.1957

potassium

MOLECULAR WEIGHT	# OF Si GROUPS	# OF BRIDGING Os	# OF OH GROUPS	# OF OR GROUPS	CALCULATED MOLECULAR WEIGHT
770.2637	7	7	6	8	770.7609
	9	10	13	3	768.9783
	9	13	5	5	770.9783
	11	16	12	0	769.1957
	11	19	4	2	771.1957

potassium

MOLECULAR WEIGHT	# OF Si GROUPS	# OF BRIDGING Os	# OF OH GROUPS	# OF OR GROUPS	CALCULATED MOLECULAR WEIGHT
770.357	7	7	6	8	770.7609
	9	10	13	3	768.9783
	9	13	5	5	770.9783
	11	16	12	0	769.1957
	11	19	4	2	771.1957

potassium

MOLECULAR WEIGHT	# OF Si GROUPS	# OF BRIDGING Os	# OF OH GROUPS	# OF OR GROUPS	CALCULATED MOLECULAR WEIGHT
770.4503	7	7	6	8	770.7609
	9	10	13	3	768.9783
	9	13	5	5	770.9783
	11	16	12	0	769.1957
	11	19	4	2	771.1957

potassium

MOLECULAR WEIGHT	# OF Si GROUPS	# OF BRIDGING Os	# OF OH GROUPS	# OF OR GROUPS	CALCULATED MOLECULAR WEIGHT
771.1971	7	7	6	8	770.7609
	10	12	15	1	773.087
	9	13	5	5	770.9783
	11	19	4	2	771.1957

potassium

MOLECULAR WEIGHT	# OF Si GROUPS	# OF BRIDGING Os	# OF OH GROUPS	# OF OR GROUPS	CALCULATED MOLECULAR WEIGHT
771.2905	7	7	6	8	770.7609
	10	12	15	1	773.087
	9	13	5	5	770.9783
	11	19	4	2	771.1957

potassium

MOLECULAR WEIGHT	# OF Si GROUPS	# OF BRIDGING Os	# OF OH GROUPS	# OF OR GROUPS	CALCULATED MOLECULAR WEIGHT
773.0656	8	9	8	6	774.8696
	10	12	15	1	773.087
	11	19	4	2	771.1957

potassium

MOLECULAR WEIGHT	# OF Si GROUPS	# OF BRIDGING Os	# OF OH GROUPS	# OF OR GROUPS	CALCULATED MOLECULAR WEIGHT
773.1591	8	9	8	6	774.8696
	10	12	15	1	773.087
	10	15	7	3	775.087
	11	19	4	2	771.1957

potassium

MOLECULAR WEIGHT	# OF Si GROUPS	# OF BRIDGING Os	# OF OH GROUPS	# OF OR GROUPS	CALCULATED MOLECULAR WEIGHT
773.2525	8	9	8	6	774.8696
	10	12	15	1	773.087
	10	15	7	3	775.087

potassium

MOLECULAR WEIGHT	# OF Si GROUPS	# OF BRIDGING Os	# OF OH GROUPS	# OF OR GROUPS	CALCULATED MOLECULAR WEIGHT
773.346	8	9	8	6	774.8696
	10	12	15	1	773.087
	10	15	7	3	775.087
	12	21	6	0	775.3044

potassium

MOLECULAR WEIGHT	# OF Si GROUPS	# OF BRIDGING Os	# OF OH GROUPS	# OF OR GROUPS	CALCULATED MOLECULAR WEIGHT
773.4395	8	9	8	6	774.8696
	10	12	15	1	773.087
	10	15	7	3	775.087
	12	21	6	0	775.3044

potassium

MOLECULAR WEIGHT	# OF Si GROUPS	# OF BRIDGING Os	# OF OH GROUPS	# OF OR GROUPS	CALCULATED MOLECULAR WEIGHT
774.0942	8	9	8	6	774.8696
	10	12	15	1	773.087
	10	15	7	3	775.087
	12	21	6	0	775.3044

potassium

MOLECULAR	# OF Si	# OF	# OF OH	# OF OR	CALCULATED

WEIGHT	GROUPS	BRIDGING Os	GROUPS	GROUPS	MOLECULAR WEIGHT
774.1877	8	9	8	6	774.8696
	10	12	15	1	773.087
	10	15	7	3	775.087
	12	21	6	0	775.3044

potassium

MOLECULAR WEIGHT	# OF Si GROUPS	# OF BRIDGING Os	# OF OH GROUPS	# OF OR GROUPS	CALCULATED MOLECULAR WEIGHT
774.2812	8	9	8	6	774.8696
	10	12	15	1	773.087
	10	15	7	3	775.087
	12	21	6	0	775.3044

potassium

MOLECULAR WEIGHT	# OF Si GROUPS	# OF BRIDGING Os	# OF OH GROUPS	# OF OR GROUPS	CALCULATED MOLECULAR WEIGHT
774.3748	8	9	8	6	774.8696
	10	12	15	1	773.087
	10	15	7	3	775.087
	12	21	6	0	775.3044

potassium

MOLECULAR WEIGHT	# OF Si GROUPS	# OF BRIDGING Os	# OF OH GROUPS	# OF OR GROUPS	CALCULATED MOLECULAR WEIGHT
775.0298	9	8	18	2	776.9783
	6	6	1	11	776.6522
	8	9	8	6	774.8696
	10	12	15	1	773.087
	8	12	0	8	776.8696
	10	15	7	3	775.087
	12	21	6	0	775.3044

potassium

MOLECULAR WEIGHT	# OF Si GROUPS	# OF BRIDGING Os	# OF OH GROUPS	# OF OR GROUPS	CALCULATED MOLECULAR WEIGHT
775.1234	9	8	18	2	776.9783
	6	6	1	11	776.6522
	8	9	8	6	774.8696
	8	12	0	8	776.8696
	10	15	7	3	775.087
	12	21	6	0	775.3044

potassium

MOLECULAR WEIGHT	# OF Si GROUPS	# OF BRIDGING Os	# OF OH GROUPS	# OF OR GROUPS	CALCULATED MOLECULAR WEIGHT
775.217	9	8	18	2	776.9783
	6	6	1	11	776.6522
	8	9	8	6	774.8696
	8	12	0	8	776.8696
	10	15	7	3	775.087
	12	21	6	0	775.3044

potassium

MOLECULAR WEIGHT	# OF Si GROUPS	# OF BRIDGING Os	# OF OH GROUPS	# OF OR GROUPS	CALCULATED MOLECULAR WEIGHT
779.153	10	10	20	0	781.087
	7	8	3	9	780.7609
	9	11	10	4	778.9783
	9	14	2	6	780.9783
	11	17	9	1	779.1957

potassium

MOLECULAR WEIGHT	# OF Si GROUPS	# OF BRIDGING Os	# OF OH GROUPS	# OF OR GROUPS	CALCULATED MOLECULAR WEIGHT
779.2468	10	10	20	0	781.087
	7	8	3	9	780.7609
	9	11	10	4	778.9783
	9	14	2	6	780.9783
	11	17	9	1	779.1957
	11	20	1	3	781.1957

potassium

MOLECULAR WEIGHT	# OF Si GROUPS	# OF BRIDGING Os	# OF OH GROUPS	# OF OR GROUPS	CALCULATED MOLECULAR WEIGHT
785.0748	9	9	15	3	786.9783
	8	10	5	7	784.8696
	10	13	12	2	783.087
	10	16	4	4	785.087
	12	22	3	1	785.3044

potassium

MOLECULAR WEIGHT	# OF Si GROUPS	# OF BRIDGING Os	# OF OH GROUPS	# OF OR GROUPS	CALCULATED MOLECULAR WEIGHT
785.169	9	9	15	3	786.9783
	8	10	5	7	784.8696
	10	16	4	4	785.087
	12	22	3	1	785.3044

potassium

MOLECULAR WEIGHT	# OF Si GROUPS	# OF BRIDGING Os	# OF OH GROUPS	# OF OR GROUPS	CALCULATED MOLECULAR WEIGHT
785.2632	9	9	15	3	786.9783
	8	10	5	7	784.8696
	11	15	14	0	787.1957
	10	16	4	4	785.087
	12	22	3	1	785.3044

potassium

MOLECULAR WEIGHT	# OF Si GROUPS	# OF BRIDGING Os	# OF OH GROUPS	# OF OR GROUPS	CALCULATED MOLECULAR WEIGHT
785.3574	9	9	15	3	786.9783
	8	10	5	7	784.8696
	11	15	14	0	787.1957
	10	16	4	4	785.087
	12	22	3	1	785.3044

potassium

MOLECULAR WEIGHT	# OF Si GROUPS	# OF BRIDGING Os	# OF OH GROUPS	# OF OR GROUPS	CALCULATED MOLECULAR WEIGHT
785.4515	9	9	15	3	786.9783
	8	10	5	7	784.8696
	11	15	14	0	787.1957
	10	16	4	4	785.087
	12	22	3	1	785.3044

potassium

MOLECULAR WEIGHT	# OF Si GROUPS	# OF BRIDGING Os	# OF OH GROUPS	# OF OR GROUPS	CALCULATED MOLECULAR WEIGHT
785.5457	9	9	15	3	786.9783
	8	10	5	7	784.8696
	11	15	14	0	787.1957
	10	16	4	4	785.087
	12	22	3	1	785.3044

potassium

MOLECULAR WEIGHT	# OF Si GROUPS	# OF BRIDGING Os	# OF OH GROUPS	# OF OR GROUPS	CALCULATED MOLECULAR WEIGHT
786.111	9	9	15	3	786.9783
	8	10	5	7	784.8696
	11	15	14	0	787.1957
	10	16	4	4	785.087
	12	22	3	1	785.3044

potassium

MOLECULAR WEIGHT	# OF Si GROUPS	# OF BRIDGING Os	# OF OH GROUPS	# OF OR GROUPS	CALCULATED MOLECULAR WEIGHT
786.2052	9	9	15	3	786.9783
	8	10	5	7	784.8696
	11	15	14	0	787.1957
	10	16	4	4	785.087
	12	22	3	1	785.3044

potassium

MOLECULAR WEIGHT	# OF Si GROUPS	# OF BRIDGING Os	# OF OH GROUPS	# OF OR GROUPS	CALCULATED MOLECULAR WEIGHT
786.2995	9	9	15	3	786.9783
	8	10	5	7	784.8696
	11	15	14	0	787.1957
	10	16	4	4	785.087
	12	22	3	1	785.3044

potassium

MOLECULAR WEIGHT	# OF Si GROUPS	# OF BRIDGING Os	# OF OH GROUPS	# OF OR GROUPS	CALCULATED MOLECULAR WEIGHT
786.3937	9	9	15	3	786.9783
	8	10	5	7	784.8696
	11	15	14	0	787.1957
	10	16	4	4	785.087
	12	22	3	1	785.3044

potassium

MOLECULAR WEIGHT	# OF Si GROUPS	# OF BRIDGING Os	# OF OH GROUPS	# OF OR GROUPS	CALCULATED MOLECULAR

					WEIGHT
787.1478	7	6	8	8	788.7609
	9	9	15	3	786.9783
	9	12	7	5	788.9783
	11	15	14	0	787.1957
	12	22	3	1	785.3044

potassium

MOLECULAR WEIGHT	# OF Si GROUPS	# OF BRIDGING Os	# OF OH GROUPS	# OF OR GROUPS	CALCULATED MOLECULAR WEIGHT
787.2421	7	6	8	8	788.7609
	9	9	15	3	786.9783
	9	12	7	5	788.9783
	11	15	14	0	787.1957
	11	18	6	2	789.1957
	12	22	3	1	785.3044

potassium

MOLECULAR WEIGHT	# OF Si GROUPS	# OF BRIDGING Os	# OF OH GROUPS	# OF OR GROUPS	CALCULATED MOLECULAR WEIGHT
787.3364	7	6	8	8	788.7609
	9	9	15	3	786.9783
	9	12	7	5	788.9783
	11	15	14	0	787.1957
	11	18	6	2	789.1957

potassium

MOLECULAR WEIGHT	# OF Si GROUPS	# OF BRIDGING Os	# OF OH GROUPS	# OF OR GROUPS	CALCULATED MOLECULAR WEIGHT
787.4307	7	6	8	8	788.7609
	9	9	15	3	786.9783
	9	12	7	5	788.9783
	11	15	14	0	787.1957
	11	18	6	2	789.1957

potassium

MOLECULAR WEIGHT	# OF Si GROUPS	# OF BRIDGING Os	# OF OH GROUPS	# OF OR GROUPS	CALCULATED MOLECULAR WEIGHT
788.1853	7	6	8	8	788.7609
	9	9	15	3	786.9783
	9	12	7	5	788.9783
	11	15	14	0	787.1957
	11	18	6	2	789.1957

potassium

MOLECULAR WEIGHT	# OF Si GROUPS	# OF BRIDGING Os	# OF OH GROUPS	# OF OR GROUPS	CALCULATED MOLECULAR WEIGHT
788.2796	7	6	8	8	788.7609
	9	9	15	3	786.9783
	9	12	7	5	788.9783
	11	15	14	0	787.1957
	11	18	6	2	789.1957

potassium

MOLECULAR WEIGHT	# OF Si GROUPS	# OF BRIDGING Os	# OF OH GROUPS	# OF OR GROUPS	CALCULATED MOLECULAR WEIGHT

789.0346	7	6	8	8	788.7609
	7	9	0	10	790.7609
	9	12	7	5	788.9783
	11	15	14	0	787.1957
	11	18	6	2	789.1957

potassium

MOLECULAR WEIGHT	# OF Si GROUPS	# OF BRIDGING Os	# OF OH GROUPS	# OF OR GROUPS	CALCULATED MOLECULAR WEIGHT
789.129	7	6	8	8	788.7609
	10	11	17	1	791.087
	7	9	0	10	790.7609
	9	12	7	5	788.9783
	11	15	14	0	787.1957
	11	18	6	2	789.1957

potassium

MOLECULAR WEIGHT	# OF Si GROUPS	# OF BRIDGING Os	# OF OH GROUPS	# OF OR GROUPS	CALCULATED MOLECULAR WEIGHT
789.2234	7	6	8	8	788.7609
	10	11	17	1	791.087
	7	9	0	10	790.7609
	9	12	7	5	788.9783
	11	18	6	2	789.1957

potassium

MOLECULAR WEIGHT	# OF Si GROUPS	# OF BRIDGING Os	# OF OH GROUPS	# OF OR GROUPS	CALCULATED MOLECULAR WEIGHT
789.3178	7	6	8	8	788.7609
	10	11	17	1	791.087
	7	9	0	10	790.7609
	9	12	7	5	788.9783
	11	18	6	2	789.1957

potassium

MOLECULAR WEIGHT	# OF Si GROUPS	# OF BRIDGING Os	# OF OH GROUPS	# OF OR GROUPS	CALCULATED MOLECULAR WEIGHT
790.0732	7	6	8	8	788.7609
	10	11	17	1	791.087
	7	9	0	10	790.7609
	9	12	7	5	788.9783
	11	18	6	2	789.1957

potassium

MOLECULAR WEIGHT	# OF Si GROUPS	# OF BRIDGING Os	# OF OH GROUPS	# OF OR GROUPS	CALCULATED MOLECULAR WEIGHT
790.1677	7	6	8	8	788.7609
	10	11	17	1	791.087
	7	9	0	10	790.7609
	9	12	7	5	788.9783
	11	18	6	2	789.1957

potassium

MOLECULAR WEIGHT	# OF Si GROUPS	# OF BRIDGING Os	# OF OH GROUPS	# OF OR GROUPS	CALCULATED MOLECULAR WEIGHT
791.018	8	8	10	6	792.8696

	10	11	17	1	791.087
	7	9	0	10	790.7609
	11	18	6	2	789.1957

potassium

MOLECULAR WEIGHT	# OF Si GROUPS	# OF BRIDGING Os	# OF OH GROUPS	# OF OR GROUPS	CALCULATED MOLECULAR WEIGHT
791.1125	8	8	10	6	792.8696
	10	11	17	1	791.087
	7	9	0	10	790.7609
	10	14	9	3	793.087
	11	18	6	2	789.1957

potassium

MOLECULAR WEIGHT	# OF Si GROUPS	# OF BRIDGING Os	# OF OH GROUPS	# OF OR GROUPS	CALCULATED MOLECULAR WEIGHT
791.207	8	8	10	6	792.8696
	10	11	17	1	791.087
	7	9	0	10	790.7609
	10	14	9	3	793.087

potassium

MOLECULAR WEIGHT	# OF Si GROUPS	# OF BRIDGING Os	# OF OH GROUPS	# OF OR GROUPS	CALCULATED MOLECULAR WEIGHT
791.3016	8	8	10	6	792.8696
	10	11	17	1	791.087
	7	9	0	10	790.7609
	10	14	9	3	793.087

potassium

MOLECULAR WEIGHT	# OF Si GROUPS	# OF BRIDGING Os	# OF OH GROUPS	# OF OR GROUPS	CALCULATED MOLECULAR WEIGHT
801.1609	8	9	7	7	802.8696
	10	12	14	2	801.087
	10	15	6	4	803.087
	11	19	3	3	799.1957
	13	25	2	0	799.4131

potassium

MOLECULAR WEIGHT	# OF Si GROUPS	# OF BRIDGING Os	# OF OH GROUPS	# OF OR GROUPS	CALCULATED MOLECULAR WEIGHT
801.256	8	9	7	7	802.8696
	10	12	14	2	801.087
	10	15	6	4	803.087
	13	25	2	0	799.4131

potassium

MOLECULAR WEIGHT	# OF Si GROUPS	# OF BRIDGING Os	# OF OH GROUPS	# OF OR GROUPS	CALCULATED MOLECULAR WEIGHT
801.3511	8	9	7	7	802.8696
	10	12	14	2	801.087
	10	15	6	4	803.087
	12	21	5	1	803.3044
	13	25	2	0	799.4131

potassium

MOLECULAR WEIGHT	# OF Si GROUPS	# OF BRIDGING Os	# OF OH GROUPS	# OF OR GROUPS	CALCULATED MOLECULAR WEIGHT
804.9685	9	8	17	3	804.9783
	6	6	0	12	804.6522
	11	14	16	0	805.1957
	10	15	6	4	803.087
	12	21	5	1	803.3044

potassium

MOLECULAR WEIGHT	# OF Si GROUPS	# OF BRIDGING Os	# OF OH GROUPS	# OF OR GROUPS	CALCULATED MOLECULAR WEIGHT
805.0638	9	8	17	3	804.9783
	6	6	0	12	804.6522
	9	11	9	5	806.9783
	11	14	16	0	805.1957
	10	15	6	4	803.087
	12	21	5	1	803.3044

potassium

MOLECULAR WEIGHT	# OF Si GROUPS	# OF BRIDGING Os	# OF OH GROUPS	# OF OR GROUPS	CALCULATED MOLECULAR WEIGHT
805.1591	9	8	17	3	804.9783
	6	6	0	12	804.6522
	9	11	9	5	806.9783
	11	14	16	0	805.1957
	12	21	5	1	803.3044

potassium

MOLECULAR WEIGHT	# OF Si GROUPS	# OF BRIDGING Os	# OF OH GROUPS	# OF OR GROUPS	CALCULATED MOLECULAR WEIGHT
805.2544	9	8	17	3	804.9783
	6	6	0	12	804.6522
	9	11	9	5	806.9783
	11	14	16	0	805.1957
	11	17	8	2	807.1957
	12	21	5	1	803.3044

potassium

MOLECULAR WEIGHT	# OF Si GROUPS	# OF BRIDGING Os	# OF OH GROUPS	# OF OR GROUPS	CALCULATED MOLECULAR WEIGHT
805.3497	9	8	17	3	804.9783
	6	6	0	12	804.6522
	9	11	9	5	806.9783
	11	14	16	0	805.1957
	11	17	8	2	807.1957

potassium

MOLECULAR WEIGHT	# OF Si GROUPS	# OF BRIDGING Os	# OF OH GROUPS	# OF OR GROUPS	CALCULATED MOLECULAR WEIGHT
806.0171	9	8	17	3	804.9783
	6	6	0	12	804.6522
	9	11	9	5	806.9783
	11	14	16	0	805.1957

	11	17	8	2	807.1957

potassium

MOLECULAR WEIGHT	# OF Si GROUPS	# OF BRIDGING Os	# OF OH GROUPS	# OF OR GROUPS	CALCULATED MOLECULAR WEIGHT
806.1124	9	8	17	3	804.9783
	6	6	0	12	804.6522
	9	11	9	5	806.9783
	11	14	16	0	805.1957
	11	17	8	2	807.1957

potassium

MOLECULAR WEIGHT	# OF Si GROUPS	# OF BRIDGING Os	# OF OH GROUPS	# OF OR GROUPS	CALCULATED MOLECULAR WEIGHT
806.2078	9	8	17	3	804.9783
	6	6	0	12	804.6522
	9	11	9	5	806.9783
	11	14	16	0	805.1957
	11	17	8	2	807.1957

potassium

MOLECULAR WEIGHT	# OF Si GROUPS	# OF BRIDGING Os	# OF OH GROUPS	# OF OR GROUPS	CALCULATED MOLECULAR WEIGHT
806.9709	9	8	17	3	804.9783
	7	8	2	10	808.7609
	9	11	9	5	806.9783
	11	14	16	0	805.1957
	11	17	8	2	807.1957

potassium

MOLECULAR WEIGHT	# OF Si GROUPS	# OF BRIDGING Os	# OF OH GROUPS	# OF OR GROUPS	CALCULATED MOLECULAR WEIGHT
807.0663	7	8	2	10	808.7609
	9	11	9	5	806.9783
	11	14	16	0	805.1957
	9	14	1	7	808.9783
	11	17	8	2	807.1957

potassium

MOLECULAR WEIGHT	# OF Si GROUPS	# OF BRIDGING Os	# OF OH GROUPS	# OF OR GROUPS	CALCULATED MOLECULAR WEIGHT
807.1617	10	10	19	1	809.087
	7	8	2	10	808.7609
	9	11	9	5	806.9783
	11	14	16	0	805.1957
	9	14	1	7	808.9783
	11	17	8	2	807.1957

potassium

MOLECULAR WEIGHT	# OF Si GROUPS	# OF BRIDGING Os	# OF OH GROUPS	# OF OR GROUPS	CALCULATED MOLECULAR WEIGHT
807.2571	10	10	19	1	809.087
	7	8	2	10	808.7609
	9	11	9	5	806.9783
	9	14	1	7	808.9783
	11	17	8	2	807.1957

	11	20	0	4	809.1957

potassium

MOLECULAR WEIGHT	# OF Si GROUPS	# OF BRIDGING Os	# OF OH GROUPS	# OF OR GROUPS	CALCULATED MOLECULAR WEIGHT
807.3526	10	10	19	1	809.087
	7	8	2	10	808.7609
	9	11	9	5	806.9783
	9	14	1	7	808.9783
	11	17	8	2	807.1957
	11	20	0	4	809.1957

potassium

MOLECULAR WEIGHT	# OF Si GROUPS	# OF BRIDGING Os	# OF OH GROUPS	# OF OR GROUPS	CALCULATED MOLECULAR WEIGHT
808.0207	10	10	19	1	809.087
	7	8	2	10	808.7609
	9	11	9	5	806.9783
	9	14	1	7	808.9783
	11	17	8	2	807.1957
	11	20	0	4	809.1957

potassium

MOLECULAR WEIGHT	# OF Si GROUPS	# OF BRIDGING Os	# OF OH GROUPS	# OF OR GROUPS	CALCULATED MOLECULAR WEIGHT
808.1162	10	10	19	1	809.087
	7	8	2	10	808.7609
	9	11	9	5	806.9783
	9	14	1	7	808.9783
	11	17	8	2	807.1957
	11	20	0	4	809.1957

potassium

MOLECULAR WEIGHT	# OF Si GROUPS	# OF BRIDGING Os	# OF OH GROUPS	# OF OR GROUPS	CALCULATED MOLECULAR WEIGHT
808.2117	10	10	19	1	809.087
	7	8	2	10	808.7609
	9	11	9	5	806.9783
	9	14	1	7	808.9783
	11	17	8	2	807.1957
	11	20	0	4	809.1957

potassium

MOLECULAR WEIGHT	# OF Si GROUPS	# OF BRIDGING Os	# OF OH GROUPS	# OF OR GROUPS	CALCULATED MOLECULAR WEIGHT
809.0712	8	7	12	6	810.8696
	10	10	19	1	809.087
	7	8	2	10	808.7609
	9	14	1	7	808.9783
	11	17	8	2	807.1957
	11	20	0	4	809.1957

potassium

MOLECULAR WEIGHT	# OF Si GROUPS	# OF BRIDGING Os	# OF OH GROUPS	# OF OR GROUPS	CALCULATED MOLECULAR WEIGHT
809.1667	8	7	12	6	810.8696

	10	10	19	1	809.087
	7	8	2	10	808.7609
	10	13	11	3	811.087
	9	14	1	7	808.9783
	11	17	8	2	807.1957
	11	20	0	4	809.1957

potassium

MOLECULAR WEIGHT	# OF Si GROUPS	# OF BRIDGING Os	# OF OH GROUPS	# OF OR GROUPS	CALCULATED MOLECULAR WEIGHT
809.2623	8	7	12	6	810.8696
	10	10	19	1	809.087
	7	8	2	10	808.7609
	10	13	11	3	811.087
	9	14	1	7	808.9783
	11	20	0	4	809.1957

potassium

MOLECULAR WEIGHT	# OF Si GROUPS	# OF BRIDGING Os	# OF OH GROUPS	# OF OR GROUPS	CALCULATED MOLECULAR WEIGHT
817.0186	7	6	7	9	816.7609
	9	12	6	6	816.9783
	11	15	13	1	815.1957
	11	18	5	3	817.1957
	13	24	4	0	817.4131

potassium

MOLECULAR WEIGHT	# OF Si GROUPS	# OF BRIDGING Os	# OF OH GROUPS	# OF OR GROUPS	CALCULATED MOLECULAR WEIGHT
817.1145	7	6	7	9	816.7609
	10	11	16	2	819.087
	9	12	6	6	816.9783
	11	15	13	1	815.1957
	11	18	5	3	817.1957
	13	24	4	0	817.4131

potassium

MOLECULAR WEIGHT	# OF Si GROUPS	# OF BRIDGING Os	# OF OH GROUPS	# OF OR GROUPS	CALCULATED MOLECULAR WEIGHT
817.2105	7	6	7	9	816.7609
	10	11	16	2	819.087
	9	12	6	6	816.9783
	11	18	5	3	817.1957
	13	24	4	0	817.4131

potassium

MOLECULAR WEIGHT	# OF Si GROUPS	# OF BRIDGING Os	# OF OH GROUPS	# OF OR GROUPS	CALCULATED MOLECULAR WEIGHT
817.3065	7	6	7	9	816.7609
	10	11	16	2	819.087
	9	12	6	6	816.9783
	11	18	5	3	817.1957
	13	24	4	0	817.4131

potassium

MOLECULAR WEIGHT	# OF Si GROUPS	# OF BRIDGING Os	# OF OH GROUPS	# OF OR GROUPS	CALCULATED MOLECULAR WEIGHT
819.0352	8	8	9	7	820.8696
	10	11	16	2	819.087
	11	18	5	3	817.1957
	13	24	4	0	817.4131

potassium

MOLECULAR WEIGHT	# OF Si GROUPS	# OF BRIDGING Os	# OF OH GROUPS	# OF OR GROUPS	CALCULATED MOLECULAR WEIGHT
819.1313	8	8	9	7	820.8696
	10	11	16	2	819.087
	10	14	8	4	821.087
	11	18	5	3	817.1957
	13	24	4	0	817.4131

potassium

MOLECULAR WEIGHT	# OF Si GROUPS	# OF BRIDGING Os	# OF OH GROUPS	# OF OR GROUPS	CALCULATED MOLECULAR WEIGHT
819.2274	8	8	9	7	820.8696
	10	11	16	2	819.087
	10	14	8	4	821.087
	13	24	4	0	817.4131

potassium

MOLECULAR WEIGHT	# OF Si GROUPS	# OF BRIDGING Os	# OF OH GROUPS	# OF OR GROUPS	CALCULATED MOLECULAR WEIGHT
819.3235	8	8	9	7	820.8696
	10	11	16	2	819.087
	10	14	8	4	821.087
	12	20	7	1	821.3044
	13	24	4	0	817.4131

potassium

MOLECULAR WEIGHT	# OF Si GROUPS	# OF BRIDGING Os	# OF OH GROUPS	# OF OR GROUPS	CALCULATED MOLECULAR WEIGHT
819.4196	8	8	9	7	820.8696
	10	11	16	2	819.087
	10	14	8	4	821.087
	12	20	7	1	821.3044

potassium

MOLECULAR WEIGHT	# OF Si GROUPS	# OF BRIDGING Os	# OF OH GROUPS	# OF OR GROUPS	CALCULATED MOLECULAR WEIGHT
819.9963	8	8	9	7	820.8696
	10	11	16	2	819.087
	10	14	8	4	821.087
	12	20	7	1	821.3044

potassium

MOLECULAR WEIGHT	# OF Si GROUPS	# OF BRIDGING Os	# OF OH GROUPS	# OF OR GROUPS	CALCULATED MOLECULAR WEIGHT
820.0925	8	8	9	7	820.8696
	10	11	16	2	819.087

	10	14	8	4	821.087
	12	20	7	1	821.3044

potassium

MOLECULAR WEIGHT	# OF Si GROUPS	# OF BRIDGING Os	# OF OH GROUPS	# OF OR GROUPS	CALCULATED MOLECULAR WEIGHT
820.1886	8	8	9	7	820.8696
	10	11	16	2	819.087
	10	14	8	4	821.087
	12	20	7	1	821.3044

potassium

MOLECULAR WEIGHT	# OF Si GROUPS	# OF BRIDGING Os	# OF OH GROUPS	# OF OR GROUPS	CALCULATED MOLECULAR WEIGHT
820.2848	8	8	9	7	820.8696
	10	11	16	2	819.087
	10	14	8	4	821.087
	12	20	7	1	821.3044

potassium

MOLECULAR WEIGHT	# OF Si GROUPS	# OF BRIDGING Os	# OF OH GROUPS	# OF OR GROUPS	CALCULATED MOLECULAR WEIGHT
820.381	8	8	9	7	820.8696
	10	11	16	2	819.087
	10	14	8	4	821.087
	12	20	7	1	821.3044

potassium

MOLECULAR WEIGHT	# OF Si GROUPS	# OF BRIDGING Os	# OF OH GROUPS	# OF OR GROUPS	CALCULATED MOLECULAR WEIGHT
821.0542	6	5	2	12	822.6522
	8	8	9	7	820.8696
	10	11	16	2	819.087
	8	11	1	9	822.8696
	10	14	8	4	821.087
	12	20	7	1	821.3044

potassium

MOLECULAR WEIGHT	# OF Si GROUPS	# OF BRIDGING Os	# OF OH GROUPS	# OF OR GROUPS	CALCULATED MOLECULAR WEIGHT
821.1504	6	5	2	12	822.6522
	8	8	9	7	820.8696
	8	11	1	9	822.8696
	10	14	8	4	821.087
	10	17	0	6	823.087
	12	20	7	1	821.3044

potassium

MOLECULAR WEIGHT	# OF Si GROUPS	# OF BRIDGING Os	# OF OH GROUPS	# OF OR GROUPS	CALCULATED MOLECULAR WEIGHT
821.2466	6	5	2	12	822.6522
	8	8	9	7	820.8696
	11	13	18	0	823.1957
	8	11	1	9	822.8696
	10	14	8	4	821.087
	10	17	0	6	823.087

	12	20	7	1	821.3044

potassium

MOLECULAR WEIGHT	# OF Si GROUPS	# OF BRIDGING Os	# OF OH GROUPS	# OF OR GROUPS	CALCULATED MOLECULAR WEIGHT
822.0165	6	5	2	12	822.6522
	8	8	9	7	820.8696
	11	13	18	0	823.1957
	8	11	1	9	822.8696
	10	14	8	4	821.087
	10	17	0	6	823.087
	12	20	7	1	821.3044

potassium

MOLECULAR WEIGHT	# OF Si GROUPS	# OF BRIDGING Os	# OF OH GROUPS	# OF OR GROUPS	CALCULATED MOLECULAR WEIGHT
822.1128	6	5	2	12	822.6522
	8	8	9	7	820.8696
	11	13	18	0	823.1957
	8	11	1	9	822.8696
	10	14	8	4	821.087
	10	17	0	6	823.087
	12	20	7	1	821.3044

potassium

MOLECULAR WEIGHT	# OF Si GROUPS	# OF BRIDGING Os	# OF OH GROUPS	# OF OR GROUPS	CALCULATED MOLECULAR WEIGHT
822.9793	6	5	2	12	822.6522
	9	10	11	5	824.9783
	11	13	18	0	823.1957
	8	11	1	9	822.8696
	10	14	8	4	821.087
	10	17	0	6	823.087
	12	20	7	1	821.3044

potassium

MOLECULAR WEIGHT	# OF Si GROUPS	# OF BRIDGING Os	# OF OH GROUPS	# OF OR GROUPS	CALCULATED MOLECULAR WEIGHT
823.0756	6	5	2	12	822.6522
	9	10	11	5	824.9783
	11	13	18	0	823.1957
	8	11	1	9	822.8696
	10	14	8	4	821.087
	10	17	0	6	823.087
	12	20	7	1	821.3044

potassium

MOLECULAR WEIGHT	# OF Si GROUPS	# OF BRIDGING Os	# OF OH GROUPS	# OF OR GROUPS	CALCULATED MOLECULAR WEIGHT
823.1719	6	5	2	12	822.6522
	9	10	11	5	824.9783
	11	13	18	0	823.1957
	8	11	1	9	822.8696
	10	17	0	6	823.087
	12	20	7	1	821.3044

potassium

MOLECULAR WEIGHT	# OF Si GROUPS	# OF BRIDGING Os	# OF OH GROUPS	# OF OR GROUPS	CALCULATED MOLECULAR WEIGHT
831.0882	9	8	16	4	832.9783
	8	9	6	8	830.8696
	10	15	5	5	831.087
	12	18	12	0	829.3044
	12	21	4	2	831.3044

potassium

MOLECULAR WEIGHT	# OF Si GROUPS	# OF BRIDGING Os	# OF OH GROUPS	# OF OR GROUPS	CALCULATED MOLECULAR WEIGHT
831.1849	9	8	16	4	832.9783
	8	9	6	8	830.8696
	10	15	5	5	831.087
	12	18	12	0	829.3044
	12	21	4	2	831.3044

potassium

MOLECULAR WEIGHT	# OF Si GROUPS	# OF BRIDGING Os	# OF OH GROUPS	# OF OR GROUPS	CALCULATED MOLECULAR WEIGHT
831.2817	9	8	16	4	832.9783
	8	9	6	8	830.8696
	11	14	15	1	833.1957
	10	15	5	5	831.087
	12	18	12	0	829.3044
	12	21	4	2	831.3044

potassium

MOLECULAR WEIGHT	# OF Si GROUPS	# OF BRIDGING Os	# OF OH GROUPS	# OF OR GROUPS	CALCULATED MOLECULAR WEIGHT
831.3785	9	8	16	4	832.9783
	8	9	6	8	830.8696
	11	14	15	1	833.1957
	10	15	5	5	831.087
	12	21	4	2	831.3044

potassium

MOLECULAR WEIGHT	# OF Si GROUPS	# OF BRIDGING Os	# OF OH GROUPS	# OF OR GROUPS	CALCULATED MOLECULAR WEIGHT
832.056	9	8	16	4	832.9783
	8	9	6	8	830.8696
	11	14	15	1	833.1957
	10	15	5	5	831.087
	12	21	4	2	831.3044

potassium

MOLECULAR WEIGHT	# OF Si GROUPS	# OF BRIDGING Os	# OF OH GROUPS	# OF OR GROUPS	CALCULATED MOLECULAR WEIGHT
832.1528	9	8	16	4	832.9783
	8	9	6	8	830.8696
	11	14	15	1	833.1957
	10	15	5	5	831.087
	12	21	4	2	831.3044

potassium

MOLECULAR	# OF Si	# OF BRIDGING	# OF OH	# OF OR	CALCULATED

WEIGHT	GROUPS	Os	GROUPS	GROUPS	MOLECULAR WEIGHT
832.2497	9	8	16	4	832.9783
	8	9	6	8	830.8696
	11	14	15	1	833.1957
	10	15	5	5	831.087
	12	21	4	2	831.3044

potassium

MOLECULAR WEIGHT	# OF Si GROUPS	# OF BRIDGING Os	# OF OH GROUPS	# OF OR GROUPS	CALCULATED MOLECULAR WEIGHT
832.3465	9	8	16	4	832.9783
	8	9	6	8	830.8696
	11	14	15	1	833.1957
	10	15	5	5	831.087
	12	21	4	2	831.3044

potassium

MOLECULAR WEIGHT	# OF Si GROUPS	# OF BRIDGING Os	# OF OH GROUPS	# OF OR GROUPS	CALCULATED MOLECULAR WEIGHT
832.9276	9	8	16	4	832.9783
	11	14	15	1	833.1957
	10	15	5	5	831.087
	12	21	4	2	831.3044

potassium

MOLECULAR WEIGHT	# OF Si GROUPS	# OF BRIDGING Os	# OF OH GROUPS	# OF OR GROUPS	CALCULATED MOLECULAR WEIGHT
833.0244	9	8	16	4	832.9783
	9	11	8	6	834.9783
	11	14	15	1	833.1957
	10	15	5	5	831.087
	12	21	4	2	831.3044

potassium

MOLECULAR WEIGHT	# OF Si GROUPS	# OF BRIDGING Os	# OF OH GROUPS	# OF OR GROUPS	CALCULATED MOLECULAR WEIGHT
833.1213	9	8	16	4	832.9783
	9	11	8	6	834.9783
	11	14	15	1	833.1957
	12	21	4	2	831.3044

potassium

MOLECULAR WEIGHT	# OF Si GROUPS	# OF BRIDGING Os	# OF OH GROUPS	# OF OR GROUPS	CALCULATED MOLECULAR WEIGHT
833.2182	9	8	16	4	832.9783
	9	11	8	6	834.9783
	11	14	15	1	833.1957
	11	17	7	3	835.1957
	12	21	4	2	831.3044

potassium

MOLECULAR WEIGHT	# OF Si GROUPS	# OF BRIDGING Os	# OF OH GROUPS	# OF OR GROUPS	CALCULATED MOLECULAR WEIGHT
834.9629	9	8	16	4	832.9783
	7	8	1	11	836.7609
	9	11	8	6	834.9783
	11	14	15	1	833.1957
	11	17	7	3	835.1957
	13	23	6	0	835.4131

potassium

MOLECULAR WEIGHT	# OF Si GROUPS	# OF BRIDGING Os	# OF OH GROUPS	# OF OR GROUPS	CALCULATED MOLECULAR WEIGHT
835.0598	7	8	1	11	836.7609
	9	11	8	6	834.9783
	11	14	15	1	833.1957
	9	14	0	8	836.9783
	11	17	7	3	835.1957
	13	23	6	0	835.4131

potassium

MOLECULAR WEIGHT	# OF Si GROUPS	# OF BRIDGING Os	# OF OH GROUPS	# OF OR GROUPS	CALCULATED MOLECULAR WEIGHT
835.1568	10	10	18	2	837.087
	7	8	1	11	836.7609
	9	11	8	6	834.9783
	11	14	15	1	833.1957
	9	14	0	8	836.9783
	11	17	7	3	835.1957
	13	23	6	0	835.4131

potassium

MOLECULAR WEIGHT	# OF Si GROUPS	# OF BRIDGING Os	# OF OH GROUPS	# OF OR GROUPS	CALCULATED MOLECULAR WEIGHT
835.2538	10	10	18	2	837.087
	7	8	1	11	836.7609
	9	11	8	6	834.9783
	9	14	0	8	836.9783
	11	17	7	3	835.1957
	13	23	6	0	835.4131

potassium

MOLECULAR WEIGHT	# OF Si GROUPS	# OF BRIDGING Os	# OF OH GROUPS	# OF OR GROUPS	CALCULATED MOLECULAR WEIGHT
835.3508	10	10	18	2	837.087
	7	8	1	11	836.7609
	9	11	8	6	834.9783
	9	14	0	8	836.9783
	11	17	7	3	835.1957
	13	23	6	0	835.4131

potassium

MOLECULAR WEIGHT	# OF Si GROUPS	# OF BRIDGING Os	# OF OH GROUPS	# OF OR GROUPS	CALCULATED MOLECULAR WEIGHT

835.9329	10	10	18	2	837.087
	7	8	1	11	836.7609
	9	11	8	6	834.9783
	9	14	0	8	836.9783
	11	17	7	3	835.1957
	13	23	6	0	835.4131

potassium

MOLECULAR WEIGHT	# OF Si GROUPS	# OF BRIDGING Os	# OF OH GROUPS	# OF OR GROUPS	CALCULATED MOLECULAR WEIGHT
836.0299	10	10	18	2	837.087
	7	8	1	11	836.7609
	9	11	8	6	834.9783
	9	14	0	8	836.9783
	11	17	7	3	835.1957
	13	23	6	0	835.4131

potassium

MOLECULAR WEIGHT	# OF Si GROUPS	# OF BRIDGING Os	# OF OH GROUPS	# OF OR GROUPS	CALCULATED MOLECULAR WEIGHT
836.127	10	10	18	2	837.087
	7	8	1	11	836.7609
	9	11	8	6	834.9783
	9	14	0	8	836.9783
	11	17	7	3	835.1957
	13	23	6	0	835.4131

potassium

MOLECULAR WEIGHT	# OF Si GROUPS	# OF BRIDGING Os	# OF OH GROUPS	# OF OR GROUPS	CALCULATED MOLECULAR WEIGHT
836.224	10	10	18	2	837.087
	7	8	1	11	836.7609
	9	11	8	6	834.9783
	9	14	0	8	836.9783
	11	17	7	3	835.1957
	13	23	6	0	835.4131

potassium

MOLECULAR WEIGHT	# OF Si GROUPS	# OF BRIDGING Os	# OF OH GROUPS	# OF OR GROUPS	CALCULATED MOLECULAR WEIGHT
837.0005	8	7	11	7	838.8696
	10	10	18	2	837.087
	7	8	1	11	836.7609
	9	14	0	8	836.9783
	11	17	7	3	835.1957
	13	23	6	0	835.4131

potassium

MOLECULAR WEIGHT	# OF Si GROUPS	# OF BRIDGING Os	# OF OH GROUPS	# OF OR GROUPS	CALCULATED MOLECULAR WEIGHT
837.0976	8	7	11	7	838.8696
	10	10	18	2	837.087
	7	8	1	11	836.7609
	10	13	10	4	839.087
	9	14	0	8	836.9783
	11	17	7	3	835.1957

	13	23	6	0	835.4131

potassium

MOLECULAR WEIGHT	# OF Si GROUPS	# OF BRIDGING Os	# OF OH GROUPS	# OF OR GROUPS	CALCULATED MOLECULAR WEIGHT
837.1947	8	7	11	7	838.8696
	10	10	18	2	837.087
	7	8	1	11	836.7609
	10	13	10	4	839.087
	9	14	0	8	836.9783
	11	17	7	3	835.1957
	13	23	6	0	835.4131

potassium

MOLECULAR WEIGHT	# OF Si GROUPS	# OF BRIDGING Os	# OF OH GROUPS	# OF OR GROUPS	CALCULATED MOLECULAR WEIGHT
839.0406	8	7	11	7	838.8696
	10	10	18	2	837.087
	8	10	3	9	840.8696
	10	13	10	4	839.087
	12	19	9	1	839.3044

potassium

MOLECULAR WEIGHT	# OF Si GROUPS	# OF BRIDGING Os	# OF OH GROUPS	# OF OR GROUPS	CALCULATED MOLECULAR WEIGHT
844.9798	7	6	6	10	844.7609
	9	12	5	7	844.9783
	11	15	12	2	843.1957
	11	18	4	4	845.1957
	13	24	3	1	845.4131

potassium

MOLECULAR WEIGHT	# OF Si GROUPS	# OF BRIDGING Os	# OF OH GROUPS	# OF OR GROUPS	CALCULATED MOLECULAR WEIGHT
845.0774	7	6	6	10	844.7609
	9	12	5	7	844.9783
	11	15	12	2	843.1957
	11	18	4	4	845.1957
	13	24	3	1	845.4131

potassium

MOLECULAR WEIGHT	# OF Si GROUPS	# OF BRIDGING Os	# OF OH GROUPS	# OF OR GROUPS	CALCULATED MOLECULAR WEIGHT
845.1749	7	6	6	10	844.7609
	10	11	15	3	847.087
	9	12	5	7	844.9783
	11	15	12	2	843.1957
	11	18	4	4	845.1957
	13	24	3	1	845.4131

potassium

MOLECULAR WEIGHT	# OF Si GROUPS	# OF BRIDGING Os	# OF OH GROUPS	# OF OR GROUPS	CALCULATED MOLECULAR WEIGHT
846.053	7	6	6	10	844.7609
	10	11	15	3	847.087
	9	12	5	7	844.9783

	12	17	14	0	847.3044
	11	18	4	4	845.1957
	13	24	3	1	845.4131

potassium

MOLECULAR WEIGHT	# OF Si GROUPS	# OF BRIDGING Os	# OF OH GROUPS	# OF OR GROUPS	CALCULATED MOLECULAR WEIGHT
846.9315	8	8	8	8	848.8696
	10	11	15	3	847.087
	9	12	5	7	844.9783
	12	17	14	0	847.3044
	11	18	4	4	845.1957
	13	24	3	1	845.4131

potassium

MOLECULAR WEIGHT	# OF Si GROUPS	# OF BRIDGING Os	# OF OH GROUPS	# OF OR GROUPS	CALCULATED MOLECULAR WEIGHT
847.0291	8	8	8	8	848.8696
	10	11	15	3	847.087
	12	17	14	0	847.3044
	11	18	4	4	845.1957
	13	24	3	1	845.4131

potassium

MOLECULAR WEIGHT	# OF Si GROUPS	# OF BRIDGING Os	# OF OH GROUPS	# OF OR GROUPS	CALCULATED MOLECULAR WEIGHT
847.1268	8	8	8	8	848.8696
	10	11	15	3	847.087
	10	14	7	5	849.087
	12	17	14	0	847.3044
	11	18	4	4	845.1957
	13	24	3	1	845.4131

potassium

MOLECULAR WEIGHT	# OF Si GROUPS	# OF BRIDGING Os	# OF OH GROUPS	# OF OR GROUPS	CALCULATED MOLECULAR WEIGHT
847.2244	8	8	8	8	848.8696
	10	11	15	3	847.087
	10	14	7	5	849.087
	12	17	14	0	847.3044
	13	24	3	1	845.4131

potassium

MOLECULAR WEIGHT	# OF Si GROUPS	# OF BRIDGING Os	# OF OH GROUPS	# OF OR GROUPS	CALCULATED MOLECULAR WEIGHT
847.3221	8	8	8	8	848.8696
	10	11	15	3	847.087
	10	14	7	5	849.087
	12	17	14	0	847.3044
	12	20	6	2	849.3044
	13	24	3	1	845.4131

potassium

MOLECULAR WEIGHT	# OF Si GROUPS	# OF BRIDGING Os	# OF OH GROUPS	# OF OR GROUPS	CALCULATED MOLECULAR WEIGHT
847.4198	8	8	8	8	848.8696

	10	11	15	3	847.087
	10	14	7	5	849.087
	12	17	14	0	847.3044
	12	20	6	2	849.3044

potassium

MOLECULAR WEIGHT	# OF Si GROUPS	# OF BRIDGING Os	# OF OH GROUPS	# OF OR GROUPS	CALCULATED MOLECULAR WEIGHT
848.0058	8	8	8	8	848.8696
	10	11	15	3	847.087
	10	14	7	5	849.087
	12	17	14	0	847.3044
	12	20	6	2	849.3044

potassium

MOLECULAR WEIGHT	# OF Si GROUPS	# OF BRIDGING Os	# OF OH GROUPS	# OF OR GROUPS	CALCULATED MOLECULAR WEIGHT
848.1035	8	8	8	8	848.8696
	10	11	15	3	847.087
	10	14	7	5	849.087
	12	17	14	0	847.3044
	12	20	6	2	849.3044

potassium

MOLECULAR WEIGHT	# OF Si GROUPS	# OF BRIDGING Os	# OF OH GROUPS	# OF OR GROUPS	CALCULATED MOLECULAR WEIGHT
848.2012	8	8	8	8	848.8696
	10	11	15	3	847.087
	10	14	7	5	849.087
	12	17	14	0	847.3044
	12	20	6	2	849.3044

potassium

MOLECULAR WEIGHT	# OF Si GROUPS	# OF BRIDGING Os	# OF OH GROUPS	# OF OR GROUPS	CALCULATED MOLECULAR WEIGHT
848.299	8	8	8	8	848.8696
	10	11	15	3	847.087
	10	14	7	5	849.087
	12	17	14	0	847.3044
	12	20	6	2	849.3044

potassium

MOLECULAR WEIGHT	# OF Si GROUPS	# OF BRIDGING Os	# OF OH GROUPS	# OF OR GROUPS	CALCULATED MOLECULAR WEIGHT
849.1786	6	5	1	13	850.6522
	8	8	8	8	848.8696
	8	11	0	10	850.8696
	10	14	7	5	849.087
	12	17	14	0	847.3044
	12	20	6	2	849.3044

potassium

MOLECULAR WEIGHT	# OF Si GROUPS	# OF BRIDGING Os	# OF OH GROUPS	# OF OR GROUPS	CALCULATED MOLECULAR WEIGHT
851.1349	6	5	1	13	850.6522
	9	10	10	6	852.9783
	11	13	17	1	851.1957
	8	11	0	10	850.8696
	12	20	6	2	849.3044

potassium

MOLECULAR WEIGHT	# OF Si GROUPS	# OF BRIDGING Os	# OF OH GROUPS	# OF OR GROUPS	CALCULATED MOLECULAR WEIGHT
851.2327	6	5	1	13	850.6522
	9	10	10	6	852.9783
	11	13	17	1	851.1957
	8	11	0	10	850.8696
	11	16	9	3	853.1957
	12	20	6	2	849.3044

potassium

MOLECULAR WEIGHT	# OF Si GROUPS	# OF BRIDGING Os	# OF OH GROUPS	# OF OR GROUPS	CALCULATED MOLECULAR WEIGHT
851.918	6	5	1	13	850.6522
	9	10	10	6	852.9783
	11	13	17	1	851.1957
	8	11	0	10	850.8696
	11	16	9	3	853.1957
	13	22	8	0	853.4131

potassium

MOLECULAR WEIGHT	# OF Si GROUPS	# OF BRIDGING Os	# OF OH GROUPS	# OF OR GROUPS	CALCULATED MOLECULAR WEIGHT
852.0159	6	5	1	13	850.6522
	9	10	10	6	852.9783
	11	13	17	1	851.1957
	8	11	0	10	850.8696
	11	16	9	3	853.1957
	13	22	8	0	853.4131

potassium

MOLECULAR WEIGHT	# OF Si GROUPS	# OF BRIDGING Os	# OF OH GROUPS	# OF OR GROUPS	CALCULATED MOLECULAR WEIGHT
852.8974	7	7	3	11	854.7609
	9	10	10	6	852.9783
	11	13	17	1	851.1957
	11	16	9	3	853.1957
	13	22	8	0	853.4131

potassium

MOLECULAR WEIGHT	# OF Si GROUPS	# OF BRIDGING Os	# OF OH GROUPS	# OF OR GROUPS	CALCULATED MOLECULAR WEIGHT
852.9953	7	7	3	11	854.7609
	9	10	10	6	852.9783
	11	13	17	1	851.1957

	9	13	2	8	854.9783
	11	16	9	3	853.1957
	13	22	8	0	853.4131

potassium

MOLECULAR WEIGHT	# OF Si GROUPS	# OF BRIDGING Os	# OF OH GROUPS	# OF OR GROUPS	CALCULATED MOLECULAR WEIGHT
853.0933	10	9	20	2	855.087
	7	7	3	11	854.7609
	9	10	10	6	852.9783
	11	13	17	1	851.1957
	9	13	2	8	854.9783
	11	16	9	3	853.1957
	13	22	8	0	853.4131

potassium

MOLECULAR WEIGHT	# OF Si GROUPS	# OF BRIDGING Os	# OF OH GROUPS	# OF OR GROUPS	CALCULATED MOLECULAR WEIGHT
853.1913	10	9	20	2	855.087
	7	7	3	11	854.7609
	9	10	10	6	852.9783
	11	13	17	1	851.1957
	9	13	2	8	854.9783
	11	16	9	3	853.1957
	13	22	8	0	853.4131

potassium

MOLECULAR WEIGHT	# OF Si GROUPS	# OF BRIDGING Os	# OF OH GROUPS	# OF OR GROUPS	CALCULATED MOLECULAR WEIGHT
853.9753	10	9	20	2	855.087
	7	7	3	11	854.7609
	9	10	10	6	852.9783
	9	13	2	8	854.9783
	11	16	9	3	853.1957
	11	19	1	5	855.1957
	13	22	8	0	853.4131
	13	25	0	2	855.4131

potassium

MOLECULAR WEIGHT	# OF Si GROUPS	# OF BRIDGING Os	# OF OH GROUPS	# OF OR GROUPS	CALCULATED MOLECULAR WEIGHT
854.0733	10	9	20	2	855.087
	7	7	3	11	854.7609
	9	10	10	6	852.9783
	9	13	2	8	854.9783
	11	16	9	3	853.1957
	11	19	1	5	855.1957
	13	22	8	0	853.4131
	13	25	0	2	855.4131

potassium

MOLECULAR WEIGHT	# OF Si GROUPS	# OF BRIDGING Os	# OF OH GROUPS	# OF OR GROUPS	CALCULATED MOLECULAR WEIGHT
854.9558	10	9	20	2	855.087
	7	7	3	11	854.7609
	9	10	10	6	852.9783

9	13	2	8	854.9783
11	16	9	3	853.1957
11	19	1	5	855.1957
13	22	8	0	853.4131
13	25	0	2	855.4131

potassium

MOLECULAR WEIGHT	# OF Si GROUPS	# OF BRIDGING Os	# OF OH GROUPS	# OF OR GROUPS	CALCULATED MOLECULAR WEIGHT
858.9815	9	8	15	5	860.9783
	11	11	22	0	859.1957
	8	9	5	9	858.8696
	10	12	12	4	857.087
	10	15	4	6	859.087
	12	18	11	1	857.3044
	12	21	3	3	859.3044
	14	27	2	0	859.5218

potassium

MOLECULAR WEIGHT	# OF Si GROUPS	# OF BRIDGING Os	# OF OH GROUPS	# OF OR GROUPS	CALCULATED MOLECULAR WEIGHT
859.0798	9	8	15	5	860.9783
	11	11	22	0	859.1957
	8	9	5	9	858.8696
	10	12	12	4	857.087
	10	15	4	6	859.087
	12	18	11	1	857.3044
	12	21	3	3	859.3044
	14	27	2	0	859.5218

potassium

MOLECULAR WEIGHT	# OF Si GROUPS	# OF BRIDGING Os	# OF OH GROUPS	# OF OR GROUPS	CALCULATED MOLECULAR WEIGHT
859.1782	9	8	15	5	860.9783
	11	11	22	0	859.1957
	8	9	5	9	858.8696
	10	15	4	6	859.087
	12	18	11	1	857.3044
	12	21	3	3	859.3044
	14	27	2	0	859.5218

potassium

MOLECULAR WEIGHT	# OF Si GROUPS	# OF BRIDGING Os	# OF OH GROUPS	# OF OR GROUPS	CALCULATED MOLECULAR WEIGHT
859.2765	9	8	15	5	860.9783
	11	11	22	0	859.1957
	8	9	5	9	858.8696
	11	14	14	2	861.1957
	10	15	4	6	859.087
	12	18	11	1	857.3044
	12	21	3	3	859.3044
	14	27	2	0	859.5218

potassium

MOLECULAR WEIGHT	# OF Si GROUPS	# OF BRIDGING Os	# OF OH GROUPS	# OF OR GROUPS	CALCULATED MOLECULAR WEIGHT

860.0632	9	8	15	5	860.9783
	11	11	22	0	859.1957
	8	9	5	9	858.8696
	11	14	14	2	861.1957
	10	15	4	6	859.087
	12	21	3	3	859.3044
	14	27	2	0	859.5218

potassium

MOLECULAR WEIGHT	# OF Si GROUPS	# OF BRIDGING Os	# OF OH GROUPS	# OF OR GROUPS	CALCULATED MOLECULAR WEIGHT
860.1615	9	8	15	5	860.9783
	11	11	22	0	859.1957
	8	9	5	9	858.8696
	11	14	14	2	861.1957
	10	15	4	6	859.087
	12	21	3	3	859.3044
	14	27	2	0	859.5218

potassium

MOLECULAR WEIGHT	# OF Si GROUPS	# OF BRIDGING Os	# OF OH GROUPS	# OF OR GROUPS	CALCULATED MOLECULAR WEIGHT
860.9486	9	8	15	5	860.9783
	11	11	22	0	859.1957
	11	14	14	2	861.1957
	10	15	4	6	859.087
	12	21	3	3	859.3044
	14	27	2	0	859.5218

potassium

MOLECULAR WEIGHT	# OF Si GROUPS	# OF BRIDGING Os	# OF OH GROUPS	# OF OR GROUPS	CALCULATED MOLECULAR WEIGHT
861.047	9	8	15	5	860.9783
	11	11	22	0	859.1957
	9	11	7	7	862.9783
	11	14	14	2	861.1957
	10	15	4	6	859.087
	12	21	3	3	859.3044
	14	27	2	0	859.5218

potassium

MOLECULAR WEIGHT	# OF Si GROUPS	# OF BRIDGING Os	# OF OH GROUPS	# OF OR GROUPS	CALCULATED MOLECULAR WEIGHT
861.1454	9	8	15	5	860.9783
	11	11	22	0	859.1957
	9	11	7	7	862.9783
	11	14	14	2	861.1957
	12	21	3	3	859.3044
	14	27	2	0	859.5218

potassium

MOLECULAR WEIGHT	# OF Si GROUPS	# OF BRIDGING Os	# OF OH GROUPS	# OF OR GROUPS	CALCULATED MOLECULAR WEIGHT
861.2438	9	8	15	5	860.9783
	9	11	7	7	862.9783
	11	14	14	2	861.1957

	11	17	6	4	863.1957
	12	21	3	3	859.3044
	14	27	2	0	859.5218

potassium

MOLECULAR WEIGHT	# OF Si GROUPS	# OF BRIDGING Os	# OF OH GROUPS	# OF OR GROUPS	CALCULATED MOLECULAR WEIGHT
862.9178	9	8	15	5	860.9783
	7	8	0	12	864.7609
	9	11	7	7	862.9783
	11	14	14	2	861.1957
	11	17	6	4	863.1957
	13	23	5	1	863.4131

potassium

MOLECULAR WEIGHT	# OF Si GROUPS	# OF BRIDGING Os	# OF OH GROUPS	# OF OR GROUPS	CALCULATED MOLECULAR WEIGHT
863.0163	7	8	0	12	864.7609
	9	11	7	7	862.9783
	11	14	14	2	861.1957
	11	17	6	4	863.1957
	13	23	5	1	863.4131

potassium

MOLECULAR WEIGHT	# OF Si GROUPS	# OF BRIDGING Os	# OF OH GROUPS	# OF OR GROUPS	CALCULATED MOLECULAR WEIGHT
863.1148	10	10	17	3	865.087
	7	8	0	12	864.7609
	9	11	7	7	862.9783
	11	14	14	2	861.1957
	11	17	6	4	863.1957
	13	23	5	1	863.4131

potassium

MOLECULAR WEIGHT	# OF Si GROUPS	# OF BRIDGING Os	# OF OH GROUPS	# OF OR GROUPS	CALCULATED MOLECULAR WEIGHT
863.2134	10	10	17	3	865.087
	7	8	0	12	864.7609
	9	11	7	7	862.9783
	11	17	6	4	863.1957
	13	23	5	1	863.4131

potassium

MOLECULAR WEIGHT	# OF Si GROUPS	# OF BRIDGING Os	# OF OH GROUPS	# OF OR GROUPS	CALCULATED MOLECULAR WEIGHT
863.3119	10	10	17	3	865.087
	7	8	0	12	864.7609
	9	11	7	7	862.9783
	12	16	16	0	865.3044
	11	17	6	4	863.1957
	13	23	5	1	863.4131

potassium

MOLECULAR WEIGHT	# OF Si GROUPS	# OF BRIDGING Os	# OF OH GROUPS	# OF OR GROUPS	CALCULATED MOLECULAR WEIGHT
863.9032	10	10	17	3	865.087

	7	8	0	12	864.7609
	9	11	7	7	862.9783
	12	16	16	0	865.3044
	11	17	6	4	863.1957
	13	23	5	1	863.4131

potassium

MOLECULAR WEIGHT	# OF Si GROUPS	# OF BRIDGING Os	# OF OH GROUPS	# OF OR GROUPS	CALCULATED MOLECULAR WEIGHT
864.0018	10	10	17	3	865.087
	7	8	0	12	864.7609
	9	11	7	7	862.9783
	12	16	16	0	865.3044
	11	17	6	4	863.1957
	13	23	5	1	863.4131

potassium

MOLECULAR WEIGHT	# OF Si GROUPS	# OF BRIDGING Os	# OF OH GROUPS	# OF OR GROUPS	CALCULATED MOLECULAR WEIGHT
864.1004	10	10	17	3	865.087
	7	8	0	12	864.7609
	9	11	7	7	862.9783
	12	16	16	0	865.3044
	11	17	6	4	863.1957
	13	23	5	1	863.4131

potassium

MOLECULAR WEIGHT	# OF Si GROUPS	# OF BRIDGING Os	# OF OH GROUPS	# OF OR GROUPS	CALCULATED MOLECULAR WEIGHT
864.1989	10	10	17	3	865.087
	7	8	0	12	864.7609
	9	11	7	7	862.9783
	12	16	16	0	865.3044
	11	17	6	4	863.1957
	13	23	5	1	863.4131

potassium

MOLECULAR WEIGHT	# OF Si GROUPS	# OF BRIDGING Os	# OF OH GROUPS	# OF OR GROUPS	CALCULATED MOLECULAR WEIGHT
865.185	8	7	10	8	866.8696
	10	10	17	3	865.087
	7	8	0	12	864.7609
	10	13	9	5	867.087
	12	16	16	0	865.3044
	11	17	6	4	863.1957
	13	23	5	1	863.4131

potassium

MOLECULAR WEIGHT	# OF Si GROUPS	# OF BRIDGING Os	# OF OH GROUPS	# OF OR GROUPS	CALCULATED MOLECULAR WEIGHT
865.9743	8	7	10	8	866.8696
	10	10	17	3	865.087
	7	8	0	12	864.7609
	10	13	9	5	867.087
	12	16	16	0	865.3044
	12	19	8	2	867.3044

potassium

MOLECULAR WEIGHT	# OF Si GROUPS	# OF BRIDGING Os	# OF OH GROUPS	# OF OR GROUPS	CALCULATED MOLECULAR WEIGHT
880.8369	7	7	2	12	882.7609
	9	10	9	7	880.9783
	11	13	16	2	879.1957
	11	16	8	4	881.1957
	13	22	7	1	881.4131

potassium

MOLECULAR WEIGHT	# OF Si GROUPS	# OF BRIDGING Os	# OF OH GROUPS	# OF OR GROUPS	CALCULATED MOLECULAR WEIGHT
880.9364	7	7	2	12	882.7609
	9	10	9	7	880.9783
	11	13	16	2	879.1957
	11	16	8	4	881.1957
	13	22	7	1	881.4131

potassium

MOLECULAR WEIGHT	# OF Si GROUPS	# OF BRIDGING Os	# OF OH GROUPS	# OF OR GROUPS	CALCULATED MOLECULAR WEIGHT
881.0359	7	7	2	12	882.7609
	9	10	9	7	880.9783
	11	13	16	2	879.1957
	9	13	1	9	882.9783
	11	16	8	4	881.1957
	13	22	7	1	881.4131

potassium

MOLECULAR WEIGHT	# OF Si GROUPS	# OF BRIDGING Os	# OF OH GROUPS	# OF OR GROUPS	CALCULATED MOLECULAR WEIGHT
881.1354	10	9	19	3	883.087
	7	7	2	12	882.7609
	9	10	9	7	880.9783
	11	13	16	2	879.1957
	9	13	1	9	882.9783
	11	16	8	4	881.1957
	13	22	7	1	881.4131

potassium

MOLECULAR WEIGHT	# OF Si GROUPS	# OF BRIDGING Os	# OF OH GROUPS	# OF OR GROUPS	CALCULATED MOLECULAR WEIGHT
881.2349	10	9	19	3	883.087
	7	7	2	12	882.7609
	9	10	9	7	880.9783
	9	13	1	9	882.9783
	11	16	8	4	881.1957
	11	19	0	6	883.1957
	13	22	7	1	881.4131

potassium

MOLECULAR WEIGHT	# OF Si GROUPS	# OF BRIDGING Os	# OF OH GROUPS	# OF OR GROUPS	CALCULATED MOLECULAR WEIGHT
881.9316	10	9	19	3	883.087
	7	7	2	12	882.7609

	9	10	9	7	880.9783
	12	15	18	0	883.3044
	9	13	1	9	882.9783
	11	16	8	4	881.1957
	11	19	0	6	883.1957
	13	22	7	1	881.4131

potassium

MOLECULAR WEIGHT	# OF Si GROUPS	# OF BRIDGING Os	# OF OH GROUPS	# OF OR GROUPS	CALCULATED MOLECULAR WEIGHT
882.0312	10	9	19	3	883.087
	7	7	2	12	882.7609
	9	10	9	7	880.9783
	12	15	18	0	883.3044
	9	13	1	9	882.9783
	11	16	8	4	881.1957
	11	19	0	6	883.1957
	13	22	7	1	881.4131

potassium

MOLECULAR WEIGHT	# OF Si GROUPS	# OF BRIDGING Os	# OF OH GROUPS	# OF OR GROUPS	CALCULATED MOLECULAR WEIGHT
882.1307	10	9	19	3	883.087
	7	7	2	12	882.7609
	9	10	9	7	880.9783
	12	15	18	0	883.3044
	9	13	1	9	882.9783
	11	16	8	4	881.1957
	11	19	0	6	883.1957
	13	22	7	1	881.4131

potassium

MOLECULAR WEIGHT	# OF Si GROUPS	# OF BRIDGING Os	# OF OH GROUPS	# OF OR GROUPS	CALCULATED MOLECULAR WEIGHT
882.9274	10	9	19	3	883.087
	7	7	2	12	882.7609
	9	10	9	7	880.9783
	12	15	18	0	883.3044
	9	13	1	9	882.9783
	11	16	8	4	881.1957
	11	19	0	6	883.1957
	13	22	7	1	881.4131

potassium

MOLECULAR WEIGHT	# OF Si GROUPS	# OF BRIDGING Os	# OF OH GROUPS	# OF OR GROUPS	CALCULATED MOLECULAR WEIGHT
883.027	10	9	19	3	883.087
	7	7	2	12	882.7609
	12	15	18	0	883.3044
	9	13	1	9	882.9783
	11	16	8	4	881.1957
	11	19	0	6	883.1957
	13	22	7	1	881.4131

potassium

MOLECULAR WEIGHT	# OF Si GROUPS	# OF BRIDGING Os	# OF OH GROUPS	# OF OR GROUPS	CALCULATED MOLECULAR

					WEIGHT
883.1266	10	9	19	3	883.087
	7	7	2	12	882.7609
	10	12	11	5	885.087
	12	15	18	0	883.3044
	9	13	1	9	882.9783
	11	16	8	4	881.1957
	11	19	0	6	883.1957
	13	22	7	1	881.4131

potassium

MOLECULAR WEIGHT	# OF Si GROUPS	# OF BRIDGING Os	# OF OH GROUPS	# OF OR GROUPS	CALCULATED MOLECULAR WEIGHT
890.9126	9	8	14	6	888.9783
	9	11	6	8	890.9783
	11	14	13	3	889.1957
	11	17	5	5	891.1957
	13	20	12	0	889.4131
	13	23	4	2	891.4131

potassium

MOLECULAR WEIGHT	# OF Si GROUPS	# OF BRIDGING Os	# OF OH GROUPS	# OF OR GROUPS	CALCULATED MOLECULAR WEIGHT
891.0127	9	11	6	8	890.9783
	11	14	13	3	889.1957
	11	17	5	5	891.1957
	13	20	12	0	889.4131
	13	23	4	2	891.4131

potassium

MOLECULAR WEIGHT	# OF Si GROUPS	# OF BRIDGING Os	# OF OH GROUPS	# OF OR GROUPS	CALCULATED MOLECULAR WEIGHT
891.1127	10	10	16	4	893.087
	9	11	6	8	890.9783
	11	14	13	3	889.1957
	11	17	5	5	891.1957
	13	20	12	0	889.4131
	13	23	4	2	891.4131

potassium

MOLECULAR WEIGHT	# OF Si GROUPS	# OF BRIDGING Os	# OF OH GROUPS	# OF OR GROUPS	CALCULATED MOLECULAR WEIGHT
891.2128	10	10	16	4	893.087
	9	11	6	8	890.9783
	11	17	5	5	891.1957
	13	20	12	0	889.4131
	13	23	4	2	891.4131

potassium

MOLECULAR WEIGHT	# OF Si GROUPS	# OF BRIDGING Os	# OF OH GROUPS	# OF OR GROUPS	CALCULATED MOLECULAR WEIGHT
891.3128	10	10	16	4	893.087
	9	11	6	8	890.9783
	12	16	15	1	893.3044
	11	17	5	5	891.1957
	13	20	12	0	889.4131

	13	23	4	2	891.4131

potassium

MOLECULAR WEIGHT	# OF Si GROUPS	# OF BRIDGING Os	# OF OH GROUPS	# OF OR GROUPS	CALCULATED MOLECULAR WEIGHT
891.9132	10	10	16	4	893.087
	9	11	6	8	890.9783
	12	16	15	1	893.3044
	11	17	5	5	891.1957
	13	23	4	2	891.4131

potassium

MOLECULAR WEIGHT	# OF Si GROUPS	# OF BRIDGING Os	# OF OH GROUPS	# OF OR GROUPS	CALCULATED MOLECULAR WEIGHT
892.0133	10	10	16	4	893.087
	9	11	6	8	890.9783
	12	16	15	1	893.3044
	11	17	5	5	891.1957
	13	23	4	2	891.4131

potassium

MOLECULAR WEIGHT	# OF Si GROUPS	# OF BRIDGING Os	# OF OH GROUPS	# OF OR GROUPS	CALCULATED MOLECULAR WEIGHT
892.1134	10	10	16	4	893.087
	9	11	6	8	890.9783
	12	16	15	1	893.3044
	11	17	5	5	891.1957
	13	23	4	2	891.4131

potassium

MOLECULAR WEIGHT	# OF Si GROUPS	# OF BRIDGING Os	# OF OH GROUPS	# OF OR GROUPS	CALCULATED MOLECULAR WEIGHT
892.2135	10	10	16	4	893.087
	9	11	6	8	890.9783
	12	16	15	1	893.3044
	11	17	5	5	891.1957
	13	23	4	2	891.4131

potassium

MOLECULAR WEIGHT	# OF Si GROUPS	# OF BRIDGING Os	# OF OH GROUPS	# OF OR GROUPS	CALCULATED MOLECULAR WEIGHT
892.9143	8	7	9	9	894.8696
	10	10	16	4	893.087
	9	11	6	8	890.9783
	12	16	15	1	893.3044
	11	17	5	5	891.1957
	13	23	4	2	891.4131

Appendix D: Kinetic Model: Fortran Program/Subroutine

```
PROGRAM: ATEOSFA
C     MAIN PROGRAM FOR CALCULATING THE CONCENTRATION OF SPECIES
C     AND THE WEIGHT AVERAGE MOLECULAR WEIGHT
C     BY KIMBERLY BROWN
C
      INTEGER IDO,NEQ, NPARAM, IEND, IMETH, INORM,
      &      NOUT
      PARAMETER (NEQ=8 ,NPARAM=50)
C
C
      REAL RK1,RKH1,RKC2,RKC4,RK3,RKE,RKH2,RKC3,RK4,RK2,RKC1
      &      TOL, A(1,1), FCN, FCNJ, HINIT,
      &   PARAM(NPARAM), T, TEND, P(NEQ), FLOAT
      EXTERNAL FCN, FCNJ, IVPAG, SSET, UMACH
      INTRINSIC FLOAT
      COMMON /C1/ RK1,RKH1,RKC2,RKC4,RK3,RKE,RKH2,RKC3,RK4,RK2,RKC1
      OPEN (UNIT=5,FILE='C:\tfafor',STATUS='UNKNOWN')
C      INITIALIZE
      HINIT=.001
      INORM=1
      IMETH=1
      CALL SSET (NPARAM, 0.0, PARAM, 1)
      PARAM(1)=HINIT
      PARAM(10)=INORM
      PARAM(12)=IMETH
      PARAM(4)=5000000
C
C
      IDO=1
      T=0.0
      P(1)=9.0
      P(2)=13.25
      P(3)=0.0
      P(4)=0.0
      P(5)=0.0
      P(6)=0.0
      P(7)=0.0
      P(8)=0.0
C
      TOL=0.000001
C

      WRITE (NOUT,98)
      WRITE(5,98)
C
      IEND1=1
      DO 10 IEND=1,3400
            TEND=FLOAT(IEND)
            CALL IVPAG (IDO,NEQ,FCN,FCNJ,A,T,TEND,TOL,PARAM,P)
            IEND2=IEND/300
            TMIN=TEND/60
            IF(IEND2.EQ.IEND1)THEN
          WRITE (NOUT,99)TMIN,P
            WRITE(5,99)TMIN,P
```

```
            IEND1=IEND1+1
            END IF
   10 CONTINUE
C
      CLOSE(UNIT=5)
      IDO=3
      CALL IVPAG(IDO,NEQ,FCN,FCNJ,A,T,TEND,TOL,PARAM,P)
C
       98
FORMAT(6X,'T',9X,'[SiOR]',9X,'[HCOOH]',9X,'[SiOH]',9X,'[SiOSi]
     & ',9X,'[SiOOCH]',9X,'[ROH]',9X,'[H2O]',9X,'[ROOCH]')
       99 FORMAT (6F12.8)
      END
C      SUBROUTINE FUNCTIONJ
      SUBROUTINE FCNJ (NEQ,T,P,DYPDY)
      INTEGER NEQ
      REAL T,P(NEQ),DYPDY(*)
      RETURN
      END
C    SUBROUTINE CONTAINING DIFFERENTIAL EQUATIONS WHICH MODEL THE
C    THE REACTION OF TEOS AND FORMIC ACID
C
C
      SUBROUTINE FCN(NEQ,T,P,PPRIME)
C
C
      INTEGER NEQ,ITMAX,NZ
      REAL RK1, RKH1, RKC2,RKC4,RK3,RKE,RKH2,RKC3,RK4,RK2,RKC1,
      &     T,P(NEQ),PPRIME(NEQ),ERREL
      INTEGER K,NOUT2
      PARAMETER (NZ=1)
      REAL FCN2,FNORM,X(NZ),XGUESS(NZ)
      EXTERNAL FCN2,NEQNF,UMACH
      ERREL=.0001
      ITMAX=1000
C     RATE CONSTANTS FOR TEOS FORMIC ACID REACTION
      RK1=0.00003
      RK2= 0.05
      RK3=0.0
      RKE=0.0
      RKH1=0.0
      RKH2=0.0
      RKC1=0.02
      RKC2=0.001
      RKC3=0.9
      RKC4=0.0004
      RK4=0.0

C
      PPRIME(1)=(-RK1*P(1)*P(2))-(RKC2*P(3)*P(1))
     &              -(RKC4*P(1)*P(5))
      PPRIME(2)=(-RK1*P(1)*P(2))
      &       +(RKC3*P(3)*P(5))
      PPRIME(3)=(RK2*P(5)*P(6))
      &      -(2*RKC1*(P(3)**2))-(RKC2*P(3)*P(1))
      &           -(RKC3*P(3)*P(5))
      PPRIME(4)=(2*RKC1*(P(3)**2))+(RKC2*P(3)*P(1))+(RKC3*P(3)*P(5))
```

```
      &              +(RKC4*P(1)*P(5))
      PPRIME(5)=(RK1*P(1)*P(2)) -(RK2*P(6)*P(5))
      &          -(RKC3*P(3)*P(5))-(RKC4*P(1)*P(5))
      PPRIME(6)=(RK1*P(1)*P(2))
      &             +(RKC2*P(3)*P(1))
      PPRIME(7)=(2*RKC1*(P(3)**2))
      PPRIME(8)=(RK2*P(6)*P(5)) +(RKC4*P(1)*P(5))
C
C

      RETURN
      END
```

REFERENCES

M. J. Adeogun, J. P. A. Fairclough, J. N. Hay, and A. J. Ryan*, J. Sol-Gel Science and Technology*, **13** (1998) 27.

R. Aelion, A. Loebell, and F. Eirich, *J. Am. Chem. Soc.*, **72** (1950) 5705.

R. M. Almeida, *J. Sol-Gel Science and Technology*, **13** (1998) 51.

I. Artaki, S. Sinha, A.D. Irwin, and J.Jonas, *J. Non-Crystalline Solids*, **72** (1985) 391.

R. A. Assink and B. D. Kay, *J. Non-Crystalline Solids*, **99** (1988) 359.

J. K. Bailey, C. W. Macosko, and M. L. Mercartney, *J. Non-Crystalline Solids*, **125** (1990) 208.

D. C. Bradley, R. Gaze, and W. Wardlaw, *J. Chem. Soc*., (1955) 3977.

D. C. Bradley, R. Gaze, and W. Wardlaw, *J. Chem. Soc*., (1957) 469.

E.G. Braume and J.G. Grasselli, *Infrared and Raman Spectroscopy*. Marcel Dekker, New York, 1976.

C. J. Brinker, K. D. Keefer, D. W. Schaefer, C. S. Ashley, *J. Non-Crystalline Solids*, **48** (1982) 47.

C. J. Brinker, K. D. Keefer, D. W. Schaefer, R. A. Assink, B. D. Kay, and C. S. Ashley, *J. Non-Crystalline Solids*, **63** (1984) 45.

C.J. Brinker and G.W. Scherer, *Sol-Gel Science*. Academic Press, San Diego, 1990.

C.J. Brinker and G. W. Scherer, *The Physics and Chemistry of Sol-Gel Processing*. Academic Press, San Diego, 1990b.

H. Brumberger ed., *Modern Aspects of Small Angle Scattering*. Kluwer, Dordrecht, 1995.

A. Campero, R. Arroyo, C. Sanchez, and J. Livage, in

S. Y. Chang and T. A. Ring, *J. Non-Cryst. Solids*, **147 & 1**48 (1992) 56.

B. K. Coltrain, L. W. Kelts, N. J. Armstrong, and J. M. Salva, *J. Sol-Gel Science and*

Technology, **3** (1994) 83.

R. J. Davis and Z. Liu, *Chem. Mater*., **9** (1997) 2311.

L. Delattre and F. Babonneau, *Chem. Mater*., **9** (1997) 2385.

S. Dire and F. Babonneau, *J. Non-Cryst. Solids*, **167** (1994) 29.

D. M. Doddrell, D. T. Pegg, and M. R. Bendall, *J. Magnetic Resonance*, **48** (1982) 323.

D. H. Doughty R. A. Assink, and B. D. Kay, *J. Am. Chem Soc.* **224** (1990) 241.

W. Eitel, *Silicate Science I*. Academic Press, New York, 1964.

H. G. Emblem, K. Hargreaves, and C. E. Oxley, *J. Appl. Chem*., **18** (1968) 97.

M.T. Harris, A. Singhal, J. L. Look, J. R. Smith-Kristensen, J. S. Lin, and L. M. Toth, *J. Sol-Gel Sci. and Tech.*, **8** (1997) 41.

S. D. Hanton, *Chem. Rev*., **101** (2001) 527.

Hayashi, H. Suzuki, and S. Kaneko, *J. Sol-Gel Science and Technology*, **12** (1998) 87.

R.K. Iler, *The Chemistry of Silica*. Wiley, New York, 1979,

B. Karmakar, G. De, D. Kundu, and D. Ganguli, *J. Non-Crystalline Solids*, **135** (1991) 29.

L. W. Kelts and N. J. Armstrong, *Mat. Res. Soc. Symp. Proc*., **121** (1988) 519.

M. Kursawe, W. Glaubitt, and A. Thurauf, *J. Sol-Gel Science and Technology*, **13** (1998) 267.

I. Laaziz, A. Larbot, A. Julbe, C. Gurzard, L. Cott, *J. Solid State Chem.,* **98** (1992) 393.

J. A. Lake, *Acta. Cryst*. **23** (1967), 191.

C. Lin and J. D. Basil in *Better Ceramics through Chemistry II*, eds. C. J. Brinker, D. E. Clark, and D. R. Ulrich, Materials Research Society, Pittsburgh, 1986.

L. Malier, F. Devreux, F. Chaput, J. P. Boilot, and M. A. V. Axelos, *J. Non-Crystalline Solids*, **147** (1992) 686.

M. Michalczyk, W. Simonsick, and K.G. Sharp*, J. Organometallic Chem.,* **521** (1996) 261.

W. McFarlane and J. M. Seaby, *J. Chemical Society Perkins II* (1972) 1561.

L. Ng and A. V. McCormick, *J. Phys. Chem.,* **100** (1996) 12517.

E. Oldfield and R. J. Kirkpatrick*, J. Magnetic Resonance*, **227** (1985) 1537.

M. P. J. Peeters, T. N. M. Bernards, M. J. VanBommel, *J. Sol-Gel Science and Technology*, **13** (1998) 71.

E. J. A. Pope and J. D. Mackenzie, *J. Non-Crystalline Solids*, **87** (1986) 185.

J.C. Pouxviel, J.P. Boilot, J. C. Beloeil, J.Y. Lallemand, *J. Non-Cryst. Solids*, **89** (1987) 345.

D. Ridge and M. Todd, *J. Chem. Soc*., (1949) 2637.

N.P.G. Roeges, *A Guide to the Complete Interpretation of Infrared Spectra of Organic Structures.* Wiley, Chichester, 1994.

J. Retuert, R. Quijada, V. Arias, *Chem. Mater.*, **10** (1998) 3923.

S. Sakka, H. Kozuka, S. H. Kim, in *Ultrastructure Processing of Advanced Ceramics*, eds. J. Mackenzie and D. R. Ulrich, Wiley, New York, 1988.

C. Sanchez, J. Livage, M. Henry, F. Babonneau, *J. Non-Cryst. Solids*, **100** (1988) 65.
B. Schrader, in *Practical Fourier Transform Infrared Spectroscopy*, eds. J. R. Ferraro and K. Krishnan, Academic Press, San Diego, 1990.

K. G. Sharp, *J. Sol-Gel Science and Technology*, **2** (1994) 35.

G. Sumrell and G. J. Ham, *J. Am. Chem. Soc*. **78** (1956) 5573.

C. W. Turner and K. J. Franklin, *J. Non-Cryst. Solids*, **91** (1987) 402.

U.S. Patent *4732750*, March 22, 1988.

J. J. van Beek, D. Seykens, J.B. H. Jansen, and R. D. Schuiling, *J. Non-Cryst. Solids*, **134** (1991) 14.

M. G. Voronkov, Y. A. Yuzhelevskii, and V.P. Mileshkevich, *The Siloxane Bond*. Plenum, New York, 1978.

W. E. Wallace, C. M. Guttman, and J. M. Antonucci, *J. Am. Soc. Mass Spectrom*, **10** (1999) 224.

L.A. Woodward, *Introduction to the Theory of molecular Vibrations and Vibrational Spectroscopy*. Oxford University Press, London, 1972.

M. Yamane, S. Inoue, K. Nakazawa, *J. Non-Cryst. Solids*, **48** (1982) 153.

B. E. Yoldas, *J. Mat. Sci*. **12** (1977) 1203.

B. E. Yoldas, *J. Non-Crystalline Solids*, **83** (1986) 375.